HYDRODYNAMIC AND PARTICULATE RECOVERY STUDIES IN MOBILE-BED CONTACTING

by

Bekir Zühtü Uysal

A Thesis Submitted to the Faculty of Graduate Studies
and Research in Partial Fulfilment of the
Requirements for the Degree of
Doctor of Philosophy

Department of Chemical Engineering
McGill University
Montreal

September 1978

To

My Parents

ABSTRACT

Hydrodynamic and particulate recovery characteristics of mobile-bed contacting (MBC) were studied in a 0.29 m diameter column over the range of gas and liquid flow rates $0.5 < G < 5.5$ and $4.7 < L < 33$ kg/m^2-s. Packing of density 157 kg/m^3, of diameter 38, 25 and 19 mm, was used to obtain static bed heights of 0.29, 0.44 and 0.58 m.

Correlations were developed for bed expansion, minimum fluidization velocity, pressure drop and liquid holdup.

Inertial impaction was found to be the dominant aerodynamic mechanism for particle collection in MBC.

A general theory for particle collection in any scrubber was developed. Analogous to mass transfer, a particle transfer coefficient, k_p, was defined. A general correlation for k_p was obtained for MBC, incorporating experimentally determined effects of liquid and gas flow rate, packing size, static bed height, particle size, and hydrophobicity of particles. The correlation was validated for particles in the size range 0.35 - 5.5 μm. Experiments confirmed the conclusion, from a theoretical analysis for effect of hydrophobicity of particles, that recovery is unaffected by wettability for contact angles up to 90^o.

The effect of diffusiophoresis on particle collection was also incorporated into the theory and applied successfully experimentally. Practical expressions to estimate the contribution of diffusiophoresis to overall scrubber efficiency are presented.

RESUME

On a étudie les caractéristiques hydrodynamiques et les caractéristiques de la récupération des particules pour le processus de "mobile-bed contacting (MBC)" à l'aide d'une colonne de diamètre 0.29 m pour des débits du gaz de 0.5 à 5.5 kg/m^2-s et du liquide de 4.7 à 33 kg/m^2-s. On a obtenu des hauteurs de lit statique de 0.29, 0.44 et 0.58 m à l'aide de garnissages de 157 kg/m^3 de densité, et de 38, 25 et 19 mm de diamètre.

Des corrélations ont pu être établies quant à la dilatation du lit, la vitesse minimum de fluidisation, la perte de charge et la quantité de liquide retenue au lit.

On a montré que les collisions dûes à l'inertie constituent le mécanisme aérodynamique principal de récupération des particules dans le MBC.

On a développé une théorie générale de récupération des particules valable pour tout contacteur gaz-liquide. On a defini un coefficient de transfert de particules, k_p, par analogie au coefficient de transfert de masse. Dans le cas particulier du MBC on a obtenu une corrélation générale pour le coefficient k_p tenant compte des effets du débit de liquide, du débit de gaz, de la dimension du garnissage, de la hauteur du lit statique, de la taille des particules et de leur caractère hydrophobe, ces effets ayant été déterminés expérimentalement. Cette corrélation a été vérifiée pour des particules de taille variant entre 0.35 et 5.5 µm. Des expériences ont confirmé la conclusion d'une étude théorique de l'effet du caractère hydrophobe des particules selon laquelle la récupération est indépendante de la mouillabilité pour des angles de contact allant jusqu'à 90^o.

L'effet de la diffusiophorèse sur la récupération des particules est aussi pris en compte dans la théorie et appliqué expérimentalement avec succès. Des expressions pratiques pour l'estimation de la contribution de la diffusiophorèse à l'efficacité d'un épurateur sont présentées.

ACKNOWLEDGEMENTS

The author wishes to express his sincere gratitude and appreciation to all those who, in various ways, contributed to this work.

To Dr W.J.M. Douglas for his constructive advice and encouragement.

To Dr J.R. Grace, Dr A.S. Mujumdar and Dr P.J. Whitmore for interesting and fruitful discussions.

To The Pulp and Paper Research Institute of Canada for the award of a post-graduate scholarship, and for the extensive use of their various facilities.

To the Occupational Health and Safety Unit of the Institute for Mineral Industry Research for their courtesy in permitting the use of the Model 202 Royco particle counter and for providing the silica particles used in this work.

To Messrs A. Krish, H. Alexander of the Chemical Engineering Workshop of McGill University, and D.P.W. Pounds and W. Davidson of the PPRIC machine shop for their help in constructing the equipment.

To Mr W. Hoogendoorn and Mr O. Vadas for their help in connection with electronic instruments.

To fellow graduate students, Mr O.Biceroglu, Mr E. Bayramlı, Mr T. Mehmetoglu, Mr H. Seoud and Mr N.T. Obot, for their generous help in the construction of the experimental unit and interesting discussions.

To Miss L. Strath for her help while working as a summer student.

To Mr M. Inoue for preparing the latex particles used in prime calibration of the particle counter.

To Mr S. Kelebek, a graduate student in the Mining and Metallurgical Engineering Department of McGill University, for his help in the measurements of contact angle.

To Mrs H. Rousseau and Mrs D. Ross for their great care, patience and excellent typing of the manuscript.

To my mother, who passed away one year before completion of this work, for sustaining me through the long and arduous years.

To the rest of my family for their continued moral support.

TABLE OF CONTENTS

LIST OF FIGURES

List of Figures (continued)

List of Figures (continued)

List of Figures (continued)

List of Figures (continued)

LIST OF TABLES

List of Tables (continued)

CHAPTER 1

INTRODUCTION

1.1. MOBILE-BED CONTACTING

A novel method of gas-liquid contacting involves counter-current flow of gas and liquid phases through a bed of low density packing. Under these flow conditions the bed expands so that, for typical gas and liquid velocities used, the expanded bed height may be two or three times the static height of the bed. Typically, the packing consists of hollow molded polyethylene or polypropylene or foamed polystyrene spheres, of density about 150 kg/m^3, and 38 mm or less in diameter. The upper and lower retaining grids for the bed must naturally be spaced at about three times the static bed height. Due to the counter flow of gas and liquid, the packing balls in the expanded bed experience a turbulent random motion which in turn creates an intense level of mixing between gas and liquid. This vigorous contacting provides high interfacial transfer rates. Because of its ability to expand, a bed of this kind permits much higher gas and liquid flow rates than are possible in conventional columns such as plate towers or columns with fixed beds of packing.

From a historical point of view, this technique was invented by Kielback (1959, 1960, and 1961) who was concerned with a problem of fouling by particulate matter in the scrubbing of a gaseous stream at the smelter of the Aluminum Company of Canada, Arvida, Quebec. Further modification of the process for use in the pulp and paper industry was reported by Douglas et al. (1963).

This process has been described by a variety of names. Kielback termed it a "floating bed wet scrubber", based on its original use as a scrubber. As the modification made subsequently by Domtar Pulp and Paper Ltd concerned an application for gas absorption, their description was "turbulent contact absorber", or simply, TCA. As this technique may also be regarded as basically gas-solid fluidization modified by the presence of a liquid phase, the name "three-phase fluidized bed" has also been employed. A disadvantage of this term is that others have used the same designation for the case of gas and liquid flowing cocurrently upward through the bed being fluidized. Another disadvantage of the term three-phase fluidization is that, in all other fluidized bed processes, some essential interaction occurs between the fluid and solid phases, such as the frequent case of the fluidized solids being a catalyst or a reactant. By contrast, in the operation under consideration here, the solid phase does not interact in any way with the gas or liquid. Rather, the low density solid phase is present to achieve a specific type of contacting between the gas and liquid phases. Thus the process is essentially one in which an expandable bed of packing, the elements of which are in continuous motion, serves to impart unique contacting characteristics to a gas-liquid countercurrent flow. It appears, therefore, that the designation "mobile-bed contactor", or MBC as used by Douglas and co-workers at McGill University, remains the most comprehensive and descriptive name. Of the various terms which have been proposed, this is the only one which is equally applicable for all uses

of the technique, i.e. whether for gas absorption, direct contact heat transfer, dehumidification, or, as in the present study, as a wet scrubber for particulate removal. The designation mobile-bed contacting, MBC, is therefore used henceforth in this thesis.

In the early applications of this operation, design procedures were based on limited available operating experience of units already installed. A number of investigators subsequently published results of the studies on various aspects of MBC, such as hydrodynamics, liquid holdup, axial liquid mixing, heat transfer and mass transfer. In fact, it is the high heat and mass transfer rates, superior to other gas-liquid contactors, reported by the early investigators (Douglas et al. (1963) and Douglas (1964)), that made MBC so attractive originally.

It should be recalled that the original conception of this technique by Kielback was to solve a particularly difficult gas scrubbing problem. Thus, a fundamental advantage of MBC over other scrubbers is its self-cleaning feature when used with gases or liquids which contain suspended particulate material. The moving packing spheres are continuously cleaned by tumbling against one another, thus effectively preventing particulate build-up on the packing and subsequent shutdowns for cleaning. This non-clogging feature remains a key reason in the use of MBC for removal of particulates from gas streams.

1.2. PARTICULATE RECOVERY

In many processing operations such as combustion, smelting, calcining, drying and crushing, the effluent gases contain suspended particles. Discharge of this emission to the atmosphere creates

environmental pollution, including environmental health hazards. There may, moreover, be an appreciable economic loss, as in the case of entrainment of particles of expensive catalyst in petroleum refining. Thus, for several reasons, development and improvement of particulate removal devices has become a recognized need in industry.

Equipment used for particulate recovery may be classified as cyclone separators, baghouses, electrostatic precipitators, settling chambers, and wet scrubbers. In selecting the optimum device for a specific application, information is required on particle characteristics, (concentration, size, distribution, shape, density and physico-chemical properties), flow rate, temperature, pressure and humidity of carrier gas, collection efficiency required, allowable pressure drop, space and material limitations. As wet scrubbers, in contrast to baghouses, are not cyclic in operation, their constant pressure drop operation is sometimes an important advantage. The ability of wet scrubbers to handle high temperature and moisture-laden gases is another important characteristic. Although use of wet scrubbers avoids the secondary dust problem associated with disposal of collected particulates from dry recovery processes, disposal or clarification of the particulate-laden waste water from wet scrubbers may, however, pose another problem. Space requirements of wet scrubbers are reasonable. Commercially available types of wet scrubbers include principally spray columns, cyclone-type scrubbers, orifice-type scrubbers, centrifugal scrubbers, plate columns, packed towers, venturi scrubbers and the newest wet scrubber, the MBC process. Provided that high pressure drop may be used, wet scrubbers such as a venturi scrubber may collect particles down to 0.05 micron in size.

In spite of its high potential for use of particulate recovery, there are very few studies published for this application of MBC (Pollack et al. (1966), Epstein et al. (1971), Calvert et al. (1972), Rowbottom (1973), Calvert et al. (1974), Mlodzinski and Warych (1975)). Unfortunately, none of these are thorough investigations, and each suffers from important deficiencies. As the limited studies available are quite inadequate for developing a reliable mathematical model of particulate collection in MBC for use in industrial design, the present study has been undertaken.

1.3. OBJECTIVES AND SCOPE

The objective of the present study is then to investigate the characteristics and performance of MBC for particulate recovery from gases, an application for which the industrial potential of the MBC process is very important. The need in the particulate recovery study to have accurate information on the hydrodynamics of MBC, and the discrepancies among previous studies of MBC hydrodynamics lead to extending this work to include studies of bed expansion, minimum fluidization velocity, pressure drop and liquid holdup.

More specifically, for the hydrodynamics of MBC, the objective was to obtain experimental data and a general correlation for:

(i) minimum fluidization velocity

(ii) bed expansion

(iii) pressure drop

(iv) liquid holdup

For particulate recovery in MBC, the objectives were:

(i) Identification of the major particle collection mechanism(s).

(ii) Development of a general theory for particulate recovery both at conditions where only aerodynamic mechanisms exist, and at conditions where diffusiophoresis, the most important phoretic mechanism in scrubbers, co-exists with aerodynamic mechanisms.

(iii) To obtain extensive data for particle collection in MBC at conditions where only aerodynamic mechanisms exist, and to study the effect of basic variables such as liquid and gas flow rate, packing size, static bed height, particle size and nature (hydrophobicity) of particles.

(iv) To investigate the effect of diffusiophoresis.

(v) To test the proposed theory under conditions with and without diffusiophoresis.

To accomplish the above objectives and to obtain results applicable for the reliable design of full-scale industrial units, a pilot-plant size experimental facility was constructed with all necessary auxiliary equipment.

CHAPTER 2

LITERATURE SURVEY

The literature relevant to this thesis on mobile-bed contacting (MBC) is summarized in this chapter. The first section concerns general characteristics of MBC, i.e. hydrodynamics and interphase transfer. Subsequently, particle collection mechanisms are reviewed and particle collection in MBC is discussed.

2.1 HYDRODYNAMICS OF MOBILE-BED CONTACTING

Although studies of several aspects of MBC have now been reported, a fundamental limitation is that most published data were strongly affected either by wall effects or by the use of small open area of the grid supporting the mobile-bed. Small open area in the packing support grids and small ratios of column diameter to packing size, D_c/d_{pb}, strongly affect hydrodynamic behaviour of the system. For example, Gel'perin et al. (1960 and 1966), Blyakher et al. (1967), Aksel'rod et al. (1969), Balabekov et al. (1969) reported data on hydrodynamics of MBC using plates with open areas 34.5, 25-70, 41, 35.5-55.5 and 40%, respectively. However, a typical supporting grid used in industry would have more than 70% open area. The data presented by Levsh et al. (1968) and by Krainev et al. (1968) are for packing consisting of rings, which is not a packing used in industry. Some of the data reported by Khanna (1971) and by Tichy and Douglas (1972) were for values of D_c/d_{pb} as low as 3.7, for which wall effects were evidently present. In the subsequent study of Kito et al. (1976) the ratio $D_c/d_{pb} = 5$ no

doubt caused strong wall effects. Only the early studies of Chen (1965) and Chen and Douglas (1968) were free from these side effects. Thus the number of published studies in which the results are not of limited generality is indeed very few, much less even than the rather small total number of studies available.

2.1.1 Minimum Fluidization Velocity

As gas flow rate is increased from zero at a constant liquid flow rate, an MBC column behaves first simply as a packed bed. Upon further increase of gas flow rate, the low density packing starts fluidizing and the bed begins to expand because the spacing between the upper and lower retaining grids for an MBC column is always greater than the static bed height. With the change in state of the packing from a static to a mobile bed, the column enters the normal operating range of MBC. Thus one may visualize an MBC column as a gas-liquid contactor which operates at flow conditions corresponding to flooding conditions of a fixed-bed contactor, but where the flooding conditions are stabilized in MBC by the ability of the mobile-bed to expand. Thus the minimum gas fluidization velocity, G_{mf}, defines the lower limit of the operating conditions of MBC.

Table 2.1 summarizes the equations found in the literature for estimation of minimum fluidization velocity. As will be discussed further in Chapter 6, the significant differences in values of G_{mf} estimated by these equations emphasize the importance of the effect of physical characteristics and dimensions on the hydrodynamic behaviour of the system. Only the correlation reported by Chen (1965), and Chen and Douglas (1968), was obtained using a column with large open-area grid

TABLE 2.1 Correlations for Minimum Fluidization Velocity

Reference	Open Area of Grid	D_c/d_{pb}	Equation
Gel'perin et al. (1966)	34.5%	10	$u_{G,mf} = 109.5\ L^{-.21}$
Blyakher et al. (1967)	41%	9.2	$u_{G,mf} = (u_{G,mf})_{L=0} + 1.25\times10^{-6}L^{.9}/(37.5 + 1.25\times10^{-6}L^{.9})$
Chen (1965) Chen and Douglas (1968)	80%	8-24	$G_{mf} = 98.46\ d_{pb}^{1.1}10^{-.03683\ L}$
Khanna (1971)	70%	3.7-11	$G_{mf} = 526.47\ d_{pb}^{1.5}10^{-.0317\ L}$
Tichy and Douglas (1972)	70%	3.7-11	$G_{mf} = .36355 + 57.9\ d_{pb} - 1.848\ L^{.6}d_{pb}^{.5}$
Kito et al. (1976)	4-84%	5	$u_{G,mf} = 3.44(u_{G,mf})_{L=0}h_{G,mf}^{2.27}$

and with large ratios of D_c/d_{pb}. But unfortunately, the maximum liquid flow rate in this study was limited to 15 kg/m^2-s, lower than the range now preferred in industry. As a matter of fact, a study of G_{mf} for higher liquid flow rates is needed. It should also be mentioned that, in spite of quantitative differences among reported studies, the basic qualitative conclusion that G_{mf} decreases with increasing liquid flow rate is common to all.

2.1.2 Bed Expansion

For the design or analysis of performance of any MBC column, information on height of the mobile-bed is essential. Although Chen (1965) and Chen and Douglas (1968) obtained for the first time extensive data for a column of 0.29 m diameter, no correlation was given. These data are also limited to liquid flow rates lower than about 15 kg/m^2-s. Their main observation, that bed height increased linearly with gas flow rate, has subsequently been confirmed at conditions of negligible grid effects by Blyakher et al. (1967), Khanna (1971) and Tichy and Douglas (1972). There are, however, significant differences between the bed expansion data of these authors. One source of these differences may be the criteria used for bed height. Although it is not clear in their paper, Blyakher et al. (1967) probably considered bed height to be the maximum height attained by any packing ball because their values of bed height are consistently much higher than others who reported the average height over a period of observation. The presence of wall effects also reduce bed height for otherwise comparable conditions, as observed by Khanna (1971) and Tichy and Douglas (1972).

TABLE 2.2 Correlations for Bed Expansion

Reference	Equation	Limitations
Blyakher et al. (1967)	$H/H_{st} = 1.17 + (.65 + .053\ Q_L^{.75})(u_G - u_{G,mf})$	Q_L: liquid flow rate, m^3/m^2-hr 19-90% grid open area
Gel'perin et al. (1968)	$H = (h_{pb}H_{st} + Q_L/S_c)/(1-h_G)$	h_G: gas holdup 25-70% grid open area
Levsh et al. (April 1968)	$H = .13\ H_{st}Q_L^{n}u_G^{2}$	plastic rings are used as packing $n = .43$ for $L < 28$ $n = .35$ for $L > 28$
Aksel'rod et al. (1969)	$H = .08\ Q_L^{.3}H_{st}^{.6}u_G^{.93}$	30-65% grid open area
Khanna (1971)	$h = .414\ \Delta G_{mf}^{1.2}$	$D_c/d_{pb} = 3.7$-11
Tichy and Douglas (1972)	$H/H_{st} = .8849 + .3166G - 18.33d_{pb} + .5852L^{.6}d_{pb}^{.5}$	$D_c/d_{pb} = 3.7$-11

Unfortunately, other reported data on bed expansion are strongly affected by the use of small open area of the bottom grids (Gel'perin et al. (1968), Levsh et al. (April 1968 and October 1968), Krainev et al. (1968), Aksel'rod et al. (1969)). When grids of small open-area are used, a liquid layer may be established above the supporting grid over some range of gas and liquid flow rates. This liquid build-up has not only been observed, but some authors have even attempted to correlate the height of this liquid layer (Levsh et al. (April 1968 and October 1968), Krainev (1968)). As the operating characteristics would change significantly in the presence of such a liquid layer, which becomes in effect a bubble column or a sieve tray, results under these conditions cannot be considered representative of MBC operation, and therefore are not further discussed here. Nevertheless for the sake of completeness, all available equations for bed expansion are summarized in Table 2.2. It should again be emphasized that these results are of limited applicability due in some cases to wall effects (low values of D_c/d_{pb}) and other cases to the use of bed support grid open-area uncharacteristically low for true MBC operation. Analysis of the literature thus clearly indicates the necessity of determining a correlation for expansion of mobile-beds for conditions free from the limitations noted of previous studies.

2.1.3 Pressure Drop

Most of the papers concerning pressure drop in MBC provide graphical relationships as a function of gas and liquid flow rates, but in which the pressure drop includes implicitly the contribution from the

bottom grid (Gel'perin et al. (1966), Blyakher et al. (1967), Gel'perin et al. (1968), Levsh et al. (April 1968 and October 1968), Krainev et al. (1968), Aksel'rod et al. (1969), Mayak et al. (1969), Balabekov et al. (July 1969 and October 1969)). Because of the use of support grids of such small open-area in these studies, the total pressure drop data reported depends to a significant extent on the specific bottom grids used.

More fundamental and dependable studies were made subsequently by Barile et al. (1971), Tichy et al (1972 and 1973), Wozniak (1977). A common feature of these more recent studies is that they equate the total pressure drop in MBC to the sum of the weights per unit area of packing and liquid holdup, or

$$\Delta P_c = (h_L \rho_L + h_{pb} \rho_{pb}) gH$$

$$= (h_{L,st} \rho_L + h_{pb,st} \rho_{pb}) gH_{st} \qquad (2.1.1)$$

Although there is agreement on the form of Equation (2.1.1), there are discrepancies quantitatively between the data of these studies and in the effect reported of some variables. For example, Tichy et al. (1972) claimed that pressure drop is independent of packing size over the range 0.0127 - 0.019 m for flow rates $0.4 \leq G \leq 4.2$ kg/m^2-s and $5.5 \leq L \leq 32.$ kg/m^2-s in 0.14 m column. On the other hand Barile and Meyer (1971), using a 0.29 m column and 0.019 m and 0.038 m packing, reported pressure drop data in graphical form which showed that pressure drop increased with a decrease in the packing size. Moreover, they also report a

TABLE 2.3 Correlations for Pressure Drop

Author	Equation	Comments
Tichy and Douglas (1972)	$4.003 - 2.24G + .84G^2 - .127G^3 = \log(2\rho_G \Delta P_c (H_{st})_{std}/G^2 (H_{st})(1 + cG_L))$	$c = f(H_{st})$ $\Delta P \neq f(d_{pb})$
Wozniak (1977)	$\Delta P_c^* = \Delta P_c - m_{pb} g/S_c$ $Eu^* = 4.672(H_{st}/D_c)^{.4515}(Re_G)_{d_{pb}}^{-1.798}(Re_L)_{d_{pb}}^{.8261}$	One packing size, 19 mm, was used.
Barile and Meyer (1971)	$\Delta P_c = m_{pb} g/S_c + \rho_L g H_{st}(1160\ Fr^{.78} Re_L^{-.51}(H_{st}/d_{pb})^{-.36}$	82% grid open area
UOP(1970)-BECHTEL(1971)	$\Delta P_c = (54.4\ u_L^{.33} + 353(90.12\ u_L^{-.25} - 197\ u_G)^{-1.02})H$	Equation is not consistent, predicts negative pressure drop for some conditions.
Levsh et al. (April 1968)* and Krainev et al. (1968)	$\Delta P_c = m_{pb} g/S_c + .043L^{.55} u_G (H_{st}/.07)^m$	Plastic rings are used as packing. $m = .75$-$.8$ for $L < 28.8$ $m = 1$ for $28.8 < L < 61.5$
Blyakher et al. (1967)	$\Delta P_c = \beta_G u_G^2 \rho_G/2g + 6.13(\rho_{pb} - \rho_G)H_{st} + \beta_f u_G^{1.75} u_L^{.5} + \beta_b L H_{st}$	41% grid open area β_G = hydrolic resistance coeff. of the grid β_f and β_b are coefficients.
Uchida et al. (1977) and Kito et al. (1976)	$\Delta P_c = \rho_b h_{pb} g H_{st} + 9.38 \times 10^4 \mu_L^{2.3} f^{-.42}(d_{eq}/D_c)^{-.84} d_{pb}^{-.84} \rho_{pb}^{-.18} H_{st} u_L$	d_{eq} = equivalent diameter of the hole on plate f = grid open area

* corrected form

dependence of liquid holdup on packing size, as will be discussed in the next section. Thus Barile and Meyer's results consistently show an effect of packing size.

Wozniak (1977) indicates that the pressure drop due to liquid holdup is proportional to $(H_{st}/D_c)^{0.4515}$. Since he used one column size only, dependence of pressure drop on column diameter is not clear unless there were strong wall effects. A choice of H_{st}/d_{pb} would have been a better choice than H_{st}/D_c, but unfortunately Wozniak could not investigate the importance of this term as he used only one packing size, 0.019 m.

Finally, Uchida et al. (1977) attempted to evaluate pressure drop in MBC using the relation given in Equation (2.1.1) and the liquid holdup results obtained by Kito et al. (1976). But as mentioned in Section 2.1.1, the results of Kito et al were undoubtedly affected by their use of a low value (5) for the ratio, D_c/d_{pb}. Although Uchida et al. stated that they had modified Kito's liquid holdup correlation to be also applicable to a larger column, they did not specify clearly how this modification was made.

Table 2.3 gives all the equations found in the literature discussed above.

It should also be mentioned that if the liquid holdup per static volume of the bed is independent of gas flow rate, as reported by Chen (1965), Chen and Douglas (1968), Barile and Meyer (1971), and Tichy and Douglas (1973) for normal operating conditions, then Equation (2.1.1) implies that pressure drop is also independent of gas flow rate over the same range (Figure 2.1). When the gas flow rate is increased to extremely

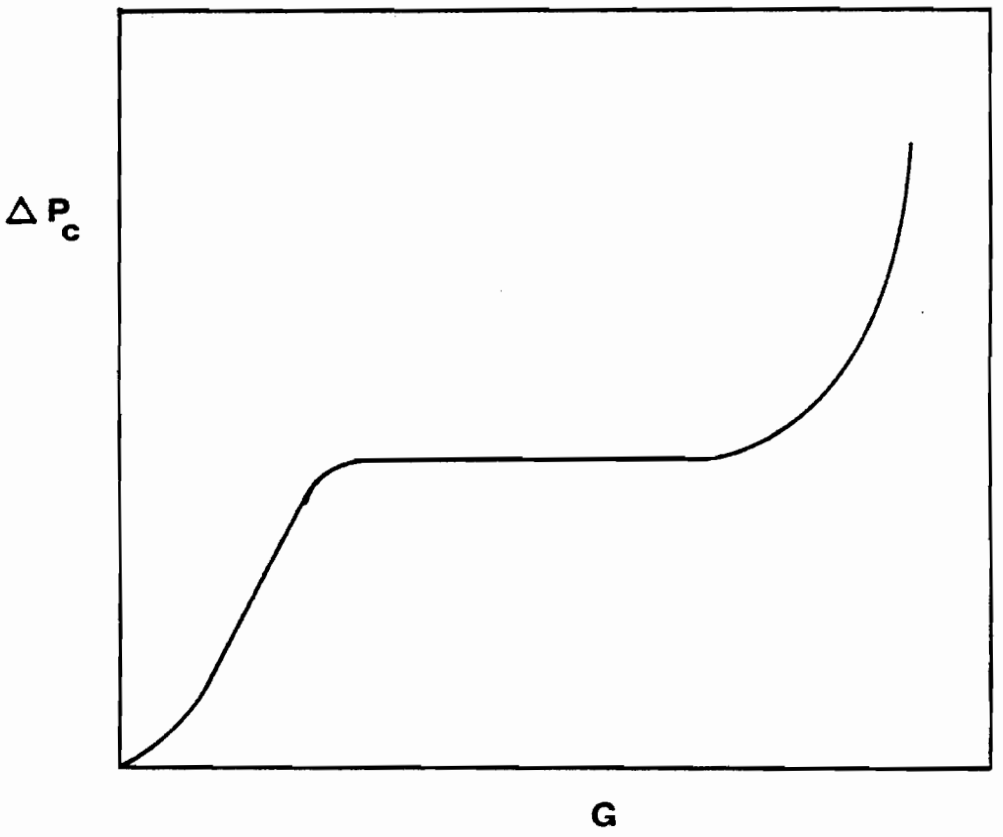

FIGURE 2.1. Effect of gas flow rate on pressure drop in M.B.C.

high values, pressure drop can be made to increase further due to the increase of liquid holdup in the bed. Data reported by Douglas et al. (1963) fall into this region of very high gas velocity. If gas flow rate is increased further yet, the mobile-bed can of course eventually be forced to flood.

It can be concluded from observations of appreciable differences in the available data and correlations in the literature that a definitive study of the pressure drop in MBC is necessary.

2.1.4 Holdup and Mixing of Liquid

A key characteristic of MBC is the capacity for exceptionally high gas and liquid flow rates, and associated with these large countercurrent flows are correspondingly high values of liquid holdup. In spite of the important role of liquid holdup in the performance of an MBC column, there are unfortunately very few studies of this aspect. Chen (1965), and Chen and Douglas (1968) studied liquid holdup in MBC for the first time, using a transient-response technique. Employing a step input technique and using 0.1 N KCl solution as the tracer, they obtained liquid holdup data for a 0.29 m column and for 12, 25 and 38 mm packing sizes. The maximum flow rate was limited to about 15 kg/m^2-s. The central feature of the results of this study was that, over the flow ranges investigated, the amount of liquid holdup was independent of gas velocity but dependent on liquid flow rate and packing size. The following is their suggested correlation:

$$h_{L,st} = 0.02 + 2.369 \times 10^{-3} {}_{L}0.6 d_{pb}^{-0.5} \qquad (2.1.2)$$

It is important to note that for this equation liquid holdup is defined as volume of liquid per volume of static bed, not per volume of actual expanded bed.

Khanna (1971), using the same experimental technique measured liquid holdup in a smaller column ($D_c = 0.14$ m), reported an extensive amount of data but gave no correlation. Khanna's experiments indicated that the liquid holdup in MBC decreases with gas velocity whereas those of Chen on a larger diameter column showed no effect of gas flow rate. Inspection of Khanna's data reveals that the effect of packing size is not explicit. At low liquid flow rates Khanna's data show a decrease in liquid holdup with an increase in packing size, the same result as that of Chen. However, at high liquid flow rates the reverse trend was observed by Khanna. Furthermore the values of liquid holdup reported by Khanna were about twice those obtained by Chen. Although the same technique was employed in both studies, such a large difference cannot be explained. There were probably strong wall effects in Khanna's study as he used a smaller column but it may be wrong to attribute the whole difference to the different size of the columns used in these two studies.

The measurements of liquid holdup by Wozniak (1977) agree with neither of the earlier studies. Wozniak used a 0.2 m diameter column, i.e. intermediate in size between those of Chen and Khanna, and 19 mm packing, corresponding to $D_c/d_{pb} = 10.5$. Wozniak obtained liquid holdup data by a direct volumetric method, measuring the volume of liquid retained in the column when the inlet and outlet valves of the liquid line were suddenly closed, and reported the results in the form of a graphical relationship of liquid holdup per static volume of bed

with liquid flow rate. His results were much higher than those of either Chen or Khanna. Furthermore, Wozniak found that liquid holdup increases with gas velocity whereas Khanna showed the reverse and Chen showed no effect of gas velocity. These two distinct differences between Wozniak's results and earlier studies are probably due to his use of a support grid of low (60%) open area.

Barile and Meyer (1971) used yet another approach to determine liquid holdup in MBC. They measured pressure drop across the bed and used Equation (2.1.1) to obtain liquid holdup indirectly. Their correlation is:

$$h_{L,st} = 1160\ Fr_L^{0.78}\ Re_L^{-0.51}(H_{st}/d_{pb})^{-0.36} \qquad (2.1.3)$$

The liquid holdup values predicted by Equation (2.1.3) are smaller than Chen's results but show similar effect of packing size. This approach of determining liquid holdup from pressure drop is probably more accurate than other methods provided that the pressure drop measurements are correct. Since the static pressure fluctuates significantly in MBC during operation, the average of extensive pressure measurements must be taken. This becomes difficult if a simple u-tube manometer is used. Since Barile and Meyer used a manometer for the measurements of pressure drop and observed oscillations in the manometer, the experimental accuracy of their data is uncertain. Other than this, their method should be dependable.

Further analysis and comparison of these studies will be deferred to Chapter 6.

There are only two studies on liquid mixing in MBC. From measurement of residence time distribution by a transient response technique, Chen (1965) and Khanna (1971) determined the axial dispersion characteristics of the liquid phase. The liquid flow pattern was found to be intermediate between piston and completely mixed flow, in general somewhat closer to the latter. Chen and Douglas (1969) correlated the data on liquid mixing by Equation (2.1.4):

$$\frac{Pe}{Pe_o} = \left(\frac{d_{pb}}{D_c}\right)^{-0.304} F(\Delta) \qquad (2.1.4)$$

where the liquid phase Peclet number is Pe for MBC, Pe_o for a fixed-bed contactor, and Δ is a dimensionless excess gas mass velocity, defined as $(G - G_{mf})/G_{mf}$. The data for fixed-bed operation was correlated as:

$$Pe_o = 0.07\ Re_L^{0.583} Ga^{-0.081} \qquad (2.1.5)$$

Chen and Douglas (1969) give the generalized function, $F(\Delta)$, in graphical form.

In the subsequent study using the smaller diameter column noted previously, Khanna (1971) correlated his data for the column when operated as a fixed-bed contactor in the form:

$$Pe_o = 1.06\ Re_L^{0.41} Ga^{-0.095} \qquad (2.1.6)$$

Therefore if the total volume of packing is known and the height of the bed and the liquid holdup can be determined, then Equation (2.1.7) permits calculation of gas holdup. This, of course, requires a dependable correlation for the liquid holdup. Other than this indirect way of evaluation of gas holdup, no research, designed specifically for direct measurement of gas holdup, has yet been published for MBC.

Kito et al. (1976) describe an indirect method of evaluation of gas holdup using Equation (2.1.7), but in that study there was no flow of liquid through the bed. In this way they evaluated gas holdup from expansion of the bed of their column which was fitted with a support grid of only 1.27 - 31.5% open area and charged with a static quantity of water. Since such conditions differ in two crucial ways from MBC industrial operation, i.e. no liquid through flow and small open area grids, the results by Kito et al. may be more akin to bubble column studies and are not relevant to true MBC studies.

As the axial distribution of particle concentration in the gas phase through any scrubber may be a significant factor, axial mixing of the gas phase would be of interest but no study has as yet been published.

2.2 PARTICLE COLLECTION MECHANISMS

In order to make a fundamental analysis of the performance of any particle collection device, a thorough knowledge of the mechanisms by which particles are removed from gas streams is necessary. All the particle collection mechanisms are therefore reviewed in this section in accordance with the classification given in Table 2.4, with particular emphasis on collection by spherical objects and from bubbles.

TABLE 2.4 Classification of the Particle Collection Mechanisms

Particle Collection Mechanisms:

A. Aerodynamic Capture Mechanisms

i. Inertial Impaction
ii. Interception
iii. Diffusion
iv. Gravitational Collection
v. Electrostatic Attraction

B. Phoretic Mechanisms

i. Diffusiophoresis
ii. Thermophoresis
iii. Electrophoresis
iv. Magnetophoresis

The listing of particle collection mechanisms according to two classifications derives from the fact that aerodynamic mechanisms may occur in any particle collection device, but phoretic mechanisms are involved only when the relevant flux forces are present.

2.2.1 Aerodynamic Capture Mechanisms

2.2.1.1 Inertial impaction

Inertial impaction, the most frequently encountered mechanism of particle deposition, applies to many processes in nature as well as in man-made devices. Development of the theory of inertial impaction began in Germany during World War I, where an acute shortage of natural materials for air filters led to development of both artificial materials and the underlying theoretical principles involved in their use. Sell (1931) presented the first reasonably complete statement of these theories. Albrecht (1931) is also among the pioneers of this work. The theory was later refined by Taylor (1940), Langmuir (1946 and 1948), Lewin (1953), Fuchs (1964), Ranz (1951 and 1956), Ranz et al. (1952), among many other investigators.

According to the theory of inertial impaction, an aerosol particle in a suspending fluid stream tends to move in a straight line because of its inertia. However, when a moving aerosol stream approaches an obstacle, the fluid stream lines spread around it. Inertial forces carry particles across the stream, thus reducing the particle-obstacle distance below that between the obstacle and the streamline on which the particle was originally located. Particles originally on streamlines closer than some critical value impact on the obstacle, and depending

on the nature of the particle and the obstacle, may be retained by the obstacle after impaction. Figure 2.2 illustrates the inertial impaction process. The shaded bounding surface represents the envelope of trajectories of the particles which just graze the surface of the obstacle. It divides the particles which impact from those which do not impact. The efficiency of impaction, E, is the ratio of the number of particles flowing through the cross section S_o to the number of particles flowing through the target projected area, S_p. If the particles are uniformly distributed throughout the approaching gas stream, then the collection efficiency equals the ratio of the area swept clean, S_o, to the cross sectional area of the obstacle, S_p;

$$E_I = (y_o/r_c)^2 \qquad \text{for spheres} \qquad (2.2.1\text{-a})$$

and

$$E_I = y_o/r_c \qquad \text{for cylinders} \qquad (2.2.1\text{-b})$$

This definition provides an upper limit on efficiency corresponding to the case for which all particles which impact are also retained by the obstacle. Obviously, if some particles bounce rather than stick on impaction, this definition of efficiency would be too high. Factors which determine the ratio y_o/r_c are the velocity distribution of the gas flowing past the collector, the mass of the particle, its aerodynamic drag coefficient, the size and the shape of the collector, and the rate of flow of the gas stream.

Velocity distribution of the gas flowing past the collector depends on the Reynolds number of the gas with respect to the collector.

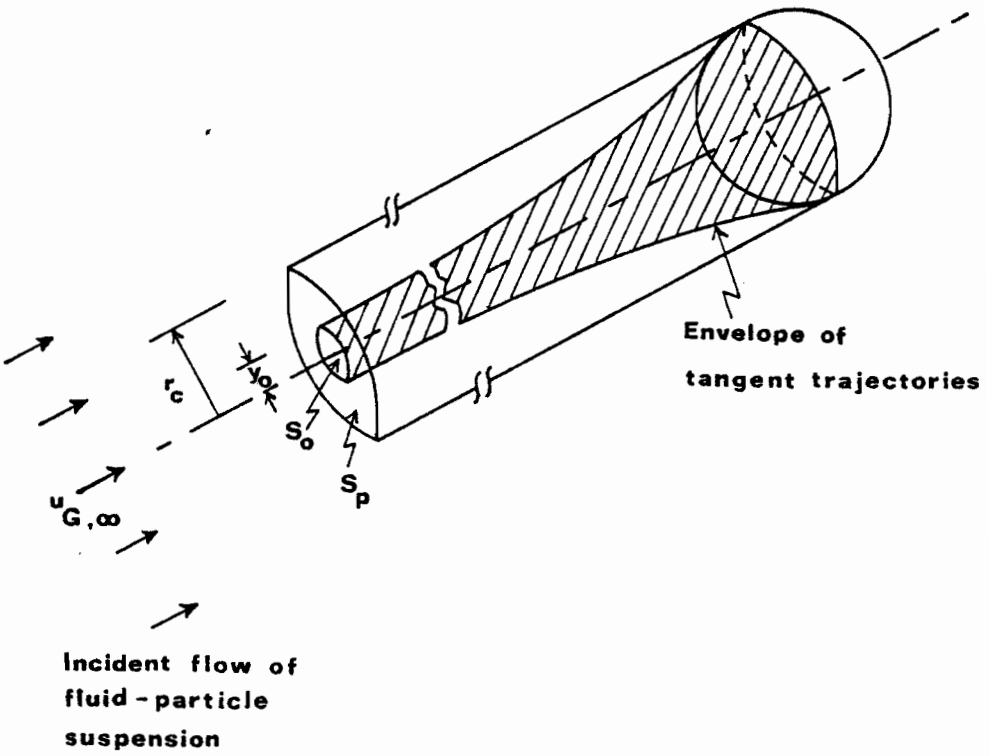

FIGURE 2.2. Inertial impaction efficiency of a sphere

$$Re_c = u_G \rho_G d_c / \mu_G \tag{2.2.2}$$

At high values of Re_c (potential flow), the parting of the gas streamlines occurs close to the collector. Except near the collector surface, the flow pattern corresponds to that of an ideal gas. When the Re_c is low, flow is governed by viscosity (viscous flow) and the effect of the disturbance created by the collector is felt at relatively large distances upstream. The effect of sudden spreading of the stream lines at high Reynolds numbers is to enhance the influence of particle inertia and therefore cause a higher collection efficiency.

To determine the trajectory of the particle one starts with the equation of motion of the particle. Assuming Stokes law holds for the particles studied (Stokesian particles);

$$m_p \frac{d\vec{u}_p}{dt} = - \frac{3\pi\mu_G d_p}{c'}(\vec{u}_p - \vec{u}_G) + m_p \vec{g} + \Sigma \vec{F}_{ext} \tag{2.2.3}$$

In the absence of external forces and also neglecting the gravity,

$$m_p \frac{d\vec{u}_p}{dt} = - \frac{3\pi\mu d_p}{c'}(\vec{u}_p - \vec{u}_G) \tag{2.2.4}$$

This can be put into dimensionless form as follows,

$$\frac{d\vec{U}_p}{d\theta} = - \frac{1}{St}(\vec{U}_p - \vec{U}_G) \tag{2.2.5}$$

when, $$St = \frac{c' d_p^2 \rho_p u_{G,\infty}}{9 \mu_G d_c} \quad (*) \qquad (2.2.6\text{-a})$$

$$\theta = \frac{2tu_{G,\infty}}{d_c} \qquad (2.2.6\text{-b})$$

$$U = \frac{u}{u_{G,\infty}} \qquad (2.2.6\text{-c})$$

The dimensionless Stokes number, St, (Equation (2.2.6-a)) which characterizes the particle motion has also the physical meaning of the ratio of the particle "stopping distance" to the radius of the collector. A particle's stopping distance is that distance it would travel before coming to rest if injected into a still gas at velocity $u_{G,\infty}$, when all forces on the particle except the drag force are zero.

Solutions to the equation of motion for the particle depend on the choice of velocity field. These equations have been solved by numerical methods for collectors of several simple shapes, such as a sphere, cylinder or ellipsoid, under specific boundary conditions (Glauert et al., Landahl et al. (1949), Torobin et al. (1959), Dorsch et al. (1955), Blodgett et al. (1946), Ranz (1956), Langmuir (1948), Fond et al. (1957), Stairmand (1950), Das (1950), Beard et al. (1974), Herne (1960), Flint et al. (1971)).

These numerical solutions yield a critical value for Stokes number below which no inertial deposition takes place. For spherical collectors, $St_{cr} = 0.083$, and for cylindrical collectors, $St_{cr} = 0.125$. These theoretical limits are all subject to the assumption that inertial

---

* Stokes number is also referred to as inertial impaction parameter, K.

impaction is the only collection mechanism. In reality, however, in case of turbulence for instance, particles are collected at the back as well as the front of the collector and collection efficiency for $St \leq St_{cr}$ is not zero (Goldshmid et al. (1963)).

It is also worth stressing the important assumption, not always made explicitly that the particles stick to the obstacle upon impaction. Only recently has this point attracted the attention of some investigators. In spite of the great simplification brought by this assumption, experimental evidence shows that this may not always be true. Goldshmid and Calvert (1963) showed experimentally for small particle collection by liquid drops that non-wetting particle-liquid pairs give lower collection efficiencies than the mutually wetting pairs for the same Stokes number. Moreover, collection efficiency seems to drop with increase in contact angle or with decrease of mutual wetting. More recently Montagna (1974) and Allen (1975) have confirmed this finding experimentally and proposed theoretical models.

Using the change in Helmholtz force energy of the surface during particle capture, Montagna (1974) derived the work of coalescence, W_c. Since the colliding particle will be captured only if the normal incident kinetic energy of the particle equals or exceeds the minimum work required for coalescence, the following relation may be written:

$$\tfrac{1}{2} m_p u_p^2 \geq W_c = \gamma_{SL} \int_0^{h_e} 2\pi(2r_c h - h^2)^{\frac{1}{2}} dh \qquad (2.2.7)$$

where, h = depth of particle penetration through the interface, and

h_e = penetration depth required for capture.

If the incident kinetic energy of the particle is sufficiently high, the particle could completely penetrate into the drop. For this case, Montagna (1974) derived

$$\frac{2(u^2\cos^2 x - x)^{1/2}}{u^2 - x^2} \geq \left(\frac{\mu_G}{\mu_L}\right) St \qquad (2.2.8)$$

where, $x = u_w/u_{G,\infty} = f(\theta_c)$, and

u_w = minimum normal velocity of particle required for capture.

Montagna used the last two equations as boundary conditions in the inertial impaction model, rather than the earlier assumption that every colliding particle is captured.

In a similar study, having shown experimentally that hydrophobic particles are collected less efficiently than hydrophilic particles, Allen (1975) proposed the following equality to calculate the minimum velocity for penetration of the particle into the liquid drop.

$$\frac{u_G^2}{u^2_{G,\infty}} = -\frac{12\cos\theta_c}{We} \qquad (2.2.9)$$

In the above discussion, generally, gas phase has been assumed to be the continuous phase. However, there are some industrial applications of gas-liquid contacting, such as bubble or sieve plate columns, for which gas phase is the dispersed phase. In such cases, particles may be collected from bubbles by the continuous liquid phase. Due to the internal circulation of gas inside the bubble a centrifugal force is applied on the particles. This force may carry the particles to the

surface and cause them to be captured by the surrounding liquid. This mechanism is called inertial collection by bubbles. Fuchs (1964) gives the following equation for the rate of inertial collection by spherical bubbles:

$$\phi_{b,I} = \frac{c'\pi u_b^2 n_p d_b d_p^2 (\rho_p - p_G)}{6\mu_G} \qquad (2.2.10)$$

where u_b is the bubble velocity and d_b the bubble diameter. The total number of particles collected at the surface during the rise of a bubble by one unit length is

$$R = \phi/u_b \qquad (2.2.11)$$

The efficiency per one unit length rise can then be defined as

$$E = 6R/\pi d_b^3 n_p \qquad (2.2.12)$$

Combining Equations (2.2.10) to (2.2.12),

$$E_{b,I} = c'u_b d_p^2 (\rho_p - \rho_G)/d_b^2 \mu_G \qquad (2.2.13)$$

This equation is useful for defining a parameter to which inertial collection by bubbles is proportional. This parameter will be defined here as

$$N_{b,I} = c'u_b d_p^2 (\rho_p - \rho_G)/d_b^2 \mu_G \qquad (2.2.14)$$

Usefulness of the definition of such a parameter will become clearer in Chapter 3.

In summary, the inertial impaction mechanism is the most frequently encountered and, in most cases, the dominant particle capture mechanism. For particle collection from continuous gas streams, Stokes number is the characteristic parameter to determine the efficiency of collection. Equation (2.2.14) defines a similar parameter for particle collection from bubbles by surrounding liquid.

Although there have been intensive studies in this field during the past thirty years, some aspects of this problem of inertial collection have still not been understood completely. For example, only very recently the first study about the effect of particles already collected on solid collectors on the capture of new particles appeared in the literature (Wang (1977)). This is a very important problem for filters. Moreover, it is very difficult to predict the effect of boundary layer flow on the trajectories of aerosol particles. The effect on particle collection of the complex flow field with eddies in the wake behind collectors remains another incompletely resolved problem.

2.2.1.2 Interception

In the above section for particle collection by inertial impaction it was assumed that the particle has a finite size only for determining the resistance to its motion relative to the fluid, and a finite mass only for determining the effect of this resistance on its motion. As far as the motion of the particle was concerned, the particle was considered to be a massive point. No particle was assumed to touch

the surface of the collector unless its trajectory was tangent to or intersects the surface. However, since the trajectory is the path of the center of the particle, a large particle will come in contact with the collector when its trajectory passes the collector surface at a distance less than or equal to the radius of the particle, r_p. This mechanism which results from the finite size of the particles is known as interception mechanism, and is described by the following parameter:

$$N_R \triangleq d_p/d_c \tag{2.2.15}$$

The efficiency of particle removal due to this mechanism can be obtained very easily for two limiting cases.

Interception Efficiency for St $\to \infty$

For very large Stokes numbers, the inertia of the particles is so big that their trajectories can be assumed rectilinear in the vicinity of the collector. Therefore,

$$E_R = \frac{\pi(d_p + d_c)^2/4 - \pi d_c^2/4}{\pi d_c^2/4} = \frac{(d_p + d_c)^2 - d_c^2}{d_c^2} \tag{2.2.16}$$

For small particle sizes, this can be approximated as

$$E_R = \frac{d_p^2 + 2d_p d_c}{d_c^2} \approx 2d_p/d_c \approx 2N_R \tag{2.2.17}$$

Interception Efficiency for St → 0

For very small Stokes numbers, the inertia of the particles is so small that it may now be considered a massless particle with finite size. Neglecting all other forces as well as the inertia, the particle's equation of motion (Equation (2.2.5)) implies that particle's center will exactly follow the fluid stream lines, i.e. $u_p = u_g$. For the motion of the gas there are again two limiting cases corresponding to creeping flow ($Re_c \to 0$) and potential flow ($Re_c \to \infty$).

For Creeping Flow

Using the standard result for the stream function, ψ, in Stokes flow around a sphere (Doganoglu (1975)),

$$E_R = \frac{\psi(r = (d_p + d_c)/2 \ , \ \theta = \pi/2)}{\pi d_c^{\,2}/4}$$

$$= (1 + d_p/d_c)^2 - 3/2(1 + d_p/d_c) + \frac{1}{2(1 + d_p/d_c)}$$

$$= (1 + N_R)^2 - 3/2(1 + N_R) + \frac{1}{2(1 + N_R)} \qquad (2.2.18)$$

For small particle sizes this can be approximated as

$$E_R = 1 + 2N_R + N_R^{\,2} - 3/2(1 + N_R) + 1/2(1 - N_R + N_R^{\,2} \ldots.)$$

$$\approx 3/2 \ N_R^{\,2} \qquad (2.2.19)$$

For Potential Flow

Following a similar procedure as above,

$$E_R = (1 + d_p/d_c)^2 - \frac{1}{(1 + d_p/d_c)}$$

$$= (1 + N_R)^2 - \frac{1}{(1 + N_R)}$$

$$= 1 + 2N_R + N_R^2 - (1 - N_R + N_R^2 \ldots.)$$

$$= 3N_R \qquad (2.2.20)$$

It should be noted that the above equations are for spherical collectors. Similarly, expressions for other shapes can be derived. For a cylindrical collector, for example, Equation (2.2.20) becomes:

$$E_R \approx 2N_R - N_R^2 \qquad (2.2.21)$$

As far as particle collection from bubbles is concerned, a similar treatment to the above approach may be attempted. But, since the particles are usually much smaller than the bubbles, interception effects can usually be neglected (Fuchs (1964)).

2.2.1.3 Diffusion

Capture due to diffusion may occur when the particles are sufficiently sub-micron in size that their motion is influenced by the irregular collisions with gas molecules. For such cases Brownian motion

will be superimposed upon the trajectory of a particle. This relatively slow diffusional velocity may be sufficient to cause the particle to come into contact with the collector if the particle passes sufficiently closely and slowly by the collecting body.

Assuming that the particles possess no ordered motion, Fuchs (1964) expressed the rate of deposition of particles on a sphere from a stationary gas as

$$\phi_D = 2\pi D_p d_c n_{p_i} \left(1 + \frac{d_c/2}{\sqrt{\pi D_p t}}\right) \qquad (2.2.22)$$

where, n_{p_i} is the initial particle concentration, and
D_p is the diffusivity of the particle.

If $D_p t/d_c^2 \ll 1$, particles are deposited on the surface of the sphere from a thin adjacent layer of aerosols at the same rate as onto a flat surface,

$$\phi_D = n_{p_i} \sqrt{D_p/\pi t} \qquad (2.2.23)$$

If $D_p t/d_c^2 \gg 1$, a practically constant concentration distribution is established around a sphere, as given by the following equation (Fuchs (1964), Hidy and Brock (1970)).

$$n_{p_r} = n_p \left(1 - \frac{(d_c/2)}{\delta}\right) \qquad (2.2.24)$$

where δ is the distance from the collector center and n_p is the particle number concentration in the main body of the gas. Then the concentration gradient at the collector surface is given by

$$\left.\frac{\partial n_{p_r}}{\partial \delta}\right|_{\delta = d_c/2} = 2n_p/d_c \qquad (2.2.25)$$

and the rate of deposition on a spherical collector from a gas at rest becomes constant and equal to

$$\phi_D = 2\pi D_p d_c n_p \qquad (2.2.26)$$

When there is a gas flow, continuity equation of the particle can be written as follows:

$$\frac{\partial n_p}{\partial t} + \vec{\nabla} \cdot n_p \vec{u} = D_p \nabla^2 n_p \qquad (2.2.27)$$

This may be solved to find the diffusional efficiency. For incompressible fluids this equation reduces to

$$\frac{\partial n_p}{\partial t} + \vec{u} \cdot \vec{\nabla} n_p = D_p \nabla^2 n_p \qquad (2.2.28)$$

Equation (2.2.28) can be written in terms of dimensionless Peclet number as

$$\frac{\partial n_p}{\partial t} + \vec{u}^* \cdot \vec{\nabla}^* n_p = \frac{1}{Pe} \nabla^{*2} n_p \qquad (2.2.29)$$

for which $\theta = tu_{G,\infty}/d_c$

$$\vec{\nabla}^* = d_c\vec{\nabla}$$

$$\nabla^{*2} = d_c^2\nabla^2$$

$$\underrightarrow{u}^* = \underrightarrow{u}/u_{G,\infty}$$

Therefore, the efficiency of particle collection due to diffusion should be a function of Peclet number. In fact, Langmuir (1942), Johnstone and Roberts (1949), Ranz (1951) have shown that the efficiency due to diffusion is an inverse function of Peclet number.

$$Pe = u_G d_c/D_p$$

$$= Re_c Sc \qquad (2.2.30)$$

Studies reported by Ranz (1951), Friedlander (1957), and Langmuir (1942) indicate that the efficiency due to diffusion is not significant if the value of Pe number is much above 10. Since the diffusion coefficient of the particle, D_p, is an inverse function of the particle size, the Peclet number can also be written as

$$Pe \propto u_G d_c d_p \qquad (2.2.31)$$

This relation indicates that, as the particle size increases, Peclet number also increases and the effect of diffusion decreases.

Approximate values of the diffusion coefficient of particles varying in size from hydrogen molecules up to 100 μm in diameter are given in Table 2.5 (Davies (1966)). It can be noticed that particle diffusivities are several orders of magnitude smaller than the diffusivities of gases. The particle diffusivities in this table are calculated from Einstein's relation and the slip factor c' (Davies (1945)).

$$D_p = kTc/3\pi\mu_G d_p \qquad (2.2.32)$$

$$c' = 1 + \frac{10^{-4}}{Pr_p}\{6.32 + 2.01 \exp(-2190\ Pr_p)\} \qquad (2.2.33)$$

k is Boltzmann's constant, 1.38054×10^{-23} J/°K, T the absolute temperature (°K), r_p the radius of particle in cm and P the pressure in cm of mercury.

It is more appropriate to extend the physical significance of Equation (2.2.29) and to consider also the effect of velocity distribution of gas around the collector. In this connection it is helpful to consider Pe number as the product of Re_c and Sc (Equation (2.2.30)). In view of the definition

$$Sc = \mu_G/\rho_G D_p \qquad (2.2.34)$$

Schmidt number indicates the ratio of convective to diffusive transfer rates. When $Sc \approx 1$, the thickness of the diffusion layer and the hydrodynamic boundary layer around a body are of the same order of magnitude.

TABLE 2.5 Diffusion Coefficients of Small Particles in Air at 760 mm Hg and 20°C

Particle Radius (μm)	Diffusion Coefficient, D_p (m^2/s)
10^{-4} (hydrogen molecule)	$7x10^{-5}$
$5x10^{-4}$	5.2x10
10^{-3}	$1.3x10^{-6}$
$5x10^{-3}$	$5.3x10^{-8}$
10^{-2}	$1.4x10^{-8}$
$2x10^{-2}$	$3.6x10^{-9}$
$5x10^{-2}$	$6.8x10^{-10}$
10^{-1}	$2.2x10^{-10}$
$2x10^{-1}$	$8.4x10^{-11}$
$5x10^{-1}$	$2.76x10^{-11}$
1	$1.3x10^{-11}$
2	$6.16x10^{-12}$
5	$2.4x10^{-12}$
10	$1.2x10^{-12}$
20	$5.9x10^{-13}$
50	$2.4x10^{-13}$
100	$1.2x10^{-13}$

When Sc >> 1, diffusive and convective transfer are comparable only at a very short distance from the surface of the body, because the diffusion layer is very thin in comparison with the friction layer. For particles, Sc is very large, being about 10^5 for $r_p = 10^{-5}$cm and about 10^3 for $r_p = 10^{-6}$cm. Consequently, this analysis yields the importance of the effect of Re_c on collection efficiency. For high Schmidt number ($Sc \approx 10^6$) and low Reynolds numbers ($Re_c < 3$), Levich (1952) offered the following relation for spherical collectors.

$$\phi_D = \pi D_p d_c n_p Re_c^{1/3} Sc^{1/3} \qquad (2.2.35)$$

For larger Reynolds numbers ($600 < Re_c < 2{,}600$) and the same value of Schmidt number, Aksel'rod (1953) showed that

$$\phi_D = 0.8\ \pi D_p d_c n_p Re_c^{1/2} Sc^{1/3} \qquad (2.2.36)$$

Garner and Suckling (1958) and Garner and Keey (1958) presented the following correlation for Reynolds numbers between 100 - 700 and Schmidt numbers about 10^3:

$$\phi_D = 0.95\ \pi D_p d_c n_p Re_c^{1/2} Sc^{1/3} \qquad (2.2.37)$$

As the flow rate of the gas passing by a collector increases, theoretical and experimental study of particle deposition from turbulent streams becomes naturally much more difficult. In spite of the recent

advances in the study of turbulence, little is known about the motion of particles suspended in a turbulent flow. In particular, the extent to which particles follow the turbulent fluctuations has not been fully understood yet. Besides the effect of turbulent flow on suspended particles the reverse problem of the effect that the particles have on the structure of turbulent flow carrying them is also important and experimentally confirmed (Fuchs (1964)). Theoretically the situation is very complex, and experimentally there is little data on the deposition of particles from turbulent flow. The size and mass of the particles are important for turbulent deposition. If the particles are small enough to follow the turbulent fluctuations of fluid motion, the rate of deposition from a turbulent boundary layer, due to eddy diffusion followed by molecular diffusion, is negligibly small because eddy diffusion cannot transport an appreciable number of particles all the way to the surface. Interposition of even a thin layer of very low turbulence constitutes an effective obstacle to deposition unless the inertia of the particles is sufficient for them to travel some distance independently. In this case, the particles may reach the surface by eddy impingement. This latter phenomenon is called "inertial deposition from turbulent flow". Pioneering work in this field was done by Friedlander and Johnstone (1957). The cited authors were the first to present a model based on the idea that the particles and fluid may behave alike in the core of the turbulent fluid but act differently near the wall, and that particles diffuse from the turbulent core region towards the collector surface due to eddy diffusion. While gas molecules diffuse through the relatively stagnant layer to the surface, particles

diffuse from the turbulent core to within one stopping distance of the surface, then penetrate the quiescent region due to their large inertia. Researchers studying this phenomenon have examined only very simple systems such as deposition on flat plates and on the walls of pipes. The reason for these choices is of course that the velocity distribution for such systems are well known for turbulent conditions. Further discussion of this topic is beyond the scope of this work but can be found elsewhere (Davies (1966), Forney and Spielman (1973), Schmel (1970 and 1971), Beal (1968), Montgomery and Corn (1970), Hutchison et al. (1971), Claver and Yates (1973), and Azarniouch (1973)).

Finally, as was done for inertial impaction and interception, a characteristic parameter for diffusion, N_D, can be defined, so that

$$E_D = \alpha_D N_D \tag{2.2.38}$$

The particle collection efficiency of spherical objects due to diffusion can be defined as

$$E_D = \frac{\phi_D}{\frac{\pi d_c^2}{4} u_{G,\infty} n_p} \tag{2.2.39}$$

Depending on the values of Re_c and Sc, ϕ can be evaluated from one of the Equations (2.2.35), (2.2.36) and (2.2.37).

If Equation (2.2.35) is used

$$N_D = d_c^{-2/3} u_{G,\infty}^{-2/3} D_p^{2/3} \tag{2.2.40}$$

If Equation (2.2.36) or (2.2.37) is used,

$$N_D = d_c^{-1/2} u_{G,\infty}^{-1/2} D_p^{2/3} \gamma_G^{-1/6} \tag{2.2.41}$$

A similar parameter for particle collection from bubbles due to diffusion can also be defined. The rate of diffusional collection in this case is given by Fuchs (1964) as

$$\phi_{b,D} = \frac{2.4}{\sqrt{8}} \pi n_p (D_p u_b d_b^3)^{1/2} \tag{2.2.42}$$

Following the same approach given in Section 2.2.1.1 and using Equations (2.2.11) and (2.2.12)

$$E_{b,D} = 5.091 \, D_p^{1/2} u_b^{-1/2} d_b^{-3/2} \tag{2.2.43}$$

The diffusional parameter for bubbles, therefore, could be defined as

$$N_{b,D} = D_p^{1/2} u_b^{-1/2} d_b^{-3/2} \tag{2.2.44}$$

Depending on the type of process the contribution of diffusion to particle collection can then be evaluated using the parameters defined by Equations (2.2.40), (2.2.41) and (2.2.44).

2.2.1.4 Gravitational collection

Gravitational forces are of course present in all particle collection devices, and become particularly important for gravity separators where the gas stream is slowed down sufficiently to allow particles to settle.

The parameter for gravitational deposition, N_G, may be defined as (Ranz and Wong (1952)):

$$N_G = u_T/u_G \tag{2.2.45}$$

and the gravitational collection efficiency as

$$E_G = \alpha_G N_G \tag{2.2.46}$$

As the above two equations imply, this mechanism of particle collection is not very significant under normal conditions and becomes important only when the terminal velocity of the particle becomes quite large or the gas velocity quite low.

The terminal settling velocity of a spherical particle is

$$u_T = c'(\rho_p - \rho_G)g d_p^{\,2}/18\,\mu_G \tag{2.2.47}$$

The Cunningham correction factor, c', is included in Equation (2.2.47) because, when particle size approaches the mean free path of the gas molecules, particles "slip" between air molecules and the resistance of the air becomes discontinuous. The Cunningham correction factor accounts for the increased rate of particle fall.

Gravity may improve particle collection from bubbles as well. The number of particles deposited inside the bubble by sedimentation is:

$$\phi_{b,G} = \pi d_b^2 n_p u_T/4 \qquad (2.2.48)$$

Using Equations (2.2.11), (2.2.12) and (2.2.47),

$$E_{b,G} = c' d_p^2 (\rho_p - \rho_G) g/12\ u_b d_b \mu_G \qquad (2.2.49)$$

As was done for inertial and diffusional collection, the parameter for gravitational collection from bubbles could be defined as

$$N_{b,G} = c' d_p^2 (\rho_p - \rho_G) g/u_b d_b \mu_G \qquad (2.2.50)$$

2.2.1.5 Electrostatic attraction

When an aerosol particle or a collector or both are electrically charged, the trajectories of particles past the collector are affected by electrostatic forces. Ranz and Wong (1952) presented dimensionless groups of force ratios which characterize some of the electrostatic forces influencing deposition of particles. Kraemer and Johnstone (1955) presented a general theoretical solution and experimental verification for deposition of particles on spherical surfaces. They solved the equations of motion for the particle neglecting all forces but electrostatic attraction.

There are five cases of electrostatic collection. For each case Kraemer and Johnstone (1955) defined a collection parameter which is the ratio of the electrostatic force to the Stokes-Cunningham drag force. These are summarized below.

For the coulombic force between a charged collector and a charged particle:

$$N_{E_1} = c' q_p q_c / 3\pi \mu_G d_p u_r \varepsilon_o \qquad (2.2.51)$$

For the induction force between an uncharged particle and a charged spherical collector:

$$N_{E_2} = 2(\varepsilon - 1) c' d_p^2 q_c^2 / 3(\varepsilon + 2) \mu_G u_r d_c \varepsilon_o \qquad (2.2.52)$$

For the induction force between charged particles and uncharged spherical collector:

$$N_{E_3} = c' q_p^2 / 3\pi^2 \mu_G d_p u_r \varepsilon_o d_c^2 \qquad (2.2.53)$$

For the repulsion force exerted by unipolar charged particles on the aerosol particle deposited:

$$N_{E_4} = c' q_p^2 d_c n_p / 18\ \pi \mu_G d_p u_r \varepsilon_o \qquad (2.2.54)$$

For the attraction between a charged particle and a grounded collector which has a charge induced by the surrounding unipolar particles:

$$N_{E_5} = c' q_p^2 n_p b^2 / 3\pi\mu_G d_p u_r d_c \varepsilon_o \qquad (2.2.55)$$

In the above equations:

q_c = the charge on the collector per unit area, coulomb/cm^2

q_p = the charge on the particle, coulomb

ε_o = absolute dielectric constant of free space, 8.85×10^{-21} coulomb/dyne-cm^2

ε = dielectric constant of particles

u_r = relative velocity between air stream and collector, cm/s

b = radius of spherical cloud which influences the collector, cm

In most cases, only one of these five mechanisms is dominant. Hence, considering only one term of the electrostatic force, the equations for collection efficiency may be obtained. For instance, for the collection of a charged particle by a charged collector,

$$E_{E_1} = - 4N_{E_1} \qquad (2.2.56)$$

and for the collection of uncharged particles by a charged spherical collector considering only the induced charge on the particles,

$$E_{E_2} = \left(\frac{15}{8}\pi N_{E_2}\right)^{0.4} \tag{2.2.57}$$

Further discussion of this topic is beyond the scope of this work.

2.2.2 Phoretic Mechanisms

2.2.2.1 Diffusiophoresis

In a concentration gradient, which is accompanied by diffusion but not necessarily by net motion of the gas phase, the heavier molecules will impart a higher momentum to the particles than the lighter molecules. If there is a net motion of the gas phase (Stefan flow), additional force is applied to the particles. The combination of forces due to concentration gradient and Stefan flow is referred to as the diffusiophoretic force, and particle movement by this force is called diffusiophoresis. As extensive articles on diffusiophoresis have been published, only the basics of this phenomenon will be discussed here.

It was first suggested by Stefan (1881) that there must exist near a surface of an evaporating or condensing body a hydrodynamic flow of the medium directed away from the evaporating and towards the condensing surface. In a binary system of a vapor and a carrier gas the velocity of the Stefan flow is

$$u = -\frac{D_{vg}}{P_g}\frac{dP}{dx} \tag{2.2.58}$$

where D_{vg} is the diffusion coefficient of the vapor in the gas and P and P_g are the partial pressures of vapor and carrier gas, respectively. Aitken (1883) was the first who observed the formation of dust-free spaces next to moist surfaces.

Particles near a condensing or evaporating surface might be expected to move with a velocity of about that of the Stefan flow. However, the phenomenon is more complicated. The particle's total diffusiophoretic velocity is the sum of the Stefan flow velocity and the velocity due to gas-particle momentum transfer (Goldsmith and May (1966), Goldsmith et al. (1963), and Waldman (1959)), and the particle behaviour is influenced by its size. More precisely, Knudsen number, Kn, which is the ratio of gas mean free path to particle radius, is an important measure for the modifying effect of diffusion currents of the vapor and gas on the velocity of particles (Derjaguin and Duklin (1956, 1957), Freise (1957), Facy (1958)). Diffusiophoretic velocities of particles can therefore be studied in three categories, large particles ($Kn << 1$), intermediate particles ($Kn \approx 1$) and small particles ($Kn >> 1$).

Small Particles

For small particles, $r_p << \lambda$, gas molecular behaviour becomes important. Derjaguin and Bakanov (1957) and Waldmann (1959), independently derived equations for the particle velocity based on a rigorous consideration of the effects of diffusing gas molecules on particle motion using the Chapman-Enskog theory of gases (Chapman and Cowling (1964)). Waldman's treatment was more realistic because the molecule-particle collisions were assumed partly specular and partly diffuse while Derjaguin and Bakanov considered only specular collisions.

Waldmann's expression for diffusiophoretic particle velocity in a binary gas mixture undergoing equimolar counter-diffusion is

$$u_{pd} = - \frac{(1 + \frac{\pi}{8} a_1)\sqrt{m_1} - (1 + \frac{\pi}{8} a_2)\sqrt{m_2}}{(1 + \frac{\pi}{8} a_1)x_1\sqrt{m_1} + (1 + \frac{\pi}{8} a_2)x_2\sqrt{m_2}} D(\nabla x_1)_\infty \quad .....(2.2.59)$$

where x_i = mole fraction

a_i = accomodation coefficient, fraction of molecules reflected diffusely from the surface

m_i = the mass of i^{th} component of gas molecules

D = gas diffusivity

$(\nabla x_1)_\infty$ = concentration gradient in the undisturbed gas

For the case where component 1 diffuses through inert component 2 which is stagnant, diffusiophoretic particle velocity is (Schmitt (1961)),

$$u_{pd} = - \frac{(1 + \frac{\pi}{8} a_1)\sqrt{m_1}}{(1 + \frac{\pi}{8} a_1)x_1\sqrt{m_1} + (1 + \frac{\pi}{8} a_2)x_2\sqrt{m_2}} \frac{D}{x_2}(\nabla x_1)_\infty \quad .....(2.2.60)$$

Further improvements of diffusiophoretic theory for small particles have been minor. For example, the equation suggested by Mason and Chapman (1962) is only different from Waldman's equation with the factor multiplying the accomodation coefficients by 4/9 instead of $\pi/8$. Bakanov and Derjaguin (1960) improved the accuracy of their previous analysis by considering a temperature gradient in the gas. For equimolar counter diffusion, their expression is:

$$u_{pd} = - \frac{\sqrt{m_1} - \sqrt{m_2}}{x_1\sqrt{m_1} + x_2\sqrt{m_2}} - 1/2 \frac{1}{d_o x_1 x_2} \frac{x_1 d_{-1} + x_2 d_1}{x_1\sqrt{m_1} + x_2\sqrt{m_2}} D(\nabla x_2)_\infty \quad .....(2.2.61)$$

where d_o, d_1 and d_{-1} are parameters dependent on gas properties.

For the accomodation coefficients taken as unity, which is a reasonable assumption, comparison of Equations (2.2.59) and (2.2.61) indicates that Bakanov and Derjaguin's expression is different from Waldmann's equation only by the second term in Equation (2.2.61). This second term is of the same order as one fifth of thermal diffusion factor, $\alpha_T/5$ (Whitmore (1976)). However, since α_T is usually very small, this term can be neglected (Waldmann and Schmitt (1966)). With a similar study, Derjaguin and Yalamov (1972) found a value of $1/(1 + \frac{\pi}{8})$ instead of (1/2) for the coefficient in the second term of Equation (2.2.61).

Large Particles

For the case of large particles ($r_p >> \lambda$ or $Kn << 1$) the system can be considered as in the continuum regime. As a matter of fact, the continuum mechanics equations would yield a solution for diffusiophoretic particle velocity. However, the general approach to the evaluation of u_p has been such that although these continuum mechanics equations have been used for the bulk of the fluid, near the particle surface they have been regarded as not adequate due to the complex interactions of gas molecules with the particle surface. Therefore, in this range molecular mechanics has been used which results in a velocity discontinuity at the surface of the particle, i.e. the velocity of the gas is not zero at the point of one mean free path away from the surface. This velocity discontinuity is referred to as "diffusion slip". The expressions found for this slip velocity have been then used as the boundary condition for the continuum mechanics equations.

Kramers and Kistemaker (1943) offered the following equation for the slip factor

$$\sigma_{12} = \frac{m_1 - m_2}{m + \sqrt{m_1 m_2}} \tag{2.2.62}$$

For equimolar counter diffusion, using this slip velocity, Schmitt and Waldmann (1960) derived an expression for the diffusiophoretic velocity for large particles which is exactly the same as the equation for small particles (Equation (2.2.59)) with the accomodation coefficients taken as equal, $a_1 = a_2$.

$$u_{pd} = \sigma_{12} D(\nabla x_1)_\infty \ldots\ldots \tag{2.2.63}$$

$$u_{pd} = - \frac{m_1 - m_2}{m + \sqrt{m_1 m_2}} D(\nabla x_1)_\infty$$

$$= - \frac{\sqrt{m_1} - \sqrt{m_2}}{x_1\sqrt{m_1} + x_2\sqrt{m_2}} D(\nabla x_1)_\infty \tag{2.2.64}$$

As the velocities predicted by Equation (2.2.64) do not agree with the experimental results, Schmitt and Waldmann (1960) therefore proposed an empirical expression for the diffusion slip factor,

$$\sigma_{12} = 0.95 \frac{m_1 - m_2}{m_1 + m_2} - 1.05 \frac{d_1 - d_2}{d_1 + d_2} \tag{2.2.65}$$

where d_1, d_2 are the molecular diameters of gas components. For the case where component 1 is diffusing through stagnant component 2 the diffusiophoretic velocity becomes (Waldmann and Schmitt (1966)),

$$u_{pd} = - (1 \pm \sigma_{12} x_2) \frac{D}{x_2} (\nabla x_1)_\infty \qquad (2.2.66)$$

It should be again noted that if Kramers and Kistemaker's expression for the slip factor (Equation (2.2.62)) is used in Equation (2.2.66) and $a_1 = a_2$ is taken, the same particle velocity expression for small particles (Equation (2.2.60)) is obtained. However, to have agreement with the experimental results the empirical diffusion slip factor (Equation (2.2.65)) should be used in Equation (2.2.66).

Brock (1963) tried to improve the above treatment by considering diffusion heat slip as well as friction slip. The final expression is again the same as Bakanov and Derjaguin's equation for small particles (Equation (2.2.61). Nevertheless, as mentioned in the section for small particles, this extension does not improve the final result appreciably as thermal diffusion is usually negligible.

In a more recent study, Whitmore (1976), besides giving an excellent review of diffusiophoresis, calculated the energy dissipation rate in the flow field of gas with particles suspended for two cases, i.e. with slip at the particle surface and without slip. This approach led to the very important result that

$$E_{slip}/E_{no\ slip} = 2 \qquad (2.2.67)$$

As normally one would expect that the particle velocity would adjust until the energy dissipation rate is minimum, Whitmore concluded that the shear stress at the surface supresses any tendency for slip to occur and, therefore, particles move with the mean mass velocity of the gas.

Thus, the particle velocity for the case of component 1 diffusing in stagnant component 2, becomes (Whitmore (1976), Whitmore et al. (1973, 1976, 1977)),

$$u_{pd} = -\frac{M_1}{M}\frac{D}{x_2}(\nabla x_1)_\infty \qquad (2.2.68)$$

Extensive experimental results for diffusiophoresis in a wetted-wall column show excellent agreement with Equation (2.2.68) (Whitmore (1976)).

Intermediate Particles

Analysis of the motion of intermediate particles (Kn $\sim$ 1) is more difficult. There are very few works in this transition regime. Brock (1968) offered the following equation for diffusiophoretic velocity.

$$u_{pd} = \frac{\{1 - (\frac{m_2}{m_1})^{1/2} + ((\frac{2m_2}{m_1 + m_2})^{1/2} - (r_2/r_{12})^2)\ 0.311/Kn\}}{1 - 0.360/Kn} D(\nabla x_1)_\infty \qquad .....(2.2.69)$$

For large Knudsen numbers this equation reduces to the expression for small particles. However, for small Kn, it does not converge to the values predicted by the velocity expression for large particles.

Treating the particles as large molecules and using the molecular diffusion equation (Hirschfelder et al. (1964)), Annis et al. (1972, 1973) derived an equation which they claim holds for all particle sizes. This claim is, however, inconsistent with the fact that the diffusion equation on which the theory is based is correct only for very small particles.

Finally, Whitmore et al. (1977) suggest that the mean molar velocity of fluid can be used as an approximate limit for particle velocities in the transition regime.

2.2.2.2 Thermophoresis

Under a thermal gradient in an aerosol stream, particles will move along the gradient under the influence of differential molecular bombardment. The force which causes particle motion results from differences in momentum imparted to the particle on opposite sides. The hotter, and thus faster, molecules colliding with the particle impart a higher momentum to the particle than the cooler, slower, molecules. Hence particles are driven in the direction of decreasing temperature by this phenomenon, called thermophoresis, first described by Tyndall (1870).

Thermal forces, like diffusiophoretic forces or any other interactions between particles and gas, depend on the Knudsen number. A number of equations have been developed to calculate the thermophoretic velocity of particles. Some basic equations will be summarized below. In fact, all these equations can be expressed in one general form as

$$u_{pt} = - K \frac{\mu_G}{\rho_G T} \nabla T \qquad (2.2.70)$$

and differ only in the definition of K. But it should be pointed out that the agreement of any of these equations with experiments is not very satisfactory (Goldsmith and May (1966)).

Small Particles:

For small particles (Kn >> 1), the theory is simple and complete. For such particles, thermophoresis has been treated on an elementary kinetic theory as developed by Einstein (1924), Cawood (1936), Clusius

(1944), Stetter (1960). The basic treatment starts with the assumption that the distribution function of the gas molecules hitting the particle is not appreciably influenced by the presence of the particle. In fact, this is a reasonable assumption. If the mean free path is large, a gas molecule, after rebounding from the particle, will go further away from it and will have practically no chance to hit it a second time before having lost its memory. Derjaguin and Bakanov (1959) and, independently, Waldmann (1959) derived the thermophoretic velocity for small particles as

$$u_{pt} = \frac{0.75}{(1 + \frac{\pi}{8} a)} \frac{\mu_G}{\rho_G T} \nabla T \qquad (2.2.71)$$

where a, as mentioned before, is the fraction of gas molecules reflected diffusely by the particle. For smooth surface of the particles and for liquid particles, $a \approx 0.9$. For rough surfaces, $a \approx 1$.

Large Particles:

As the size of the particles increases relative to the mean free path ($Kn << 1$), the difficulty of theoretical treatment of the molecule-particle interaction also increases, as for the case of diffusiophoresis. Some drastic simplifications, and uncertainties become involved. The molecule no longer sees the particle as another molecule, but as a solid surface. For a temperature decreasing from left to right the particle surface receives an impulse directed to the right and practically an equal impulse directed to the left is imparted to the gas. Epstein (1929) derived the equation for the thermophoretic force from the above considerations and using the Stokes equation

$$F = 3\pi d_p \mu_G u_p \tag{2.2.72}$$

obtained the thermophoretic velocity of particle as

$$u_{pt} = - \frac{3\mu_G}{2\rho_G T} \left(\frac{k_G}{2k_G + k_p}\right) \nabla T \tag{2.2.73}$$

where k_G and k_p are the thermal conductivities for gas and particle, respectively. The agreement of this equation with experiments, especially for good conductors, is poor. Brock (1962) tried to improve the above equation and reported the thermophoretic velocity as,

$$u_{pt} = - \frac{3\mu_G}{2\rho_G T} \left\{\frac{1}{1 + 3c_m Kn}\right\} \left\{\frac{\left(\frac{k_G}{k_p}\right) + c_t Kn}{1 + 2\frac{k_G}{k_p} + 2c_t Kn}\right\} \nabla T \tag{2.2.74}$$

Brock (1962) suggested that c_t ranges from 1.875 to 2.48 and c_m from 1. to 1.27. Finally Derjaguin and Bakanov (1967), using a different approach, deduced the following equation:

$$u_{pt} = - \left\{\frac{4k_G + 0.5k_p}{2k_G + k_p}\right\} \frac{\mu_G}{\rho_G T} \nabla T \tag{2.2.75}$$

Intermediate Particles:

There are not many studies reported for intermediate size particles. Equation (2.2.74), given above, has been used for this transition regime. Another expression suggested by Derjaguin and Yalamov (1966) is given below.

$$u_{pt} = -3 \left\{ \frac{\frac{k_G}{k_p} + c_t K_n}{1 + 2\frac{k_G}{k_p} + 2c_t \frac{k_G}{k_p} Kn} \right\} \frac{\mu_G}{\rho_G T} \nabla T \qquad (2.2.76)$$

As an overall evaluation of thermophoresis it may be appropriate to mention here that experimental results reported by Goldsmith and May (1966) and Rosenblatt and LaMer (1964), and theoretical calculations lead to the conclusion that thermophoretic velocity is quite low. Even at temperature gradients of 10^3 $^oC/cm$, the thermophoretic velocity is only about 0.1 cm/s. Therefore, long residence times are required to accomplish significant particle separation at reasonable temperature gradients. However, thermal forces might be used to enhance the performance of certain particle collection devices (Thring and Strauss (1960) and Strauss (1966)).

2.2.2.3 Electrophoresis

If charged particles are subjected to a unidirectional electric field, they move towards the electrodes and are deposited there. The motion or migration of the particles in an electric field is called electrophoresis.

A particle carrying n_e elementary units of electrical charge ,q, in an electric field of intensity E_e experiences an electric force,

$$F = n_e q E_e \qquad (2.2.77)$$

This force causes the particle to move through the medium in which it is suspended. Neglecting second order electrostatic effects, such as

the polarizability of the particle and assuming that a spherical particle is moving in laminar flow (Re < 1), the final speed attained by the particle, when the viscous drag force acting on the particle becomes equal to the applied electrical force, can be obtained from Stokes law

$$u_{pe} = n_e \, q \, E_e / 3\pi \, \mu_G \, d_p \qquad (2.2.78)$$

This expression shows that the migration velocity of the particle is proportional to intensity of applied electric field and charge on the particle. The proportionality constant between particle velocity and field strength is, by definition, the electrical mobility of the particle, Z_E, i.e.

$$Z_E = u_{pe}/E_e = n_e \, q/3\pi \, \mu_G \, d_p \qquad (2.2.79)$$

There are two ways to charge an aerosol particle. The first one is in the absence of an applied electric field. In this case the unipolar gaseous ions diffuse toward the particle surface and impart their electric charges to the particle. Here, the collision is primarily due to the random thermal motion of the ions. This is called "diffusion charging". The second way to charge particles is accomplished with an applied electrical field of sufficient intensity, such as that encountered in the corona charger of an electrostatic precipitator. In this case, the ordered motion of the ions caused by the electric field may be the predominant charging mechanism by which ions are driven onto the particle. Applied electric field increases the frequency of collision between ions

and the particle. This type of charging is called "field charging". Under some conditions, for instance when sub-micron particles with sizes of the same order of magnitude as the mean free path are charged under moderate electric field intensities, both the field and diffusion charging mechanisms may be equally important.

For all these cases the number of elementary units of charge that a particle may carry can be evaluated theoretically (Shannon (1974)). This may then be used with Equation (2.2.79) to calculate particle mobility. Further details concerning electrophoresis are given by White (1951), Rohman (1923), Pantheniez (1932), and Cochet (1961).

2.2.2.4 Magnetophoresis

When an electrically charged particle moves in a magnetic field transverse to the field lines a force, called "Lorentz force", is generated. The direction of this force will be at right angle to both the direction of the field and the direction of motion of the particle. As a result of the change in direction of the particle due to this magnetic force, the possibility of particle deposition exists. The terminal drift velocity of a particle in a magnetic field can be obtained by equating the Lorentz force to the resistance of the gas.

$$F = n_e q u_p B = 3\pi \mu_G d_p u_{pm} \qquad (2.2.80)$$

where n_e = number of charges on particle

q = elementary charge

u_p = velocity of particle in the field

B = magnetic field strength

u_{pm} = terminal drift velocity of particle

Examination of the above equation indicates that the terminal drift velocity due to magnetic force is less than 0.01 cm/s for particles 0.1-1. μm in size except at unrealistically high particle velocities and magnetic field strengths. Therefore Lorentz force is too small for use in particle deposition. The use of magnetic fields even to agglomerate particles does not appear feasible. Only recently there are some attempts to evaluate the feasibility of specially designed high magnetic field separators for fine particle control (Gooding et al. (1977)).

2.3 PARTICLE COLLECTION IN MOBILE-BED CONTACTING

The literature concerning the particle collection in MBC is very limited. The first study is by Pollack et al. (1966) who have obtained some experimental data for fly ash recovery from a coal burning power plant flue gas. They presented results in graphical form for the effect of gas velocity, over the range of 2.5 - 4.9 m/s, on overall efficiency. A two-stage column, each stage packed with 0.25 m of 38 mm packing, was employed. Liquid flow rate was varied between 13.5 and 27.2 kg/m^2-s (also see Wet Scrubbers System Handbook, Vol. 1, Chapter 5 (1972)). Using these few experimental data Epstein et al. (1971) obtained the following equation by regression analysis.

$$E(d_p) = 1 - \exp\{-5\times10^{-17}(L/G)^{3.3}\, G^{3.66}\, K\, n\, H_{st}/d_{pb}\} \quad .....(2.3.1)$$

where, they reported,

$K = 3.28 \times 10^{-6} \rho_p u_T d_p^2 / g \mu_G d_d$

d_p = particle diameter, μm

d_d = mean diameter of droplets, μm

d_{pb} = diameter of packing spheres, ft

G = gas flow rate, lb/hr-ft^2

H_{st} = static height of packing for a single stage, ft

L/G = liquid to gas ratio, gal/mcf

n = number of stages

As can be seen, this equation incorporates a mixture of units. Although they use droplet size in the inertial impaction parameter, K_i, no comment was made concerning how they determined mean droplet size. To the author's best knowledge there is as yet no published study concerning size distribution of liquid droplets in MBC. Without such information, how mean droplet size could be evaluated and used in calculation of the inertial impaction parameter cannot be understood. This shortcoming has also confused Calvert et al. (1972). In the Wet Scrubbers System Handbook, edited by Calvert (1972), the same equation is given as

$$E(d_p) = 1 - \exp \{- 2.45 \times 10^6 u_L^{3.3} u_G^{0.36} St H/d_{pb}\} \quad (2.3.2)$$

where d_{pb} = packing size, cm

H = stage height, cm

$St = u_{Gi} d_p^2 \rho_p / g \mu_G d_{pb}$

u_G = superficial gas velocity, cm/s

u_{Gi} = interstitial gas velocity, cm/s

u_L = superficial liquid velocity, cm/s

Close examination of Equations (2.3.1) and (2.3.2) reveals that, while being transferred from the original source (Epstein et al. 1971), the equation has, remarkably, been changed. Although Calvert et al. specify use of interstitial velocity, u_{Gi}, for calculation of St, they omitted to specify the basis they used for liquid holdup and/or gas holdup, required in order to evaluate interstitial gas velocity. The same shortcoming exists for calculation of terminal velocity of the liquid drop for Equation (2.3.1). Due to the inconsistencies and incompleteness noted above, and to the lack of information concerning experimental conditions from which they were determined, such as temperature of the streams and humidity of gas, these equations cannot be considered to provide a reliable basis for prediction of particle collection in MBC.

Rowbottom (1973) reported the results of a series of pilot scale experiments to test particulate removal from Kraft recovery flue gas by a MBC column of 0.093 m^2 cross-sectional area and up to five stages high. Each stage was 1.22 m between the support grids and was packed with 38 mm diameter balls to a static height of 0.29 m. Each support grid had 65% open area. The maximum gas velocity used was about 4.72 m/s. Liquid flow rates up to 40 kg/m^2-s were used. Although no theoretical treatment or attempt to correlate the experimental data was made, the graphical presentation of these results provide a valuable indication of the effect of operating variables on the exit particulate loading.

The qualitative conclusions reached by the cited study can be summarized as follows:

i) Inlet particulate concentration over the range 1.8-3.3 gm/m^3 had no effect on exit concentration for liquid flow rates greater than 14 kg/m^2-s.

ii) Exit particle concentration decreased with increasing liquid flow rates. For high liquid flow rates this decrease of outlet concentration with liquid flow rate was only marginally significant.

iii) At similar liquid and gas flow rates, an increase in number of stages from one to three decreased outlet particle concentration appreciably. However, the difference in exit concentrations between 3-stage and 5-stage operations was not detectable.

iv) Condensation of water vapor in MBC improved performance.

Since particle size distributions at the inlet and outlet were not determined, this study provides no information concerning the effect of particle size on particulate recovery. Particle collection at the demister, consisting of 0.076 m thick mesh pad, and during backwash of the gas stream by a spray nozzle placed on the exit line were not also explicitly accounted for. Nevertheless, the qualitative conclusions summarized above were a valuable aid in design of the experiments of the present study.

Calvert et al. (1974) reported the performance of a 3-stage MBC unit installed to clean the exhaust gas stream from an electrostatic precipitator used to control particulate emission from a 165 M.W. utility

steam boiler. Cross sectional area of the column was about 13.88 m^2 and 38 mm packing was used. Inlet and outlet particle size distributions were determined when the liquid and gas flow rates were 136 and 14 kg/m^2-s, respectively. An aerodynamic mass median particle diameter of 3 μm at the inlet and 0.5 μm at the outlet was reported. Penetration as a function of particle size was calculated from the size distribution data. The graphical presentation of results shows a steep decrease of penetration from 0.86 to 0.01 over the range of particle size 0.3 to 2.5 μm. This was the first time that the effect of particle size on efficiency of MBC had been reported. Their results indicated that, for a more extensive study of particulate recovery in MBC, the range of particle size covered should be approximately 0.3 to 10 μm. Calvert et al. (1974) could not change the operating conditions of the unit, such as packing size, bed height, liquid and gas flow rates and, therefore, the effect of these variables on overall performance could not be studied. They also misinterpreted the equation reported by Epstein (1971) (Equation (2.3.1)). Although the inertial impaction parameter in that correlation was based on size of the liquid droplets and was changed to that based on packing size during the transfer to the Wet Scrubbers System Handbook, they considered the later version and claimed that the main collection mechanism in MBC was presumed to be due to inertial impaction on balls. As inertial collection parameter calculated using the ball diameter was about $5x10^{-4}$, and the collection efficiency for a sphere is, theoretically, zero for values of impaction parameter smaller than 0.083 (Section 2.2.1.1), they concluded that it was impossible to attribute high collection efficiency to this mechanism. However, packing size can be used just as a characteristic size for calculation of inertial impaction parameter. Size of liquid droplets and bubbles which may be

contributing to the performance of MBC as well as liquid films covering the balls depends on packing size at constant liquid and gas flow rates. Since neither packing size was used in Equation (2.3.1) nor their theoretical considerations against the idea of using packing size in inertial impaction parameter or Stokes number are valid, criticisms as claimed by Calvert et al. (1974) are not relevant. Furthermore, they could not explain the high efficiency of MBC with a pressure drop as small as 25 cm water column. Their attempt to explain the observed efficiencies by treating MBC as a sieve plate column and a spray column was also not successful. They attributed the unexpectedly high recovery to the condensation effect due to the presence of SO_3 and H_2SO_4 in the gas. Neither could they measure the effect of entrainment, although they knew that it existed. They concluded that their scrubber reliability had not been good and recommended that further investigation be made in order to understand the performance of MBC and to develop a realistic mathematical model.

Mlodzinski and Warych (1975) reported a study of collection of zincsulfide and superphosphate particles in a small (64 mm diameter) column. Phosphorous/bronze bed support plates with low open areas (27.5-65.2%) were used. Packing size was 2.5 - 6.8 mm. Static bed height was changed from 1.5 to 12 cm. Liquid flow rate was varied between 7.8-93.45 m^3/m^2-hr and superficial gas velocity between 1.-3.6 m/s. These specifications given on the system reflect the similarity to most of the other systems used in East-European studies. As explained in detail in Section 2.1, one must be very careful in the analysis and use of data obtained with such small scale columns. The small open area of the supporting plate affects the hydrodynamics of the bed, i.e. liquid holdup and pressure drop in the bed, and liquid buildup on the bed support grid, which in turn would affect all performance character-

istics such as heat and mass transfer and particle collection. Although the system of Mlodzinski and Warych is far from those used in industry, the results of this study will be summarized. The efficiency for hydrophilic particles (superphosphate) was found to be greater than hydrophobic particles (zincsulfide). Efficiency of particle collection increased with liquid flow rate, as was observed by Rowbottom (1973), and also increased to a lesser extent with gas flow rate. A very important result supplied in this study is that as the open-area of the lower plate increases, efficiency drops. This is the indication of the end effects present in this study. The cited authors gave the following correlations:

For superphosphate particles:

$$Pt = 1.888\ Pe^{-0.199}\ St^{-0.263} \qquad (2.3.3)$$

For zincsulfide particles:

$$Pt = 52.369(H_{st}/d_{pb})^{-0.514}\ Pe^{-0.11}\ St^{-0.572} \qquad (2.3.4)$$

where, the authors report,

$$Pe = u_{Gi}\ d_{pb}/D_p$$

$$St = u_G\ d_p^{\ 2}\ \rho_p/\mu_G\ h_o$$

It is interesting to note that although interstitial gas velocity was used for Peclet number, superficial gas velocity was used for Stokes

number. There is no theoretical background given in the paper for this choice. However, the author believes that it is not proper to use superficial velocity in Stokes number (see Chapter 6). Furthermore, in the definition of St, the cited authors used h_o, which is the gas pressure drop in MBC expressed as the height of water column in meters. However, this is not the proper way to write Stokes number (see Equation (2.2.6.a)). Moreover, introduction of Peclet number into the penetration equation implies that the diffusion mechanism is important. On the contrary, as will be shown in Chapter 3 by an order-of-magnitude analysis, this is not true for MBC. Therefore, the inappropriate introduction of Peclet number and incorrect definition of Stokes number give the impression that Equations (2.2.3) and (2.2.4) were not developed fundamentally but probably by intuition. For non-wettable particles, Weber number would be a better choice to express particle collection efficiency. Contact angle of solid particles with air and water must also be known (see Chapters 2 and 6). Mlodzinski and Warych gave no information about these.

Finally, it may be noted that Statnic and Drehmel (1975) and Bhatia et al. (1978) referred to the potential use of MBC for particle recovery. Statnic and Drehmel (1975) also reported some data obtained using the same MBC facility previously reported by Epstein (1971) and confirmed that the critical size for the particles, that should be further investigated, is between 0.3 and 10. μm.

2.4 CONCLUSION

For analysis of performance of MBC in particle collection studies, information on hydrodynamic characteristics of the system is required. Studies of hydrodynamic behaviour of MBC were therefore reviewed in the first section of this chapter. Inspection of this previous work leads to the conclusion that, unfortunately, there are appreciable differences among the data reported. Some sources for these disagreements were identified. This analysis indicated that, because of deficiencies and limitations of previous studies, a comprehensive investigation of particle collection in MBC should be preceded by determination of MBC hydrodynamic characteristics (bed expansion, minimum fluidization velocity, pressure drop and liquid holdup) in a study that would avoid limitations identified for previous studies.

In the second section, particle collection mechanisms were reviewed according to a basic system of classification. For the aerodynamic capture mechanisms, parameters for each mechanism have been defined. Efficiencies due to these mechanisms can be expressed in terms of these individual parameters. Table 2.6 summarizes these parameters for particle collection by liquid drops and spherical objects. Table 2.7 is for collection from bubbles. This analysis suggests that the effect of gas velocity and particle size on penetration, Pt = 1 - E, would be expected to be of the form shown in Figures 2.3 and 2.4. Determination of the collection efficiency under the conditions of simultaneous effect of all the aerodynamic mechanisms is more complicated. According to Fuchs (1964) the total efficiency is greater than any of the individual efficiencies and smaller than their sum. Nevertheless,

TABLE 2.6 Parameters of Individual Aerodynamic Capture Mechanisms for Collection by Drops

Mechanism	Parameter	
Inertial impaction	$St = c' d_p^2 \rho_p u_{G,\infty} / 9\mu_G d_c$	
Interception	$N_R = d_p / d_c$	
Diffusion	$N_D = d_c^{-2/3} u_{G,\infty}^{-2/3} D_p^{2/3}$	for $Re_c < 3$; $Sc \approx 10^6$
	$N_D = d_c^{-1/2} u_{G,\infty}^{-1/2} D_p^{2/3} \gamma_G^{-1/6}$	for $600 < Re_c < 2600$; $Sc \approx 10^6$ and $100 < Re_c < 700$; $Sc \approx 10^3$
Gravity	$N_G = u_T / u_G$	
Electrostatic attraction	N_E (defined by Equations (2.2.40)-(2.2.44))	

TABLE 2.7 Parameters of Individual Aerodynamic Capture Mechanisms for Collection from Bubbles

Mechanism	Parameter
Inertial deposition	$N_{b,I} = c'_b d_p^2(\rho_p - \rho_G)/d_b^2 \mu_G$
Diffusional deposition	$N_{b,D} = D_p^{1/2} {}_b^{-1/2} d_b^{-3/2}$
Gravitational deposition	$N_{b,G} = c' d_p^2(\rho_p - \rho_G) g/ {}_o d_b \mu_G$

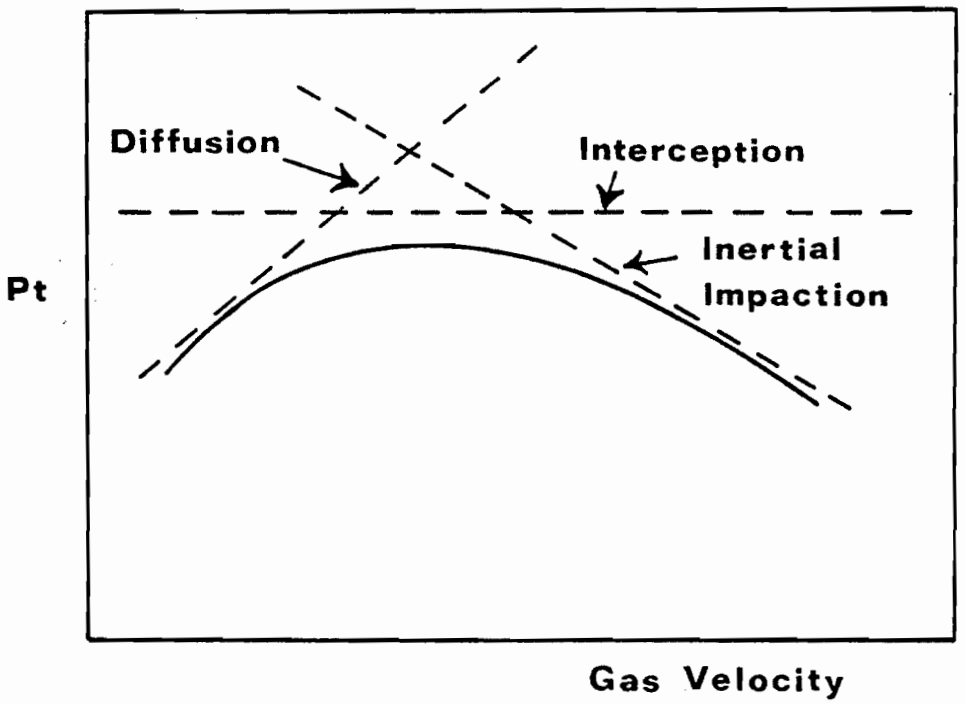

FIGURE 2.3. Schematic representation of the effect of gas velocity on particle penetration

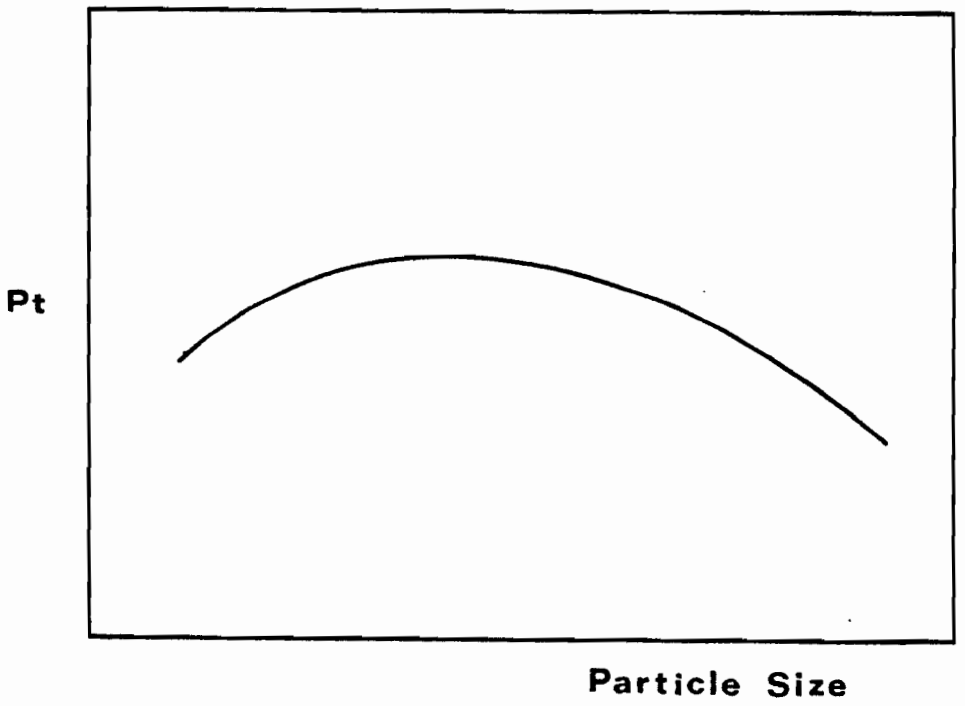

FIGURE 2.4. Schematic representation of the effect of particle size on penetration

in most cases, one mechanism is dominant to others. Under such conditions, the total efficiency can be obtained by adding the individual efficiencies. One important assumption in this procedure is that there is no appreciable interference between mechanisms. This is a reasonable assumption if all the individual mechanisms except the dominant one are very small.

As phoretic capture mechanisms are due to flux forces exerted on the system, it is possible to control these effects for any system at any flow conditions by selection of conditions which either include or exclude any of these flux forces. Furthermore, the particle velocities due to such external forces can be evaluated using equations given in Section 2.2.2. The particle velocities so evaluated are superimposed on the convective velocity.

The literature review of Section 2.3 reveals that there has not yet been published any thorough and adequate investigation of particle collection in MBC leading to reliable methods of predicting the effects on collection efficiency of all variables of interest for the application of MBC to industrial problems.

CHAPTER 3

ANALYSIS OF AERODYNAMIC CAPTURE MECHANISMS IN MOBILE-BED CONTACTING

A purely theoretical formulation of particle collection for MBC is not possible. If the geometry of the system were simple, the theoretical efficiency could have been evaluated from the trajectories of particles solving the equations of motion and using the fundamentals of collection mechanisms discussed in the previous chapter. However, the nature of gas-liquid contact in MBC is very complex. The highly turbulent conditions in a 3-phase flow make the above theoretical approach impossible. Spherical packing balls are free to move due to the counter flow of gas and liquid streams. This motion by the solid packing creates very vigorous fluid contacting inside the bed. Liquid enters the system as droplets which may collide and/or break up. In addition to droplets, liquid exists in the mobile-bed as films covering the packing spheres, and as large irregularly shaped globs. But whatever the form or shape of liquid flowing downward, all liquid contributes to particle collection. Moreover, although overall the gas is the continuous phase, a result of the vigorous interphase contacting is that some of the gas is present also in the form of bubbles within the liquid elements. Khanna (1971) estimated that gas bubbles can account for up to 60% of the total interfacial area in MBC. Thus some particle collection by bubbles as well must be allowed for.

The great complexity of gas-liquid contacting taking place in MBC does not mean that an order-of-magnitude analysis cannot be made in

order to determine the major aerodynamic capture mechanism for this scrubber. Since, as mentioned in the previous chapter, phoretic mechanisms are due to some external flux forces, their effect on the system is controllable. However, any particle collection device is characterized by the aerodynamic capture mechanisms occurring. Therefore, the following analysis is made to determine for the MBC process the relative contributions of each of the aerodynamic capture mechanisms.

For particle collection by liquid droplets and by liquid films covering the spherical packing, the parameters defined in Chapter 2 and summarized in Table 2.6 can be used. It should be noted that the diffusion parameter, N_D, depends on the Reynolds number, Re_c, and Schmidt number, Sc. For the purpose of the present calculations, typical air and water flow rates of 3 and 15 kg/m^2-s, respectively, at 20^{o}C are chosen. At these flow rates, the relative velocity between gas and liquid is about 3 m/s. The smallest spherical collector in MBC would be liquid droplets. A simple terminal velocity calculation shows that, at such intermediate flow rates, liquid droplets smaller than about 300 μm would be entrained in the gas stream. A recent experimental study by Calvert et al. (1977) concerning entrainment from MBC confirms this estimate. Therefore, 1,000 μm is chosen as an average size for liquid droplets. The largest spherical collector is of course the largest packing ball used (38 mm). For these conditions, then, Re_c is between 200 and 7500. Since the critical particle size range for MBC is between 0.35 and 10 μm, these two values are taken as the smallest and largest particles. Hence, Sc number varies between 1.6×10^5 and 6.3×10^6. Considering these values of Re_c and Sc numbers,

Equation (2.2.41) is used for evaluation of the diffusion parameter, N_D. Calculated values for the parameters of individual mechanisms are given in Table 3.1. As neither particles nor collectors are charged in this study of mobile-bed operation, electrostatic attraction is not considered.

A similar comparison of the individual aerodynamic mechanisms for the bubbles can be made. As noted in the previous chapter, due to circulation of gas inside the bubble a centrifugal force is applied on the particles. This force may carry particles to the surface and cause them to be captured by the surrounding liquid. This mechanism was identified as inertial collection by bubbles. Where internal streamlines carrying particles pass sufficiently close to the surface, diffusion of particles may enable them to reach the surface. Hence diffusional collection may contribute to the overall deposition rate. Furthermore, depending on the size and bubble velocity, gravity may help the particles to settle and be collected by the liquid surface. These three mechanisms were identified as potentially important for particle deposition from bubbles in the previous chapter and the corresponding parameters were summarized in Table 2.7.

For bubble diameters greater than 1 mm, bubbles become flattened, pulsations of shape occur and the internal circulation of gas becomes very complex (Fuchs (1964)). Since the parameters given in Table 2.7 involve the assumption of sphericity of bubbles, they are evaluated for two bubble sizes, 10^{-1} mm and 1 mm, as suggested by Fuchs (1964). The results are summarized in Table 3.2.

Inspection of Tables 3.1 and 3.2 indicates that, with respect to aerodynamic capture mechanisms, inertial impaction is not only the most important but is the dominant capture mechanism for MBC. Whether particles are collected by liquid droplets, by liquid films covering the packing or are deposited from the bubbles, inertial capture is in all cases the major mechanism. The contributions from other mechanisms to the total efficiency depend on size of the particle and the collector. Referring back to Figures 2.2 and 2.3, the analysis of this chapter leads to the important conclusion that the characteristic operating region for MBC is to the right of the maxima of these curves.

Having identified the major mechanism of particle collection in MBC, the next step is to formulate a model for the overall efficiency of particulate recovery. This analysis will be the subject of the next chapter because the procedure is entirely different from the mechanistic approach presented in the present chapter. As it is not possible to measure the size of liquid droplets or bubbles in MBC due to highly turbulent conditions, a general macroscopic treatment will be presented which may be applied not only to the MBC process but, in fact, to any scrubber.

TABLE 3.1 Parameters for Aerodynamic Collection by Liquid Droplets and Packing Spheres

		Liquid Droplet		Spherical Packing	
		$d_d = 10^{-3}$ m		$d_{pb} = .038$ m	
Mechanism	Parameter	$d_p = .35$ μm	$d_p = 10.$ μm	$d_p = .35$ μm	$d_p = 10.$ μm
Inertial impaction	St	3.22×10^{-3}	1.87 .	8.48×10^{-5}	4.91×10^{-2}
Interception	N_R	3.5×10^{-4}	10^{-2}	9.21×10^{-6}	2.63×10^{-4}
Diffusion	N_D	2.45×10^{-5}	2.08×10^{-6}	3.97×10^{-6}	3.38×10^{-7}
Gravitational Collection	N_G	1.75×10^{-6}	1.01×10^{-3}	1.75×10^{-6}	1.01×10^{-3}

TABLE 3.2 Parameters for Aerodynamic Collection in Bubbles

Mechanism	Parameter	$d_b = 10^{-4}$ m		$d_b = 10^{-3}$ m	
		d_p = .35 μm	d_p = 10. μm	d_p = .35 μm	d_p = 10. μm
Inertial collection	$N_{b,I}$	2.9×10^{3}	1.68×10^{6}	2.9×10^{1}	1.68×10^{4}
Diffusional collection	$N_{b,D}$	5.68	8.94×10^{-1}	1.8×10^{-1}	2.83×10^{-2}
Gravitational collection	$N_{b,G}$	3.16×10^{-1}	1.83×10^{2}	3.16×10^{-2}	1.83×10^{1}

CHAPTER 4

THEORY OF PARTICLE COLLECTION IN GAS-LIQUID CONTACTORS

Although flow of gases and liquids through a variety of contacting equipment is common to many industrial processes the physical description of such multiphase flows, because of their enormous complexity, remains incomplete. In its full generality, a problem involving contacting of gas and liquid would require simultaneous solution of mass, momentum and energy equations, together with information on geometry of the system. However, this approach is generally too difficult due to the complexity of the equations of change and insufficient information on the geometry of the flow media. Nevertheless, a great deal of engineering importance can be learned about a specific problem by making simplifying assumptions. The use of overall mass balances and average mass transfer coefficients for evaluation of mass transfer performance of gas-liquid contactors is a good example. This approach will be used in seeking a solution to the present specific problem of evaluation of penetration of particles through gas-liquid contactors. The general treatment presented in this chapter is not uniquely developed for MBC but is applicable to all gas-liquid contactors, such as tray columns, packed beds, spray columns, and venturi scrubbers.

With respect to the term "penetration", it will be used consistently according to the definition now generally accepted, i.e. as the ratio of the number of particles leaving the system to the number of particles entering. Thus, overall particle penetration for a scrubber is:

$$Pt = \frac{\text{number of particles leaving the scrubber}}{\text{number of particles entering the scrubber}} \qquad (4.1)$$

The overall efficiency is then

$$E = 1 - Pt \qquad (4.2)$$

The critical feature of this theoretical analysis for particle penetration through a gas-liquid contactor will be the use for the particles and for the gas phase of local volume averaged continuity equations, abbreviated subsequently for convenience as LVACE. Any small control volume of any shape in the scrubber may be chosen for taking the average of the continuity equation (CE) and this volume may contain solid phase (packing), liquid phase, gas phase and particles suspended in the fluid phases. In the analysis to follow, V represents this control volume, S the surface enveloping this volume, V_G the volume of gas and S_i the gas-liquid interfacial area. The basic idea is to associate with every point in the scrubber a local volume average of the differential equation of continuity such that at every point

$$\frac{\partial \rho}{\partial t} + \vec{\nabla} \cdot \rho \underset{\rightarrow}{u} = 0 \qquad (4.3)$$

All the phases, gas, liquid, particles in the gas and particles in the liquid are involved in Equation (4.3). A key feature of this approach is that for the specific problem of evaluation of particle collection efficiency, a solution may be obtained using only two LVACE's, i.e. for the gas phase and for the particles suspended in this gas phase.

4.1 LOCAL VOLUME AVERAGED EQUATION OF CONTINUITY FOR PARTICLES SUSPENDED IN THE GAS PHASE

The LVACE for particles in the gas can be written as

$$\frac{1}{V} \int_{V_G} \left(\frac{\partial n_p}{\partial t} + \vec{\nabla} \cdot \underset{\rightarrow}{N}_p \right) dV = 0 \qquad (4.1.1)$$

For the first term, the operations of volume integration and differentiation with respect to time may be interchanged.

$$\frac{1}{V} \int_{V_G} \frac{\partial n_p}{\partial t} dV = \frac{\partial \bar{n}_p}{\partial t} \qquad (4.1.2)$$

The second term in Equation (4.1.1) represents the divergence of total particle flux, N_p, which involves convective and other types of flux.

$$\underset{\rightarrow}{N}_p = n_p \underset{\rightarrow}{u}_p + \underset{\rightarrow}{J}_p \qquad (4.1.3)$$

The general expression for particle flux with respect to mass average velocity (because ρ_p is constant) can be written as

$$\underset{\rightarrow}{J}_p = - D_p \vec{\nabla} n_p + \Sigma \underset{\rightarrow}{J}_{p,ext} \qquad (4.1.4)$$

The first term on the right hand side of the above equation represents diffusional flux, the second is the summation of fluxes due to all other possible external forces, such as diffusiophoresis, thermophoresis, etc.

Combining Equations (4.1.1)-(4.1.4),

$$\frac{\partial \overline{n}_p}{\partial t} + \frac{1}{V}\int_{V_G} \vec{\nabla} \cdot n_p \underset{\rightarrow}{u}\, dV - \frac{1}{V}\int_{V_G} \vec{\nabla} \cdot D_p \vec{\nabla} n_p\, dV$$

$$+ \Sigma \frac{1}{V}\int_{V_G} \vec{\nabla} \cdot \underset{\rightarrow}{J}_{p,ext}\, dV = 0 \qquad \ldots\ldots(4.1.5)$$

Using the theorem of the volume average of a divergence (Slattery (1972)),

$$\frac{1}{V}\int_{V_G} \vec{\nabla} \cdot n_p \underset{\rightarrow}{u}\, dV = \vec{\nabla} \cdot \overline{n_p \underset{\rightarrow}{u}} + \frac{1}{V}\int_{S_i} n_p \underset{\rightarrow}{u} \cdot \underset{\rightarrow}{n}\, dS \qquad (4.1.6)$$

and

$$\frac{1}{V}\int_{V_G} \vec{\nabla} \cdot \underset{\rightarrow}{J}_{p,ext}\, dV = \vec{\nabla} \cdot \overline{\underset{\rightarrow}{J}}_{p,ext} + \frac{1}{V}\int_{S_i} \underset{\rightarrow}{J}_{p,ext} \cdot \underset{\rightarrow}{n}\, dS \qquad \ldots\ldots(4.1.7)$$

$$\frac{1}{V}\int_{V_G} \vec{\nabla} \cdot D_p \vec{\nabla} n_p\, dV = D_p \vec{\nabla} \cdot \overline{\vec{\nabla} n_p} + \frac{D_p}{V}\int_{S_i} \vec{\nabla} n_p \cdot \underset{\rightarrow}{n}\, dS \qquad \ldots\ldots(4.1.8)$$

Using the theorem for volume average of a gradient (Slattery (1972)),

$$\overline{\vec{\nabla} n_p} = \frac{1}{V}\int_{V_G} \vec{\nabla} n_p\, dV$$

$$= \vec{\nabla}\left(\frac{1}{V}\int_{V_G} n_p\, dV\right) + \frac{1}{V}\int_{S_i} n_p \underset{\rightarrow}{n}\, dS$$

$$= \vec{\nabla}\,\overline{n}_p + \frac{1}{V}\int_{S_i} n_p \underset{\rightarrow}{n}\, dS \qquad \ldots\ldots(4.1.9)$$

In the above equations, n represents the unit vector. From Equations (4.1.8) and (4.1.9),

$$\frac{1}{V}\int_{V_G} \vec{\nabla} \cdot D_p \vec{\nabla} n_p \, dV = D_p \nabla^2 \bar{n}_p + D_p \vec{\nabla} \cdot \frac{1}{V}\int_{S_i} n_p \underset{\rightarrow}{n} \, dS + \frac{D_p}{V}\int_{S_i} \vec{\nabla} n_p \cdot \underset{\rightarrow}{n} \, dS \quad .....(4.1.10)$$

Combining Equations (4.1.5,6,7 and 10),

$$\frac{\partial \bar{n}_p}{\partial t} + \vec{\nabla} \cdot \overline{n_p \underset{\rightarrow}{u}} + \frac{1}{V}\int_{S_i} n_p \underset{\rightarrow}{u} \cdot \underset{\rightarrow}{n} \, dS + \Sigma \vec{\nabla} \cdot \bar{\underset{\rightarrow}{J}}_{p,ext} + \Sigma \frac{1}{V}\int_{S_i} \underset{\rightarrow}{J}_{p,ext} \cdot \underset{\rightarrow}{n} \, dS + D_p \nabla^2 \bar{n}_p + D_p \vec{\nabla} \cdot \frac{1}{V}\int_{S_i} n_p \underset{\rightarrow}{n} \, dS + \frac{D_p}{V}\int_{S_i} \vec{\nabla} n_p \cdot \underset{\rightarrow}{n} \, dS = 0 \quad .....(4.1.11)$$

Equation (4.1.11) is the most general LVACE for particles. For gas-liquid scrubbers in which diffusion can be neglected, the last three terms, i.e. those involving D_p, can be dropped from Equation (4.1.11). Moreover, for a sufficiently small averaging volume,

$$\overline{n_p \underset{\rightarrow}{u}} \approx \bar{n}_p \bar{\underset{\rightarrow}{u}}$$

Therefore, LVACE of the particles becomes

$$\frac{\partial \bar{n}_p}{\partial t} + \vec{\nabla} \cdot \bar{n}_p \underline{\bar{u}} + \Sigma \vec{\nabla} \cdot \underline{\bar{J}}_{p,ext} = - \frac{1}{V} \int_{S_i} n_p \underline{u} \cdot \underline{n} \, dS$$

$$- \Sigma \frac{1}{V} \int_{S_i} \underline{J}_{p,ext} \underline{n} \, dS$$

.....(4.1.12)

The physical significance of the first term on the right hand side of the above equation is that it represents the rate of depletion of particles at the gas-liquid interface due to aerodynamic effects. Similarly the second term is the rate of depletion of particles at the interface due to external forces. Let A represent the rate of aerodynamic collection,

$$A = \frac{1}{V} \int_{S_i} n_p \underline{u} \cdot \underline{n} \, dS \qquad (4.1.13)$$

Since the geometry of the interface in a scrubber is not known it can be postulated, similarly to mass transfer, that the rate of aerodynamic capture may be written as

$$A = k'_p \, n_p \, a \qquad (4.1.14)$$

where a is gas-liquid interfacial area per unit volume of the contactor, and k'_p can by analogy to mass transfer be called the "area-based particle transfer coefficient". Likewise by analogy to mass transfer the variables

may be further consolidated by defining a "volumetric particle transfer coefficient", k_p, as

$$k_p = k'_p \, a \qquad (4.1.15)$$

The rate of aerodynamic collection may then be expressed as

$$A = k_p \, n_p \qquad (4.1.16)$$

Furthermore, the flux due to an external force can be expressed as

$$\underset{\rightarrow}{J}_{p,ext} = n_p \, \underset{\rightarrow}{u}_{p,ext} \qquad (4.1.17)$$

For the same reason of the complexity of shape of the interface, the rate of depletion of particles at the interface due to a phoretic force can be written as

$$\frac{1}{V} \int_{S_i} \underset{\rightarrow}{J}_p \cdot \underset{\rightarrow}{n} \, dS = \overline{J}_{p,ext} \, a$$

$$= \overline{n}_p \, \overline{u}_{p,ext} \, a \qquad .....(4.1.18)$$

Incorporating these several changes, the LVACE for particles becomes

$$\frac{\partial \overline{n}_p}{\partial t} + \vec{\nabla} \cdot \overline{n}_p \, \underset{\rightarrow}{\overline{u}} + \Sigma \, \vec{\nabla} \cdot \overline{n}_p \, \underset{\rightarrow}{\overline{u}}_{p,ext} = - k_p \, \overline{n}_p - \Sigma \, \overline{n}_p \, \overline{u}_{p,ext} \, a$$

.....(4.1.19)

One further consolidation may be obtained by adding the phoretic velocities to the convective velocity. Thus the final form of the LVACE for particles in any gas-liquid scrubber for which there is no significant particle collection by diffusion is as follows:

$$\frac{\partial \bar{n}_p}{\partial t} + \vec{\nabla} \cdot \bar{n}_p \vec{\bar{u}}_p = - k_p \bar{n}_p - \Sigma \bar{n}_p \bar{u}_{p,ext} a \qquad (4.1.20)$$

4.2 LOCAL VOLUME AVERAGED EQUATION OF CONTINUITY FOR THE GAS PHASE

For simplicity, the gas phase is considered here as having two components. Component "1" is a solute which transfers across the gas-liquid interface while component "2" does not transfer between the gas and liquid phase.

LVACE for Component 1:

Similarly to Section 4.1, the local volume average of the continuity equation for solute can be written as follows:

$$\frac{1}{V} \int_{V_G} \left(\frac{\partial \rho_1}{\partial t} + \vec{\nabla} \cdot \underset{\rightarrow}{n}_1 - r_1\right) dV = 0 \qquad (4.2.1)$$

Since,

$$\frac{1}{V} \int_{V_G} \frac{\partial \rho_1}{\partial t} dV = \frac{\partial \bar{\rho}_1}{\partial t} \qquad (4.2.2)$$

and,

$$\frac{1}{V} \int_{V_G} r_1 \, dV = \bar{r}_1 \qquad (4.2.3)$$

and also using the theorem of the volume average of a divergence,

$$\frac{\partial \rho_1}{\partial t} + \vec{\nabla} \cdot \underset{\rightarrow}{\overline{n}}_1 + \frac{1}{V} \int_{S_i} \underset{\rightarrow}{n}_1 \cdot \underset{\rightarrow}{n} \, dS - \overline{r}_1 = 0 \qquad (4.2.4)$$

letting,

$$\frac{1}{V} \int_{S_i} \underset{\rightarrow}{n}_1 \cdot \underset{\rightarrow}{n} \, dS = \overline{n}_1 \, a \qquad (4.2.5)$$

the continuity equation for the transferring component becomes

$$\frac{\partial \overline{\rho}_1}{\partial t} + \vec{\nabla} \cdot \underset{\rightarrow}{\overline{n}}_1 + \overline{n}_1 \, a - \overline{r}_1 = 0 \qquad (4.2.6)$$

LVACE for Component 2:

For the component for which there is no interfacial transfer one may write:

$$\frac{\partial \overline{\rho}_2}{\partial t} + \vec{\nabla} \cdot \underset{\rightarrow}{\overline{n}}_2 - \overline{r}_2 = 0 \qquad (4.2.7)$$

LVACE for the Total Gas Phase:

By adding Equations (4.2.6) and (4.2.7) one obtains

$$\frac{\partial \overline{\rho}}{\partial t} + \vec{\nabla} \cdot \overline{\rho} \, \underset{\rightarrow}{\overline{u}} = - \overline{n}_1 \, a \qquad (4.2.8)$$

The second term in the above equation is the divergence of the total flux which contains both convective and diffusional fluxes.

4.3 EVALUATION OF PARTICLE PENETRATION IN THE ABSENCE OF ANY PHORETIC FORCE

When there are no external flux forces exerted on the system, Equation (4.1.20) for the LVACE of the particle reduces to

$$\frac{\partial \bar{n}_p}{\partial t} + \vec{\nabla} \cdot \bar{n}_p \, \underset{\rightarrow}{\bar{u}}_p = - k_p \, \bar{n}_p \qquad (4.3.1)$$

As this case includes the absence of diffusiophoresis, there can be no gas-liquid interfacial component transfer. Therefore the LVACE for the gas phase (Equation (4.2.8)) becomes

$$\frac{\partial \bar{\rho}}{\partial t} + \vec{\nabla} \cdot \bar{\rho} \, \underset{\rightarrow}{\bar{u}} = 0 \qquad (4.3.2)$$

In order to proceed further an assumption must be made for the velocities of the gas phase and of particles in the gas. It is reasonable to assume that, at steady state flow, the whole stream containing gas and suspended particles will move with one velocity. According to Newton's second law, this velocity is that of the center of mass of the system. Thus the amount and density of the particles and gas affect the overall velocity of the stream. Separate evaluation of the velocity of the gas and of the particles is more complex. Particle-gas relative motion involves a drag force acting between them. Depending on the temperature of gas and conductivity of the particle, the phenomenon of thermal slip at the surface of the particles may also exist. Moreover, as mentioned in Section 2.2.1.3, the effect of particles on the gas flow carrying them is not yet well defined. Nevertheless, for

dilute particle concentrations one can generally assume that particles would adopt the gas mass velocity. This is the assumption usually made in overall balances. Even for simple problems, such as numerical solution for inertial collection efficiency of a sphere, this assumption is made for conditions upstream from the collector (Section 2.2.1.1).

For the present case of no mass transfer, neglecting temperature and pressure variations along the column, density of the gas can be assumed constant so that Equation (4.3.2) yields

$$\vec{\nabla} \cdot \underset{\rightarrow}{\bar{u}} = 0 \tag{4.3.3}$$

Hence, the LVACE of the particles becomes, for steady state,

$$\underset{\rightarrow}{\bar{u}} \cdot \vec{\nabla} \bar{n}_p = - k_p \bar{n}_p \tag{4.3.4}$$

Neglecting components of the velocity vector other than u_z, this equation upon integration yields

$$\frac{\bar{n}_{p,out}}{\bar{n}_{p,in}} = \exp \{- k_p H/u_z\} \tag{4.3.5}$$

Since mass flow rate of gas does not change along the column, particle penetration through a gas-liquid contactor in the absence of any phoretic force may then be expressed according to the definition of penetration (Equation (4.1)) as

$$Pt = \exp \{- k_p H/u_z\} \tag{4.3.6}$$

4.4 EVALUATION OF PARTICLE PENETRATION IN THE PRESENCE OF DIFFUSIOPHORESIS

The LVACE of particles written as Equation (4.1.20) permits consideration of any phoretic mechanism that may apply in a particle collection device. For scrubbers, the most likely external flux is diffusiophoresis. Depending on the direction of the flux of diffusing component, overall efficiency of a column is either increased or decreased by diffusiophoresis. In industrial applications the flux is normally towards the gas-liquid interface because of condensation of vapor, usually water, when diffusiophoresis is used to improve particle collection efficiency.

The review given in Section 2.2.2.1 indicates that Knudsen number, the relative size of the particle with respect to the mean free path of the gas molecules, is an important criterion for motion of particles due to diffusiophoresis. Using this fundamental criterion, particles may be classified for size as small, intermediate and large. As the mean free path of most common gases is of the order of 0.05 μm under typical processing conditions, particles of the size 0.35 to 10 μm of interest in the present research would exhibit large particle behaviour. It is interesting to note that, having made this classification, the diffusiophoretic particle velocities, as presented in Section 2.2.2.1, are independent of the particle size for the size ranges defined earlier as "small" and "large" particles. The remainder of the analysis applies for "large" particles, i.e. for Knudsen number less than one.

Particle velocity expressions used will be for the case where one component is diffusing through an inert component towards gas-liquid

interface. Using Kramers and Kistemaker's (1943) slip coefficient (Equation (2.2.62)), the diffusiophoretic particle velocity suggested by Waldmann and Schmitt (1966) (Equation (2.2.66)), with $a_1 = a_2$, becomes

$$u_{pd} = - \frac{\sqrt{m_1}}{x_1\sqrt{m_1} + x_2\sqrt{m_2}} \frac{D}{x_2}(\nabla x_1)_\infty \qquad (2.2.60)^*$$

Whitmore's (1976) expression for large particles is

$$u_{pd} = -\frac{M_1}{M} \frac{D}{x_2}(\nabla x_1)_\infty \qquad (2.2.68)$$

Furthermore, Whitmore et al. (1977) suggest that the mean molar velocity of the gas phase can be used as an approximate limit for intermediate particle velocities. This is then the lower limit for large particles. Therefore,

$$u_{pd} = - \frac{D}{x_2}(\nabla x_1)_\infty \qquad (4.4.1)$$

The objective is then to obtain expressions for particle penetration using these diffusiophoretic velocities. Since in the gas film at the gas-liquid interface,

$$N_1 = - \frac{cD}{x_2}(\nabla x_1)_\infty \qquad (4.4.2)$$

---

* It may be noted that molecule masses, m_i, can be replaced by the molecular weights, M_i.

and, $N_2 = 0$ (4.4.3)

The above expressions for diffusiophoretic particle velocity can be rewritten as follows for the three cases:

i) particles moving with Schmitt-Waldmann velocity

$$u_{pd} = \frac{\sqrt{M_1}}{x_1\sqrt{M_1} + x_2\sqrt{M_2}} \frac{N_1}{c} \tag{4.4.4}$$

ii) particles moving with the mean mass velocity of the gas

$$u_{pd} = \frac{M_1}{M} \frac{N_1}{c} \tag{4.4.5}$$

iii) particles moving with the mean molar velocity of the gas

$$u_{pd} = \frac{N_1}{c} \tag{4.4.6}$$

As suggested by Whitmore (1976), by making a proper choice for the velocity and concentration terms in the continuity equations for the particle and the gas, a general simultaneous solution can be obtained. For the case of particles moving with the gas mean mass velocity the natural choice would be to write the LVACE's in terms of density and mass velocity, while for the case of particles moving with the gas mean molar velocity, in terms of molar concentration and molar velocity. For the case of particles moving with the Schmitt-Waldmann velocity, Whitmore (1976) introduced "root mass" variables as follows:

$$c_i^r = c_i \sqrt{M_i} \qquad (4.4.7\text{-a})$$

$$N_i^r = N_i \sqrt{M_i} \qquad (4.4.7\text{-b})$$

$$c^r = \Sigma c_i^r \qquad (4.4.7\text{-c})$$

$$N^r = \Sigma N_i^r \qquad (4.4.7\text{-d})$$

$$u^r = \frac{N^r}{c^r} \qquad (4.4.7\text{-e})$$

From Equations (4.1.20) and (4.2.8), the general LVACE for particles and for gas can be then written as

$$\frac{\partial \bar{n}_p}{\partial t} + \vec{\nabla} \cdot \bar{n}_p \vec{\bar{u}}^{+} = - k_p \bar{n}_p - \bar{n}_p \bar{u}_{pd}^{+} a \qquad (4.4.8)$$

$$\frac{\partial \vec{\bar{c}}^{+}}{\partial t} + \vec{\nabla} \cdot \bar{c}^{+} \vec{\bar{u}}^{+} = - \bar{N}_1^{+} a \qquad (4.4.9)$$

The terms with superscript (+) correspond to those for either one of the three cases.

Multiplying the particle LVACE by $1/\bar{c}^{+}$ and the gas LVACE by $\bar{n}_p/\bar{c}^{+2}$, and subtracting the second from the first,

$$\{\frac{1}{\bar{c}^{+}} \frac{\partial \bar{n}_p}{\partial t} - \frac{\bar{n}_p}{\bar{c}^{+2}} \frac{\partial \bar{c}^{+}}{\partial t}\} + \{\frac{1}{\bar{c}^{+}} \vec{\nabla} \cdot \bar{n}_p \vec{\bar{u}}^{+} - \frac{\bar{n}_p}{\bar{c}^{+2}} \vec{\nabla} \cdot \bar{c}^{+} \vec{\bar{u}}^{+}\}$$

$$= - k_p \bar{n}_p - \frac{\bar{n}_p}{\bar{c}^{+}} \bar{u}_{pd}^{+} a + \frac{\bar{n}_p}{\bar{c}^{+2}} \bar{N}_1^{+} a \qquad (4.4.10)$$

Since, $$\overline{u}_{pd}^{+} = \frac{\overline{N}_1^{+}}{\overline{c}^{+}} \qquad (4.4.11)$$

after some simplifications,

$$\frac{\partial(\overline{n}_p/\overline{c}^{+})}{\partial t} + \vec{\overline{u}}^{+} \cdot \vec{\nabla}\,(\overline{n}_p/\overline{c}^{+}) = - k_p(\overline{n}_p/\overline{c}^{+}) \qquad (4.4.12)$$

It is appropriate to note here that when Whitmore (1976) wrote the continuity equations, he did not consider the rate of particle removal at the gas-liquid interface, represented by the terms at the right hand side of Equations (4.4.8) and (4.4.9). His analysis was not based on the use of LVACE's and he equated the left hand sides of the continuity equations to zero. Continuity equations thus written describe flow of gas-particle streams without particle transfer across the gas-liquid interface. Further, they cannot be solved due to lack of information on boundary conditions because the shape and size of the interface in scrubbers are not known. Correct forms of continuity equations of gas and particle with interphase particle transfer in a scrubber must be of the form of Equations (4.4.8) and (4.4.9) which are LVACE's. It is interesting to note that the last two terms in Equation (4.4.10) cancel due to the diffusiophoretic velocity expression as given in Equation (4.4.11). This, fortuitously, enabled Whitmore to arrive at a similar expression to Equation (4.4.12) with the right hand side as zero because he did not consider the aerodynamic collection. As a matter of fact, one should be very careful in considering the interfacial transfer and for its proper treatment, LVACE's must be used.

Equation (4.4.12) can be further simplified by making the usual assumptions for scrubbers, i.e. that steady state applies over the entire contactor and the variation of $(\bar{n}_p/\bar{c}^+)$ in the x and y directions (or r and θ directions in cylindrical coordinates) is negligible. Thus,

$$\bar{u}_z^+ \frac{d(\bar{n}_p/\bar{c}^+)}{dz} = - k_p (\bar{n}_p/\bar{c}^+) \tag{4.4.13}$$

Integration of this equation between the inlet and outlet of the column yields

$$\ln \frac{(\bar{n}_p/\bar{c}^+)_{out}}{(\bar{n}_p/\bar{c}^+)_{in}} = - \int_{z=0}^{z=H} \frac{k_p}{\bar{u}_z^+} dz \tag{4.4.14}$$

Now recalling the definition of particle penetration in a scrubber (Equation (4.1)), the general expression for penetration can be written as:

$$Pt = \frac{(\bar{n}_p/\bar{c}^+)_{out} \bar{c}^+_{out} \bar{u}^+_{out}}{(\bar{n}_p/\bar{c}^+)_{in} \bar{c}^+_{in} \bar{u}^+_{in}} \tag{4.4.15}$$

or,

$$Pt = \frac{\bar{c}^+_{out} \bar{u}^+_{out}}{\bar{c}^+_{in} \bar{u}^+_{in}} \exp \{- \int_{z=0}^{z=H} \frac{k_p}{\bar{u}_z^+} dz\} \tag{4.4.16}$$

As the exponential term is the penetration due to aerodynamic effects, the first term is the penetration due to diffusiophoresis, i.e.

$$Pt_A = \exp \{- \int_{z=0}^{z=H} \frac{k_p}{\bar{u}_z^+} dz\} \tag{4.4.17}$$

$$Pt_D = \frac{\overline{c}^{+}_{out}\ \overline{u}^{+}_{out}}{\overline{c}^{+}_{in}\ \overline{u}^{+}_{in}} \qquad (4.4.18)$$

and

$$Pt = Pt_A\ Pt_D \qquad (4.4.19)$$

The integral sign in the expression for Pt_A is retained in order to emphasize that, along the column, velocity changes, and so does the value of penetration due to aerodynamic mechanisms, because of the change in gas density. For small condensation rates and for small variations in temperature and pressure of the gas, however, an average value for velocity can be used, thus giving the simpler expression

$$Pt_A = \exp\{- k_p H/\overline{u}^{+}_{z,ave}\} \qquad (4.4.20)$$

The final integrated Equations (4.4.18) and (4.4.20) can be written more explicitly for the cases corresponding to three alternate choices for particle velocity, as follows:

i) For particles moving with the Schmitt-Waldmann velocity:

$$Pt_A = \exp\{- k_p H/u^{r}_{z,ave}\} \qquad (4.4.21)$$

$$Pt_D = \frac{\overline{c}^{r}_{out}\ \overline{u}^{r}_{out}}{\overline{c}^{r}_{in}\ \overline{u}^{r}_{in}} = \frac{\overline{N}^{r}_{out}}{\overline{N}^{r}_{in}} \qquad .....(4.4.22)$$

ii) For particles moving with the gas mean mass velocity:

$$Pt_A = \exp \{- k_p H/u_{z,ave}\} \qquad (4.4.23)$$

$$Pt_D = \frac{\overline{\rho}_{out}\ \overline{u}_{out}}{\overline{\rho}_{in}\ \overline{u}_{in}} = \frac{\overline{G}_{out}}{\overline{G}_{in}} \qquad .....(4.4.24)$$

iii) For particles moving with the gas mean molar velocity:

$$Pt_A = \exp \{- k_p H/u^*_{z,ave}\} \qquad (4.4.25)$$

$$Pt_D = \frac{\overline{c}_{out}\ \overline{u}^*_{out}}{\overline{c}_{in}\ \overline{u}^*_{in}} = \frac{\overline{F}_{out}}{\overline{F}_{in}} \qquad (4.4.26)$$

For all these cases, of course, it is to be noted that Equation (4.4.19) holds.

4.5 SUMMARY

To date there had been no general theoretical framework available as a guide to the analysis of particulate collection in gas-liquid contactors. In this connection it is to be noted that particle transfer from gas to liquid is different from mass or heat transfer in the sense that particle transfer is not linked to a gradient of some

intensive variable as mass and heat transfer are to gradients in concentration or temperature. Rather, particle transfer occurs due to aerodynamic and phoretic transfer mechanisms. A general theoretical analysis for particulate collection in gas-liquid contactors has been developed in this chapter by writing and combining appropriately the local volume averaged continuity equation (LVACE) of the particles and of the gas phase. The development has been carried out with few assumptions in order that this framework would be generally applicable to a wide variety of types of gas-liquid contactors used for particulate removal.

As the geometry of the gas-liquid interface is not known for many contacting devices, it is not possible to evaluate the term in the LVACE which requires integration over this interfacial area for particle transfer by aerodynamic mechanisms. It is therefore necessary to introduce a particle transfer coefficient, k_p, analogous to volume-based interfacial mass transfer coefficients.

The results of this theoretical treatment are given in the form of expressions for particle penetration through a contactor for two general cases. For the case when particle collection is due only to aerodynamic collection mechanisms, i.e. in the absence of any phoretic collection, particle penetration, Pt, is given as Equation (4.3.6). Then, for the case of simultaneous aerodynamic and diffusiophoretic collection, a general expression for particle penetration is presented as Equation (4.4.16). As this equation is given in completely general form with respect to diffusiophoretic velocity, the general solution is then expanded for three specific choices of diffusiophoretic particle velocity.

This theoretical treatment shows that the effect of diffusiophoresis on overall particle collection efficiency of a scrubber is directly proportional to the amount of the vapor which is transferred across the gas-liquid interface (Equation (4.4.18)). The analysis also shows that, in the case of particle collection simultaneously by aerodynamic and diffusiophoretic mechanisms, particle penetration is simply the product of the particle penetration by each mechanism independently (Equation (4.4.19)).

The theoretical framework for particulate collection provided in Chapter 4 involves a particle transfer coefficient, k_p, for whatever aerodynamic collection mechanisms apply in the specific case. The analysis of particulate collection given in Chapter 3 established that, of the various aerodynamic capture mechanisms, only inertial impaction was significant in the MBC process. As noted earlier, it is unfortunately not possible to predict the particle transfer coefficient theoretically due to the complexity of gas-liquid contacting in the mobile-bed. Experimental guidance is therefore necessary. The experimental program described in the next chapter was designed to determine k_p for the MBC process.

CHAPTER 5

EXPERIMENTAL EQUIPMENT AND PROCEDURE

5.1 GENERAL

The experimental facility and procedures were developed with the objective of determining for mobile-bed contacting the particle transfer coefficient, k_p, which is required for the general theoretical expressions (Equations (4.3.6) and (4.4.16)) for particle penetration in any gas-liquid contactor. As aerodynamic particle capture mechanisms are always present, while those due to external flux forces are involved only when such forces are exerted on the system, a particulate recovery device is characterized by its performance due to aerodynamic capture mechanisms. Thus the overall design was first to determine k_p with no external flux force, and then to study the effect of the industrially significant flux force, namely, diffusiophoresis. Characterization of MBC without diffusiophoresis took up the major part of the program, while a relatively few experiments served to determine the additional effect of diffusiophoresis. Six variables which affect inertial impaction efficiency in a MBC column are:

i) liquid flow rate,

ii) gas flow rate,

iii) packing size,

iv) static height of the bed,

v) particle size, and

vi) type (hydrophobicity) of particles.

Hence, characterization of the MBC process for particulate collection required design of experiments to study the effect of each of these variables.

In order to analyze performance with respect to particle collection the hydrodynamics of the system must be known. As appreciable differences exist among reported studies on this aspect of MBC, a new and comprehensive study was also made to define the system hydrodynamics, namely, bed expansion, minimum fluidization velocity, pressure drop and liquid holdup.

5.2 EQUIPMENT

Figure 5.1 shows the flow diagram of the pilot-plant scale MBC experimental facility. Details of this unit with all the auxiliary equipment follow.

5.2.1 Mobile-Bed Column

The test column was made of 0.29 m ID plexiglass pipe. A packing support screen with 87% open area was located between the column and inlet gas distribution section. This lower grid was made of 23 steel rods of diameter 1.5 mm. With such a large open area this grid was very similar to those used in industrial scale MBC units. The use of a high open-area grid avoided the shortcoming of most published studies, namely, low open-area supports causing the hydrodynamic behaviour of the bed to be significantly different from that which corresponds to industrial practice.

FIGURE 5.1. Flow Diagram Legend

B : Blower
DH : Duct heater
ES : Entrainment separator
F : Filter
FC : Flow controller
FS : Steam filter
FSP : Flow straightening pipes
GD : Gas distributor
HC : Humidification column
LD : Liquid distributor
LI : Level indicator
M : Manometer
MBC : Mobile bed column
MC : Mixing chamber
ME : Mist eliminator
MLD : Main liquid distributor
O : Orifice
PC : Particle counter
PG : Particle generator
PR1, PR2 : Pressure reducers
PSN : Particle sampling nozzle
RL : Liquid rotameter
RS : Steam rotameter
S : Strainer
ST : Steam trap
TC : Temperature controller
T_{db} : Dry bulb thermometer
T_{wb} : Wet bulb thermometer
V : Valve

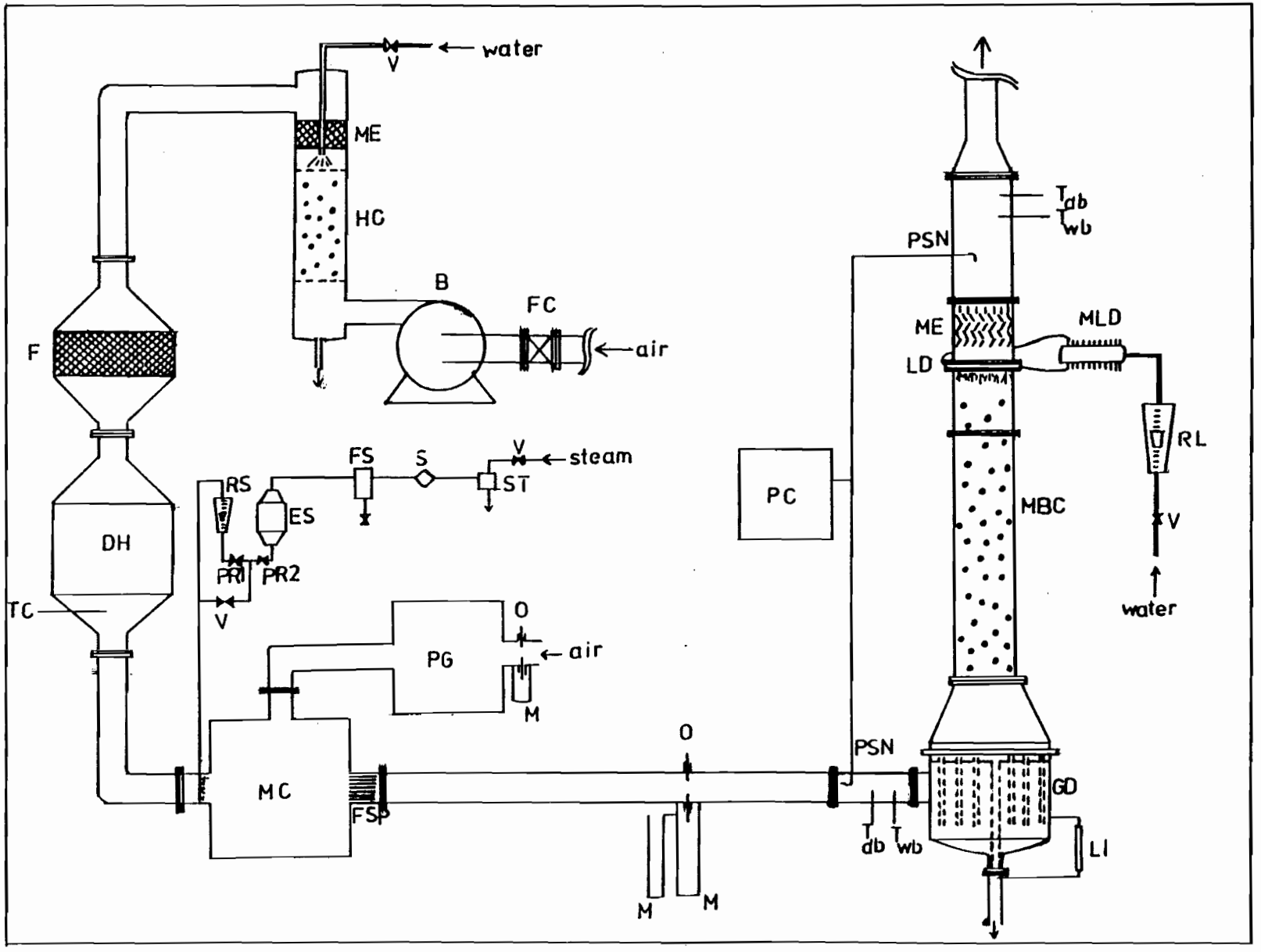

FIGURE 5.1. Mobile-bed contactor experimental facility

At a height of 0.46 m above the support grid a co-centric access port, 0.14x0.14 m, was provided for loading and unloading of the bed packing. The liquid distributer, which served also as the upper retaining grid for the packing, was located 1.5 m above the lower grid. A 5-stage baffle type entrainment separator was located 0.15 m above the liquid distributor. A further 0.6 m section of the 0.29 m column above the entrainment separator allowed for placement of a pitot-tube to measure gas velocity and a sampling probe for particle analysis. Above this there was a converging aluminum section to the air exit duct, a 0.178 m diameter flexible hose.

The column was packed with polypropylene balls of density 157 kg/m^3 (Precision Plastic Ball Co., Chicago, Illinois), which is the density of packing most commonly used in industry. Three static bed heights (0.29 m, 0.44 m and 0.58 m) and three packing sizes (38 mm, 25 mm and 19 mm) were employed in the experiments. These packings provided D_c/d_{pb} ratios between 7.6 - 15.3.

The gas distributing plenum chamber below the column was the one used by Chen and Douglas (1968 and 1969) and consisted of a conical section 0.61 m high between a 0.61 m high x 0.61 m diameter flow straightening section and the 0.29 m diameter experimental tower. Flow straightening and distribution of the inlet gas flow was achieved by passage through 32 aluminum tubes, 0.05 m diameter x 0.37 m long, housed in this 0.61 m diameter cylindrical section. Flow through the converging section (0.61 m to 0.29 m diameter) above the straightener gave a flat velocity profile gas flow to the mobile-bed. Figure 5.2 shows the velocity distribution measured at 0.05 m below the bed support grid by a standard pitot tube and a micromanometer.

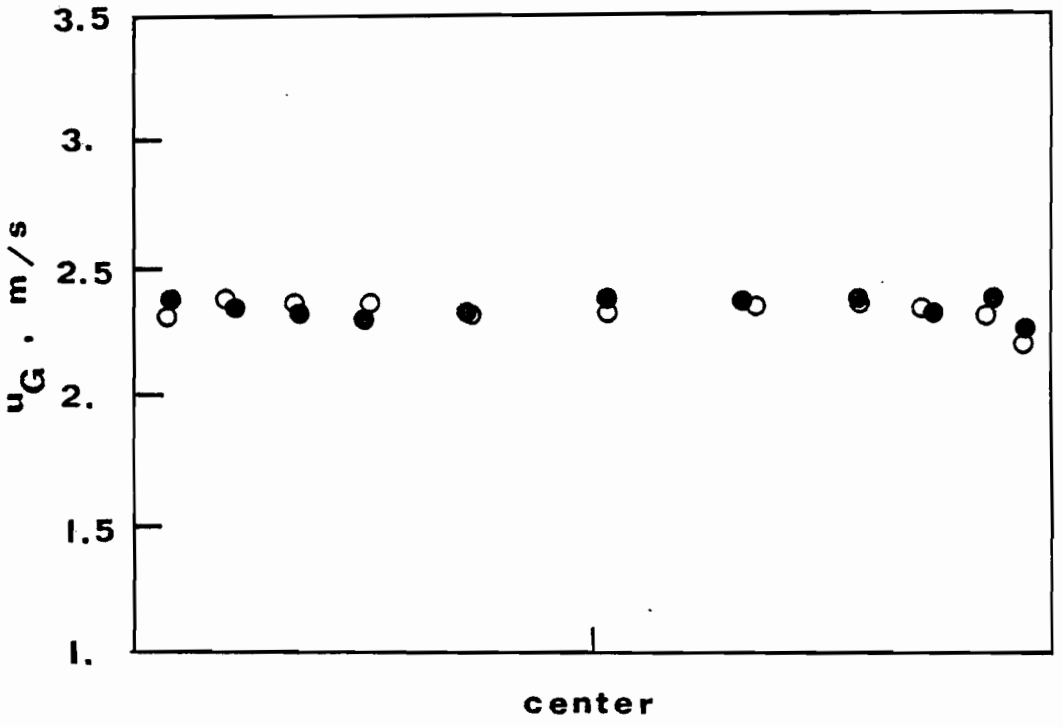

FIGURE 5.2. Air velocity profiles at the column entrance.

Average velocity = 2.4 m/s

○ Perpendicular to the air inlet duct

● Parallel to the air inlet duct

5.2.2 Gas Flow System

The relatively large air flow rates required for this study were delivered by a 30 H.P. blower. The blower discharge was conditioned by passage through a humidification column which was in fact a small MBC column with 38 mm packing, and equipped with a demister (York Company, Model 30455). In order to remove suspended particles, the air then passed through a fire resistant filter (American Air Filter of Canada Ltd., Model 6A74J/R3). This filter was guaranteed by the manufacturer to be 99.5% efficient for 0.3 μm DOP particles.

High humidity air, when required for experiments with diffusiophoresis, was provided by heating and injecting steam into the inlet air. Heating the air was accomplished by a 100 KW single stage electrical duct heater (specially manufactured by Playford Co., Montreal) equipped with a 150 A SCR proportional controller (Honeywell, Model R7308E1259) and temperature controller (United Electric, Model 5600). Building steam for humidification was admitted through a strainer, a filter and an entrainment separator (Centrifix Corp., Cleveland, Ohio) which was guaranteed to remove 99% of all entrainment. Humidity of the air stream was monitored by wet- and dry-bulb thermometers. The clean air thus heated and humidified to the desired level is mixed, in a cubical chamber 0.6x0.6x0.6 m, with the stream from the aerosol generator. A bundle of flow straightening pipes (25 mm copper pipes) were placed in the duct at the mixing chamber exit to eliminate large-scale turbulence and swirl. The orifice for flow rate measurement, located 2.1 m downstream from these flow straightening sections, was calibrated with a standard pitot tube placed 0.3 m upstream of the orifice. Velocity

readings, taken with a micromanometer, were processed following the method of "centroid of equal areas" (ASME (1971)). The average value of the orifice coefficient found was $C = 0.6259$ (details in Appendix E). A 1.27 m length of inlet pipe was provided between the orifice and the MBC column to provide sufficient distance for redevelopment of the velocity profile prior to withdrawal of the air sample for particle analysis. All piping upstream of the MBC column was aluminum, 0.216 m ID.

5.2.3 Liquid Flow System

The liquid distributor in the column consisted of a parallel array of 11 stainless steel tubes, 4.8 mm (3/16 in.) ID , with the liquid exiting from 97 downwardly-directed, uniformly spaced nozzles (10 mm long x 1.6 mm (1/16 in.) diameter). High pressure plastic tubing connected both ends of each of these 11 tubes to a main header. This main header, a 0.38 m length of 85 mm diameter aluminum pipe, had 22 short nipples, (4.8 mm (3/16 in.) ID), 11 at each side, which were connected in pairs to both ends of the 11-tube liquid distributor in the column. With this design of distributor, very uniform liquid flow over the column cross section was achieved.

In order that the liquid distributor could also function as the upper retaining grid for the smallest packing used, steel rods (1.6 mm (1/16 in.)) were placed between each water distributor tube. This design provided 70% open area.

The flow rate of the tap water used as the liquid phase was measured by a rotameter (Brooks, Emerson Electric Co., Meter Size: 13, Tube No: R-13M-25-1, Float No: 13-LJ-1394).

5.2.4 Entrainment Separator

The top of a gas-liquid contactor normally contains a highly efficient demister for elimination of liquid droplets entrained in the exit gas. A steel mesh-pad type demister, such as the one used in this study for the humidification pre-treatment column, can remove liquid droplets down to a few microns. But the use of such an efficient demister for the mobile-bed column in this study would not be appropriate. As 0.3-10 μm particles were to be used, a less efficient demister was required in order that particles in this size range not be collected by the demister upstream of the particle sampler. For this specification a zigzag baffle type entrainment separator was an appropriate choice. Calculation of terminal velocity for liquid droplets at the gas velocities in MBC showed that drops with the diameter of up to a few hundred microns would be entrained. Therefore the ideal entrainment separator would have zero efficiency for particle diameters less than 10 μm, and 100% efficiency for removal of particles from 10 μm to several hundred microns. A zigzag demister was designed for which the performance curve was a satisfactory approach to this specification. The calculations and details are given in Appendix F. The separator consisted of 4 rows of zigzag baffles, of which each comprised 7 vanes, 60 mm wide. The angle between the vanes and the vertical flow direction of air was 30^{o}. At the top of these 4 zigzag sections, a fifth section with vertical vanes, 60 mm wide, was attached in order to straighten the air flow upstream of the gas sampler. The typical S-curve on Figure 5.3 shows the theoretical prediction of performance of this zigzag baffle demister for a typical air velocity of 3 m/s. The results

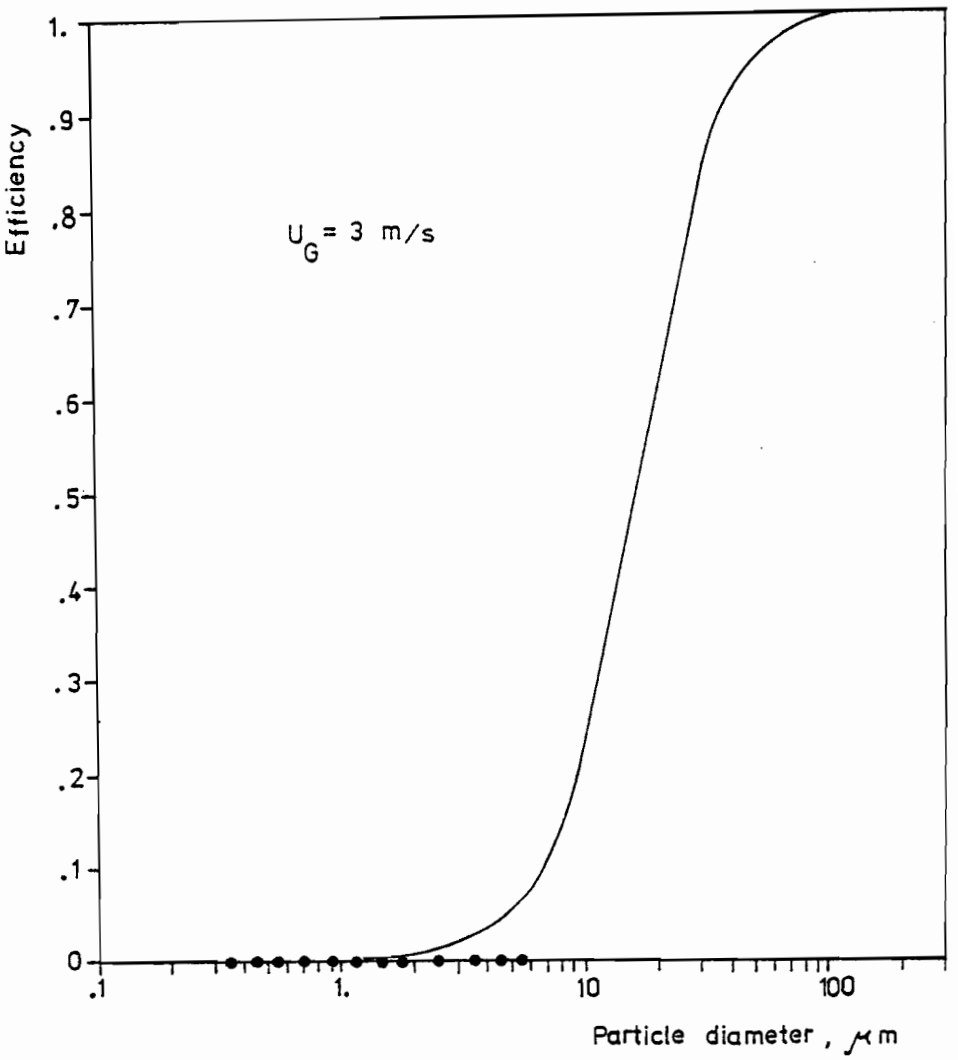

FIGURE 5.3. Collection efficiency of the zig-zag baffle type entrainment separator. Solid line is the theoretical prediction,

● Experimental

of an experimental check on the demister performance using ferrous sulphate particles, also shown on Figure 5.3, demonstrates that the actual efficiency was zero for the particle size range 0.3 to 6 μm, thus indicating that the theoretical curve is somewhat conservative.

5.2.5 Instrumentation

5.2.5.1 Pressure taps and transducer

A special pressure tap which had been successfully employed previously by Tichy et al. (1972) was used for pressure measurements (Figure 5.4). The gas-liquid mixture entering the tap was separated in a small cylindrical liquid knock-out vessel. The liquid closed the vessel in a siphon. The pressure in the vessel was therefore equal to the static pressure in the MBC column. One such pressure measurement assembly was located just above the lower grid, another just below the upper grid.

As pressure in an MBC column fluctuates appreciably, sometimes by as much as 15%, pressure measurement by a differential force balance pressure transducer is preferable to use of a U-tube manometer. A Foxboro instrument, Model 613 DM-MK-1, was used in this study. Pressure lines from the lower and upper taps were connected to the opposite sides of the twin-diaphragm differential sensing capsule of the pressure transducer. The difference between these pressures causes the diaphragm capsule to exert a force on the force bar which transmits this force to an electronic force-balance system. This system comprises a force-balance detector, a transistor-amplifier and a feedback torque motor. The pressure difference on the diaphragm capsule causes a change in

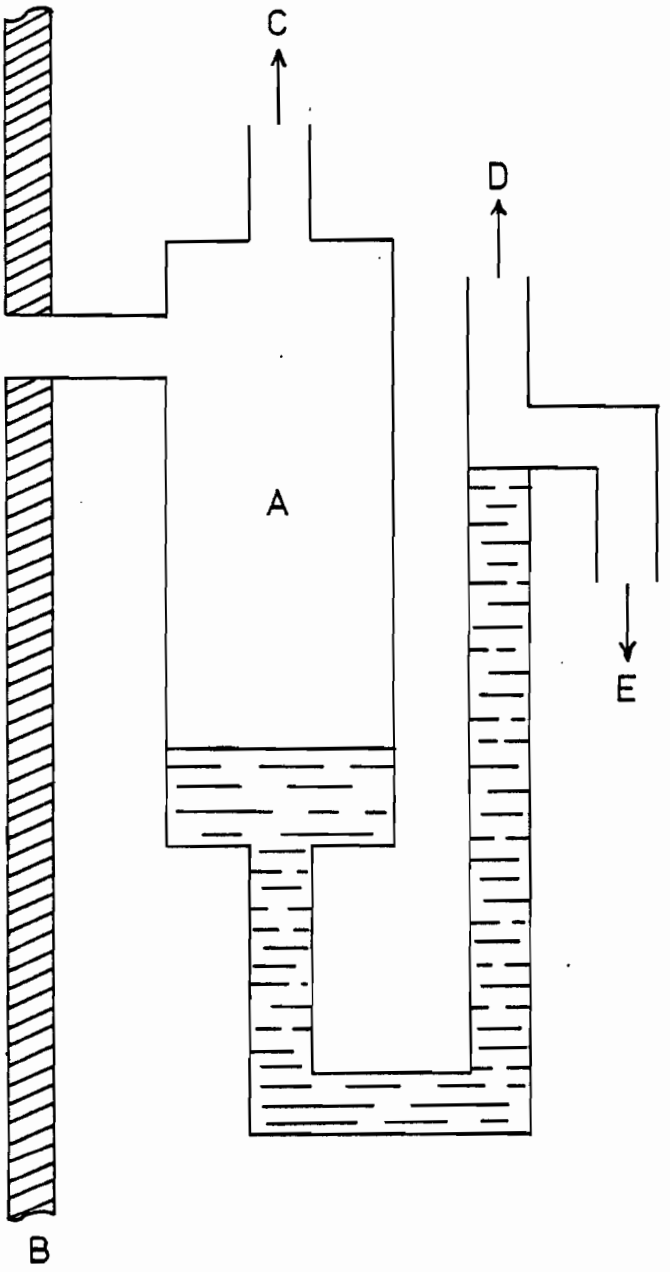

FIGURE 5.4. Tap for pressure measurements.
(To scale)

A - auxiliary vessel
B - wall of the Mobile-Bed Column
C - to the manometer and transducer
D - to atmosphere
E - overflow

output current of the transistor-amplifier which is detected by the voltmeter and transferred to the digital printer (Figure 5.5). The average of about 60 printed values during 45 seconds was taken as the pressure drop at any flow condition.

Calibration of the pressure transducer was made with a U-tube manometer at static conditions. The results are given in Appendix G.

5.2.5.2 The aerosol generator

The concentrated aerosol for introduction into the inlet stream to the MBC test column was produced by a spinning disk aerosol generator (Model 8330, Environmental Research Corporation, St.Paul, Minn.). The schematic diagram is shown in Figure 5.6. Ambient air for producing the concentrated aerosol is drawn through a calibrated orifice meter and into the mixing chamber by a blower mounted on the side of the mixing chamber. The air flow was fixed at 0.0236 m^3/s as suggested by the manufacturer. After being heated with a resistance element to ensure that the carrier liquid injected at the spinning disk would subsequently be evaporated, the air stream passes upwards through a filter into the plenum chamber. The air then flows downward through an 80 mesh stainless steel screen, to damp turbulence, into the air classifier section where the droplets from the spinning disk are injected and the associated carrier liquid is evaporated. As the final step, the air stream with the particles after evaporation of the carrier liquid then passes through an ionizer section. Here neutralization of residual electric charges on the particles is achieved by addition of a high concentration of bipolar ions generated by a Krypton 85 source.

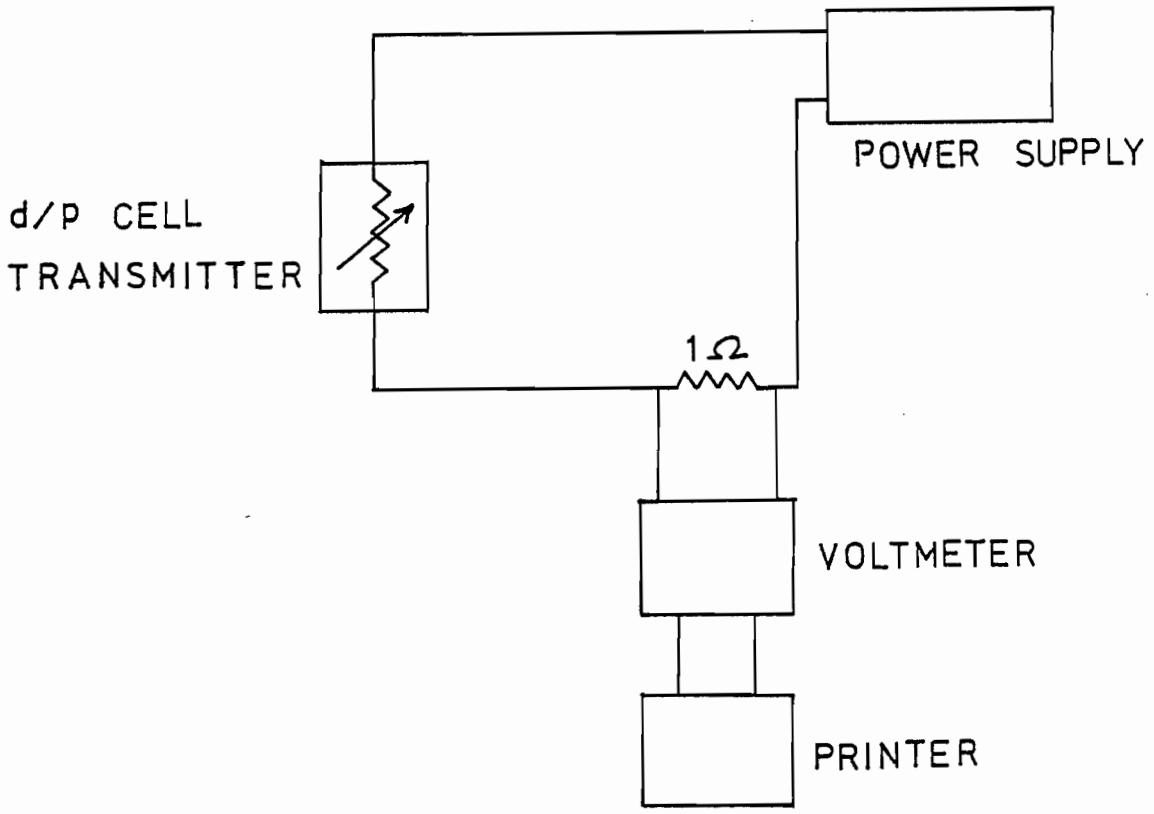

FIGURE 5.5. Circuit diagram for pressure measurements

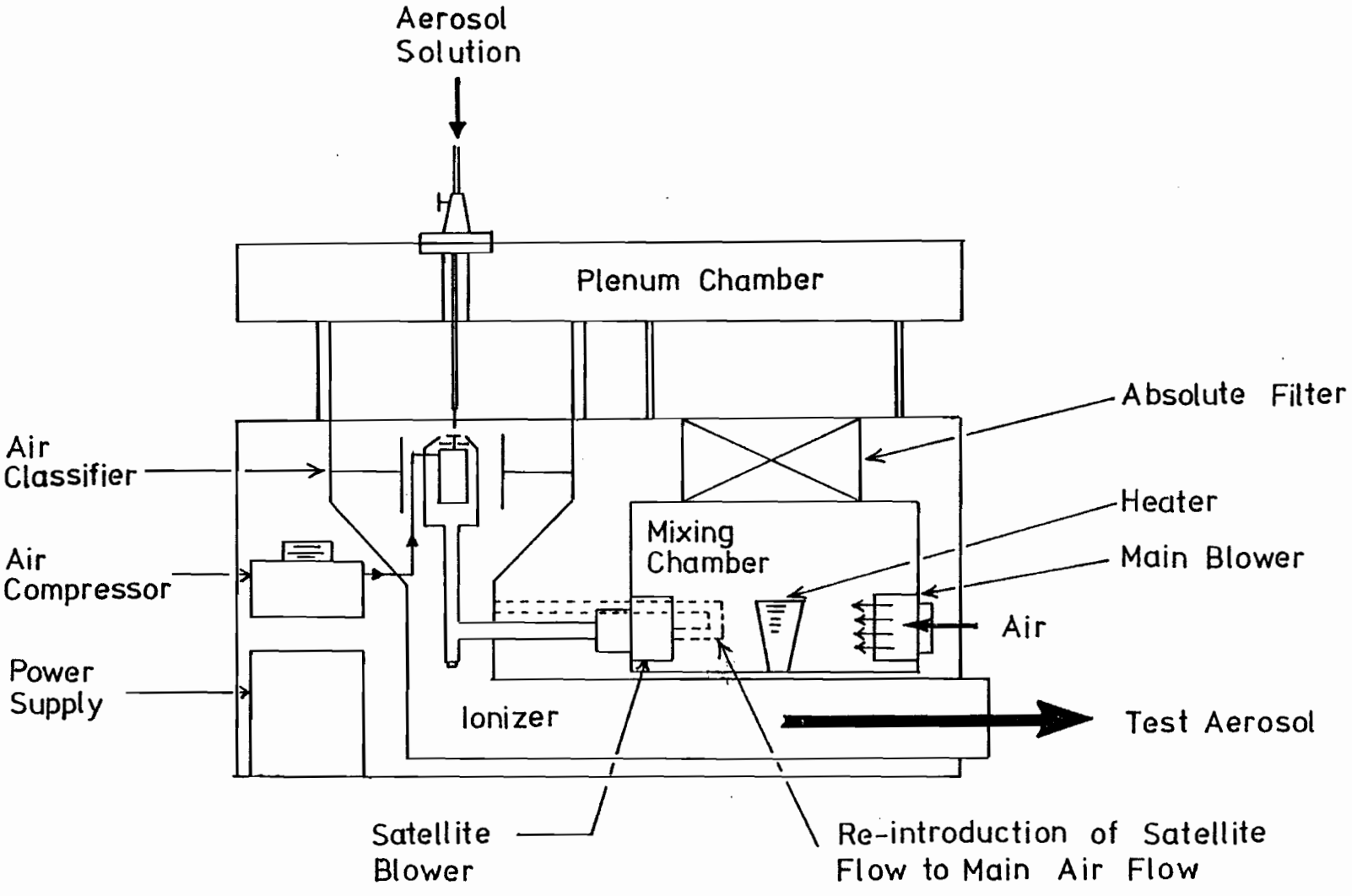

FIGURE 5.6. Schematic diagram of the spinning disk aerosol generator

The concentrated aerosol then leaves the generator unit to be mixed with the main gas inlet stream to the MBC column, as described in Section 5.2.2.

The aerosol material, in a solution or slurry of a volatile solvent carrier, is fed by a hypodermic needle (No.24) to the center of a 25.4 mm (1 in.) diameter stainless steel disk, which rotates at a speed of 60,000 r.p.m. The liquid is thereby atomized into two discrete droplet sizes. Primary droplets, approximately 30 microns in diameter, formed during liquid break-up, provide the homogeneous test aerosol. Smaller satellite droplets are also formed during liquid break-up. The size of the primary droplets, d_{pd}, is related to angular disk speed, w, disk diameter, d_{disk}, fluid surface tension, σ, and fluid density, ρ, by the following expression

$$d_{pd} = k(\sigma/\rho\ w^2\ d_{disk})^{1/2} \qquad (5.2.1)$$

The constant of proportionality, k, equal to $(12)^{1/2}$ according to theory, is reported by the aerosol generator manufacturer to vary over the range 2 to 7 depending on the disk speed and on the liquid used.

In the air classifier section of the generator, shown in great detail in Figure 5.7, the bimodal distribution from the spinning disk is separated into primary and satellite droplets. A flow rate of approximately $3x10^{-3}$ m^3/s, provided by a small satellite blower, was used to entrain the satellite droplets. In the process of passing the satellite removal head, this air flows around and cools the electric motor drive of the spinning disk.

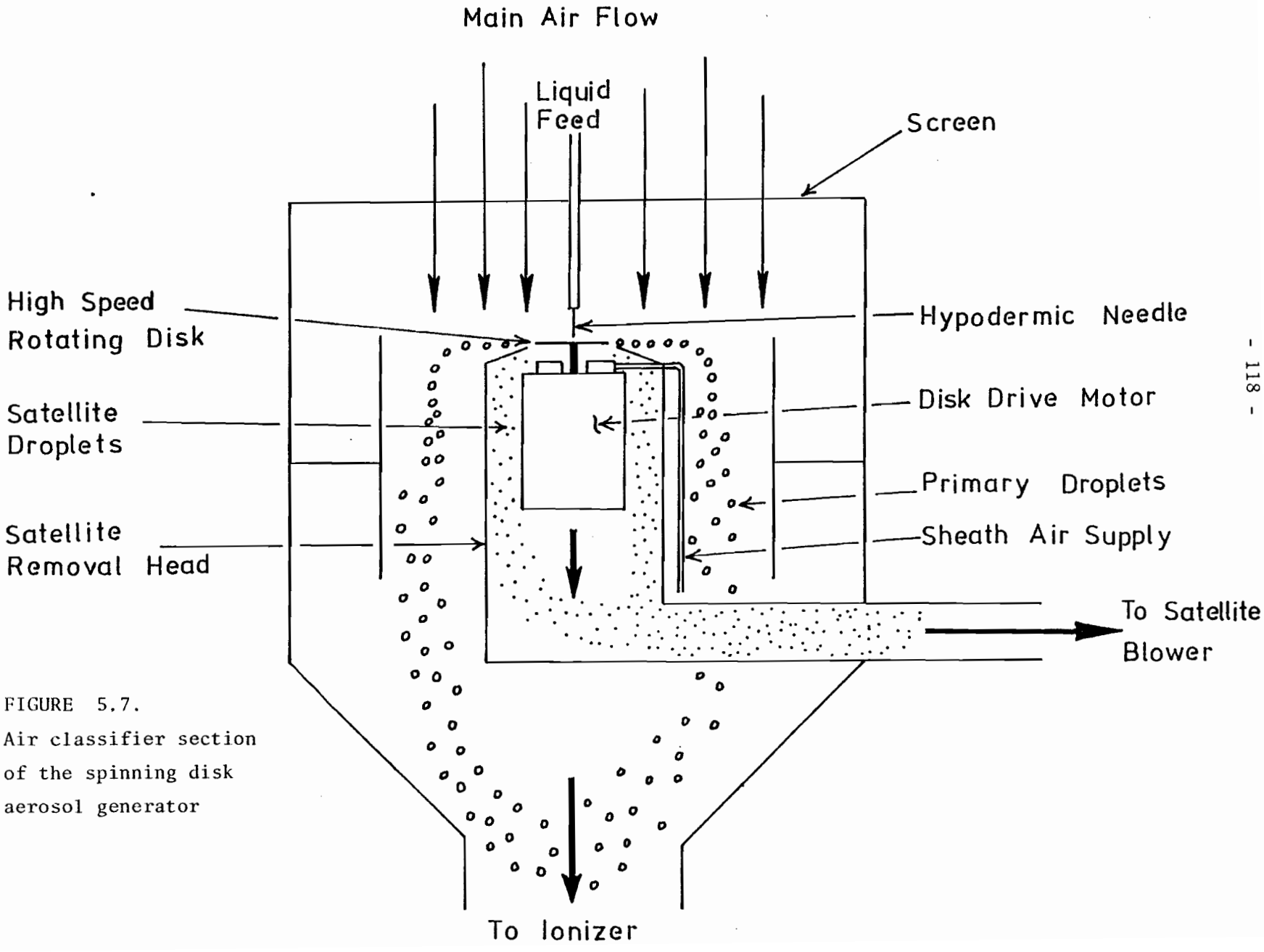

FIGURE 5.7.
Air classifier section of the spinning disk aerosol generator

In the original (1970) design of the manufacturer, the satellite droplets were discharged into the mixing chamber where evaporation of the carrier liquid was completed. The filter then captured all of these small particles. However, it was found that unavoidable small fluctuations in the satellite blower caused unacceptably large fluctuations in the concentration of aerosol produced by the generator. This operating characteristic had also been observed by the previous user, Doğanoğlu (1975). The aerosol generator was therefore modified by Doğanoğlu (1975) by connecting the output of the satellite blower to the test aerosol as shown by the broken line in Figure 5.6. This modification, which stabilized the operation of the aerosol generator, was also employed in the present study. Thus, any primary droplets captured by the satellite blower were re-introduced, with the satellite droplets, into the system. The satellite droplets are far too small to affect the monodispersity of the test aerosol around the measured peak range.

With this generator it was possible to obtain a particle concentration of around 10^8 particles/m^3 at the entrance of MBC and a standard deviation about 1.2, based on number size distribution.

This spinning disk generator was used successfully to produce all four kinds of particles used in the present study, i.e. ferrous sulphate, silica, latex and dioctyl phthalate (DOP). Most of the experiments were carried out using ferrous sulphate particles, with the other three materials being chosen in order to determine the effect of degree of hydrophobicity of the particle on collection efficiency in the MBC process. The respective solutions or dispersions fed to the

spinning disk were prepared as follows.

(1) Ferrous sulphate aerosol was produced from a 23% aqueous solution to which ethanol was added in the amount of 10%. The addition of ethanol lowers the surface tension of the solution, thus assuring that the spinning disk was well wetted.

(2) Silica particles were produced by first grinding 300 μm particles in a ball mill for 24 hours and then preparing a suspension of 15 wt% silica in a solution of 10% ethanol/90% distilled water.

(3) Latex dispersions were generated from 5 wt% of polyvinyl toluene latex dispersed in distilled water, directly as supplied by Dow Chemical Co., Midland, Michigan. The average size of these latex particles was 2 microns, the standard deviation, 0.0138 microns.

(4) Liquid aerosols were made from a 30% solution of DOP in methanol.

Two methods of supplying the feed solution to the spinning disk were tried:

(a) through a micro-metering peristaltic pump (Model 969, Harvard Apparatus Co. Inc., Dover, Mass.); and

(b) using a 4.5 ℓ bottle containing the solution at a height of 0.7 m, with gravity feed.

The second method was found to be superior, as it provided a constant aerosol concentration for much longer periods (up to 15 hours). The feeding rate of the aerosol solution to the spinning disk was about 400 mm^3/s.

5.2.5.3 The particle counter

Particle concentrations at the column inlet and outlet were determined by analysis of sample streams with a particle counter (Model 202, Royco Instruments, Inc., Menlo Park, California). This unit is an accurate instrument for determining the number concentration and size of particles in the micron and submicron size range. The principle of operation is based upon the well-established phenomena of light scattering and reflection by small particles. Light scattering is the best method to analyze particles over the size range from 0.1 to 30 μm (Jelinek (1974)).

A block diagram of the particle counter is shown in Figure 5.8. It consists of two main units, one of which houses the optics, and the other the electronics. The aerosol sample is passed through an intense beam of light from a controlled source in the optical system (Figure 5.9). Particles scatter this light onto a photomultiplier tube which produces a current for each particle. The current pulse is converted to a voltage pulse by a preamplifier and the resulting signal is passed to the electronics section of the counter. Here the voltage pulse is first amplified by a 40 DB. amplifier and the signal then goes through an attenuation circuit to the discriminator. The pulses are sized, and, depending upon the counting mode, are ignored or registered on the decade counters. The particle counter may either count all particles in one or more size ranges (single mode operation) or all particles larger than any selected size (total mode operation). Table 5.1 gives channel numbers and the corresponding size ranges for the Royco 202 counter. Any combination of particle size ranges may be preselected for automatic monitoring. The particle counter has also built-in timing circuits so

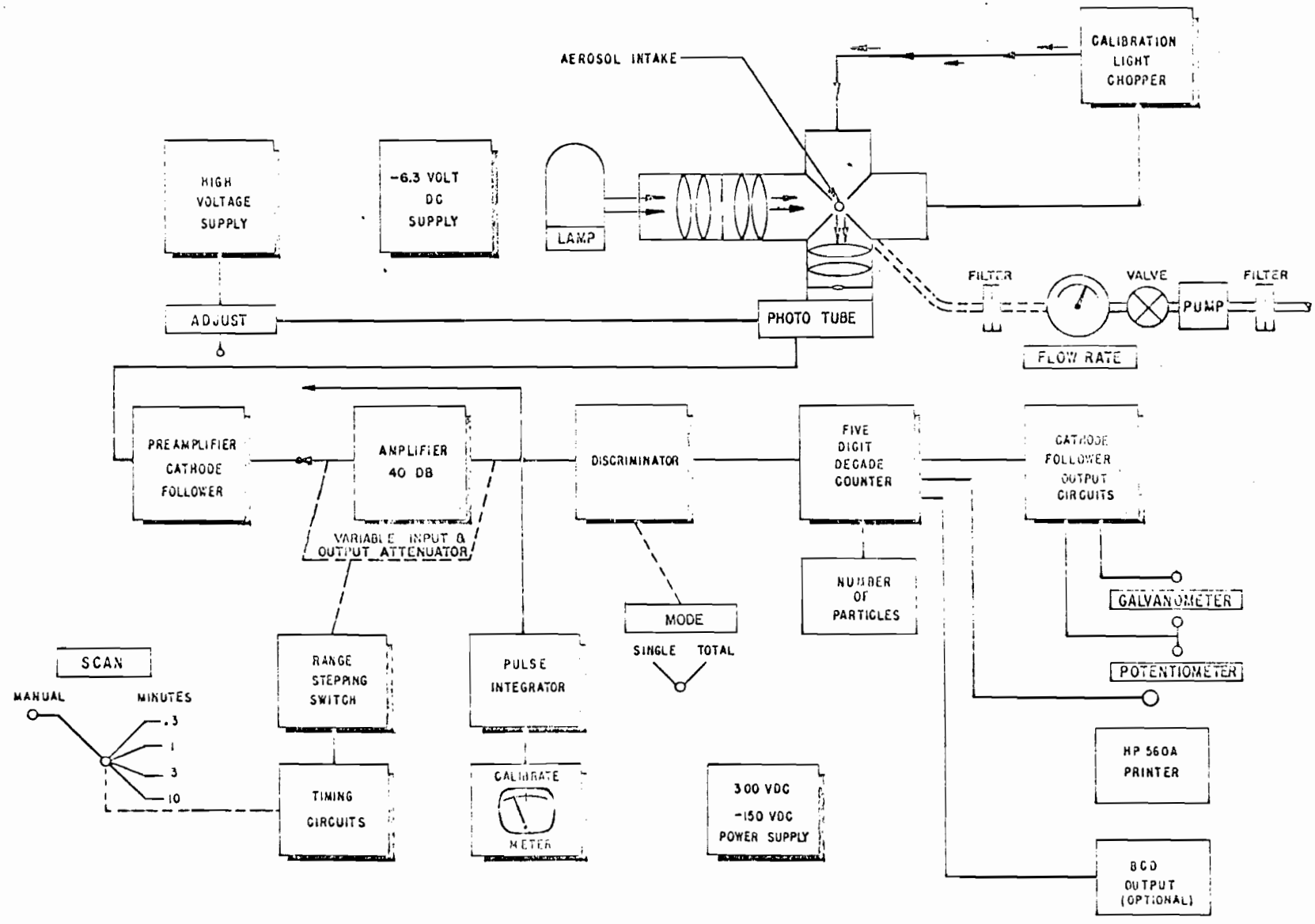

FIGURE 5.8. Block diagram of the particle counter

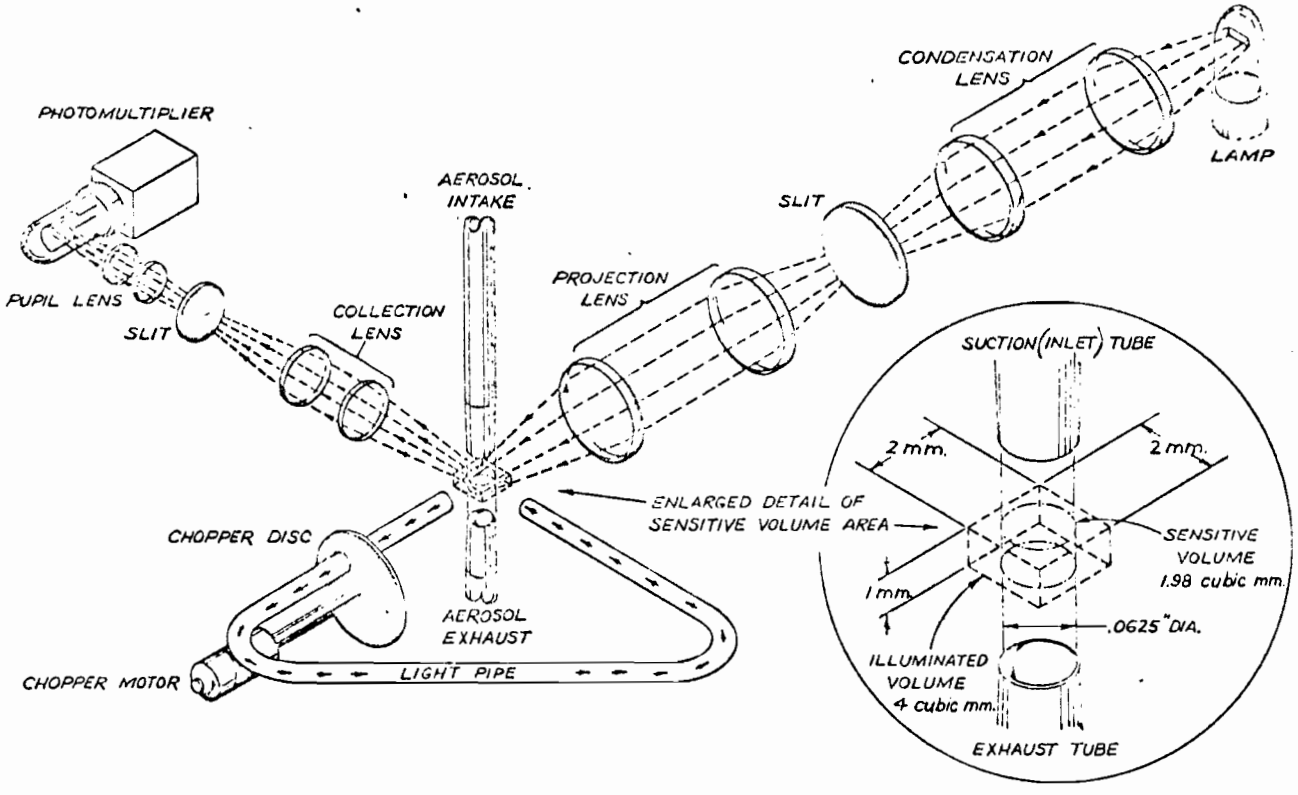

FIGURE 5.9. Optical system of Model 202 Royco particle counter

TABLE 5.1. Size Ranges of Model 202 Royco Particle Counter

Channel No.	Size Ranges, micron
1	0.3 - 0.4
2	0.4 - 0.5
3	0.5 - 0.6
4	0.6 - 0.8
5	0.8 - 1.
6	1. - 1.2
7	1.2 - 1.5
8	1.5 - 2.
9	2. - 3.
10	3. - 4.
11	4. - 5.
12	5. - 6.
13	6. - 8.
14	8. -10.
15	larger than 10.

that samples can be taken for 0.3, 1., 3. and 10. minutes.

The particle counter was "prime calibrated" every two weeks using an aerosol of latex particles. Such calibration provides comparison between the indicated size distribution with the known distribution of latex particles and permits any necessary calibration adjustment. Details of prime calibration are given in Appendix H. Furthermore, the counter is calibrated in the field daily using pulses of known magnitude created by the light chopper in the optical unit (Field Calibration).

The main source of sizing error in the particle counter is "coincidence loss". This effect results from simultaneous appearance of two particles within the sensitive volume where measurement takes place, thus causing masking of smaller particles by those larger. Coincidence loss, therefore, is not the same in all channels, but rather is a function of the count in a particular size range related to the total count in that range plus all larger particles. The instrument response is such that particles which pass through the sensitive volume less than 1 ms apart produce coincidence loss, which can be evaluated from the following expression.

$$\text{Coincidence loss in the channel} = \frac{\text{total count for all size ranges larger than the one under consideration} \quad 0.001 \quad \text{indicated count for individual channel}}{\text{time duration of test (in seconds)}} \qquad .....(5.2.2)$$

Coincidence losses in this study were corrected from a graph supplied by the manufacturer (Figure 5.10). This graph depends on a "total" mode

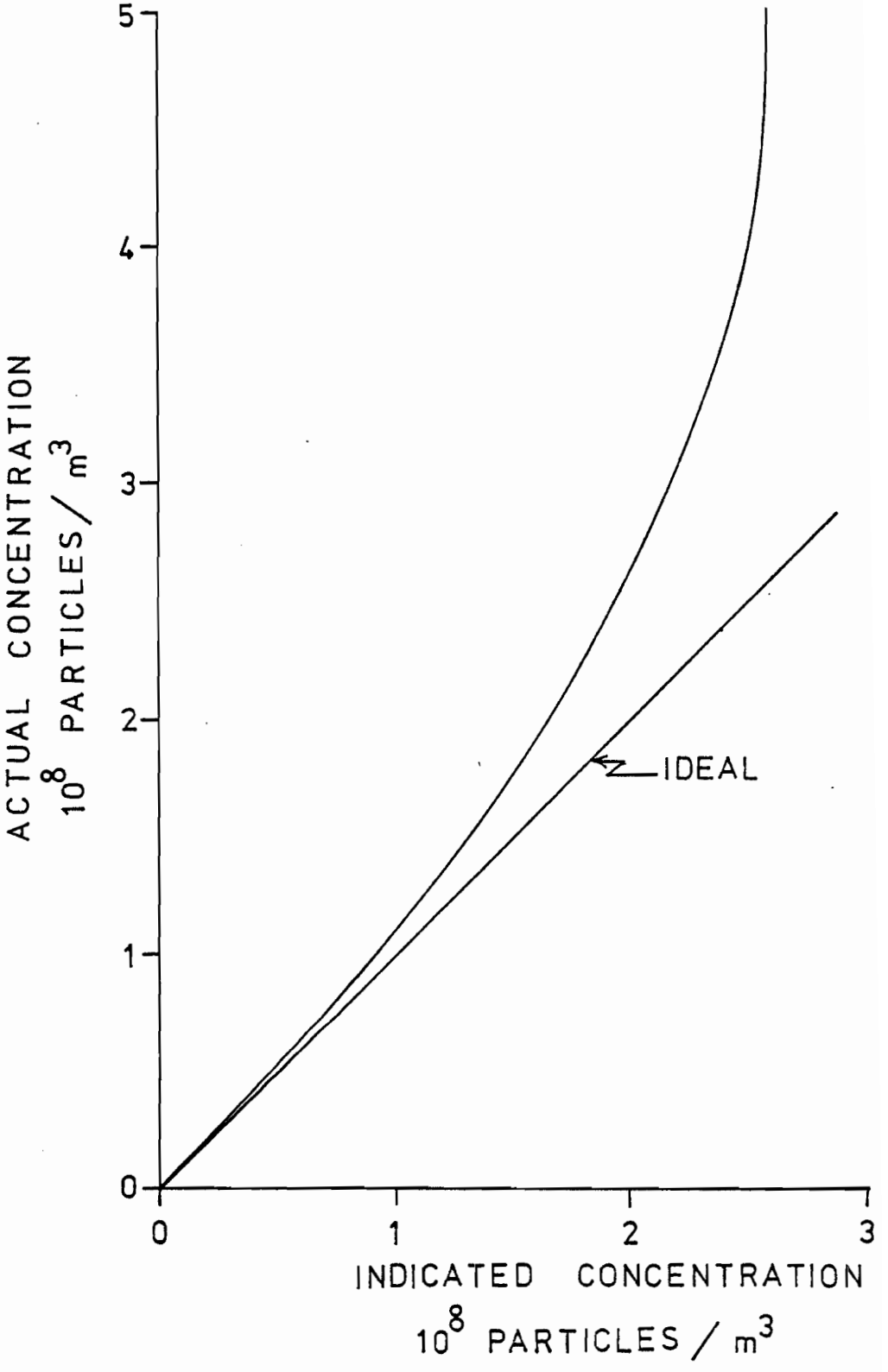

FIGURE 5.10. Correction of coincidence loss

count. The actual count for a certain size range is then the difference of the actual total counts, read from the graph, of particles equal to or larger than the specified size range and particles larger than the specified range. Although this correction is cumbersome, the effort required yields a significant increase in accuracy. All data in this study were corrected for coincidence loss as described above.

By comparison with the straight line marked "ideal", it is negligible for concentrations below 4×10^7 particles/m^3. As this study concerns concentrations about 10^8 particles/m^3, corrections were around 10% in the extreme cases.

A drawback in using this particle counter is that it is calibrated to operate at a sample flow rate of 300 cc/min. Gas velocities in MBC, however, are quite large. Therefore, in order to provide isokinetic sampling conditions, a special sampling system was designed as described in the next section.

5.2.5.4 The particle sampling system

If the velocity of the aerosol stream entering the sampling nozzle is the same as the velocity at the main stream in the column, the samping is said to be "isokinetic". If the sampling velocity is too high, large particles having greater inertia cannot follow the streamlines into the sampling nozzle. In this case, the sampling would be biased against large particles. If the sampling velocity is lower than the main stream velocity, particles with higher inertia will be oversampled, biasing the results in the opposite direction. Therefore, sampling of particles from gas streams should be made under isokinetic

conditions. Isokinetic sampling is especially necessary for particles having aerodynamic diameters, $d_{pa} = d_p\sqrt{c'\rho_p}$, greater than about 5 μm. Although this is the maximum size investigated in this present study, all sampling was done isokinetically.

Superficial gas velocities employed in the present study were in the range of 1.75-4 m/s. Although it depends on the size of the sampling nozzle chosen, the sampling flow rate from gas is then much higher than the operating flow rate of the Royco particle counter, which is 300 cc/min. This problem was solved by designing the "particle sampling system" shown in Figure 5.11.

During the experiments air was sampled at the inlet and outlet of the column (Figure 5.1). Stainless steel sampling nozzles, 6.35 mm ID, supplied by Nutech Corp., Durham, North Carolina, were used. These probes were connected to the inlet of the sampling system (Figure 5.11) by high-temperature heat-line hoses (Model 212, Technical Heaters Inc., San Fernando, California). The sampling flow rate was determined by measuring the air velocity at the point of sampling by a standard pitot tube and a micromanometer. Then, by making the necessary corrections for temperature and pressure change along the sampling line, the main sampling flow rate was adjusted by means of a rotameter and a vacuum pump. This procedure ensures isokinetic sampling from column inlet and outlet. As shown in Figure 5.11, the inlet section of the sampling system consists of diverging pipe from diameter 0.635 cm to 3.175 cm. Therefore, in this section, velocity of the aerosol stream decreases. The 4 mm diameter sliding secondary probe mounted to this section could move inward or outward. This secondary probe was connected to the Royco particle counter. Since the sampling rate of the Royco counter is constant

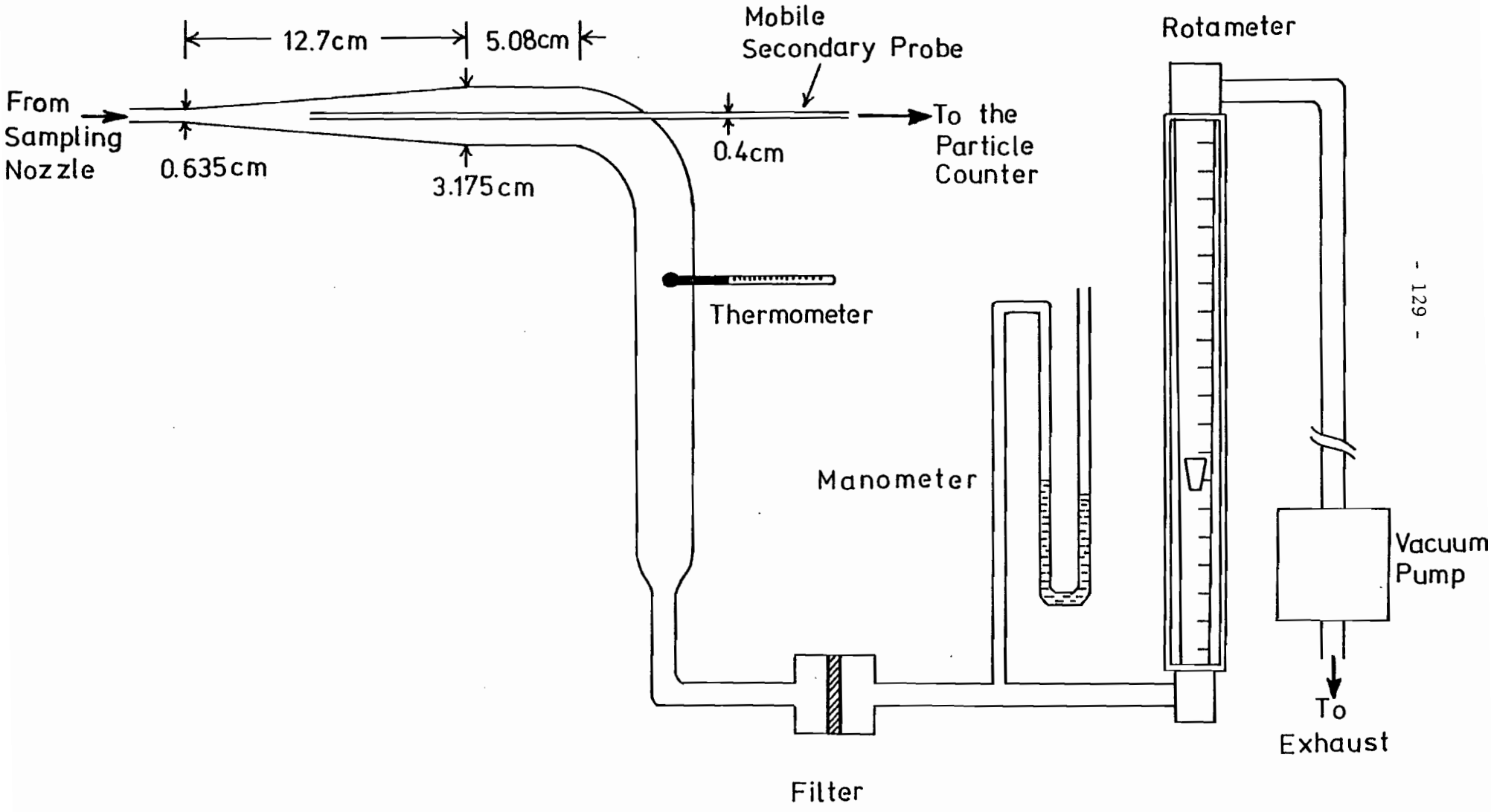

FIGURE 5.11. The particle sampling system

(300 cc/min), the velocity in the secondary probe was always 0.4 m/s. By sliding this secondary probe through the diverging pipe, it was possible to adjust the position of its tip to a point where the velocity of the main aerosol stream was also 0.4 m/s. A reference graph was prepared for the total sampling flow rate through the sampling system as a function of distance from the small area end of the diverging pipe. This graph and the calibration curve for the sampling system rotameter are given in Appendix I. By the use of such a special two-stage sampling rig, isokinetic conditions were achieved.

5.3 PROCEDURE AND DESIGN OF EXPERIMENTS

5.3.1 Minimum Fluidization Velocity Experiments

Two methods were employed to determine G_{mf}, the minimum fluidization velocity. The first method was the direct observation method. At constant liquid flow rate the gas flow rate was increased from zero and the onset of fluidization was observed visually. The gas flow rate at which the packing just starts fluidizing was recorded. This procedure becomes more difficult as liquid flow rate increases because, as will be discussed in the next chapter, minimum fluidization velocity in MBC decreases with increase in liquid flow rate.

The second method utilized bed expansion data. A least squares straight-line fit to the data for bed height as a function of gas flow rate was extrapolated to the static bed height, H_{st}, to obtain the corresponding minimum fluidization velocity.

The variables studied include three packing sizes (19, 25, 38 mm), two static bed heights (0.29 and 0.44 m) and liquid flow rates 4.7 to 23.5 kg/m^2-s.

5.3.2 Bed Expansion Experiments

The procedure followed in bed expansion experiments was to observe the value of bed height over a period of about 5 minutes and determine the maximum and minimum bed heights between which the bed continuously fluctuates. Only the height of clusters of balls was considered in this procedure, i.e. not the height reached by a single ball occasionally carried significantly above the top of the mobile-bed. The average bed height was then calculated by averaging these maximum and minimum heights.

The range of the variables d_{pb}, H_{st} and L studied in this section, are exactly the same as those noted above for G_{mf}. Gas flow rate was varied between the minimum fluidization velocity and 5.5 kg/m^2-s.

5.3.3 Pressure Drop Experiments

Pressure drop through the mobile-bed contactor was measured by using a pressure transducer. Data were collected in the form of a digital printout in millivolts, using the electronic circuit of Figure 5.5. In order to account for fluctuations in MBC, an average of about 60 printed values was taken. Pressure taps were placed just above the lower grid and just below the upper grid so that end effects were excluded. The measured pressure drop was then the actual pressure loss across the active zone of MBC. Sets of experiments, each at a constant liquid flow rate, were carried out at gas velocities over the entire operable range. Such sets were repeated for the values of d_{pb}, H_{st} and L, which were listed for the determination of G_{mf}.

5.3.4 Particle Collection Experiments

Particle concentrations at both inlet and outlet of the column were measured. Equations (4.3.5) or (4.4.15) then permit the calculation of the overall penetration.

The general procedure followed for particle collection experiments was as follows:

(1) Fill mobile-bed column with packing of desired size and seal the access lid to prevent any air or water leakage.

(2) Prepare aerosol solution to be fed to the spinning disk.

(3) Read barometric pressure.

(4) Turn on particle detector for warm-up (about one hour).

(5) Start aerosol generator, adjust the main air flow rate to 2.36×10^{-2} m^3/s and satellite flow to 3×10^{-3} m/s.

(6) Start MBC column blower, adjust flow rate by checking pressure drop across the orifice and by using Equation (E.3).

(7) Open water valves and adjust the rate.

(8) Open water valve to humidification column.

(9) Switch on duct heater and set temperature controller (for diffusiophoresis experiments).

(10) Open steam valve, adjust the rate (for diffusiophoresis experiments).

(11) Wait for system to reach steady state.

(12) Read dry-bulb and wet-bulb temperatures of inlet and outlet air.

(13) Read inlet and outlet water temperatures.

(14) Measure velocity at sampling points, calculate sampling flow rates.

(15) Check field calibration of the Royco particle counter.

(16) Connect counter to secondary sampling probe of the particle sampling system.

(17) Start vacuum pump and adjust position of the primary probe and the sampling flow rate by the rotameter valve, using calibration curve in Figure I.2 for inlet conditions. (Temperature and pressure of aerosol sample stream in the sampling system were read (Figure 5.11) and correction for the volumetric flow rate through the rotameter was made with the following standard equation.)

$$Q_{metered} = Q_{atm} \frac{493}{T} \frac{P}{29.92} \qquad (5.3.1)$$

(18) Adjust position of secondary probe in sampling system using Figure I.1.

(19) Read blank counts for inlet.

(20) Start feeding aerosol solution to the particle generator at a rate of $4 \times 10^{-7} m^3/s$.

(21) Wait until rate of particle generation reaches steady state.

(22) Take inlet particle concentration count at least five times, and take the average.

(23) Adjust position of primary and secondary probes for isokinetic sampling at outlet conditions by repeating steps (17) and (18).

(24) Take outlet concentration counts at least five times, and take the average.

(25) Stop generating particles.

(26) Take blank (background) count at outlet.

The above procedure was repeated for each experiment.

The background count at both inlet and outlet were taken in order to ensure that no contaminant particles were present. At the column inlet it was found that the maximum background count was 0.02% of the aerosol concentration. These few contaminating particles were found in the size range between 0.3-0.5 microns. This, of course, reflects the high efficiency of filters used for air (Figures 5.1 and 5.6). At the outlet of the column the background count was about 0.5-1% of the total count. Again these particles were at the low particle size range, and were evidently small liquid droplets which passed through the entrainment separator. Overall inspection of data shows that, for particles larger than about 0.8 μm, the effect of background count was nil. Particle concentrations for the lower size range were corrected by subtracting background count from the actual count.

For all experiments except those with diffusiophoresis it was essential that there be neither evaporation nor condensation in the test column, i.e. that the humidity of air at the inlet and outlet be the same. Constancy of humidity was achieved by adjusting the inlet air humidity as required. For experiments with diffusiophoresis the desired level of inlet air humidity was accomplished by injecting steam into air which had been preheated to 93°C. Due to the large air flow rates involved and limitations of the laboratory steam supply, the maximum humidity obtained at the column inlet was 0.29 kg H_2O/kg dry air.

As the mobile-bed column was designed to obtain experimental data up to quite high gas and liquid flow rates, the spacing between the retaining grids was 1.5 m. For experiments with low static bed height and low gas and liquid velocities the bed, however, does not expand to this height. In order to account for particle collection between the liquid distributor and the top of the mobile-bed, experiments were also performed without packing, i.e. the column operated as a spray column. The results of these experiments with ferrous sulphate particles are given in Appendix J. As will be discussed in the next chapter, penetration data for the test column operated as a spray column were correlated with Stokes number, liquid and gas flow rates. This correlation was then used for the correction to determine the particle penetration through just the active volume occupied by the mobile-bed.

Particle collection experiments for MBC can be classified in three groups:

i) Investigation of effect of gas flow rate, liquid flow rate, packing size, static bed height and particle dize for conditions with no diffusiophoresis;

ii) investigation of effect of hydrophobicity of particles for conditions with no diffusiophoresis; and

iii) investigation of effect of water vapor condensation (diffusiophoresis) on particle collection.

The results of the experiments of the first group give the characteristic performance of MBC due only to inertial collection. For this purpose an extensive series of experiments with ferrous sulphate

particles was made covering a wide range of variables, i.e.

$$4.7 \leq L \leq 23.5 \quad kg/m^2\text{-}s$$

$$2. \leq G \leq 4. \quad kg/m^2\text{-}s$$

$$0.29 \leq H_{st} \leq 0.58 \quad m$$

$$19 \leq d_{pb} \leq 38 \quad mm$$

$$0.35 \leq d_p \leq 5.5 \quad \mu m$$

With respect to the nature of the particles used, ferrous sulphate dissolves readily in water. Therefore these particles are hydrophilic particles, i.e. they are ideally wetted by water, as the contact angle is zero. In order to investigate whether solubility of particles has an effect on particle collection, experiments with silica particles were performed. This solid aerosol exhibits perfect wetting ($\theta_c = 0$) while being totally insoluble. Latex particles and DOP particles were used to investigate the effect of hydrophobicity on collection. Thus the inertial collection of particles in MBC was determined for a considerable range of types of particles.

As the final objective, the validity of the theoretical development given in Chapter 4 for diffusiophoretic collection was checked using ferrous sulphate particles.

CHAPTER 6

ANALYSIS AND DISCUSSION OF RESULTS

Results are grouped in two categories. The first part concerns hydrodynamic studies and the second part the particulate recovery in MBC.

6.1 STUDIES OF HYDRODYNAMICS OF MOBILE-BED CONTACTING

6.1.1 Bed Expansion and Minimum Fluidization Velocity

The expanded bed height of a mobile-bed is not only the fundamental parameter which defines the spacing between retaining grids in design of an MBC column, but is also required in interpretation of the particle collection measurements of the present study.

For each set of operating conditions used, values for both the maximum and the minimum bed height were noted, as observed visually over a period of about 5 minutes. The average value for both maximum and minimum bed height was then recorded, and "bed height" was taken as the average of the pair of maximum and minimum bed heights for each set of operating conditions. These results are given in Appendix A for two static bed heights and three packing sizes over a range of gas and liquid flow rates. The results for expanded bed height are also shown in Figures 6.1-6.6, which give the ratio, average bed height: static height, as a function of gas flow rate, with L, H_{st} and d_{pb} as parameters.

The results indicate that, at any fixed value of liquid flow rate, the bed height increases linearly with gas flow rate over the stable operating range of MBC. This finding is consistent with the previous works of Chen (1965), Blyakher et al. (1967), Chen and Douglas

LEGEND FOR FIGURES 6.1 - 6.6

L, kg/m^2-s	Symbol
4.7	○
9.4	△
14.1	□
18.8	✳
23.5	◇

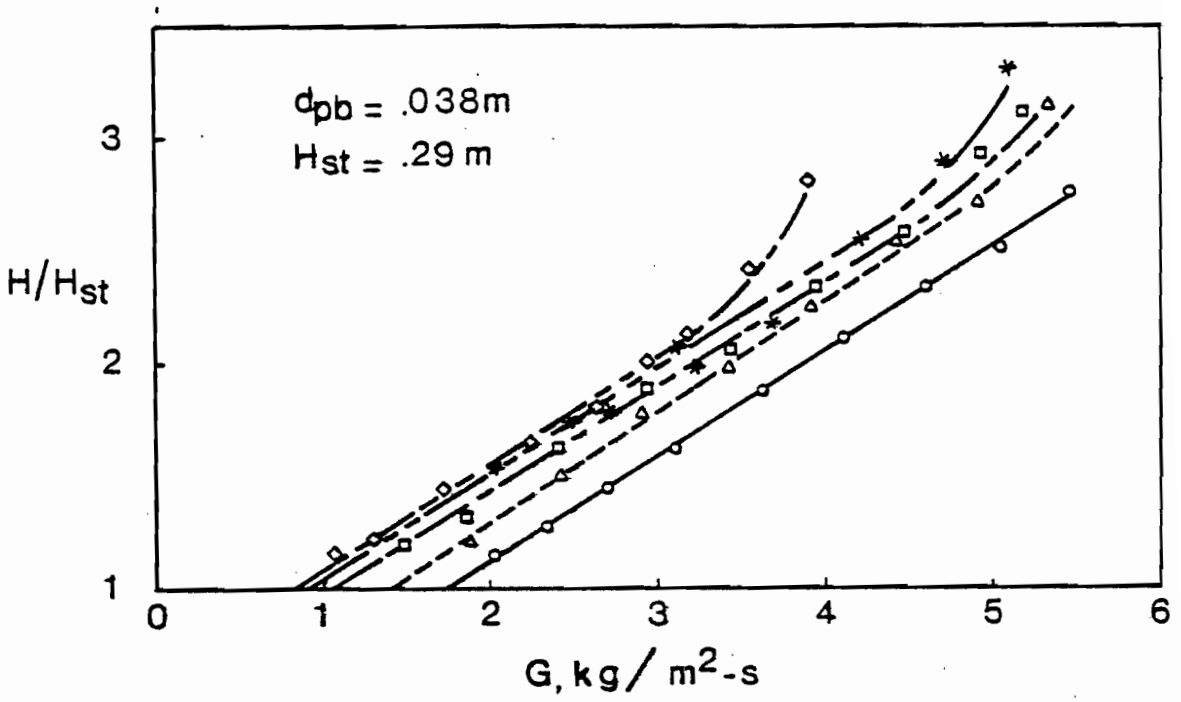

FIGURE 6.1. Effect of gas flow rate on height of mobile-bed for H_{st} = 0.29 m and d_{pb} = 38 mm

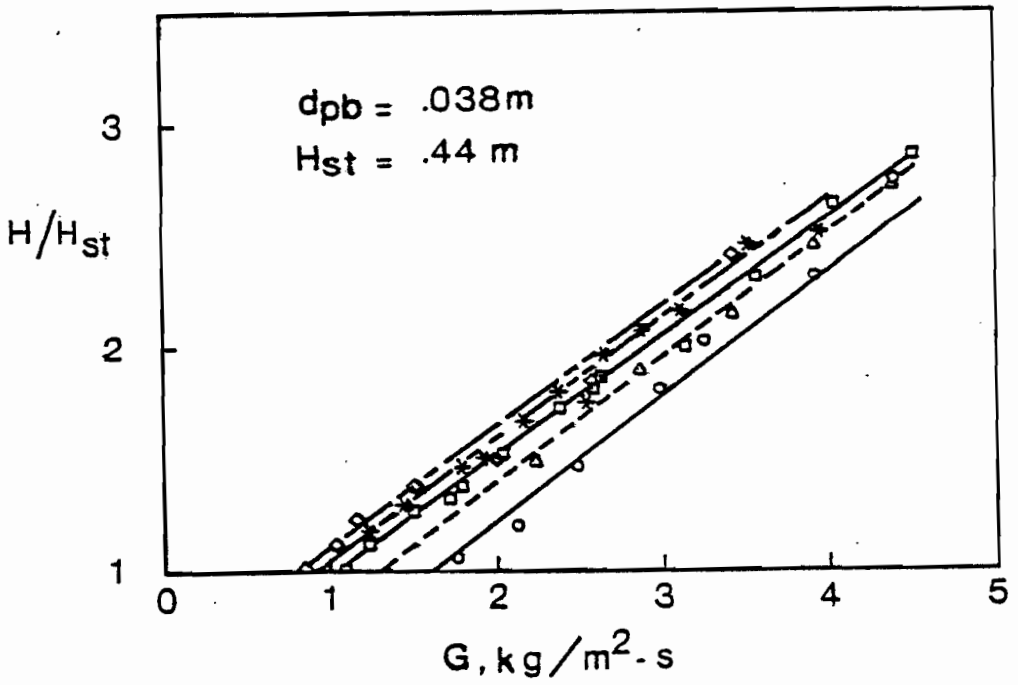

FIGURE 6.2. Effect of gas flow on height of mobile-bed for H_{st} = 0.44 m and d_{pb} = 38 mm

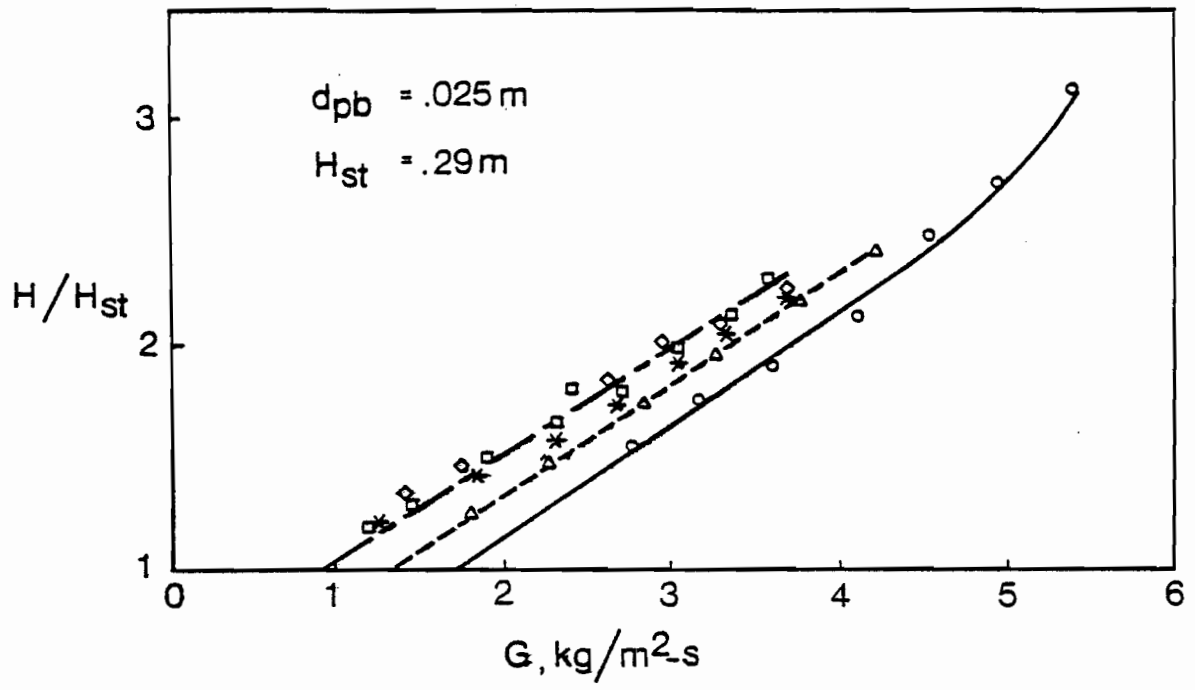

FIGURE 6.3. Effect of gas flow rate on height of mobile-bed for H_{st} = 0.29 m and d_{pb} = 25 mm

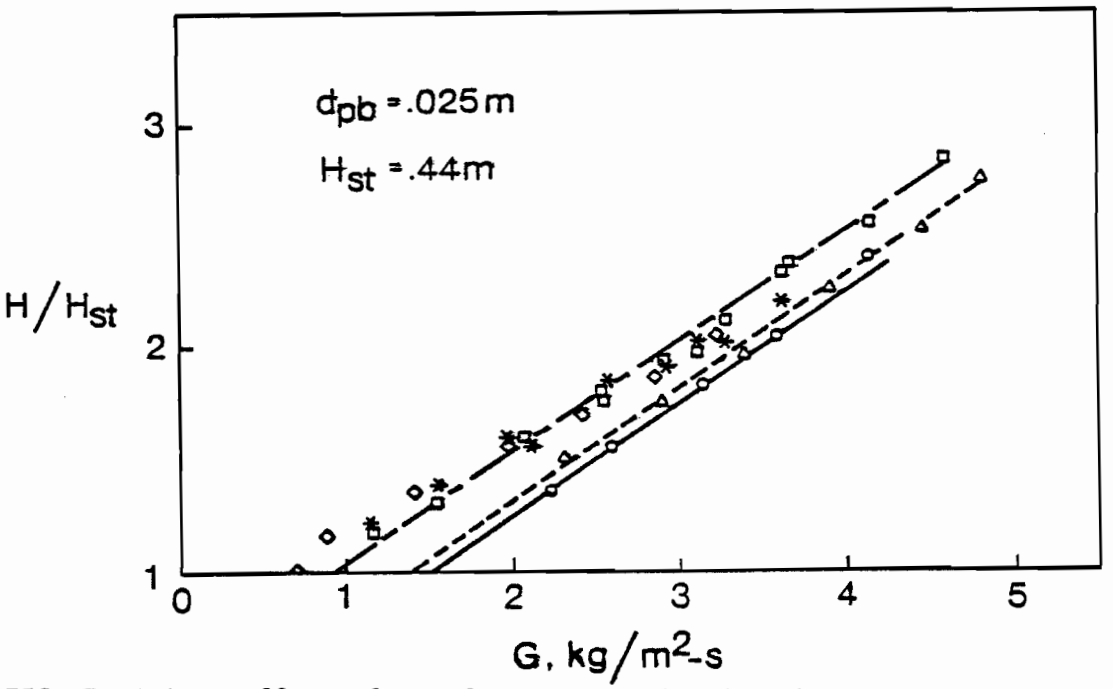

FIGURE 6.4. Effect of gas flow rate on height of mobile-bed for H_{st} = 0.44 m and d_{pb} = 25 mm

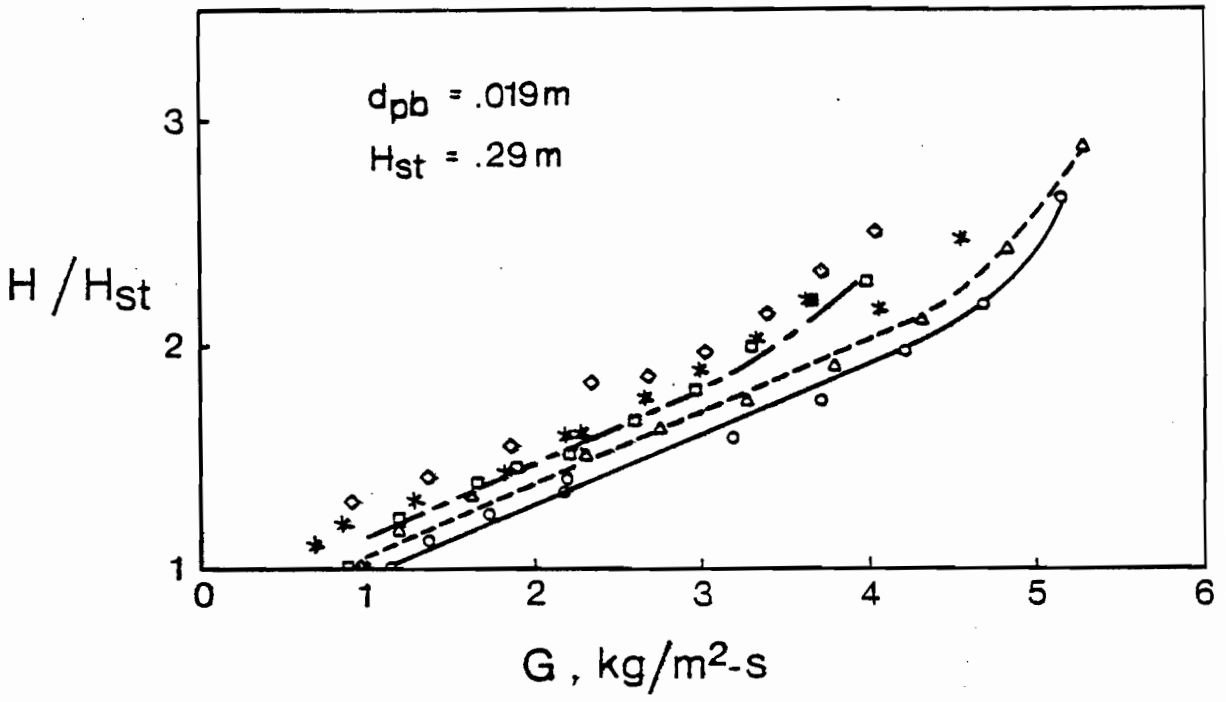

FIGURE 6.5. Effect of gas flow rate on height of mobile-bed for H_{st} = 0.29 m and d_{pb} = 19 mm

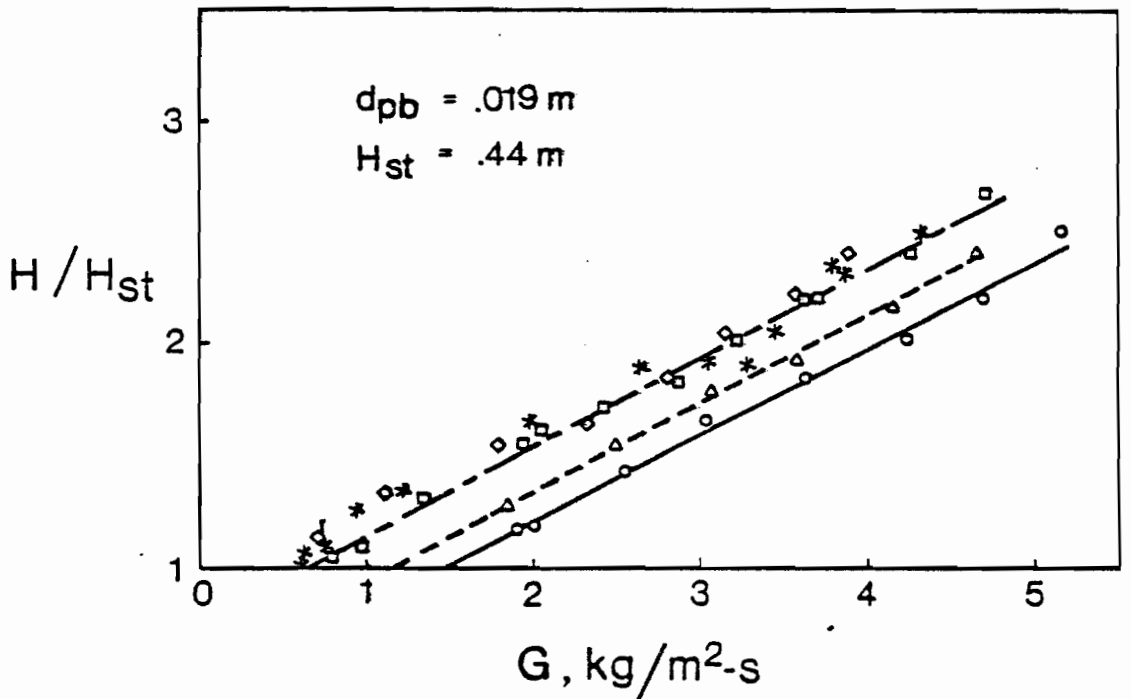

FIGURE 6.6. Effect of gas flow rate on height of mobile-bed for H_{st} = 0.44 m and d_{pb} = 19 mm

(1968), Khanna (1971), and Tichy and Douglas (1972 and 1973). At increasingly high values of G, however, the slope of these lines of constant L no longer remains constant but begins to increase. This effect is due to increase in liquid holdup, as will be discussed subsequently. As the end region of stable MBC operation is approached, the slope of the line for H/H_{st} as a function of G in fact increases sharply. The non linear region of operation is terminated by "flooding", i.e. when all the packing is carried to the upper retaining grid where the entire mobile-bed becomes a fixed-bed and the liquid is carried over the top of the bed as in flooding of any fixed-bed tower. The maximum values of G at which the slope remains constant naturally decrease with increasing L. This behaviour can be seen from Figure 6.1, where the slope is constant over the entire experimental range of G for the lowest of the five values of L used. For the other four experimental values of liquid flow rate, the value of G at which the slope begins to increase can be seen to decrease progressively with increasing L. The effect of packing diameter on extent of the linear region may also be discerned. Thus it can be observed from comparison of Figure 6.1 with Figures 6.3 and 6.5 that, for a fixed value of L, for example 14 kg/m^2-s, the onset of nonlinear increase of bed height occurs at progressively lower values of G as packing diameter is decreased over the range 38 to 19 mm. This effect is a consequence of the effect that packing size has on liquid holdup, to be discussed later. Regardless of the cause, this examination of Figures 6.1, 6.3 and 6.5 establishes that, from the practical perspective of operating an MBC column, the linear region of operation is reduced as packing diameter is reduced over the range 38 to 19 mm.

Although the general outline of the behaviour noted above had been reported previously by Tichy and Douglas (1973), that study reported data for only a single value of liquid flow rate and packing size, $L = 4.95$ kg/m^2-s and $d_{pb} = 19$ mm, for two values of H_{st}, 0.14 and 0.29 m. With this limited experimental data, Tichy and Douglas were unable to provide the general correlation which is needed for expanded bed height as a function of all variables of practical interest. The results of the present study have, therefore, documented the mobile-bed expanded height over a wide range of the controlling variables. Only on the basis of such a comprehensive study may a reliable general correlation of expanded bed height be obtained.

For each of the five values of liquid flow rate recorded in Figures 6.1 and 6.2 a least squares straight-line fit to the data is shown. For Figures 6.3 to 6.6, however, lines are shown only for the three lowest values of L (4.7, 9.4 and 14.1 kg/m^2-s). Results for the two highest liquid flow rates, 18.8 and 23.5 kg/m^2-s, are closely spaced and do not fall in any consistent relationship relative to the data for $L = 14.1$ kg/m^2-s. This inconsistent behaviour at the highest liquid velocities is believed to be associated with non-uniform distribution in the bed accompanied by occasional agglomeration of packing balls and adherence of packing to the walls. Thus the line for $L = 14.1$ kg/m^2-s in Figure 6.4, for example, may be taken also as the best estimate of bed height for values of $L > 14$ kg/m^2-s, although the accuracy of this estimate is somewhat reduced for the higher liquid rates due to less uniform bed hydrodynamics.

The gas velocity which marks transition between fixed-bed and mobile-bed operation is referred to as minimum fluidization velocity, G_{mf}. The value of G_{mf} is relevant not only to the design of an MBC column, but is as well an essential parameter in correlation of expanded bed height and of other phenomena occuring in MBC.

Previous studies by Chen (1965), Chen and Douglas (1968), Khanna (1971), Tichy and Douglas (1972 and 1973) established the method of determining minimum fluidization velocity by linear extrapolation of bed expansion to the limiting value of static bed height. Thus in Figures 6.1-6.6 the point of intersection of each line with the abscissa at $H/H_{st} = 1$ may be taken as the value of G_{mf} for the corresponding operating conditions. Table B.1 in Appendix B gives the values of minimum fluidization velocity thus determined from bed expansion results.

Equally as well as approaching G_{mf} as the minimum of those values of G for which a mobile-bed is fluidized or expanded, G_{mf} may be obtained from the opposite direction as the maximum gas velocity at which the bed just maintains its static height. Thus as an independent check on the reliability of the first method, G_{mf} was also determined in the present study by a second method, namely, by visual observation. Table B.2 in Appendix B gives the data for G_{mf} obtained by visual observation. Comparison of the results by the two methods indicates that, in spite of a certain inevitable amount of scatter, the two methods are in reasonable agreement. The transition between the fixed-bed and mobile-bed condition is not as sharp as in two-phase fluidization, (cf. Figure 2.1). Thus, it is very difficult to define the onset of fluidization visually, especially at high liquid flow rates. However, as it has now

been verified that the value of G_{mf} obtained by the extrapolation technique is indeed the minimum fluidization velocity, in future G_{mf} may be determined with confidence simply by the extrapolation technique.

Using the analogy between two-phase fluidization and MBC, which may be regarded as three-phase fluidization, Chen and Douglas (1968) suggested the following form of correlation for minimum fluidization velocity:

$$G_{mf} = \beta_o \, d_{pb}^{\beta_1} \, 10^{\beta_2 L} \qquad (6.1.1)$$

This form has been adopted for use with the data of the present investigation which covers a wider range than the cited study. The correlation proposed by Chen and Douglas, together with others found in the literature, were given in Table 2.1.

Multiple regression analysis of the two sets of data combined, i.e. those obtained visually and from bed expansion study (Tables B.1 and B.2), using the STATPK subroutine in an interactive computing system (MUSIC), gave the following equation:

$$G_{mf} = 10.86 \, d_{pb}^{0.488} \, 10^{-0.01985 \, L} \qquad (6.1.2)$$

Since the STATPK subroutine performs linear multiple regression, statistical analysis of the above correlation and others that will subsequently be presented for other hydrodynamic characteristics of MBC was made on the logarithmic forms of the equations. Therefore,

the statistics supplied by the STATPK subroutine apply to the logarithms of the variables and not to the variables themselves. The multiple correlation coefficient thus obtained for Equation (6.1.2) is 0.955. Probability associated with F evaluated is 1. These statistical measures indicate a high degree of correlation. For practical purposes, the coefficients in Equation (6.1.2) may, of course, be rounded. Thus the three constants in Equation (6.1.2) may be taken respectively as 10.9, 0.49, and -0.2 without significant loss of accuracy.

Experimental results together with the proposed correlation (Equation (6.1.2)) are plotted in Figures 6.7, 6.8 and 6.9. Also plotted for comparison is the correlation of Chen and Douglas (1968), the only other correlation obtained with both large open area grid (80%) and large D_c/d_{pb} ratio (8-24). In addition, the correlation and data obtained by Khanna (1971) and the correlation by Tichy and Douglas (1972) are included to show the effect of small D_c/d_{pb} ratio. As may be noted in these figures, Khanna's correlation does not give a good estimate of his own data for 38 mm and 25 mm packing. While Khanna predicts larger G_{mf} values for 38 mm packing, for all other cases Khanna's correlation, and other correlations for all cases, predict lower values of minimum fluidization velocity than those obtained by the present correlation (Equation (6.1.2)). This discrepancy can be better understood after inspection of their bed expansion data. As will be discussed subsequently, slopes of lines for bed height as a function of gas velocity in previous studies are mostly smaller than found in the present study. This fact suggests that there might be strong wall effects in the previous studies. Experience of operating

LEGEND FOR FIGURES 6.7, 6.8, 6.9 and 6.10:

		SYMBOL		
		PRESENT DATA		KHANNA's DATA
d_{pb}	H_{st}	determined from bed expansion data	visual observation	determined from bed expansion data
.038 m	.29 m	○	○	⊘
.038 m	.44 m	●	●	
.025 m	.29 m	□	□	▨
.025 m	.44 m	■	■	
.019 m	.29 m	△	△	◬
.019 m	.44 m	▲	▲	

CORRELATIONS

PRESENT :

$$G_{mf} = 10.86\ d_{pb}^{.488}\ 10^{-.01985\ L}$$ ————————

KHANNA :

$$G_{mf} = 526.47\ d_{pb}^{1.5}\ 10^{-.0317\ L}$$ - - - - - - - - - -

CHEN :

$$G_{mf} = 98.46\ d_{pb}^{1.1}\ 10^{-.03683\ L}$$ —— – —— –

TICHY & DOUGLAS :

$$G_{mf} = .36355 + 57.9\ d_{pb} - 1.848\ L^{.6} d_{pb}^{.5}$$ —— —— – –

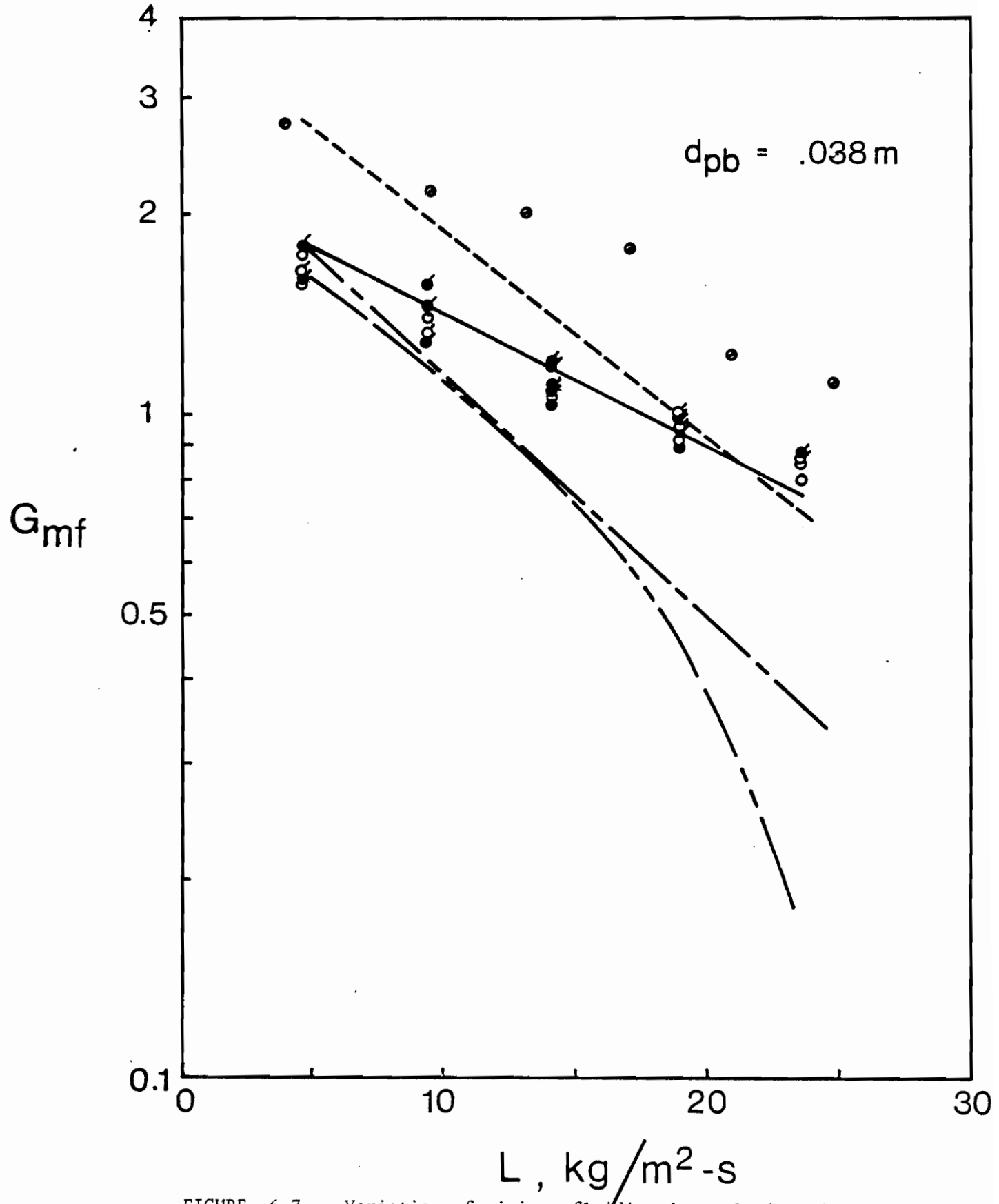

FIGURE 6.7. Variation of minimum fluidization velocity with liquid flow rate for 38 mm packing

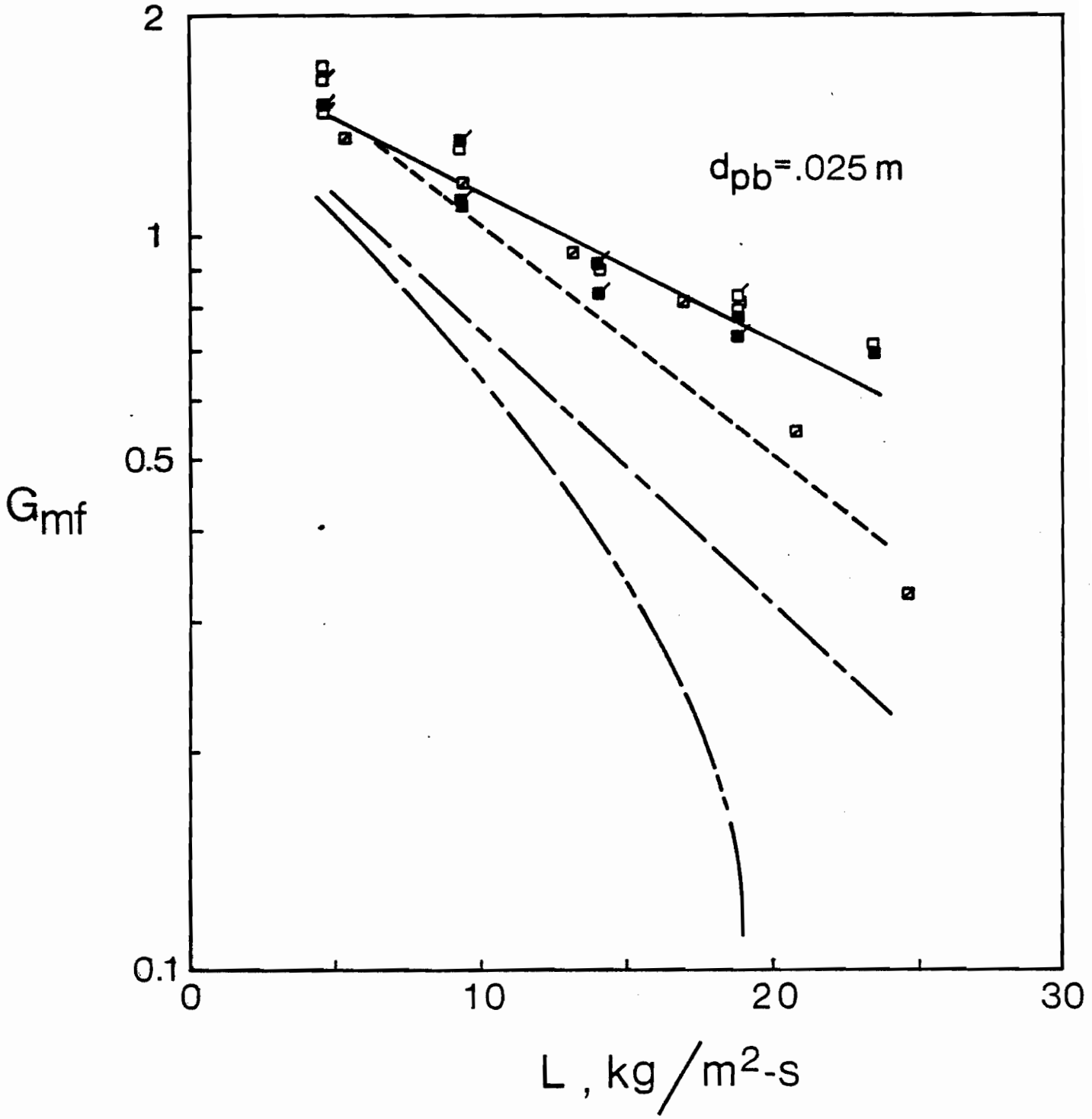

FIGURE 6.8. Variation of minimum fluidization velocity with liquid flow rate for 25 mm packing

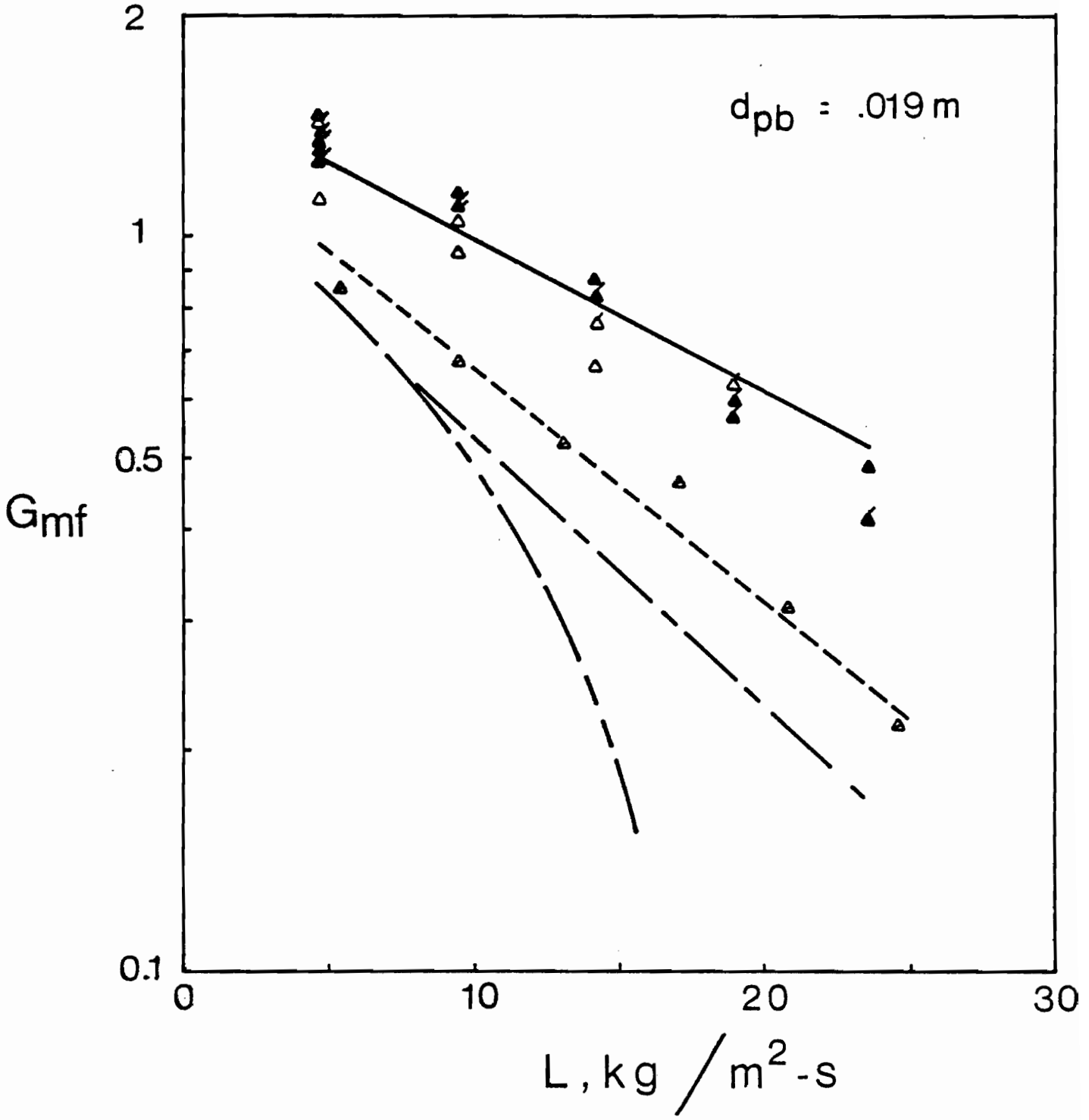

FIGURE 6.9. Variation of minimum fluidization velocity with liquid flow rate for 19 mm packing

dynamics is determination of a general correlation for expanded bed height over this linear operating region. Over the linear region one may write

$$H = m(G - G_{mf}) + H_{st} \tag{6.1.3}$$

which can be rearranged in dimensionless form as:

$$(H - H_{st})/H_{st} = (m\, G_{mf}/H_{st})(G - G_{mf})/G_{mf} \tag{6.1.4}$$

or,

$$h = (m\, G_{mf}/H_{st})\Delta \tag{6.1.5}$$

where, $$h = (H - H_{st})/H_{st} \tag{6.1.6}$$

and $$\Delta = (G - G_{mf})/G_{mf} \tag{6.1.7}$$

The excess gas mass velocity, expressed relative to G_{mf}, has been termed the stirring number, Δ. The bed expansion data and the correlation developed for minimum fluidization velocity (Equation (6.1.2)) were used to evaluate h and Δ in Equation (6.1.5). Regression analysis of these results using the STATPK subroutine yielded the following correlation:

$$h = 0.147\, G_{mf}\, \Delta/H_{st} \tag{6.1.8}$$

The correlation coefficient for the above equation is 0.89. Figure 6.11 shows the fit of experimental data with this correlation. It is interesting to note that the scatter of data becomes larger for larger values of h, which correspond to high gas velocities. At these high gas flow rates, as will be noted later in this section, fluctuations of bed height are much larger than at small gas velocities. Large fluctuations, of course, reduce the accuracy of determination of expanded bed height.

The effect of liquid flow rate and packing size is not seen explicitly from Equation (6.1.8) but, as explained previously, G_{mf} is a strong function of both of these variables.

Data reported for expanded bed height by several investigators are compared with the present work in Figure 6.12. This comparison is made for the most part at common conditions, summarized in Table 6.1. Correlations proposed previously were given in Table 2.2. Chen (1965) and Chen and Douglas (1968) presented no correlation for their data. Over the low range of gas flow rates used in that study, their experimental observations agree reasonably well with the present work. At the upper end of the range of gas flow rates covered by the cited authors there is a reduction in their bed expansion values. This reduction may not be important for prediction of bed height but may significantly effect the slope of the line, and hence the minimum fluidization velocity determined by extrapolation. This effect may be the reason why G_{mf} values of these authors are lower than those of the present study, as demonstrated in Figures 6.7-6.9.

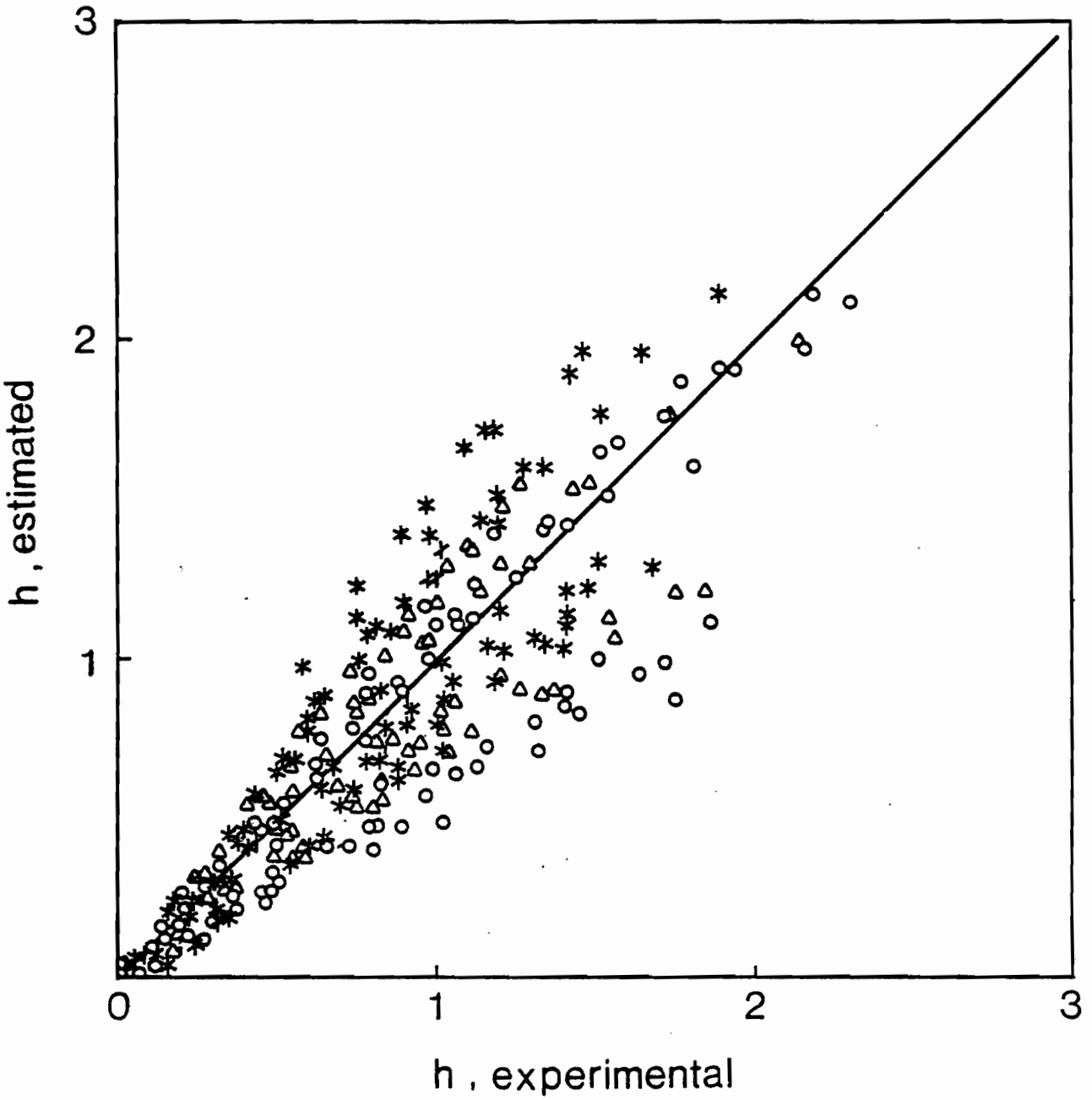

FIGURE 6.11. Comparison of experimental and estimated values for bed expansion

TABLE 6.1. Experimental Conditions of Bed Expansion Data Reported in the Literature and Used in Figure 6.12.

Author	L, kg/m^2-s	d_{pb}, mm	D_c, m	H_{st}, m
Balabekov et al. (1969)	4.17	16	0.175	0.11
Blyakher et al. (1967)	5.55	38	0.2	0.2
Chen (1965), and Chen and Douglas (1968)	6.57	38	0.29	0.3
Gel'perin et al. (1968)	5.55	16	0.165	0.09
Khanna (1971)	5.35	38	0.14	0.14
Levsh et al. (1968)	5.6	18x9x2 rings	0.178	0.21
Tichy and Douglas (1972)	4.7	38	0.14	0.14
Tichy and Douglas (1973)	4.95	19	0.29	0.29
Present	4.71	38	0.29	0.29

FIGURE 6.12. Comparison of literature data on bed expansion in MBC and the present study

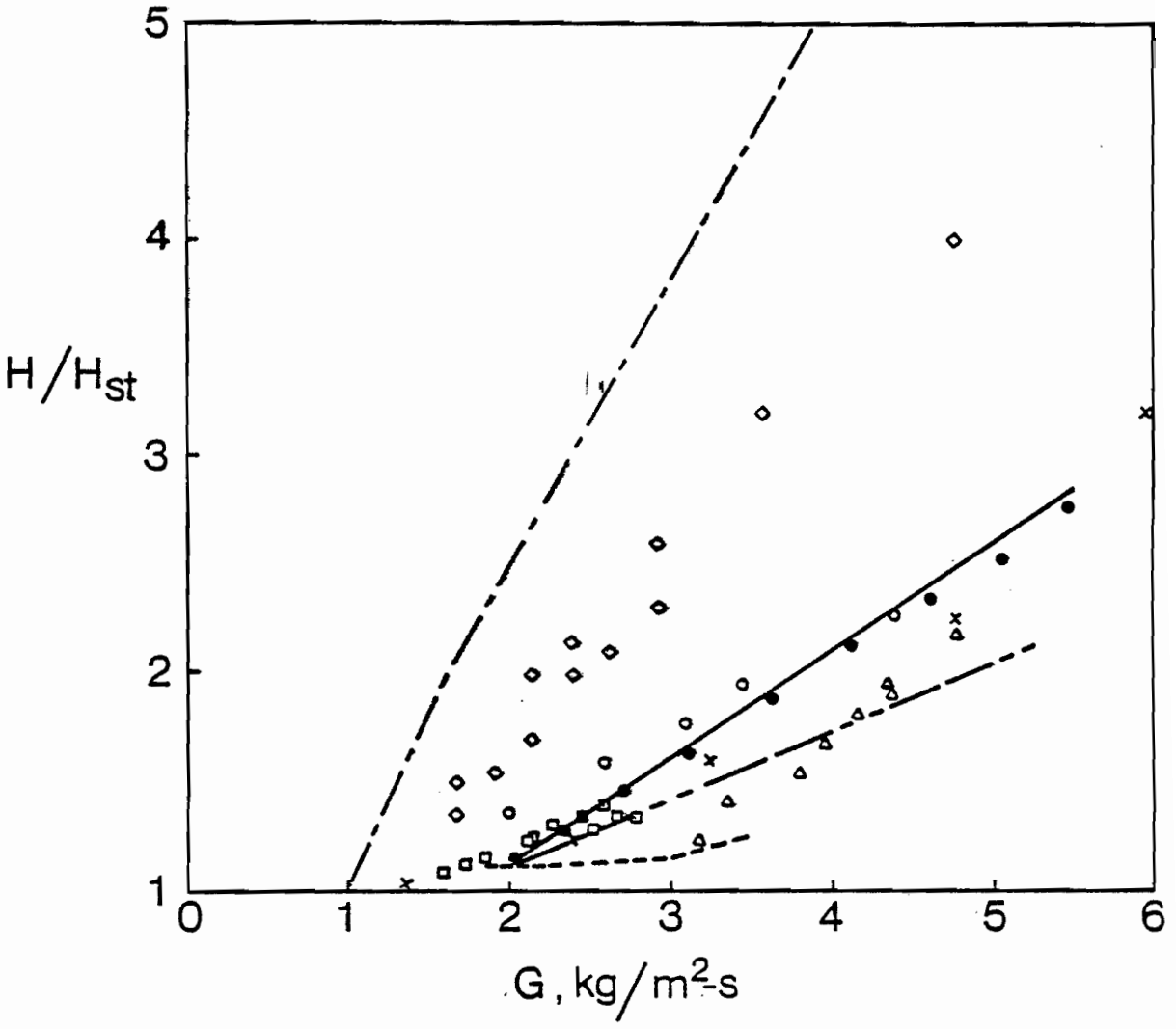

× Balabekov et al. (1969)

◇ Blyakher et al. (1967)

□ Chen (1965), Chen and Douglas (1968)

- — - — Gel'perin et al. (1968)

△ Khanna (1971)

- - - - - - Levsh et al. (1968)

- - — — Tichy and Douglas (1972)

○ Tichy and Douglas (1973)

● Present data

——— Present correlation

Khanna's data, as seen in Figure 6.12, also show lower values of bed height than the present data. Khanna (1971) presented his results only in tabular form. When the author plotted his data it was observed that, for almost all conditions, there were inconsistencies similar to those observed only at very high flow rates in the present study. This definitely implies that there were strong wall effects in Khanna's study carried out with a smaller diameter (0.14 m) column.

The same observation may be made for the studies of Levsh et al. (1968), Balabekov et al. (1969), and Tichy and Douglas (1972). The existence of a wall effect in these studies is apparently reflected in smaller slopes of their bed expansion results. Data reported by Blyakher et al. (1967) and Gel'perin et al. (1968) show quite abnormally high values for bed height. The criterion they used for bed height is a possible reason for the large differences of these studies. Although not clear from their publication, it is probable that the maximum height attained by any packing ball was reported as the bed height. If so, such a criterion for bed height does not represent a good choice. Furthermore, as noted in Section 2.1.2, the bed expansion data of both Gel'perin et al. (1968) and Levsh et al. (1968) were unfortunately strongly affected by the use of support grids of unrealistically low open area.

As noted earlier, Tichy and Douglas (1973) reported data for a large column for which wall effects should be absent, but for only a single packing size, 19 mm. These data, also shown in Figure 6.12, are in reasonable agreement with the results for the corresponding size of packing in the present study.

Finally, it should be noted that the correlation proposed in this study (Equation (6.1.8)) predicts average heights. However, fluctuations in bed height are also important in the design of MBC. Figure 6.13, a typical result for d_{pb} = 38 mm, H_{st} = 0.29 m and L = 14.1 kg/m^2-s, shows the variation of maximum and minimum height together with average values. At any gas flow rate the bed height fluctuates between limits shown by the shaded area in Figure 6.13. The complete results, presented in Appendix A, are consistent with this figure in indicating that the amplitude of height fluctuations generally increases with gas flow rate. It is also observed that a smaller packing size is generally associated with a smaller amplitude of fluctuation. Thus, for design purposes, the bed height evaluated from Equation (6.1.8) may be multiplied by 1.2 for 38 mm packing, and by 1.15 for 25 mm and 19 mm packing, in order to estimate maximum as opposed to average bed height. Maximum bed height, thus determined, would relate to fixing the spacing between bed support grids of MBC units.

6.1.2 Pressure Drop and Liquid Holdup

Two fundamental operating variables which characterize any gas-liquid contacting device are pressure drop and liquid holdup. Thus, knowledge of these parameters is essential to defining and comparing the characteristics of gas-liquid contactors.

As interstitial gas velocity is required in the analysis of particulate recovery in a gas-liquid contactor, liquid holdup in MBC must be known accurately for the present study. As reviewed in Sections 2.1.3 and 2.1.4, the results of previous studies on pressure drop and

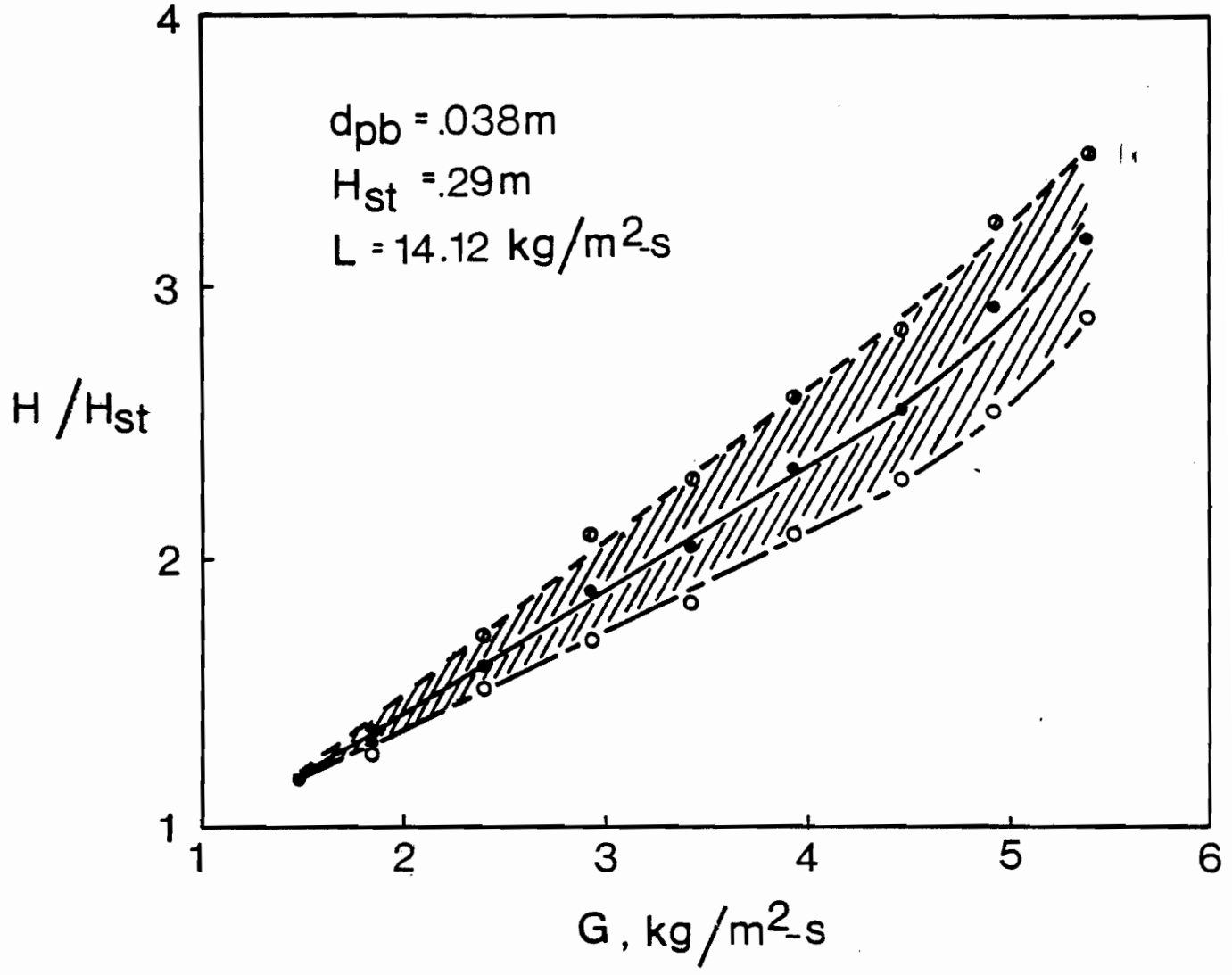

FIGURE 6.13. Fluctuations of bed height in MBC

liquid holdup in MBC are at such variance that it was not possible to predict these variables with confidence for the present study. It is liquid holdup, not pressure drop, which is specifically required in the analysis of particulate recovery in MBC. However, as it was considered that pressure drop could be measured more accurately than liquid holdup, extensive measurements of ΔP_c were made which, beyond their intrinsic interest, were used also in conjunction with Equation (2.1.1) to evaluate liquid holdup in MBC. Thus a comprehensive study of the pressure drop and liquid holdup characteristics of MBC was carried out.

It is readily demonstrated that pressure drop and liquid holdup are closely interconnected variables in a countercurrent gas-liquid contactor. The macroscopic momentum balance around an MBC column at steady state is

$$\Delta P_c = \Delta(\rho_G u_G^2) - \Delta(\rho_L u_L^2) + \frac{(m_{pb} + m_L + m_G)g + \Sigma F}{S_c} \quad (6.1.9)$$

where m_{pb}, m_L and m_G represent the mass of packing, liquid holdup and gas holdup, respectively, and ΔF can be represented as

$$\Sigma F = f A \tfrac{1}{2} \rho_G u_G^2 \quad (6.1.10)$$

where f is the friction factor, and A is total interfacial area (Bird, Stewart and Lightfoot (1960)). This force, represented by Equation (6.1.10), is composed of the sum of all viscous and pressure forces, i.e.

$$\Sigma F = F_{grid} + F_{wall} + F_{mixing} + F_{interfacial} \qquad (6.1.11)$$

As F_{grid} is the effective force of gas on the grids, this term depends on the type of grid used in a particular column. If, however, the balance is written inside the retaining grids, and pressure is correspondingly measured inside the grids, then this term does not appear. The axial drag force exerted on the wall, F_{wall}, is very small and can be neglected. The force required for overcoming surface tension, $F_{interfacial}$, and the force required for mixing, F_{mixing}, are also small relative to the weights of packing and liquid holdup and can, therefore, be neglected. An order-of-magnitude estimate of these forces justifies this. For example, Khanna (1971) reports a value of about 200 m^{-1} for the interfacial area in MBC at G = 3 kg/m^2-s and L = 15 kg/m^2-s. The surface tension between air and water at 25°C is about 7.2×10^{-2} N/m. This implies that the total force required to break the gas-liquid interface in MBC is about 0.96 N. Similarly, when the total drag force on, for example, 38 mm packing is evaluated, a value of 0.72 N is found. These values are much smaller than the force corresponding to the pressure drop in MBC due to the weights of packing and liquid holdup, which is about 32 N. Furthermore, density of the gas can be ignored relative to packing and liquid density. Thus, under conditions of negligible mass transfer between the phases, Equation (6.1.9) reduces to

$$\Delta P_c = (m_{pb} + m_L)g/S_c \qquad (6.1.12)$$

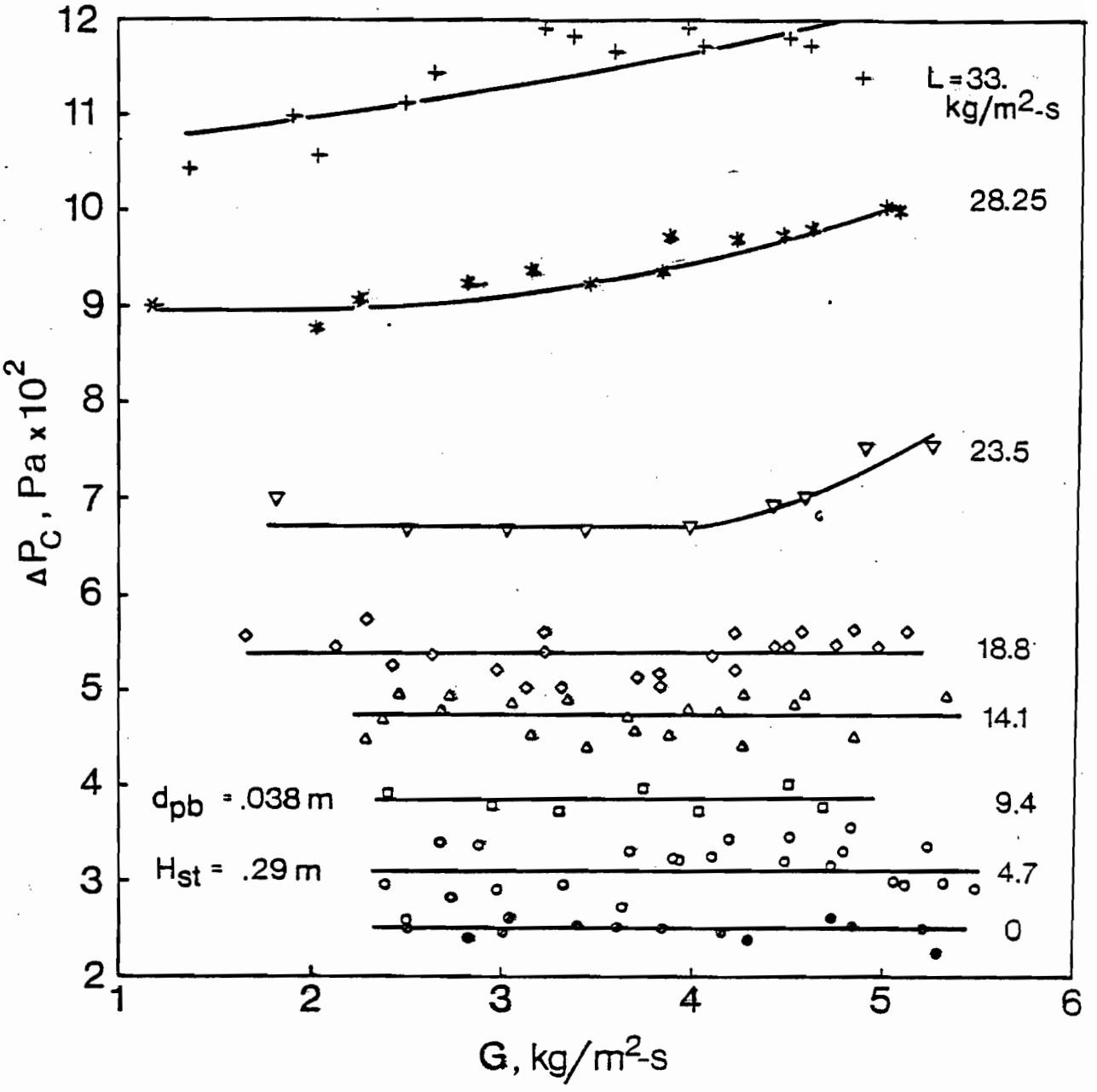

FIGURE 6.14. Pressure drop in MBC for H_{st} = 0.29 m and d_{pb} = 38 mm

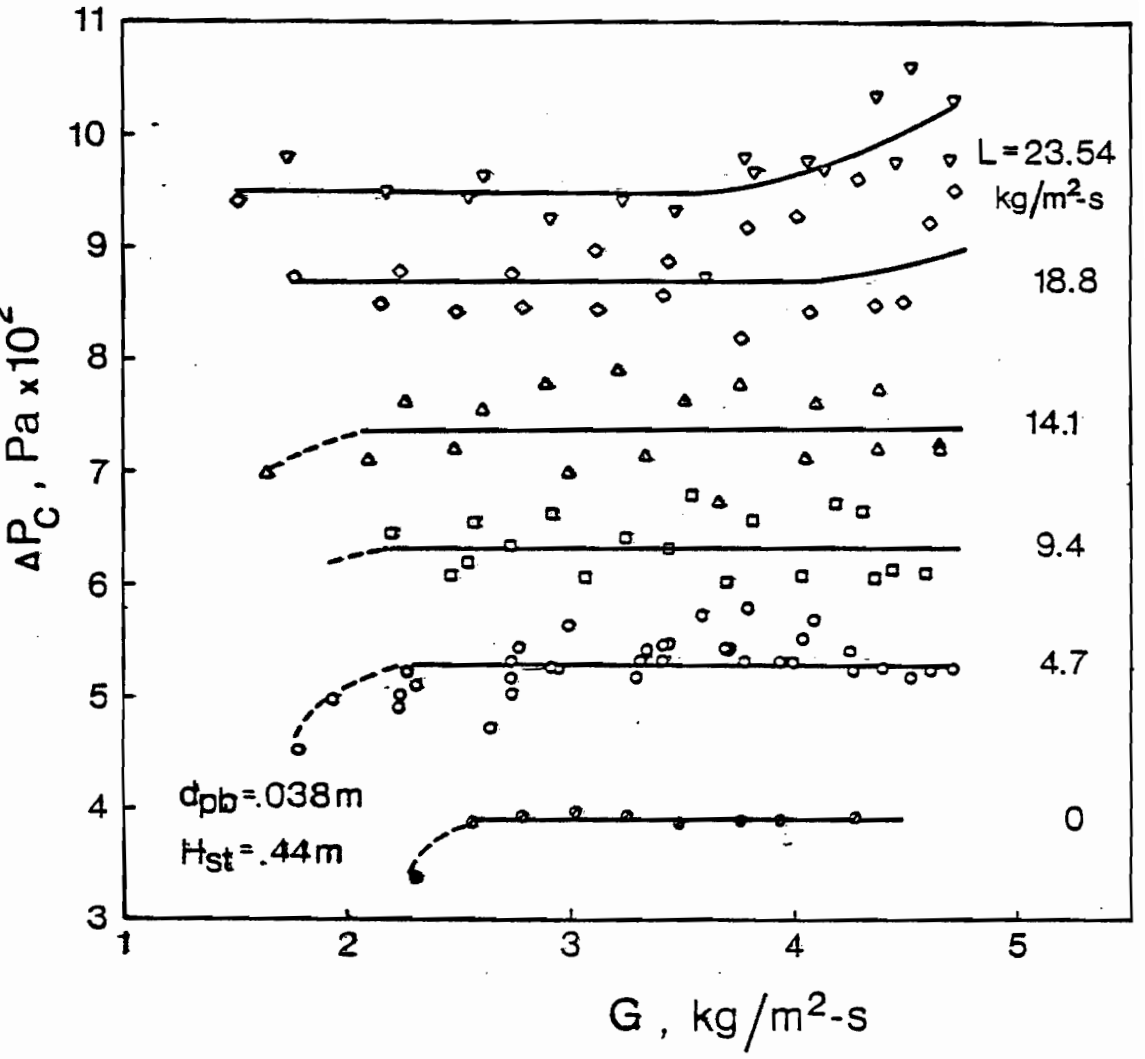

FIGURE 6.15. Pressure drop in MBC for H_{st} = 0.44 m and d_{pb} = 38 mm

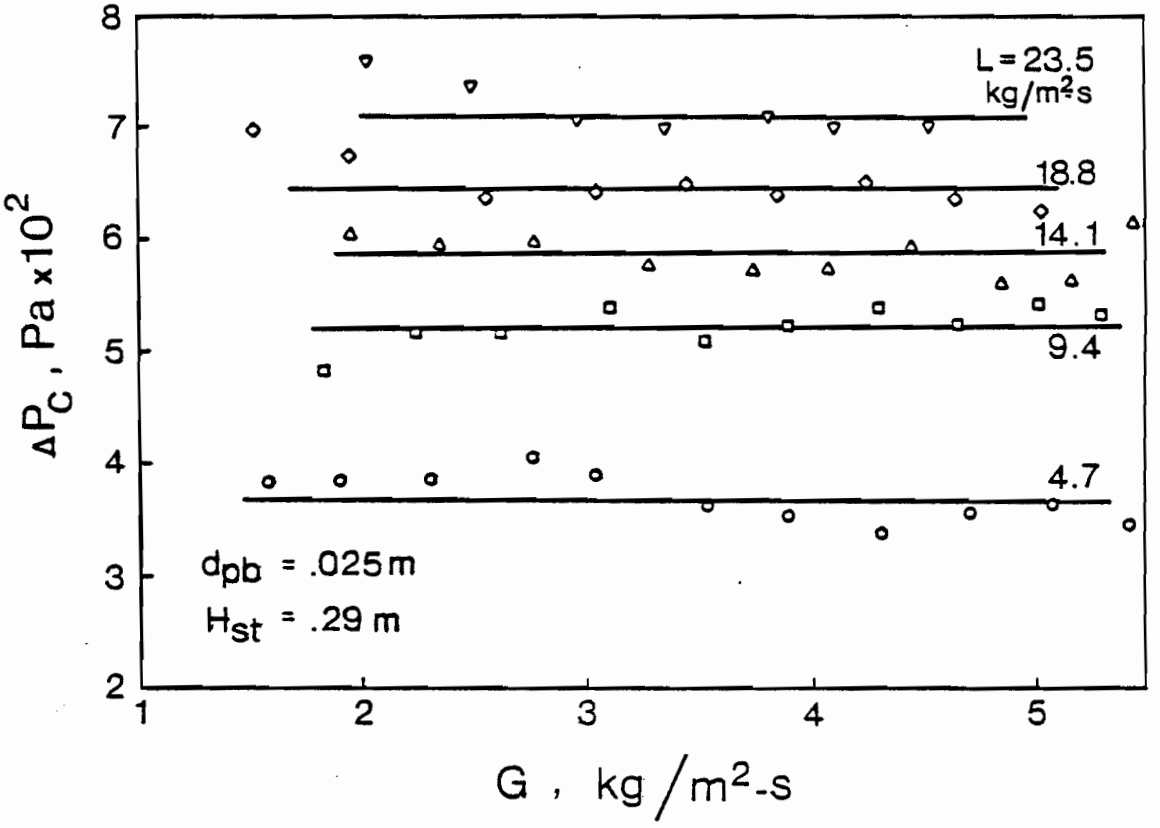

FIGURE 6.16. Pressure drop in MBC for H_{st} = 0.29 m and d_{pb} = 25 mm

FIGURE 6.17. Pressure drop in MBC for H_{st} = 0.44 m and d_{pb} = 25 mm

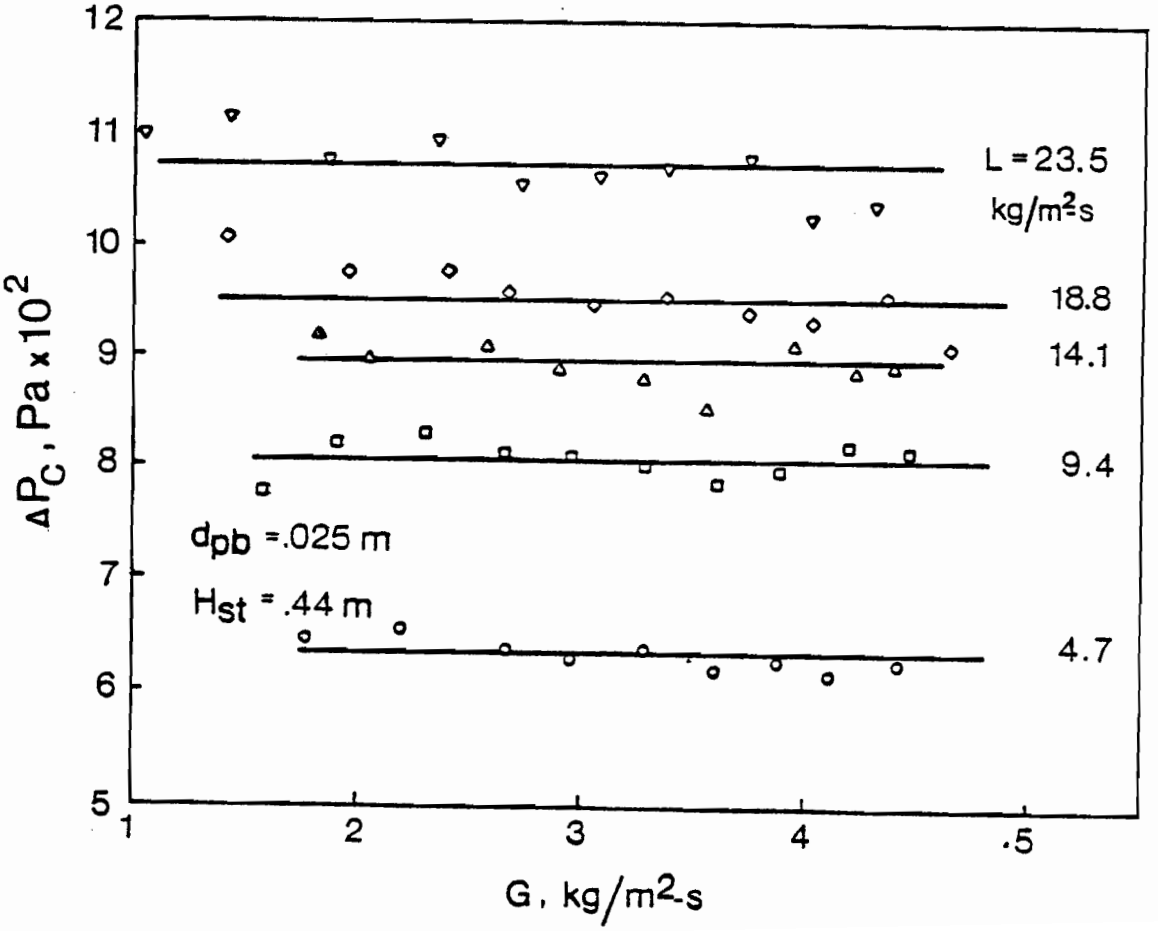

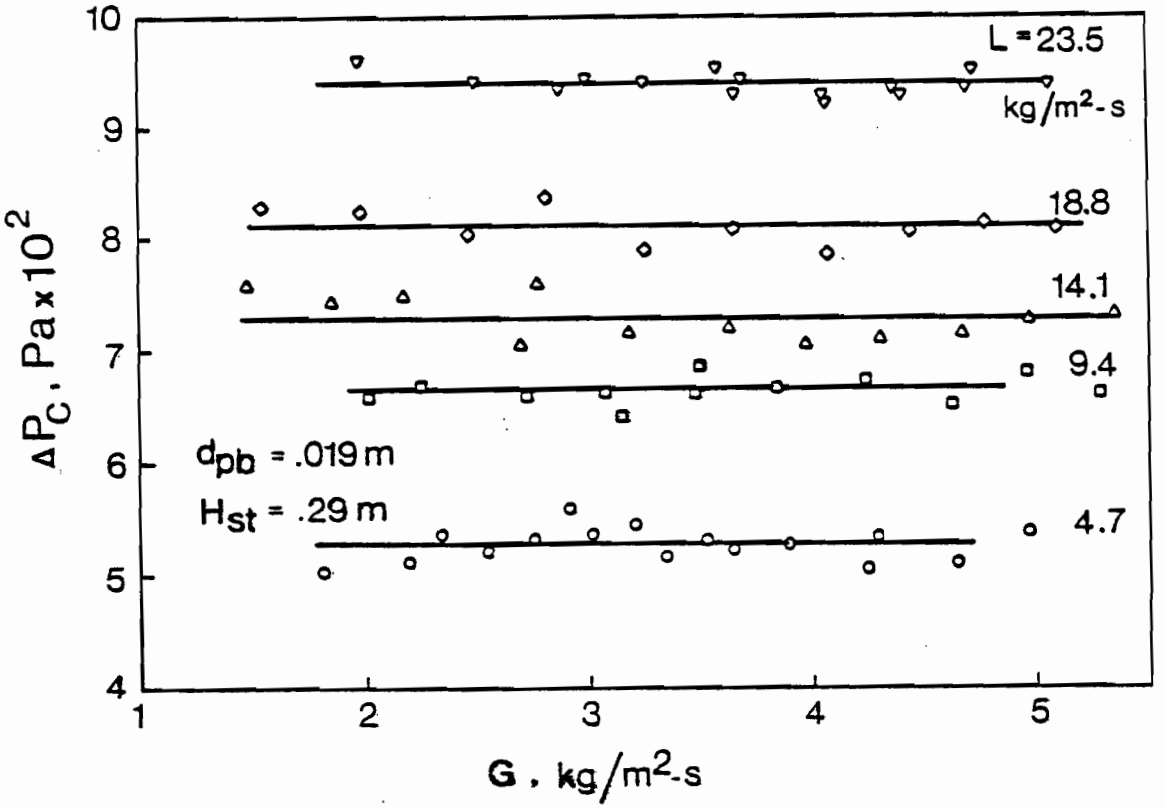

FIGURE 6.18. Pressure drop in MBC for H_{st} = 0.29 m and d_{pb} = 19 mm

FIGURE 6.19. Pressure drop in MBC for H_{st} = 0.44 m and d_{pb} = 19 mm

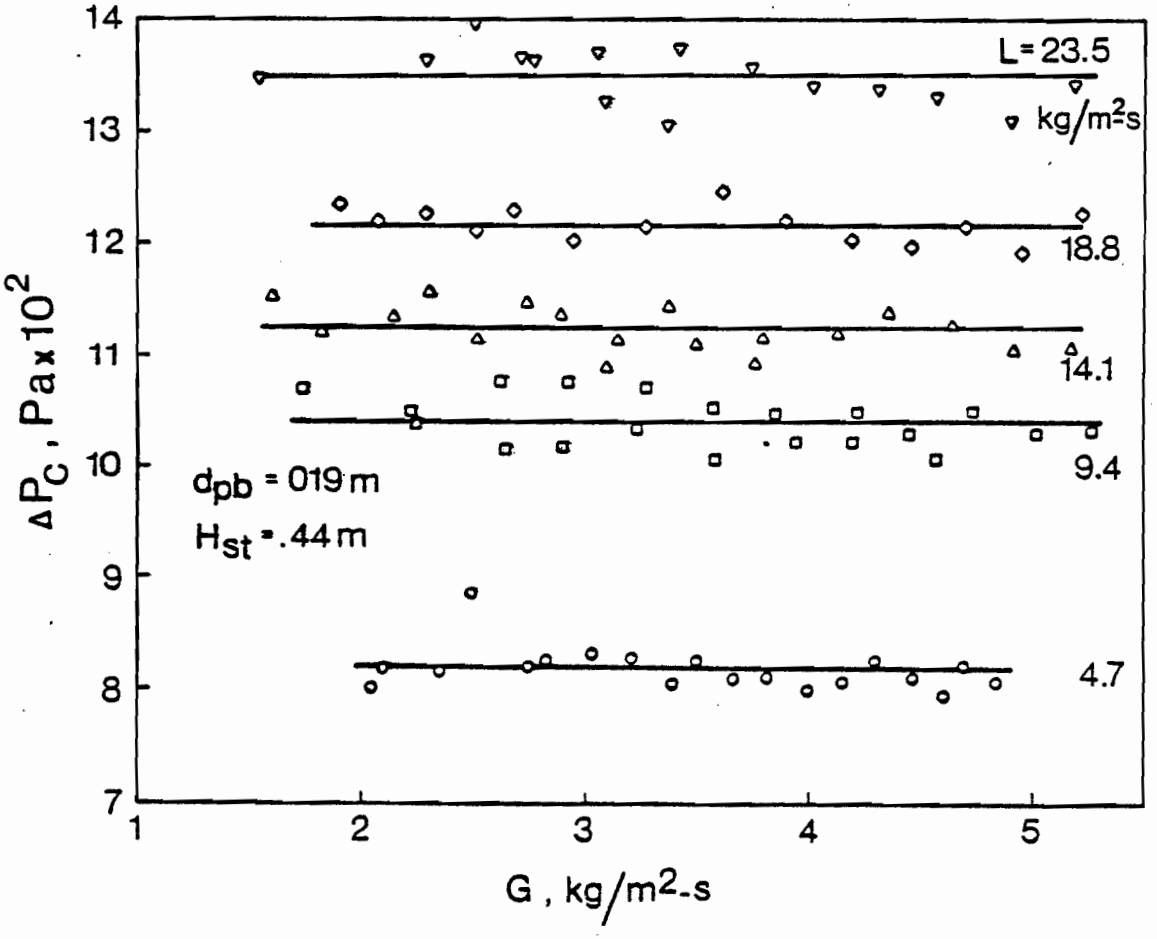

This is the same equation which appeared without comment in the earlier MBC studies of Barile et al. (1971) and Tichy and Douglas (1973), i.e.

$$\Delta P_c = (h_L \rho_L + h_{pb} \rho_{pb}) g H$$

$$= (h_{L,st} \rho_L + h_{pb,st} \rho_{pb}) g H_{st} \qquad (2.1.1)$$

Equation (2.1.1) is a very useful relation as it shows that, when the fully developed mobile state is reached by the packing, pressure drop in MBC is equal to the sum of the weights of solid packing and liquid holdup. This equation establishes then the close interconnection, referred to at the outset, between pressure drop and liquid holdup. Stated otherwise, this equation indicates that liquid holdup may be predicted from pressure drop, or vice versa. It is believed that the experimental method of determination of pressure drop (Sections 5.2.5.1 and 5.3.3) is simple, yet accurate.

Pressure drop data obtained at various gas and liquid flow rates for two static bed heights and three packing sizes are tabulated in Appendix C and plotted in Figures 6.14-6.19. The basic feature of these results is that, over normal operating conditions, pressure drop is independent of gas flow rate. This is consistent with the general characteristic behaviour of a mobile-bed contactor represented in Figure 2.1, as suggested by Chen and Douglas (1968), Barile and Meyer (1971), and Tichy and Douglas (1973). As clearly demonstrated for high liquid flow rates in Figures 6.14 and 6.15, beyond the constant pressure drop region, ΔP_c increases again with gas flow rate, due to the increase of liquid holdup in the column. At these conditions of high gas and

liquid flow rates the behaviour of the column was not uniform and there was appreciable liquid entrainment into gas. As may be noted in Figure 6.14 the transition from normal operating conditions, where pressure drop is constant, to the conditions where pressure drop increases with gas flow rate, occurs at progressively lower gas flow rates with increasing liquid rate. This trend is consistent with the observed behaviour for bed expansion discussed in the previous section. The non-linear region of increasing ΔP_c corresponds to non-linear bed expansion.

As may be noted in Figures 6.14 and 6.15 the broadest regions of stable operating conditions for MBC are for liquid flow rates smaller than about 25 kg/m^2-s. The maximum liquid flow rate was therefore limited to this value for further experiments in this study. At each liquid flow rate, then, the average values of the pressure drop data, represented by the horizontal lines in Figures 6.14-6.19, were subjected to multiple regression analysis using the STATPK subroutine of the McGill Computing Center. The following correlation was thereby obtained:

$$\Delta P_c = 112.17\ L^{0.44}\ d_{pb}^{-0.492}\ H_{st} \qquad (6.1.13)$$

The exponent of H_{st} in the above equation is specifically set equal to 1, as suggested by Equation (2.1.1). In order to verify this point, the correlation was first made allowing H_{st} to be an independent variable in the multiple regression, in which case the exponent for H_{st} was found to be 0.95. This test establishes that forcing this exponent in the regression to be 1, as suggested by the theoretical analysis, is consistent

with the experimental data. The multiple correlation coefficient found for Equation (6.1.13) is 0.93. The probability associated with the F value evaluated for the data is 1. These statistical measures show that the proposed correlation is quite adequate for the data. Figure 6.20 likewise shows the good fit of this correlation to the experimental data.

In Figure 6.21 the results of the present study are also compared with limited results reported in the literature, for conditions preferred in industry, i.e. $d_{pb} = 38$ mm and $H_{st} = 0.29$ m. Correlations previously reported were summarized in Table 2.3, not all of which are included in Figure 6.21. The correlations proposed by Blyakher et al. (1967) and by Uchida et al. (1977) - Kito et al. (1976) are not included as their results were distorted by, respectively, the use of small open-area support grids and small D_c/d_{pb} ratios. The correlation proposed by Levsh et al. (April 1968) and Krainev et al. (1968) was for plastic rings, which are of little industrial interest. The correlation of Tichy and Douglas (1972) does not consider the effect of packing size and experimental data for 38 mm packing are not available from the cited study. Also in the study of Tichy and Douglas (1973) there were no data for 38 mm packing. The correlation of UOP (1970) - Bechtel (1971) is not reliable in that it predicts negative values for some reasonable flow conditions (example: $L = 5$ kg/m^2-s and $G = 3$ kg/m^2-s). As the actual data obtained by UOP are available (UOP Bulletin No.608 and Douglas et al. (1963)), these pressure drop values over the range independent of gas flow rate are included in Figure 6.21. Only two other previous studies, those of Barile and Meyer (1971) and Wozniak (1977) could be used for comparison with the present study.

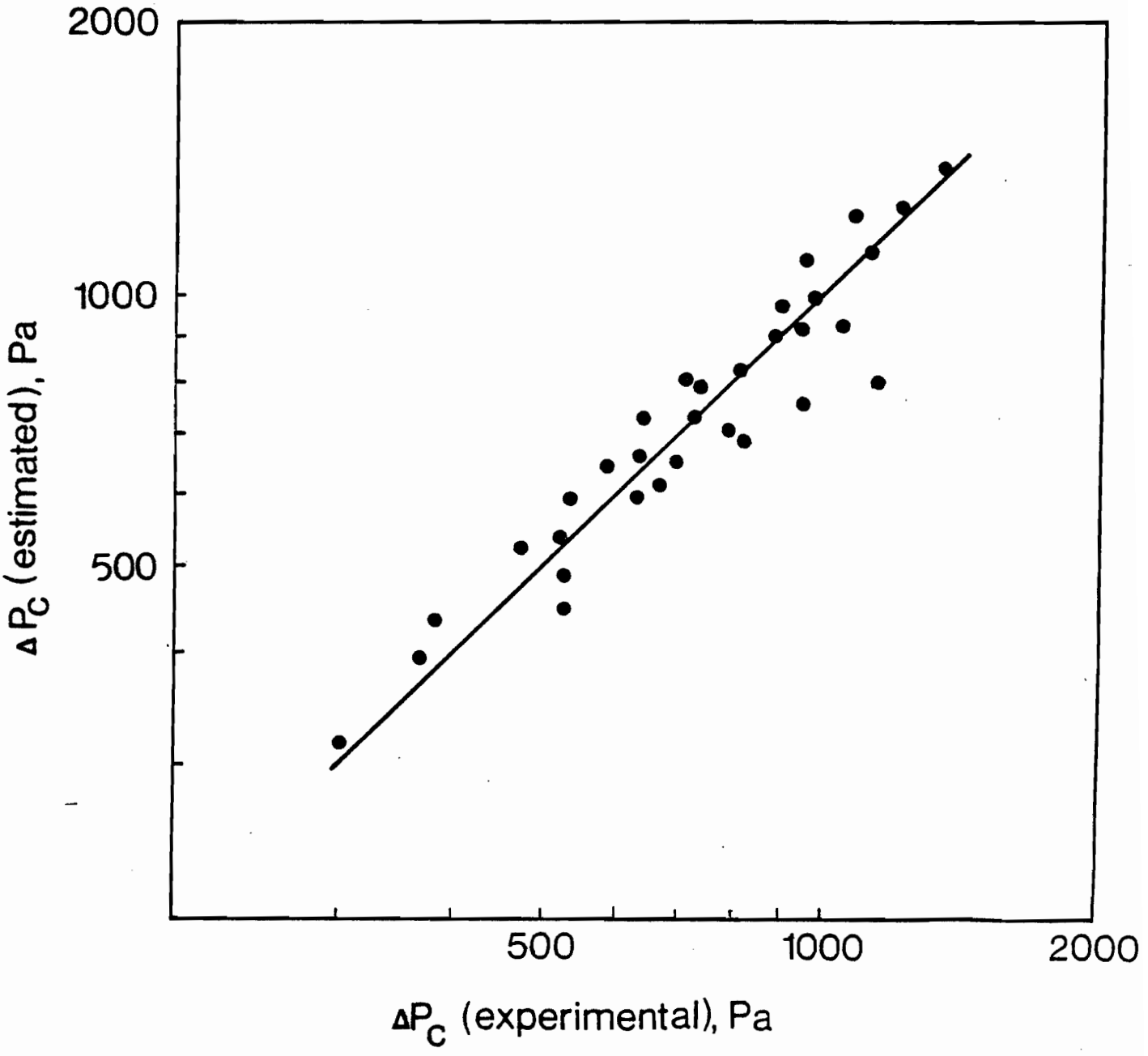

FIGURE 6.20. Comparison of experimental and estimated values of pressure drop

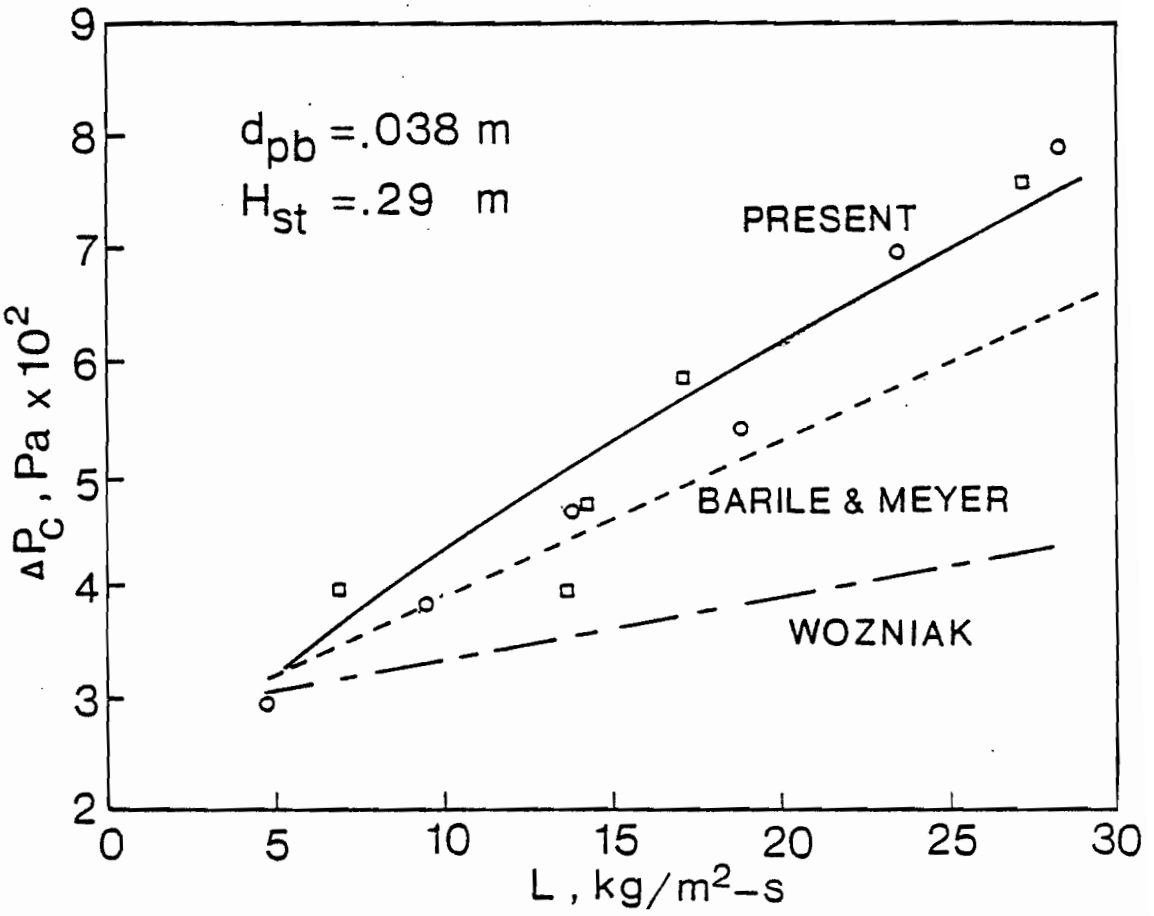

FIGURE 6.21. Comparison of present study with previous literature on pressure drop in MBC

○ Present

□ U.O.P.

As noted in Section 2.1.3, Wozniak's correlation includes an effect of gas velocity on pressure drop. However, by the extensive measurements presented in the present study, it has been shown that gas velocity does not affect pressure drop over the normal range of operating conditions. In order to be able to make a comparison, the line for Wozniak's correlation in Figure 6.21 was drawn for a typical value of gas flow rate, i.e. $G = 3$ kg/m^2-s.

The new results of the present study agree reasonably well with those of Barile and Meyer at low and intermediate liquid flow rates. At high liquid flow rates, of great importance industrially, the pressure drop predictions of the two studies of Barile and Meyer, and Wozniak diverge significantly. Predictions made by Wozniak's correlation in the important range of high liquid rates are only about half of those given by the present study. This lack of agreement for pressure drop measurement will be explained in the subsequent discussion concerning the interrelated variable, liquid holdup. The agreement of the present data and correlation with the data obtained with a full-scale MBC column by UOP is quite satisfactory.

For 19 mm packing, pressure drop results of the present study are within 10% agreement with those of the only other study performed with the same size column (0.29 m), by Tichy and Douglas (1973).

As already noted, liquid holdup in the present study is evaluated from pressure drop measurements by means of Equation (2.1.1). Thus, values of liquid holdup were calculated for conditions which correspond to those regions of Figures 6.14-6.19 over which pressure drop (and hence liquid holdup) is independent of gas velocity. Values of liquid holdup thus calculated are correlated by multiple regression

analysis using the STATPK subroutine. The following is the equation obtained from this analysis.

$$h_{L,st} = 1.15 \times 10^{-4} \, L^{0.826} \, d_{pb}^{-1.289} \qquad (6.1.14)$$

The multiple correlation coefficient obtained for the logarithmic form of this equation is 0.94, an indication of quite satisfactory fit of Equation (6.1.14) to the experimental data. Figure 6.22 also shows the adequacy of this correlation for MBC liquid holdup over the extensive operating region for which pressure drop is independent of gas velocities. Once again it may be noted that the constants determined from the statistical analysis, in this case the exponents of L and d_{pb}, can be rounded to 0.83 and -1.3, respectively, without significant loss of accuracy.

Present results agree with the previous studies reported by Chen (1965), Chen and Douglas (1968), and Barile and Meyer (1971) with respect to the lack of dependence of liquid holdup on gas flow rate over the stable operating region of MBC.

Figure 6.23 shows the effect of liquid flow rate and packing size on liquid holdup. Results of all previously published studies are also shown for comparison. The fact that the data of the present study indicate that the liquid holdup increases with a decrease in packing size is in agreement with studies reported by Chen (1965), Chen and Douglas (1968) and Barile and Meyer (1971). Figure 6.23 also shows the average experimental values of liquid holdup for liquid flow rates larger than 25 kg/m^2-s, for 38 mm packing. As noted earlier, liquid holdup increases very rapidly in this range. Beyond this limit of liquid flow rate it was observed during the experiments that the packing

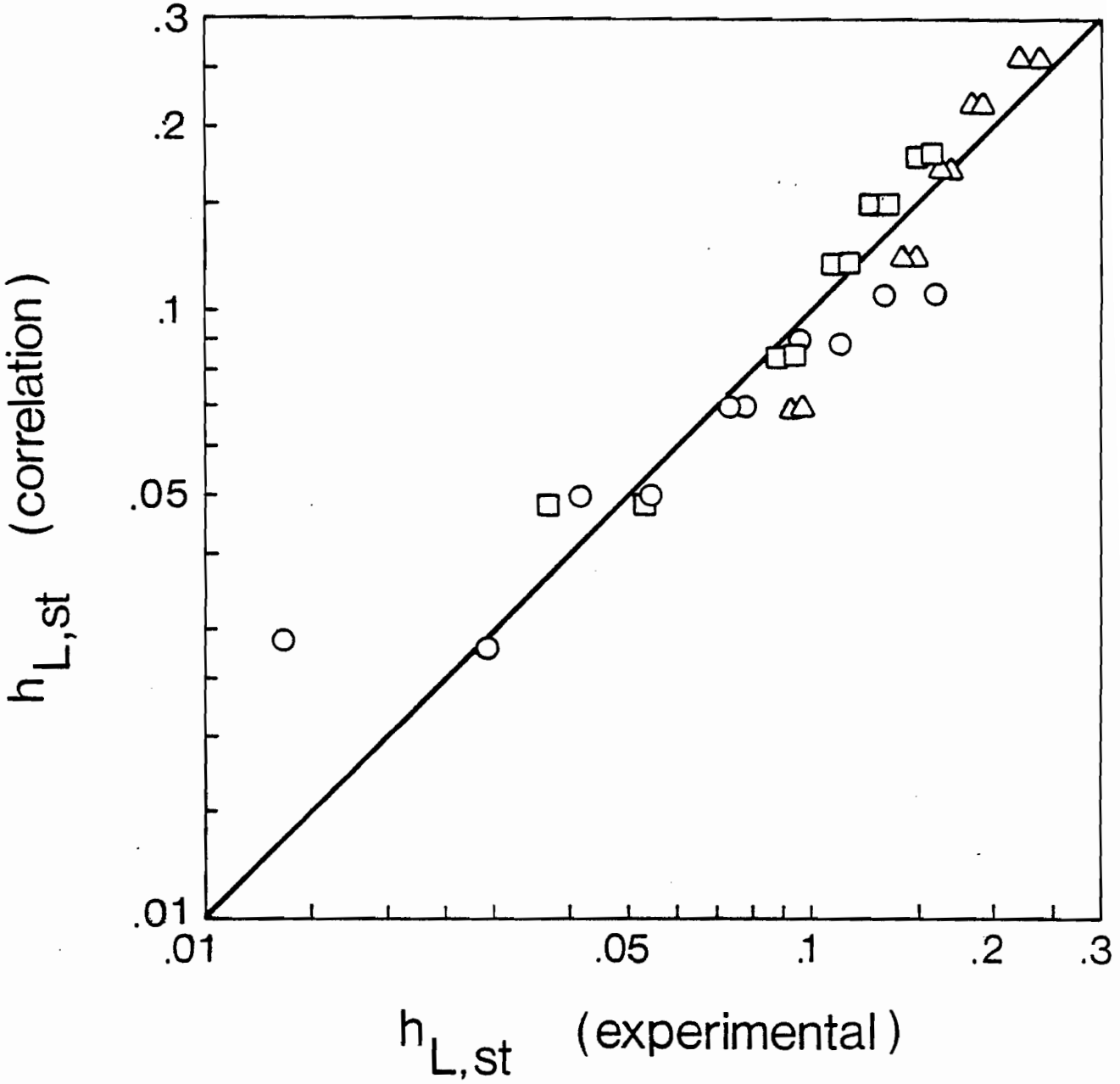

FIGURE 6.22. Comparison of experimental and estimated values of liquid holdup

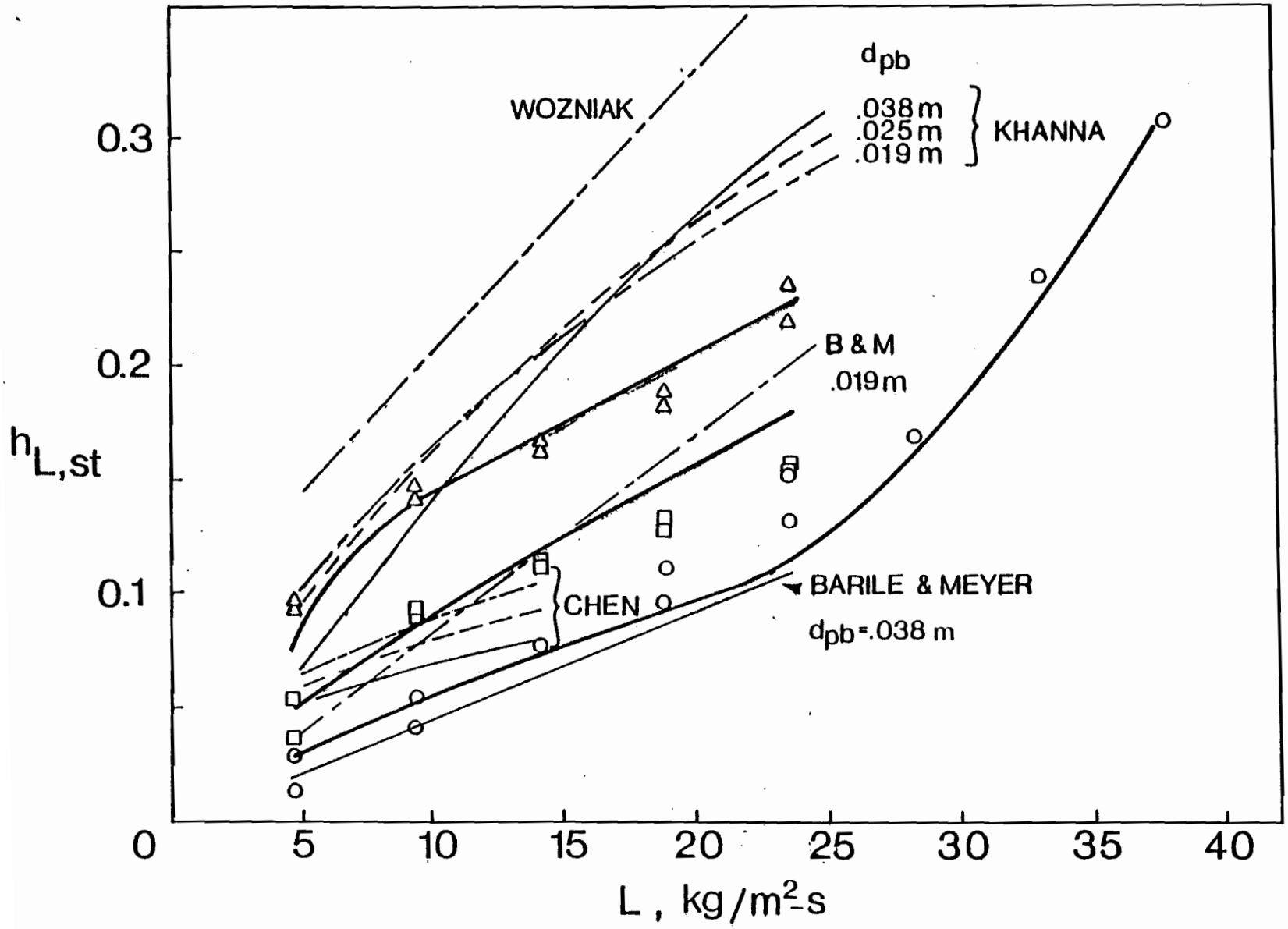

FIGURE 6.23. Liquid holdup dependence on liquid flow rate
○ d_p = 38 mm; □ d_p = 25 mm; △ d_p = 19 mm
Thick solid lines represent the present correlation

was maldistributed in the column, tended to agglomerate, adhered to the column wall, and that liquid entrainment into the gas increased very appreciably. These operating characteristics explicitly put a restriction on the upper limit of the normal operating range of MBC.

There appears to be an internal inconsistency in the results of Wozniak (1977) in that his liquid holdup data are the highest of those compared, whereas, as noted in Figure 6.21, Wozniak's data for pressure drop are the lowest. This is a contradiction. In review of the simple interrelationship between ΔP_c and h_L, given by Equation (2.1.1), either Wozniak's pressure drop measurements or liquid holdup measurements, or both, appear to be in error. It may be noted the direct volumetric measurement of liquid holdup made by Wozniak is not a very accurate method for a column in which there is such turbulent motion as MBC. It was for this reason that Chen and Douglas (1968) avoided this method and chose instead to measure h_L by a transient response technique. It is also relevant to note that in Wozniak's study pressure drop measurements were made using a simple u-tube manometer. Surprisingly, the scatter of his pressure drop data is negligible. Considering the fluctuations, sometimes as high as ± 15%, observed both in the present study and by other investigators of MBC hydrodynamics, one may therefore also question the reliability of his pressure drop data.

Khanna (1971), in his study of liquid holdup, presented his results only in graphical and tabular form. The author has correlated Khanna's results by the following equation:

$$h_L = 0.038\ L^{0.65}\ G^{-0.32}\ d_{pb}^{0.08} \qquad (6.1.15)$$

It can be noted that the basis of liquid holdup in Equations (6.1.14) and (6.1.15) are not the same, i.e. the basis is static bed and expanded bed volume, respectively. After being reduced to the same basis, i.e. to the volume of static bed by using Khanna's bed expansion data, this correlation of Khanna's results is also plotted in Figure 6.23 for a typical value of gas velocity, $G = 3$ kg/m^2-s. The values predicted by Equation (6.1.15) are unrealistically high for true MBC operation. The high values obtained by Khanna may be attributed to the small dimensions of the column used. Thus, the wall effect would have been strong, resulting in the tendency for a stationary layer of packing balls to adhere to the wall, as was indeed noted by Khanna. Such a condition leads to an increase in liquid holdup in the peripheral layer of packing and hence to the high values measured by Khanna. Furthermore, Khanna's data do not show a consistent effect of packing size (Figure 6.23). This leads one to conclude that in Khanna's experiments the dominating wall effect largely obscured the effect of packing size. It is interesting to note that over the lower range of liquid velocities ($L < 15$ kg/m^2-s) Khanna's results deviate less from the results of the present study and, moreover, indicate the smallest holdup for the largest of his packing sizes ($d_{pb} = 38$ mm). The latter trend is consistent with the extensive findings of the present study. As has also been demonstrated in the present study, maldistribution of packing and erratic behaviour are accentuated at high liquid velocities. Thus it is not surprising that as L increases, Khanna's results should diverge increasingly from those

of the present study as the wall effect in Khanna's results becomes progressively more significant. As the excess h_L for Khanna's case is primarily associated with the liquid which is trapped between the column walls and packing balls adhering to these walls it is also understandable that, at the highest liquid velocities ($L = 20, 25$ kg/m^2-s), the liquid holdup increases with d_{pb}, i.e. exactly opposite to the effect in the absence of wall effect. This trend is a natural consequence of the fact that the larger the diameter of balls adhering to the column wall, the larger the amount of liquid holdup between those balls and the wall. Thus, even though Khanna's results are not relevant to industrial conditions for MBC, they do display consistency with the phenomena which are associated with wall effects.

Although Chen (1965) used a large column (the same size as that of the present study), he covered only a relatively small range of flow rates. The maximum liquid flow rate was 14.7 kg/m^2-s. Nevertheless, the important finding of Chen that, over this operating range, the liquid holdup is not a function of gas flow rate agrees with the present work. But the values of his data for 38 mm and 25 mm packing agree reasonably with the present work. The effect of packing size on liquid holdup is also the same as determined in the present study, i.e. liquid holdup increases as packing size gets smaller, but the extent of this trend is different as represented by the exponents of d_{pb}, -0.5 in his equation (Equation (2.1.2)) and -1.29 in the present equation (Equation (6.1.14)).

As may be seen in Figure 6.23 the closest agreement of the present study is with the liquid holdup results of Barile and Meyer

(1971) for 38 mm packing. It is interesting to recall from Section 2.1.4 that they also evaluated liquid holdup from pressure drop measurements. Their results for the only other size of packing that they used (19 mm), however, are lower than the corresponding results of the present study. As may be noted from their correlation (Equation (2.1.3)), Barile and Meyer obtained a dependence of $h_{L,st}$ on $d_{pb}^{-0.93}$ using the results for two sizes. As three packing sizes were used in the present study, the exponent of d_{pb}, -1.29, in the present correlation is believed to be more dependable.

Overall comparison of the results of the present liquid holdup study with those reported by Barile and Meyer (1971) and Chen (1965) for 38 mm packing is very interesting. While the present work agrees very well with that of Barile and Meyer, Chen's liquid holdup data, which were obtained by a transient-response technique, are a little higher. If the theoretical analysis and assumptions made at the beginning of this section to obtain Equation (2.1.1) from Equation (6.1.9) had been wrong, then the effect would have been reflected in anomolously high values of liquid holdup in the present study with respect to those of Chen for 38 mm packing, due to omission of effects such as F_{mixing}, $F_{interfacial}$, etc. The comparison of results presented in Figure 6.23 indicates that this is not the case. Thus, it may be concluded that Equation (2.1.1) may with confidence be used to evaluate h_L from ΔP_c, or vice versa.

In summary, experimental results of the present study provide extensive documentation of a stable operating range of MBC where ΔP_c and $h_{L,st}$ are independent of gas flow rate and this region corresponds

to linear bed expansion region. Thus, the results of those previous studies which indicated dependence of ΔP_c or $h_{L,st}$ on G cannot be regarded as reliable. It is also shown that pressure drop and liquid holdup increase with liquid flow rate and decrease with packing size. Furthermore, considering the extensive pressure drop measurements of the present work, the dependability of the method of calculation of liquid holdup from these data, and the extensive range of variables which has been studied lead to the conclusion that Equations (6.1.13) and (6.1.14) are the most reliable correlations to evaluate, respectively, pressure drop and liquid holdup in MBC.

6.2 PARTICULATE RECOVERY

As the objective of this first comprehensive investigation of particulate recovery in MBC is to propose and validate a model for prediction of particle collection efficiency at any condition, an extensive number of experiments were performed covering a wide range of variables and operating conditions. The results of the complete set of experiments were subjected to multiple regression analysis. It was thereby found possible to obtain a single, theoretically-based empirical correlation which accounts adequately for all the results. For the case of the present study it is more convenient to present first the method of treatment of all the variables and analysis of the complete set of inertial collection data. This process leads to presentation of the general correlation for inertial collection in MBC. Following this are separate treatments of the effect on particle collection of each variable included in the present study. The effects of hydrophobicity of particles and of diffusiophoresis, being different in

character from the other variables, are analyzed in subsequent sections. The discussion is completed with a comparison of particulate recovery in other scrubbers with that in MBC.

6.2.1 Particulate Recovery Due to Inertial Collection

Data Reduction:

Theoretical analysis of particulate recovery in the absence of any phoretic force, as presented in section 4.3, has shown that particle penetration can be evaluated by means of equation 4.3.6

$$Pt = \frac{\bar{n}_{p,out}}{\bar{n}_{p,in}} = \exp\{-k_p H/u_z\} \qquad (4.3.6)$$

Penetration, therefore, can be determined experimentally by measuring the inlet and outlet particle concentrations. Inlet concentration, $\bar{n}_{p,in}$, was measured just at the entrance of the test column (as shown in Figure 5.1). However, because of the serious interference of water droplets with measurement of concentration of the aerosol, the outlet sampling nozzle could not be placed below the upper grid or liquid distributor. For this reason the outlet sampling nozzle was located at the top of the column (Figure 5.1). In designing the column for maximum gas and liquid flow rates and maximum bed height, it was necessary to fix the spacing between the upper and lower grids at 1.5 m. For experiments at low static bed height and low gas and liquid flow rates, the expanded bed height was, of course, smaller than 1.5 m. Thus, particle concentration determined at the column exit was affected

not only by particle collection in the active volume of MBC, but also by collection in the section of column between the top of the expanded bed and the liquid distributor. This upper section acts as a spray column. In other words, the change in particle concentration from $\bar{n}_{p,in}$ to $\bar{n}_{p/z = H}$ was due to collection in MBC, and from $\bar{n}_{p/z = H}$ to $\bar{n}_{p,out} = n_{p/z = 1.5\ m}$ was due to the spray section. This statement may be expressed as

$$Pt = \frac{\bar{n}_{p,out}}{\bar{n}_{p,in}} = Pt_{MBC}\ \ Pt_{H-1.5} \qquad (6.2.1)$$

In order to account correctly for particle collection in the spray column section between the liquid distributor and the top of the mobile-bed, the entire column was operated as a spray column, i.e. without packing. This auxiliary study was carried out with the ferrous sulphate particles used to develop the model for particle penetration, and details are given in Appendix J. Correlation of the results of these spray column experiments, using the general theory developed in Chapter 4, leads to an equation for particle transfer coefficient in the spray column in the form

$$k_{p,SC} = 0.0165\ L^{1.508}\ G^{0.745}\ St_d^{-0.413} \qquad (J.14)$$

Thus,

$$Pt_{H-1.5} = \exp\{-k_{p,SC}\ (1.5 - H)/u_z\} \qquad (6.2.2)$$

and

$$Pt_{MBC} = \left(\frac{\bar{n}_{p,out}}{\bar{n}_{p,in}} \right) / Pt_{H-1.5} \qquad (6.2.3)$$

Equation 6.2.3 was used to determine the particle penetration through MBC from particle concentrations measured at the inlet and outlet of the column. For the experimental conditions of the present study, maximum particulate recovery in the spray section was less than 10% of that in the mobile-bed. For large particles of a few microns, this ratio was only a few per cent.

Experimental values of the particle transfer coefficients for MBC could be calculated from the combination of equations 6.2.3 and 4.3.6 as

$$k_{p,MBC} = - u_z \, \ell n \, Pt_{MBC}/H \qquad (6.2.4)$$

Height of the mobile-bed, H, required for equations 6.2.2 and 6.2.4, was evaluated by the correlation developed for bed expansion (Equation 6.1.8). The gas velocity, represented as u_z in the above equations, is the superficial velocity, i.e. G/ρ_G.

Correlation of the Results

The order-of-magnitude analysis of Chapter 3 established that the dominant particle collection mechanism in MBC is inertial collection. This is the conclusion regardless of whether particles are collected by liquid droplets, by liquid films covering the packing, or are deposited from bubbles. Characteristic parameters for

inertial collection by these effects, namely St number and $N_{b,I}$, were defined by Equations 2.2.6-a and 2.2.14. As noted earlier in Chapter 3, the size of liquid droplets and bubbles cannot be measured due to the highly turbulent conditions of MBC. However, it can be postulated that size of packing is a key parameter affecting the agitated motion in the mobile-bed. Hence droplet and bubble sizes would be expected to depend on packing size. In this connection, it can be stated that the particle transfer coefficient for MBC would depend on Stokes number, defined as

$$St = c' \, d_p^{\,2} \, \rho_p \, u_r / 9 \, \mu_G \, d_{pb} \qquad (6.2.5)$$

The relative velocity required for Equation 6.2.5 could, because of the counter-current flow, be expressed as

$$u_r = u_{Gi} + u_{Li} \qquad (6.2.6)$$

Interstitial gas and liquid velocities can be written as

$$u_{Gi} = u_G/(1 - h_L - h_{pb}) \qquad (6.2.7)$$

$$u_{Li} = u_L/h_L \qquad (6.2.8)$$

where,

$$h_L = h_{L,st} \, H_{st}/H \qquad (6.2.9)$$

$$h_{pb} = h_{pb,st} \, H_{st}/H \qquad (6.2.10)$$

Height of the mobile-bed, H, and liquid holdup, $h_{L,st}$, can be evaluated from Equations 6.1.8 and 6.1.14, respectively, developed earlier.

Furthermore, the equation of motion for particles, as given earlier in Chapter 2,

$$\frac{d \underset{\rightarrow}{U}_p}{d\theta} = - \frac{1}{St} (\underset{\rightarrow}{U}_p - \underset{\rightarrow}{U}_G) \qquad (2.2.5)$$

implies that particle motion depends on the gas velocity field, which is characterized by gas Reynolds number,

$$Re_G = U_{Gi} \rho_G d_{pb}/\mu_G \qquad (6.2.11)$$

Since the liquid phase is also in motion, the gas velocity field, and hence particle trajectories, are also affected by this motion, which may be characterized by the liquid Reynolds number,

$$Re_L = U_{Li} \rho_L d_{pb}/\mu_L \qquad (6.2.12)$$

Moreover, Equation 4.3.6 represents a steady-state model with one distributed parameter along the height of the column. This suggests that MBC performance should depend on the ratio H_{st}/d_{pb}. All these effects must be incorporated into the correlation to be developed for particle transfer coefficient.

All the above considerations for dependence of particle transfer coefficient on relevant variables in MBC may be consolidated in a comprehensive expression,

$$k_{p,MBC} = f \{St, Re_G, Re_L, (H_{st}/d_{pb})\} \qquad (6.2.13)$$

An extensive number of experiments (602) were performed to study the effect of liquid and gas flow rates, static bed height, packing size and particle size, and thereby to determine the precise form of the general equation (6.2.13). This series of experiments was carried out using one particulate, ferrous sulphate ($\rho_p = 1900$ kg/m^3), of size range 0.35 to 5.5 μm. Operating conditions at which these experiments were carried out are summarized in Table 6.2. The complete results of these experiments are given in Table D.1 of Appendix D. Multiple regression analysis of these results, using the McGill University Computing Centre statistical program SPSSG 031, gave the following correlation:

$$k_{p,MBC} = 3765\ St^{0.8}\ Re_G^{-2.64}\ Re_L^{2.1}\ (H_{st}/d_{pb})^{1.52} \qquad (6.2.14)$$

The multiple correlation coefficient for the logarithmic form of the above equation is 0.984. The fit of this correlation to the data is shown graphically in Figures 6.24, 6.25 and 6.26, for 38 mm, 25 mm and 19 mm packing, respectively.

Use of Equation 6.2.14 together with Equation 4.3.6 gives particle penetration through MBC in the absence of any phoretic mechanism. Due to the extensive number of experiments, the wide range of variables investigated and the high value of the correlation coefficient, this first comprehensive model may be used with confidence for prediction of particulate collection in MBC.

In the following sections, the effect of the variables L, G, H_{st}, d_{pb} and d_p on particle penetration will be analysed individually.

TABLE 6.2. Operating conditions for experiments with ferrous sulphate particles in the absence of diffusiophoresis

Packing size, mm	Static bed height, m	Gas flow rates, kg/m^2-s	Liquid rates, kg/m^2-s	Particle sizes, μm
38	0.29	2.35,2.80,3.17,3.56,3.93	4.7,9.4,14.1,18.8,2.35	1.35,1.75,2.5,3.5,4.5,5.5
	0.44	2.37,2.85,3.22,3.47		
	0.58	2.85, 2.88		
25	0.29	2.85		
	0.44	2.406, 2.87		
	0.58	2.94		
19	0.29	2.4,2.86,3.23,3.56,3.88		
	0.44	2.42, 2.89		
	0.58	2.95		
38	0.44	2.86	9.4	0.35,0.45,0.55,0.7,0.9
38	0.44	2.89	18.8	1.1,1.35,1.75,2.5,3.5,4.5

LEGEND FOR FIGURES 6.24-6.43, 6.51, 6.52, 6.54 and 6.55

d_p	Symbols
.35 µm	●
.45 µm	■
.55 µm	▲
.7 µm	◆
.9 µm	▼
1.1 µm	◕
1.35 µm	◇
1.75 µm	▽
2.5 µm	○
3.5 µm	□
4.5 µm	△
5.5 µm	⬡

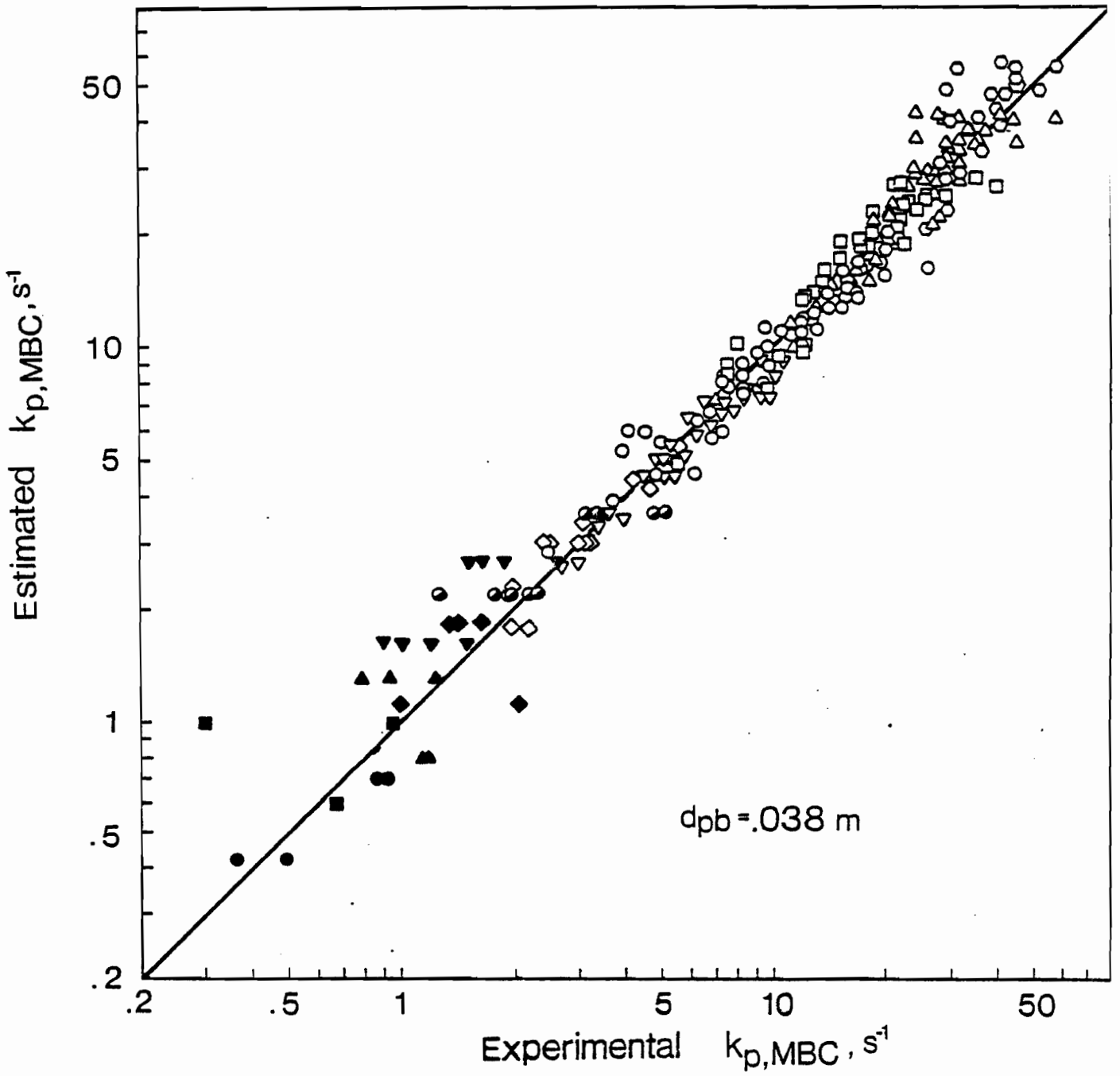

FIGURE 6.24. Comparison of experimental and estimated values of particle transfer coefficient for 38 mm packing

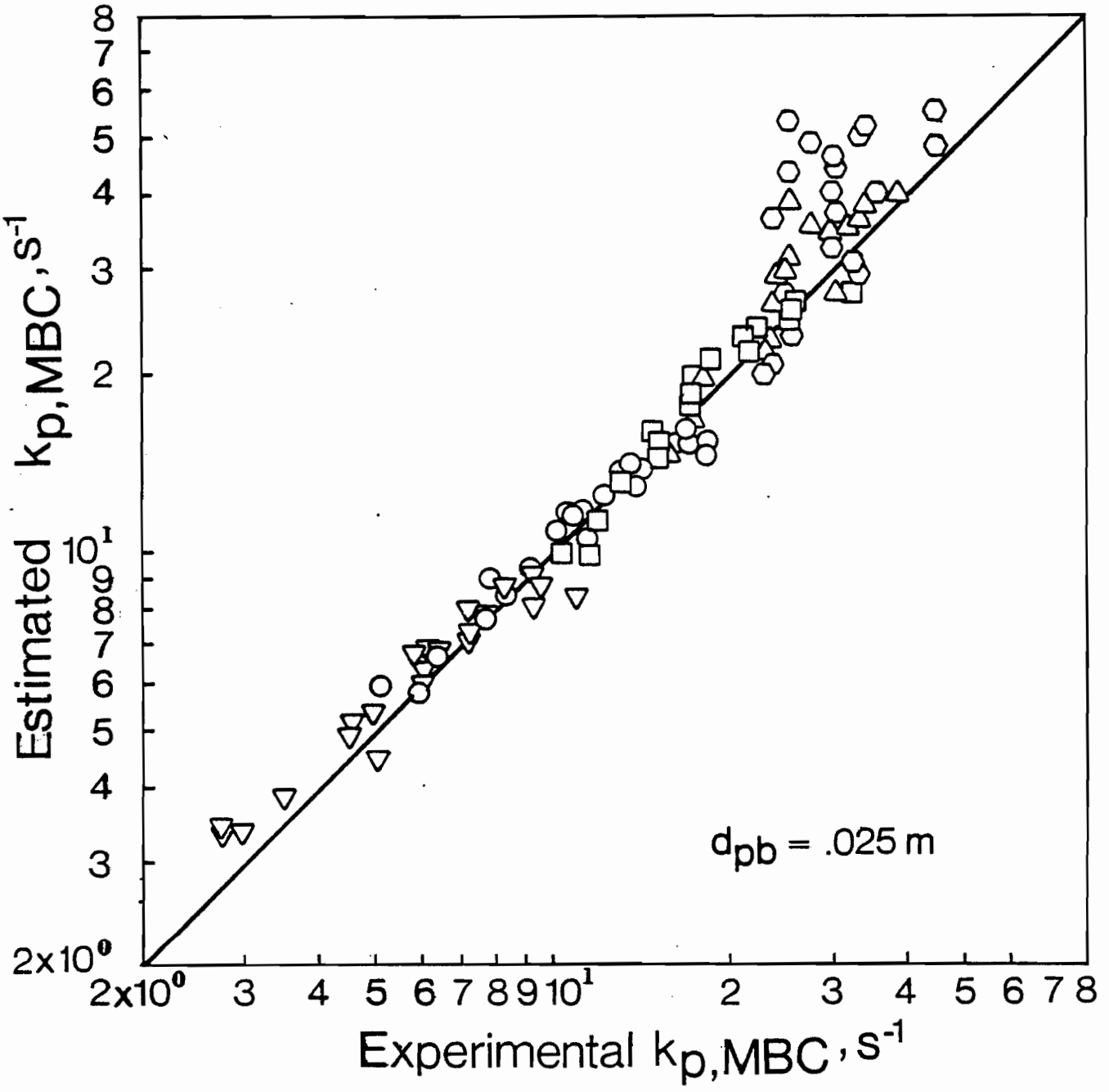

FIGURE 6.25. Comparison of experimental and estimated values of particle transfer coefficient for 25 mm packing

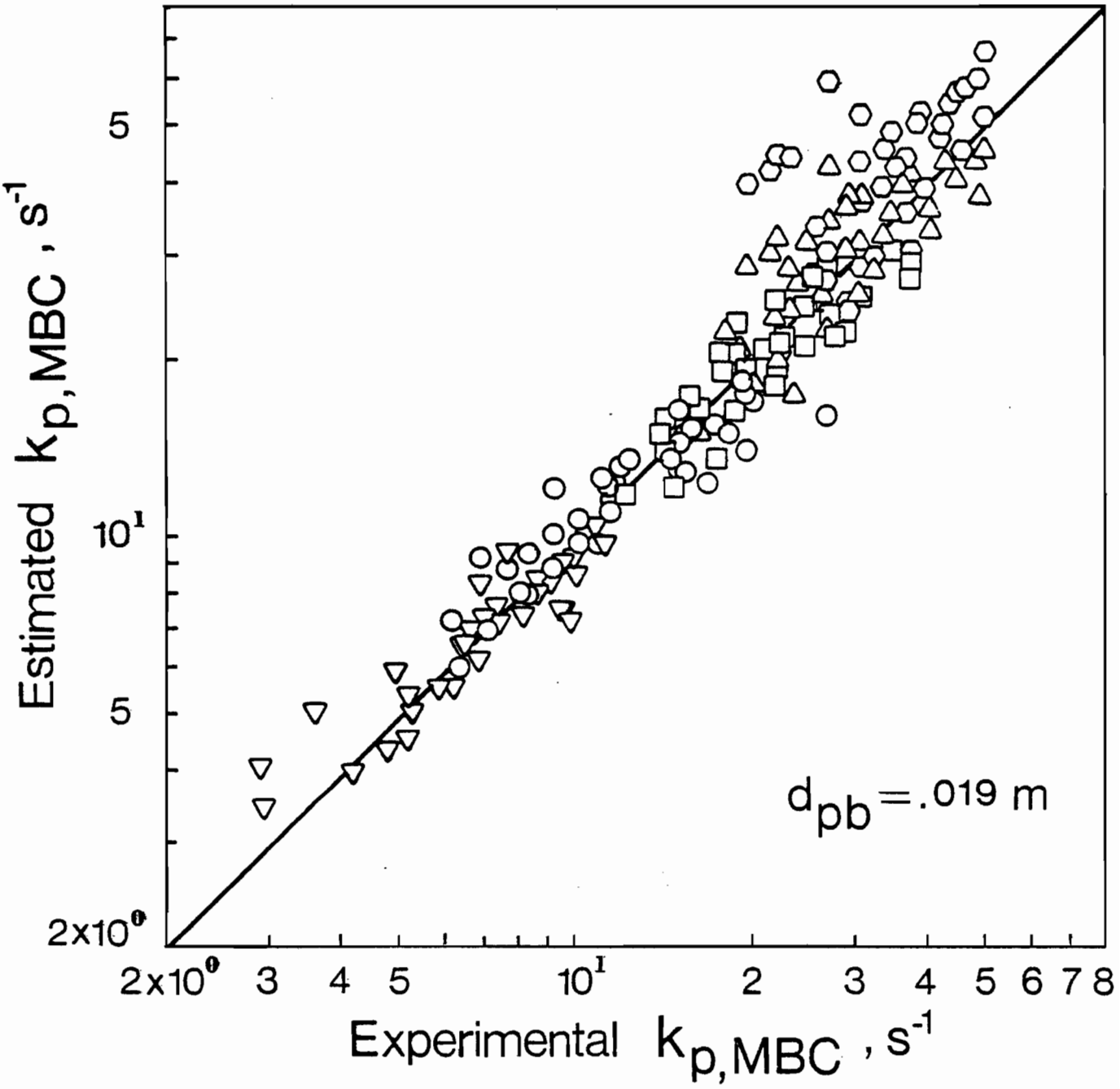

FIGURE 6.26. Comparison of experimental and estimated values of particle transfer coefficient for 19 mm packing

In so doing, it should be noted that it is not practical to present in graphical form the results of all the experiments, as their number is so large. The selection of experimental conditions for graphical presentation has been made so as to cover the extremes and the typical values of all operating variables.

6.2.1.1 Effect of Liquid Flow Rate

As in other scrubbers, liquid flow rate was found to have a very strong effect on particulate recovery in MBC. For all experiments in this study, penetration of particles decreased as liquid flow rate increased. Some typical results are shown in Figures 6.27 - 6.38. The choice for graphical representation of these 12 sets of operating conditions out of the much larger total number of experiments performed (see Table 6.2) was made so as to display at least one set of results for each of the 9 combinations of 3 packing sizes and 3 static bed heights used. In addition, for those combinations for which a wide range of gas velocities was tested, results for both the lowest and highest value of gas velocity are presented. The latter criterion applies to the pairs of Figures 6.27-6.28, 6.29-6.30, and 6.35-6.36. Finally, for each set of conditions (d_{pb}, H_{st} and G), these graphs include the results for all values of d_p tested, which correspond to from 4 to 6 values of d_p for each of the 12 sets of d_{pb} - H_{st} - G conditions.

Solid lines in Figures 6.27-6.38 do not correspond to a fit of the particular sub-set of data being displayed, but rather, represent penetration as given by the general correlation based on all of the data of the present study, i.e. Equation 6.2.14.

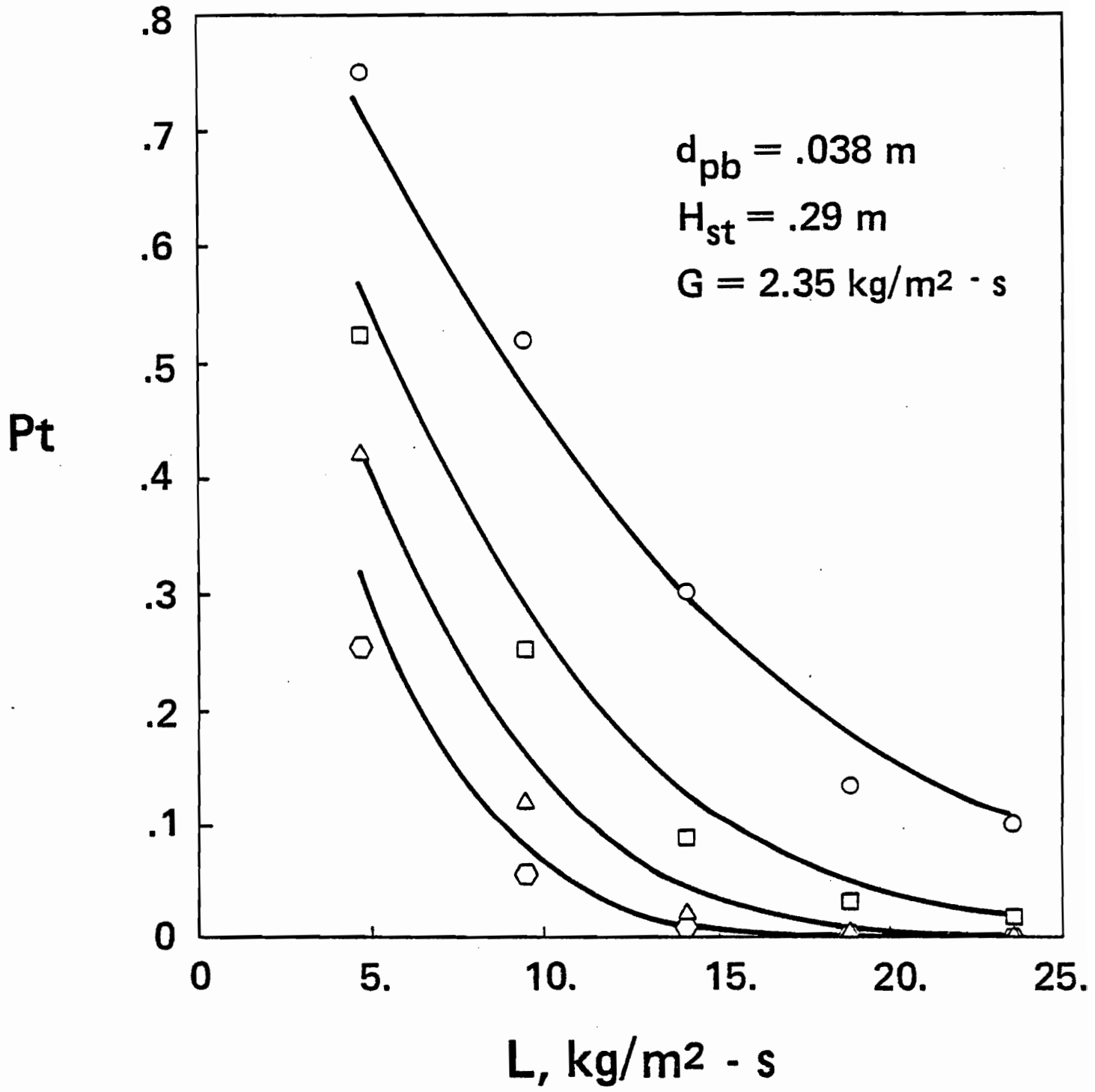

FIGURE 6.27. Effect of liquid flow rate on penetration

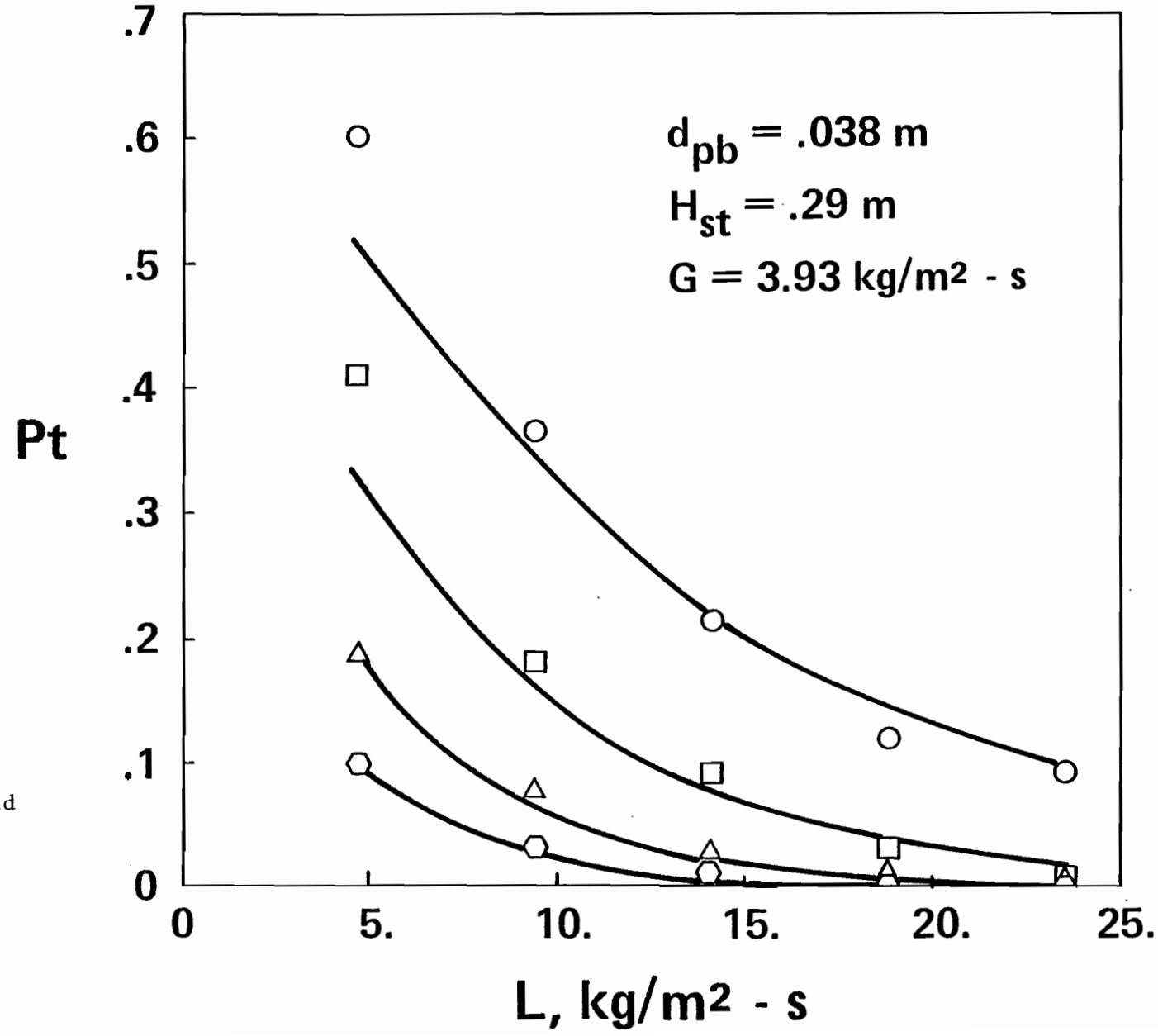

FIGURE 6.28. Effect of liquid flow rate on penetration

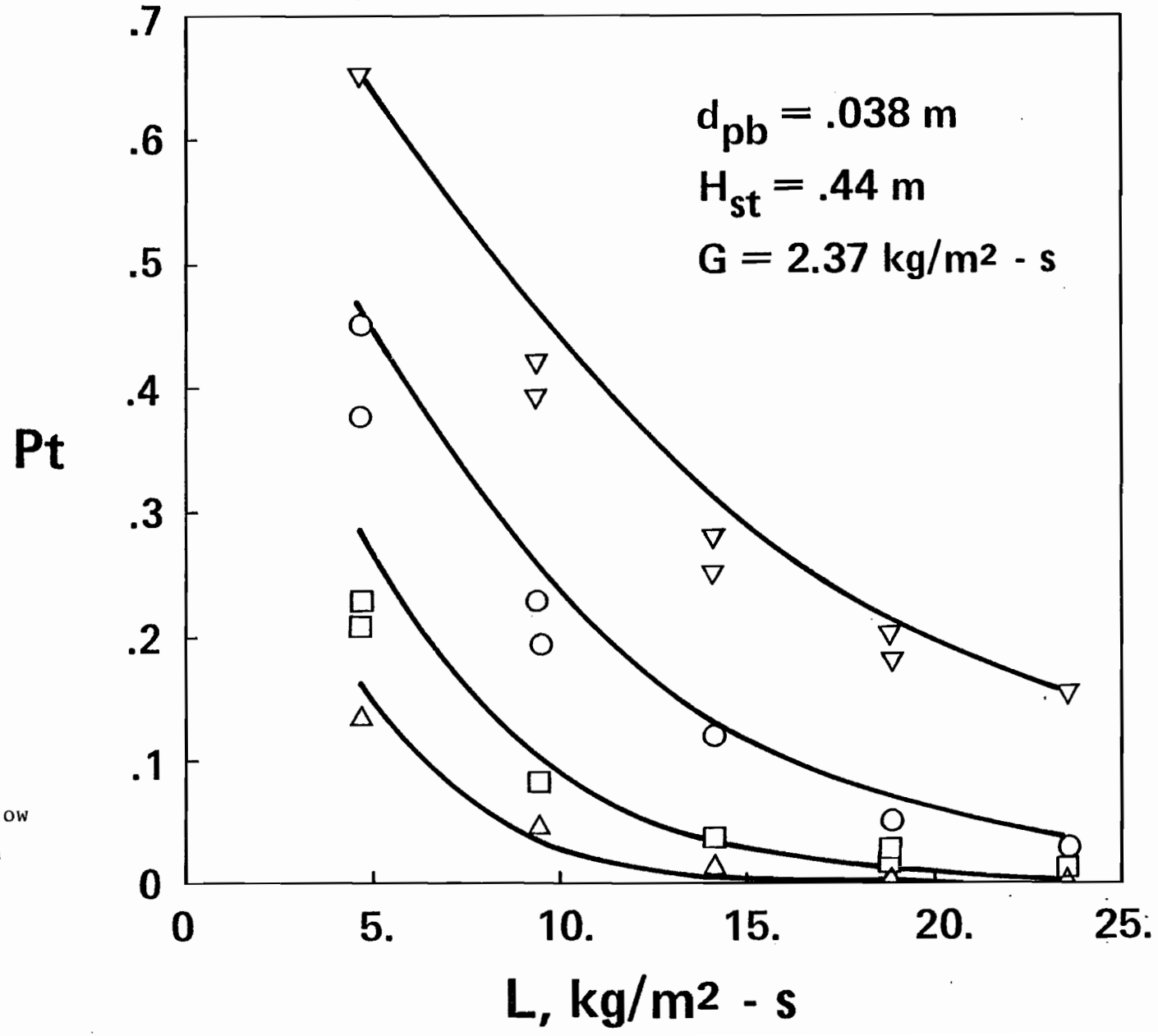

FIGURE 6.29.
Effect of liquid flow rate on penetration

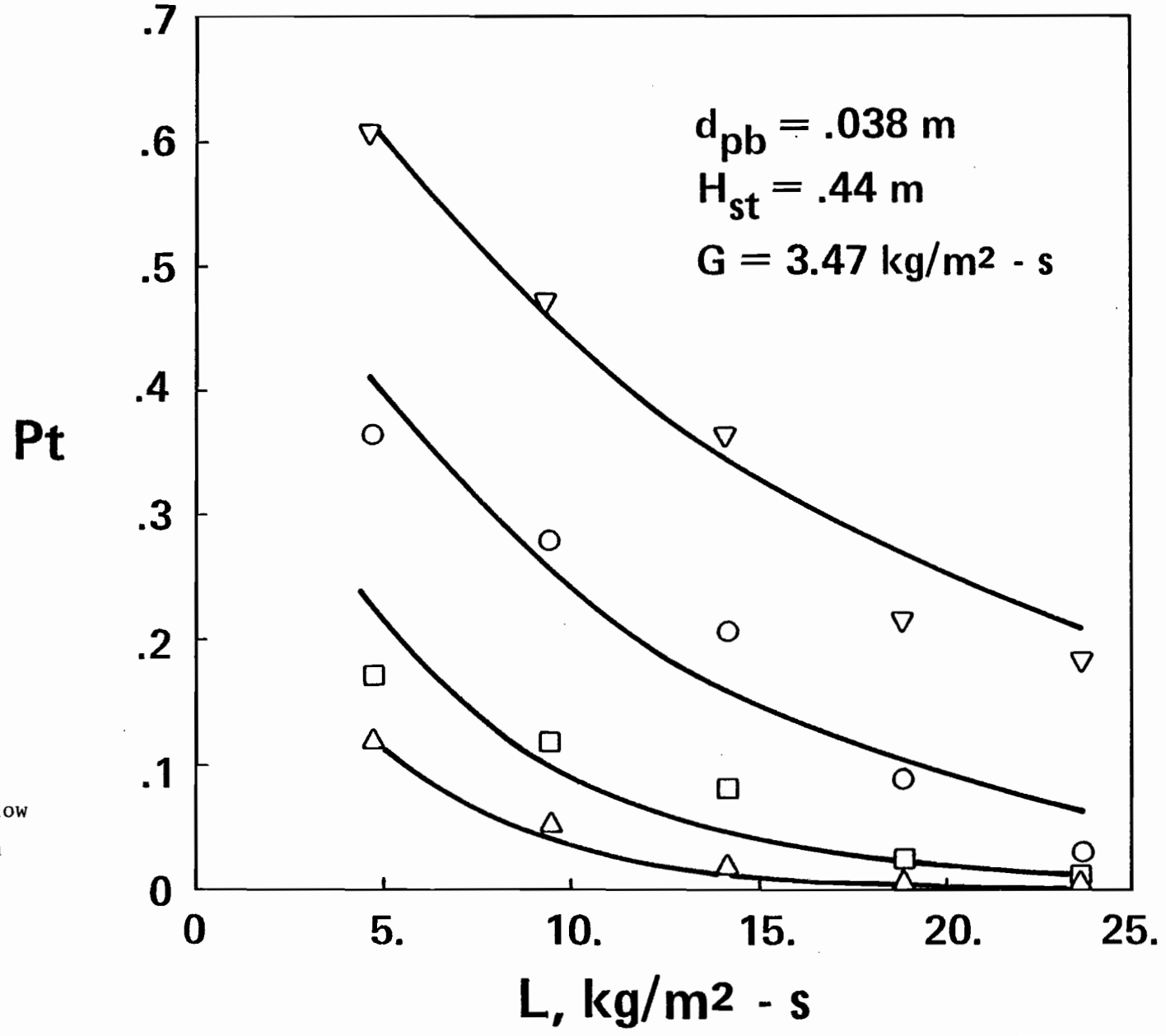

FIGURE 6.30.
Effect of liquid flow rate on penetration

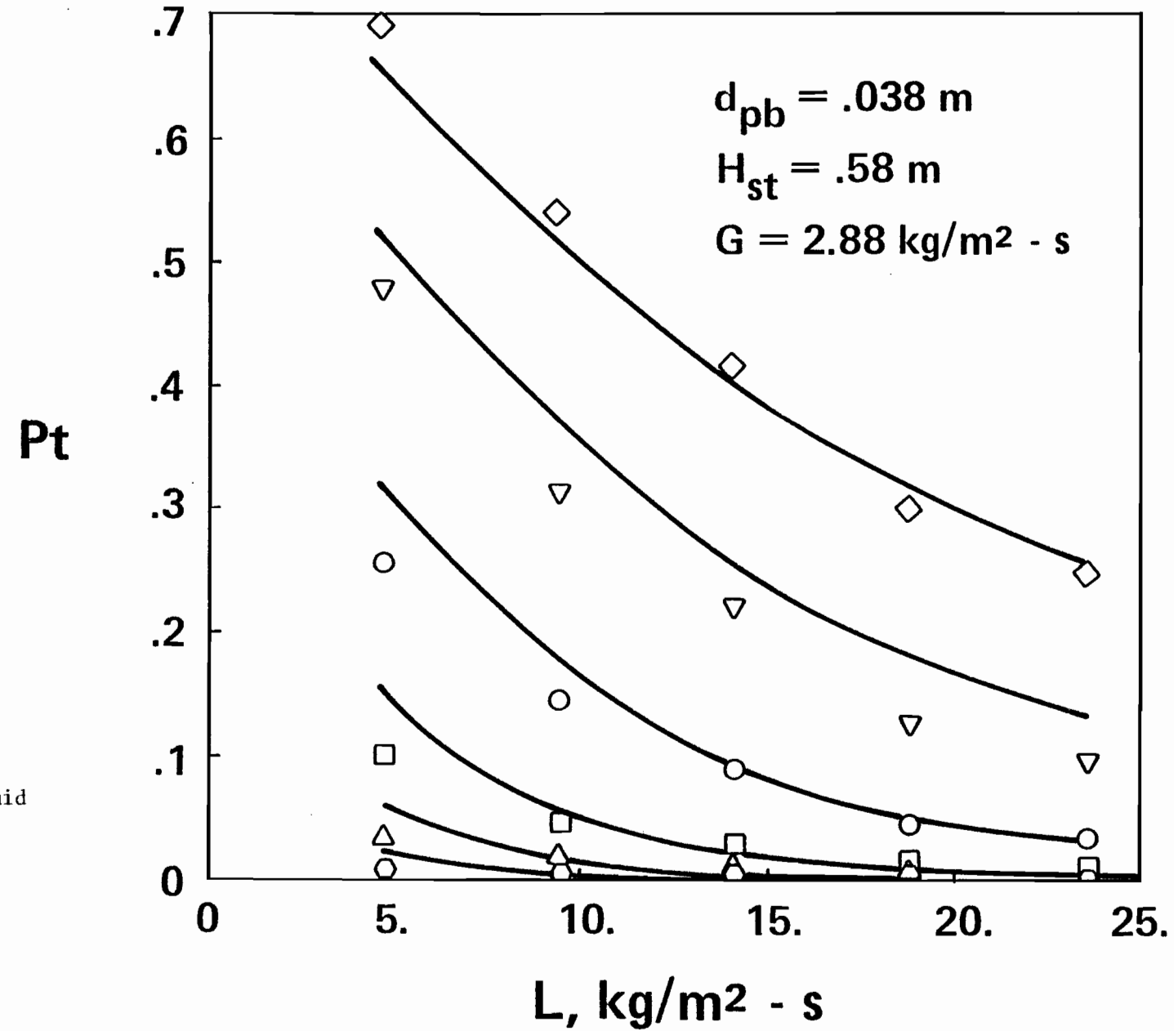

FIGURE 6.31. Effect of liquid flow rate on penetration

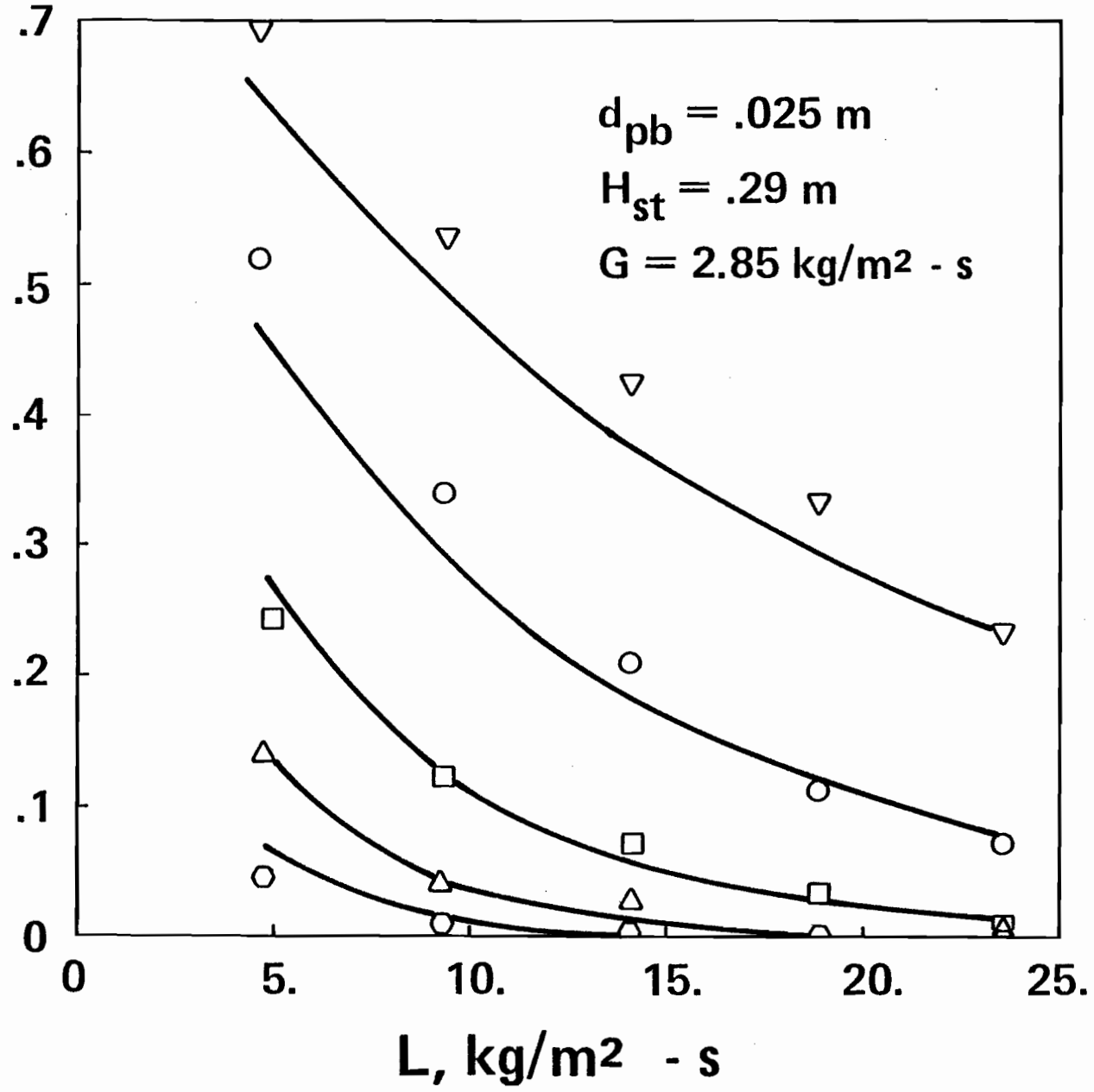

FIGURE 6.32.
Effect of liquid flow rate on penetration

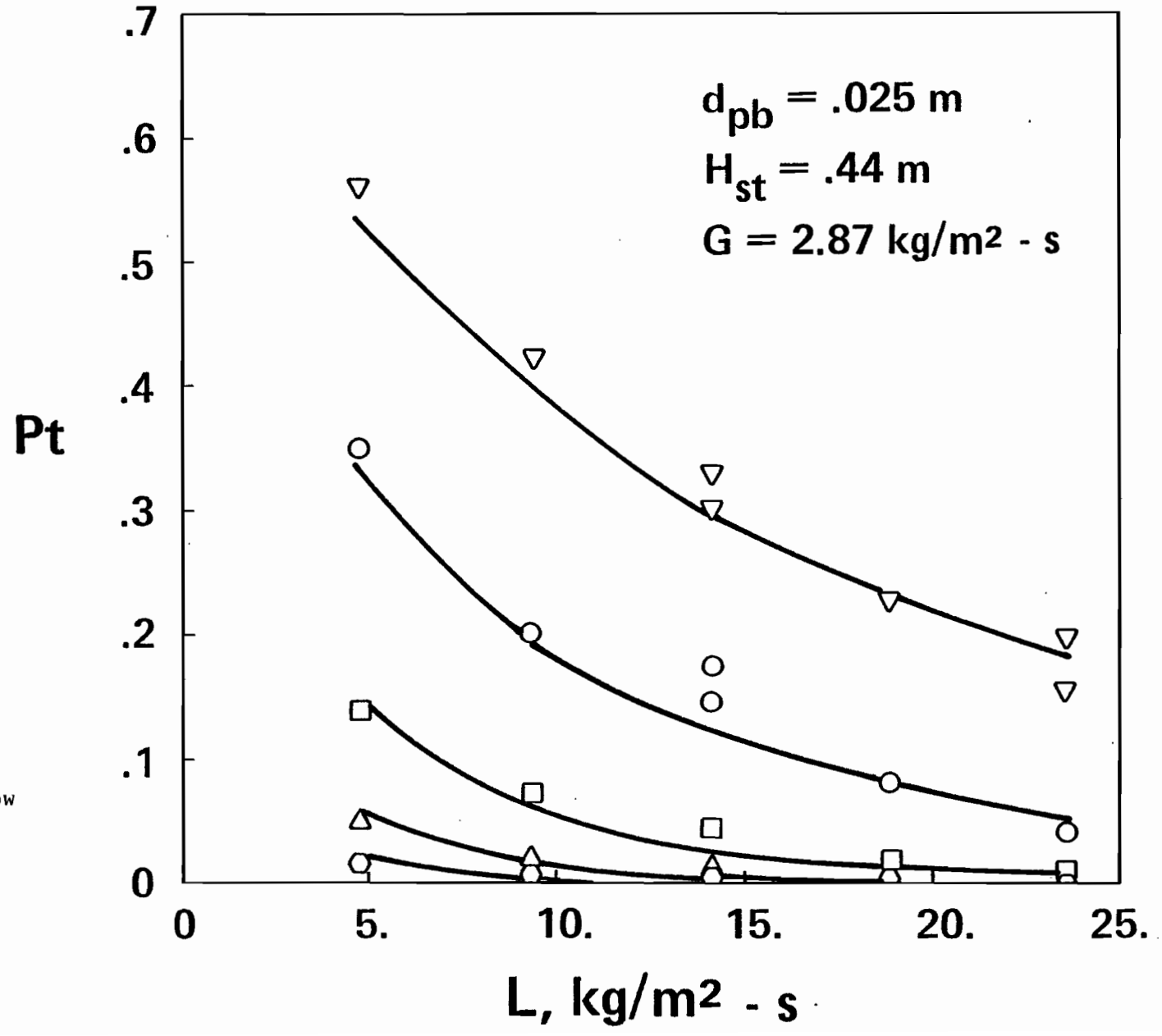

FIGURE 6.33.
Effect of liquid flow rate on penetration

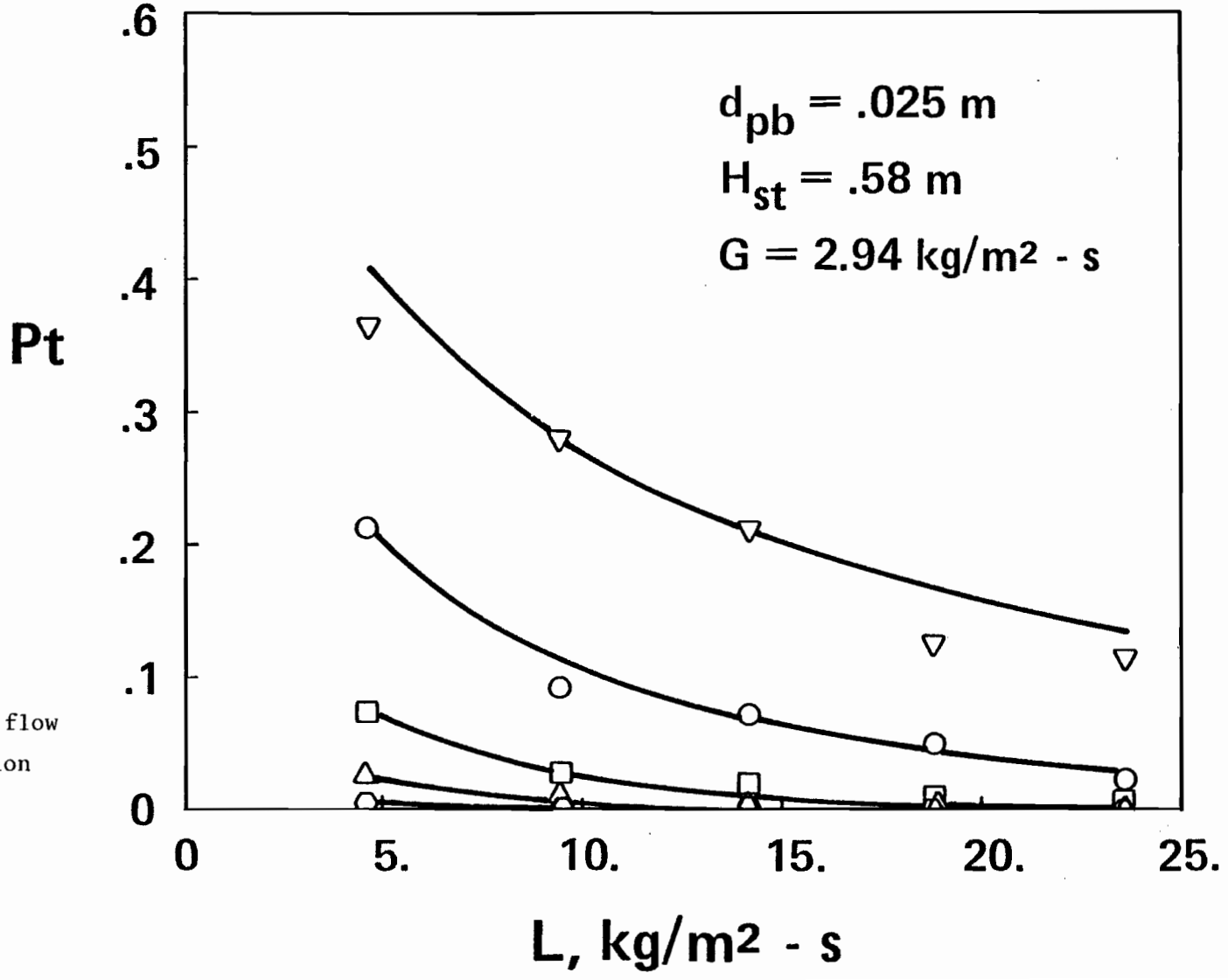

FIGURE 6.34.
Effect of liquid flow rate on penetration

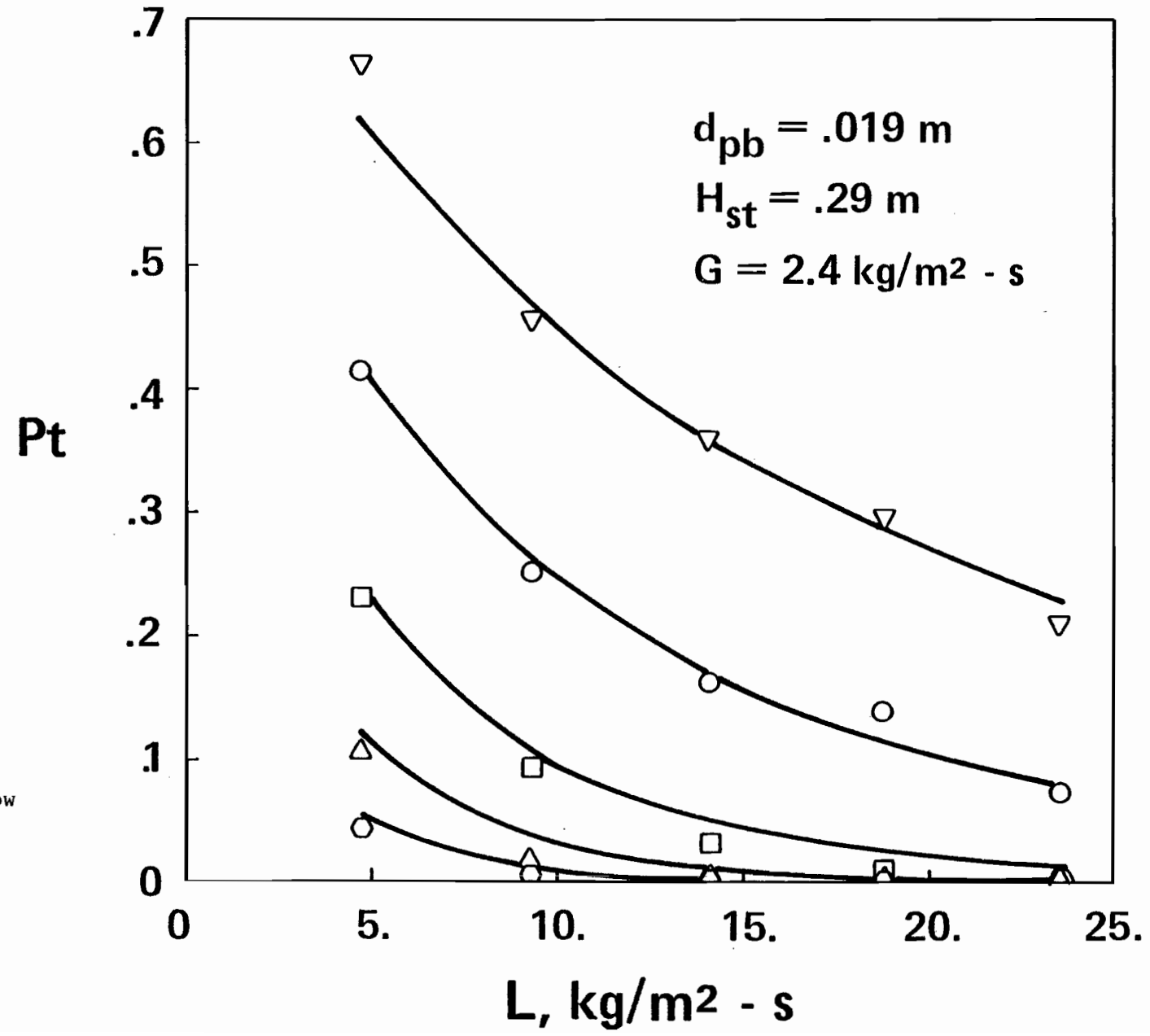

FIGURE 6.35.
Effect of liquid flow rate on penetration

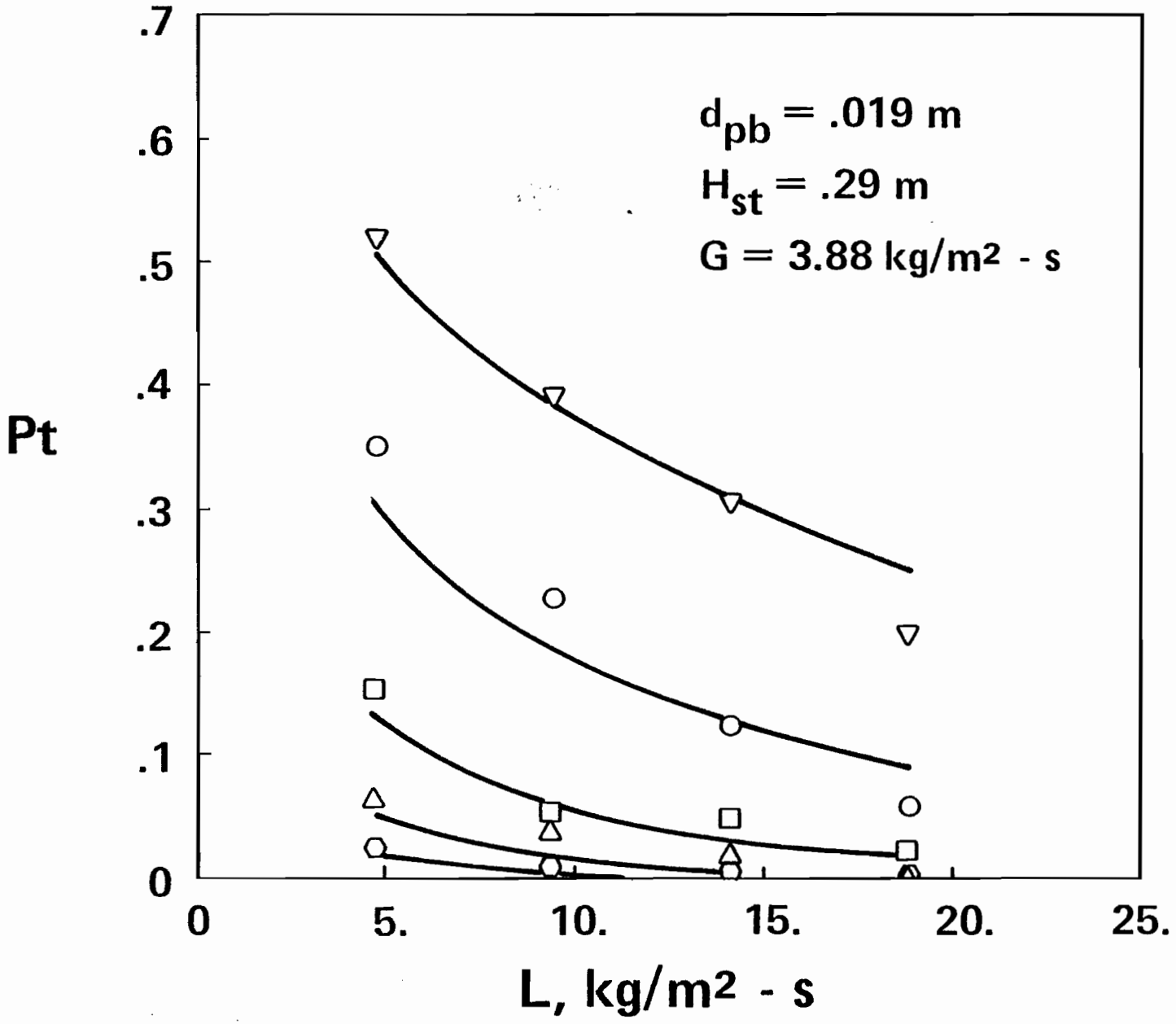

FIGURE 6.36.
Effect of liquid flow rate on penetration

6.2.1.3. Effect of Static Bed Height

Some of the experimental results for 2.5 μm ferrous sulphate particles, together with curves corresponding to the general Equation 6.2.14 for the present study, are presented in Figures 6.44 - 6.46 to illustrate the effect on penetration of static bed height. Three static bed heights, 0.29, 0.44 and 0.58 m, were studied. As would be expected, increases in static bed height improved the efficiency of the column for all packing sizes used (38 mm, 25 mm and 19 mm). This effect may, of course, be attributed to the longer residence time of gas and liquid in MBC as H_{st} increases.

The effect of static bed height for three packing sizes is shown explicitly on Figure 6.47 for 2.5 μm particles at L = 9.4 and G = 2.8 kg/m^2-s. The lines on this figure correspond to Equation 6.2.14, i.e. to the general correlation of all of the data of the present study. Table 6.2 gives the comparison of particulate recovery in a single-stage MBC with theoretical performance of a multi-stage MBC, based on values derived from the general correlation, 6.2.14. Figure 6.47 and Table 6.2 show clearly the complexity and interactions of the effects of static bed height and packing size. The presence of interaction is indicated by the curves for the three packing sizes in Figure 6.47 not being parallel. If there were no interactions, these curves would be expected to be parallel to each other. Likewise, the 4th column in Table 6.2 indicates that the decrease in total penetration when the static bed height is doubled from 0.29 m to 0.58 m is about 59% for 38 mm packing, 62% for 25 mm packing and 68% for 19 mm packing. Again, if there were no interactions, one would expect the same change in total penetration in

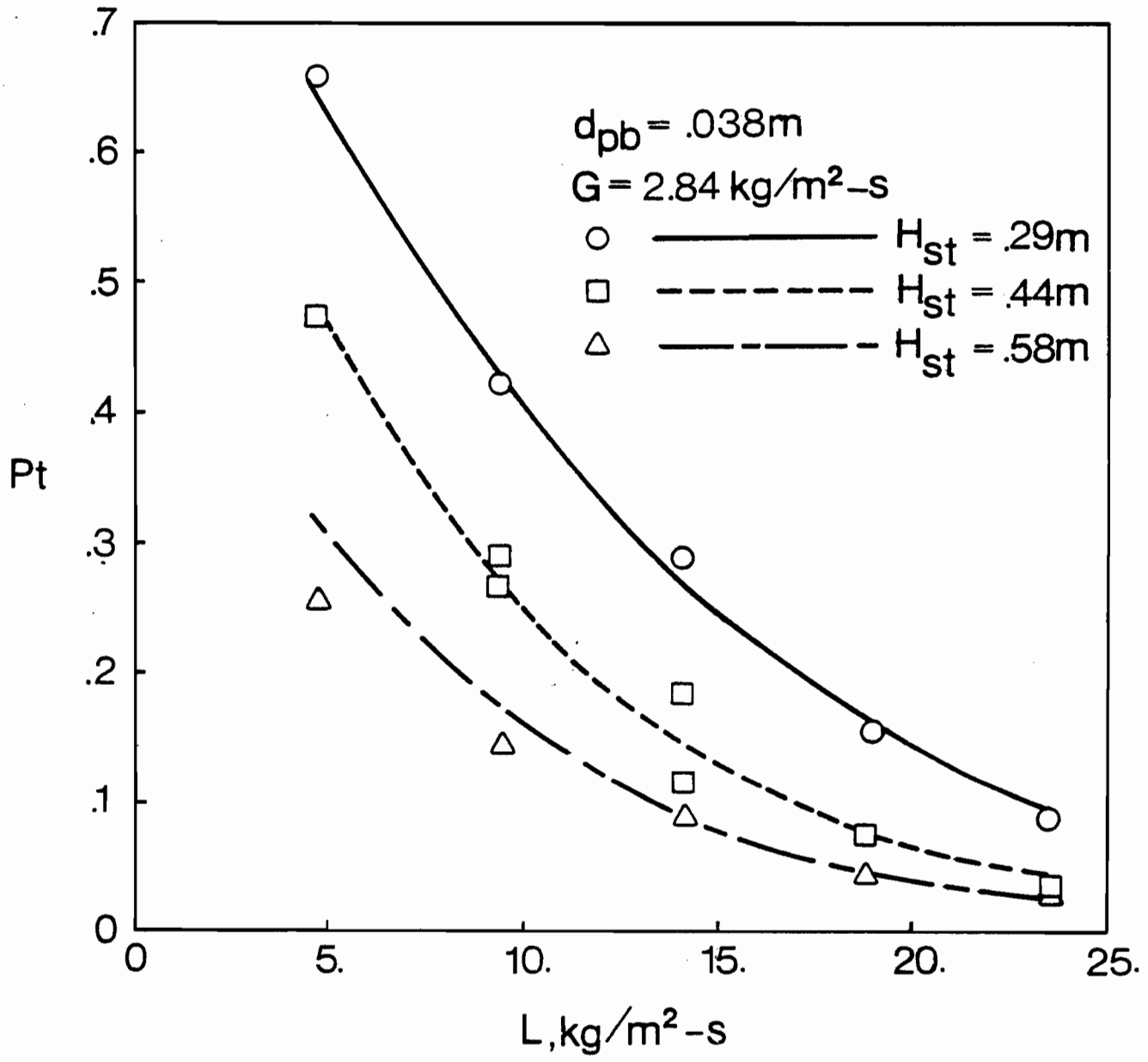

FIGURE 6.44. Variation in penetration with static bed height for 38 mm packing and d_p = 2.5 μm

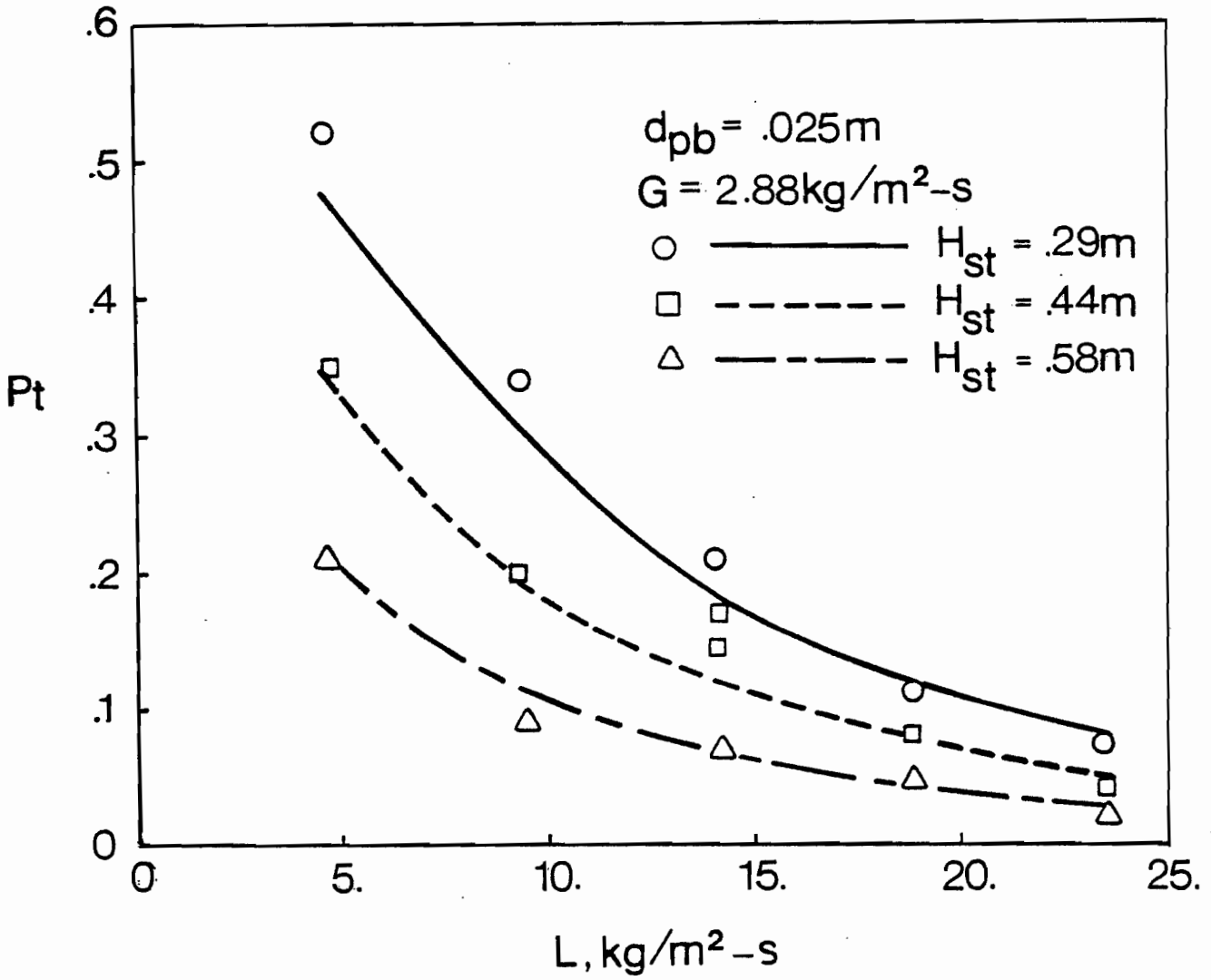

FIGURE 6.45. Variation in penetration with static bed height for 25 mm packing and d_p = 2.5 μm

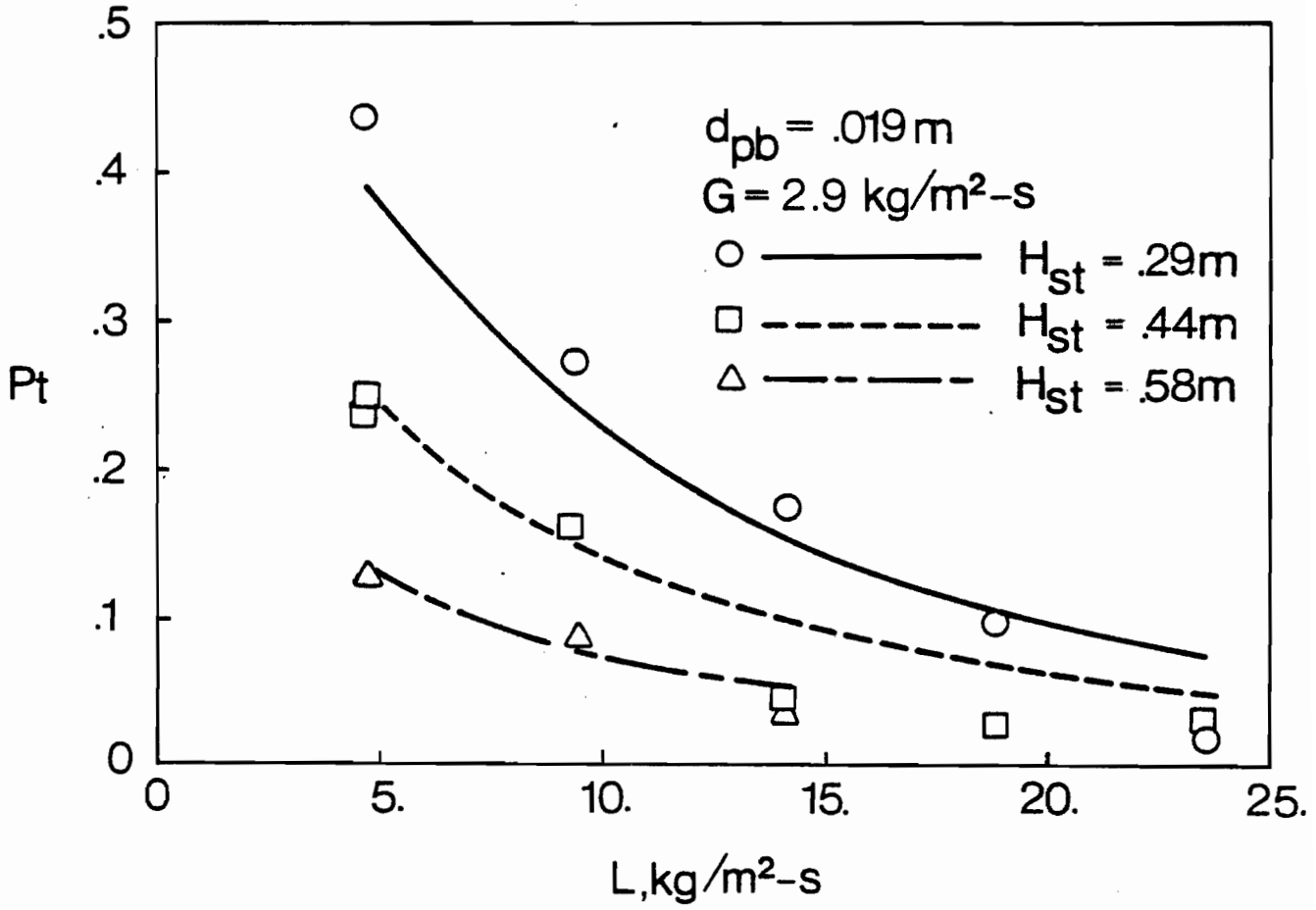

FIGURE 6.46. Variation in penetration with static bed height for 19 mm packing and d_p = 2.5 μm

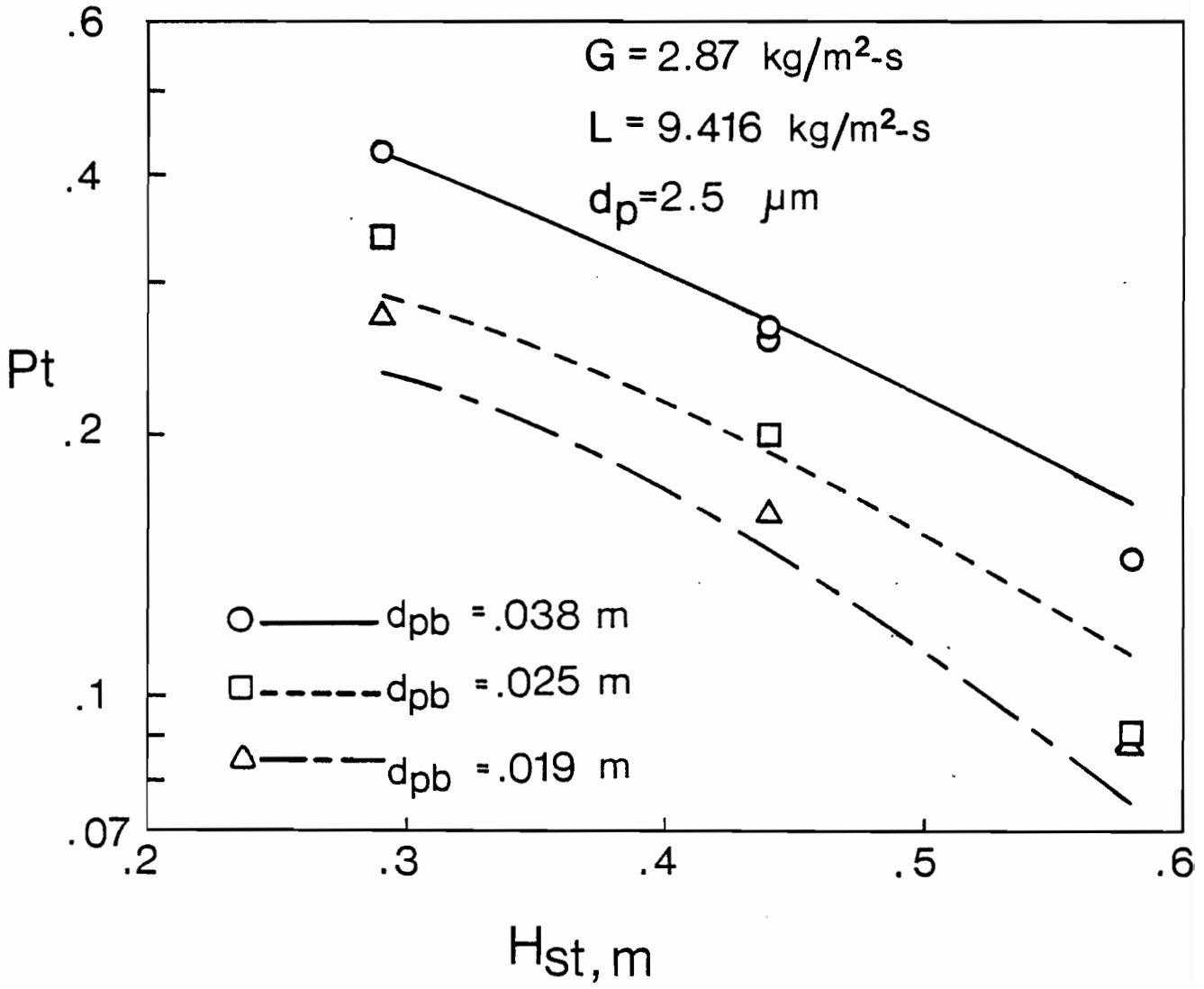

FIGURE 6.47. Effect of static bed height on penetration for d_p = 2.5 μm

TABLE 6.2. Comparison of Performance of Single-Stage and Multi-Stage MBC
($G = 2.9$ kg/m^2-s; $L = 9.4$ kg/m^2-s; $d_p = 2.5$ μm)

$d_{pb,mm}$	Total Height of Static Bed(s), m	Single-stage MBC Column			Multi-stage MBC Column		
		Total Penetration	Decrease in Total Penetration	Marginal Decrease in Penetration	Total Penetration	Decrease in Total Penetration	Marginal Decrease in Penetration
38	0.29	0.425			0.425		
	0.44	0.27	36.5%	36.5%	$(0.425)^{1.5}=0.277$	34.8%	34.8%
	0.58	0.175	58.8%	35.2%	$(0.425)^2 = 0.18$	57.7%	35. %
25	0.29	0.29			0.29		
	0.44	0.19	34.5%	34.5%	$(0.29)^{1.5} = 0.156$	46.2%	46.2%
	0.58	0.11	62.1%	42.1%	$(0.29)^2 = 0.084$	71. %	46.2%
19	0.29	0.23			0.23		
	0.44	0.15	34.8%	34.8%	$(0.23)^{1.5} = 0.11$	52.2%	52.2%
	0.58	0.074	67.8%	50.7%	$(0.23)^2 = 0.053$	77. %	51.8%

doubling static bed height for all packing sizes. Comparison of the 3rd and 6th columns in Table 6.2 shows that within the error involved in the data on which the correlation is based, and with the usual assumption that fractional penetration does not depend on particle concentration, there seems, for 38 mm packing, to be no difference between using a single-stage column with double the static bed height as compared to a two-stage column with each stage half of the total single-stage height. For the smaller packing sizes, 25 mm and 19 mm, the data clearly indicate that it would be advantageous to use a multi-stage column, i.e. 2 units in series, 0.29 m each, rather than a single column of static bed height 0.58 m.

It may also be recalled from the previous section that, for $H_{st} > 0.44$ m, penetration begins increasing somewhat with gas flow rate for approximately $L > 14$ kg/m^2-s. Therefore, when the analysis of Table 6.2 is combined with this finding of the previous section, it may be concluded that the use of a multi-stage column is generally advantageous when the alternative would be use of a single-stage unit of higher than normal static bed height.

6.2.1.4. Effect of Packing Size

Dependence on packing size of the hydrodynamics of MBC, i.e. G_{mf}, H, ΔP_c, h_L, as determined in the present study, were discussed in sections 6.1.1 and 6.1.2, and the effect of packing size on mixing has been determined by previous workers. Further, in the general correlation (Equation 6.2.14) for particle transfer coefficient, $k_{p,MBC}$, packing size enters not only explicitly in the term H_{st}/d_{pb} and as the characteristic dimension in St, Re_G, and Re_L, but indirectly has an important effect on the interstitial velocity terms used for the calculation of these three dimensionless numbers. As packing size interacts with all these hydrodynamics and particulate recovery variables, it is therefore particularly interesting to examine the net effect on penetration of this parameter.

Figures 6.48 - 6.50 show for the case of 2.5 μm particles how penetration is affected by packing size for three static bed heights. As seen in these figures, a decrease in packing size in the lower range of liquid velocities causes penetration to decrease, i.e. collection efficiency improves, while in the higher range of liquid velocities, penetration becomes independent of packing size. For the same static bed height, the increase both in intensity of mixing and in liquid holdup with decreasing packing size has been documented in the present and previous studies. Both of these effects enhance the chance of particles to be captured. In the low range of liquid velocity, the results indicate that these are the controlling phenomena.

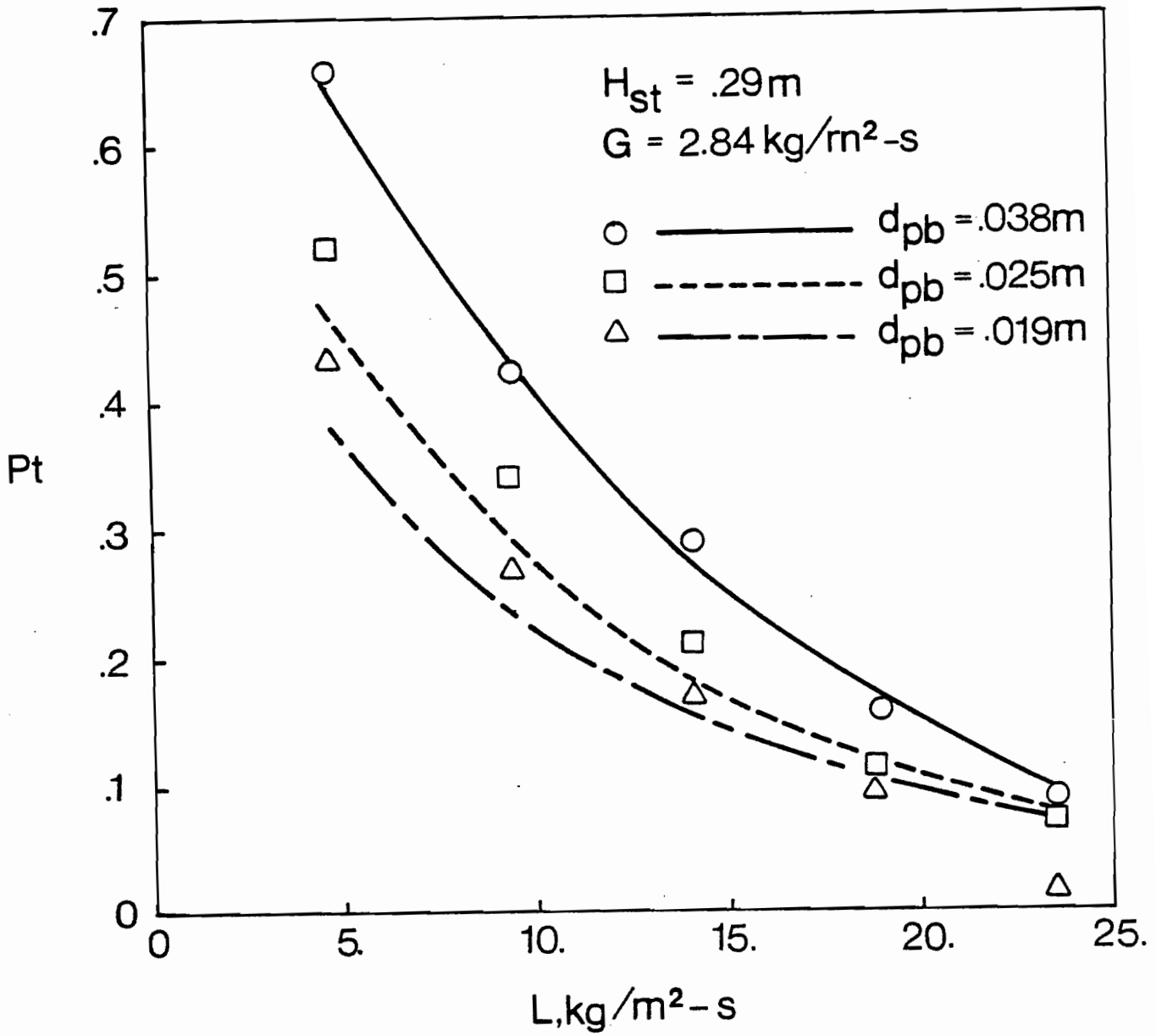

FIGURE 6.48. Variation in penetration with packing size for 0.29 m static bed height and d_p = 2.5 μm

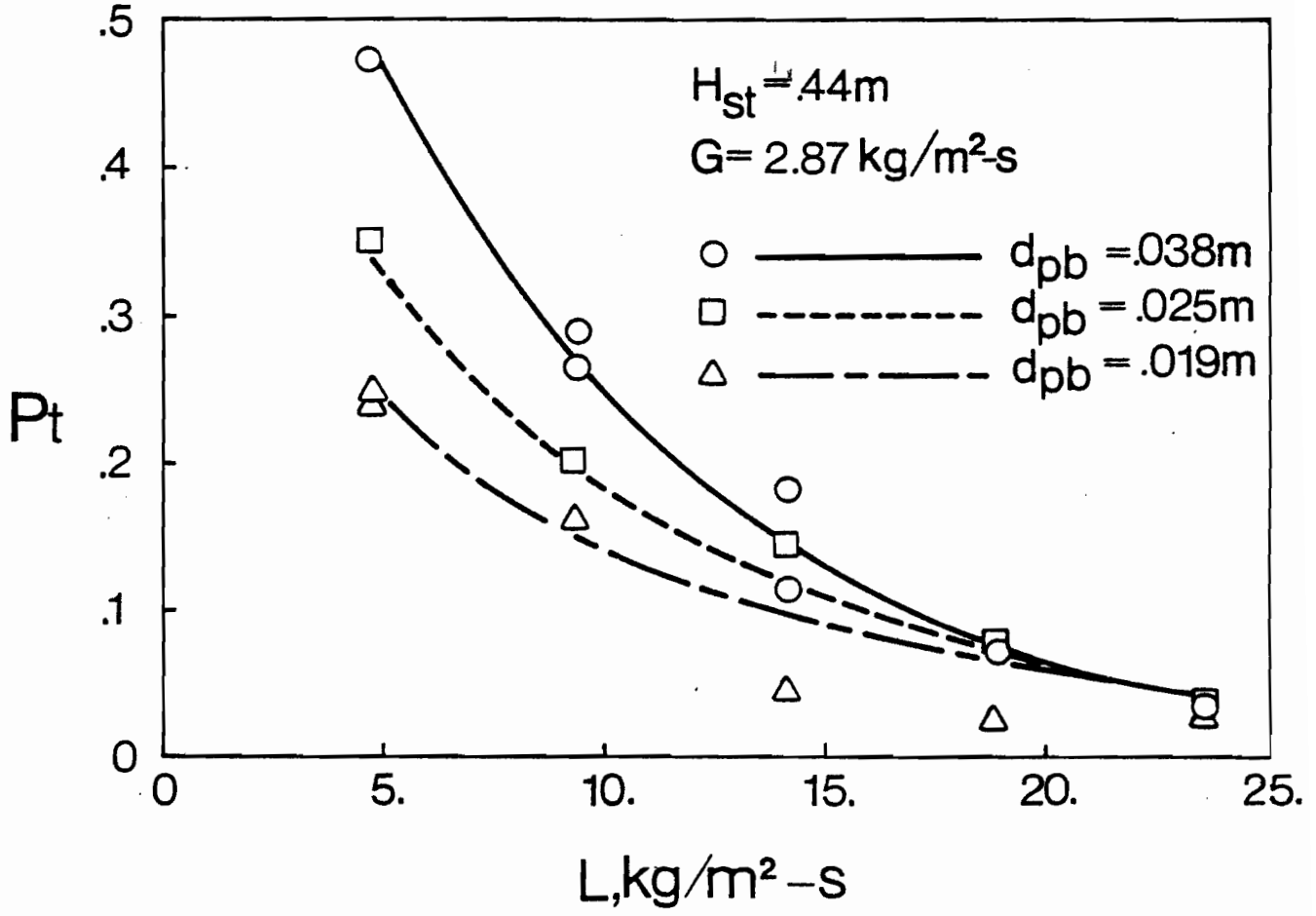

FIGURE 6.49. Variation in penetration with packing size for 0.44 m static bed height and d_p = 2.5 μm

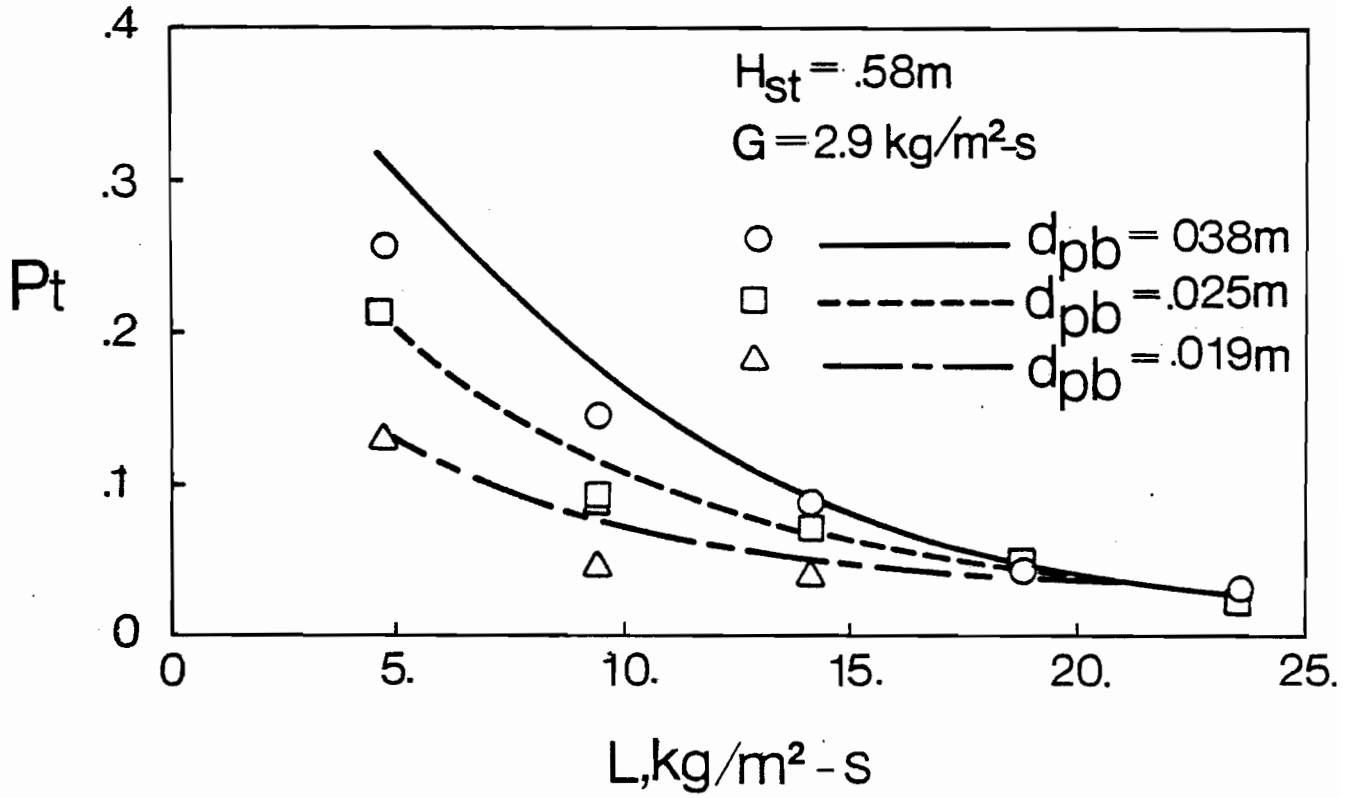

FIGURE 6.50. Variation in penetration with packing size for 0.58 m static bed height and d_p = 2.5 μm

It has already been noted that packing size affects every aspect of mobile-bed hydrodynamics and enters all four of the dimensionless variables which determine particle transfer coefficient. MBC hydrodynamics become more complex as liquid velocity increases up to the limit that the bed is no longer stable. For the upper end of the range of liquid velocities for which the bed is operationally stable, it is no longer possible to trace the complex interactions with all these variables which are affected by varying packing sizes. However, the net result of these complex interactions that is established by the present study is that, in the upper range of operability of MBC, particle penetration tends to become independent of packing size.

This is a particularly important finding from the industrial application point of view. As high liquid flow rates are advantageous economically in industry, 38 mm packing would give almost as good particle removal as 19 mm packing at these conditions. Furthermore, as it may be recalled that pressure drop in MBC is proportional to $d_{pb}^{-0.49}$ (Equation 6.1.13), the use of small packing requires more power. This suggests that, for the use of MBC in industry for particulate recovery, there is no need to be interested in packing sizes smaller than 38 mm whenever the extra pressure drop associated with smaller packing would give rise to additional operating expense.

6.2.1.5. Effect of Particle Size

Most of the literature on particulate recovery for various control devices suffers from insufficient information on the effect of particle size. Industrial studies typically treat only total concentration of particles, usually expressed as grain loading, often of a

particulate with a wide distribution of particle size. Most of the academic studies include only one or a few particle sizes. In Chapter 2 it was shown how important particle size is in recovery. A change in particle size by one order of magnitude may cause a change from one controlling mechanism to another. Especially for the submicron range, below about 0.5 μm, this aspect requires special attention. Thus it is essential to know the size distribution of the particulate emission from a source in order to choose and to design the most appropriate collection device for the specified recovery requirements. For this reason it is necessary to know the performance of any collection device as a function of particle size.

Although the theoretical analysis presented in Chapter 3 has shown that inertial impaction is the major mechanism in MBC for the particle size range between 0.35 and 10 μm, experiments were required in order to confirm this analysis (see Figure 2.4) and to establish that the model developed in terms of particle transfer coefficient (Equation 6.2.14) is applicable over the whole range of particle size. In order to obtain the complete picture, experiments have been performed with ferrous sulphate particles of sizes between 0.35 and 5.5 μm (see last two rows in Table 6.2).

The results are shown in Figures 6.51 and 6.52. These cover a range of efficiency between 5% and 99%. The agreement between the experimental data and predictions made by Equations 4.3.6 and 6.2.14 is quite satisfactory. As the correlation is based on the assumption

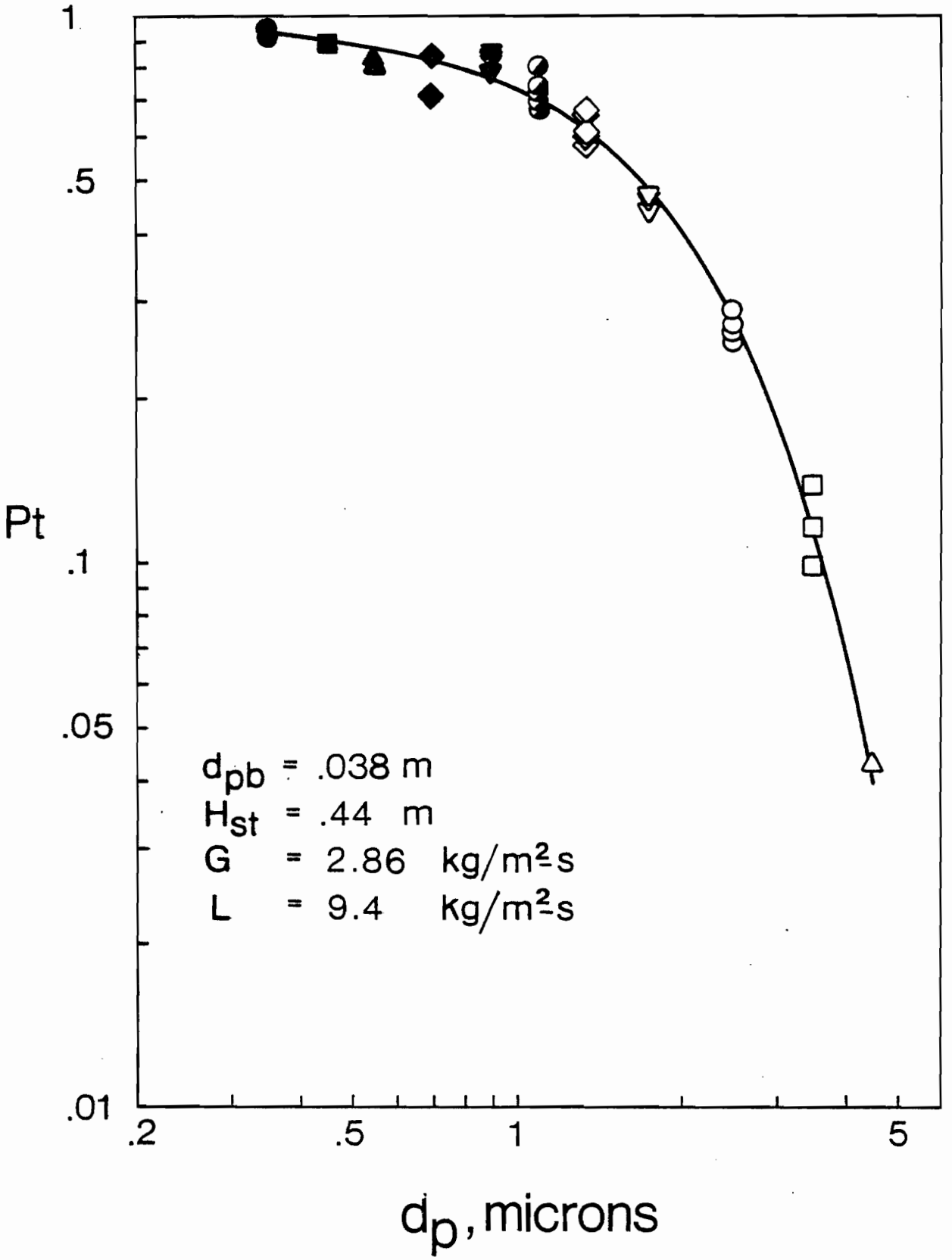

FIGURE 6.51. Effect of size of particle on penetration

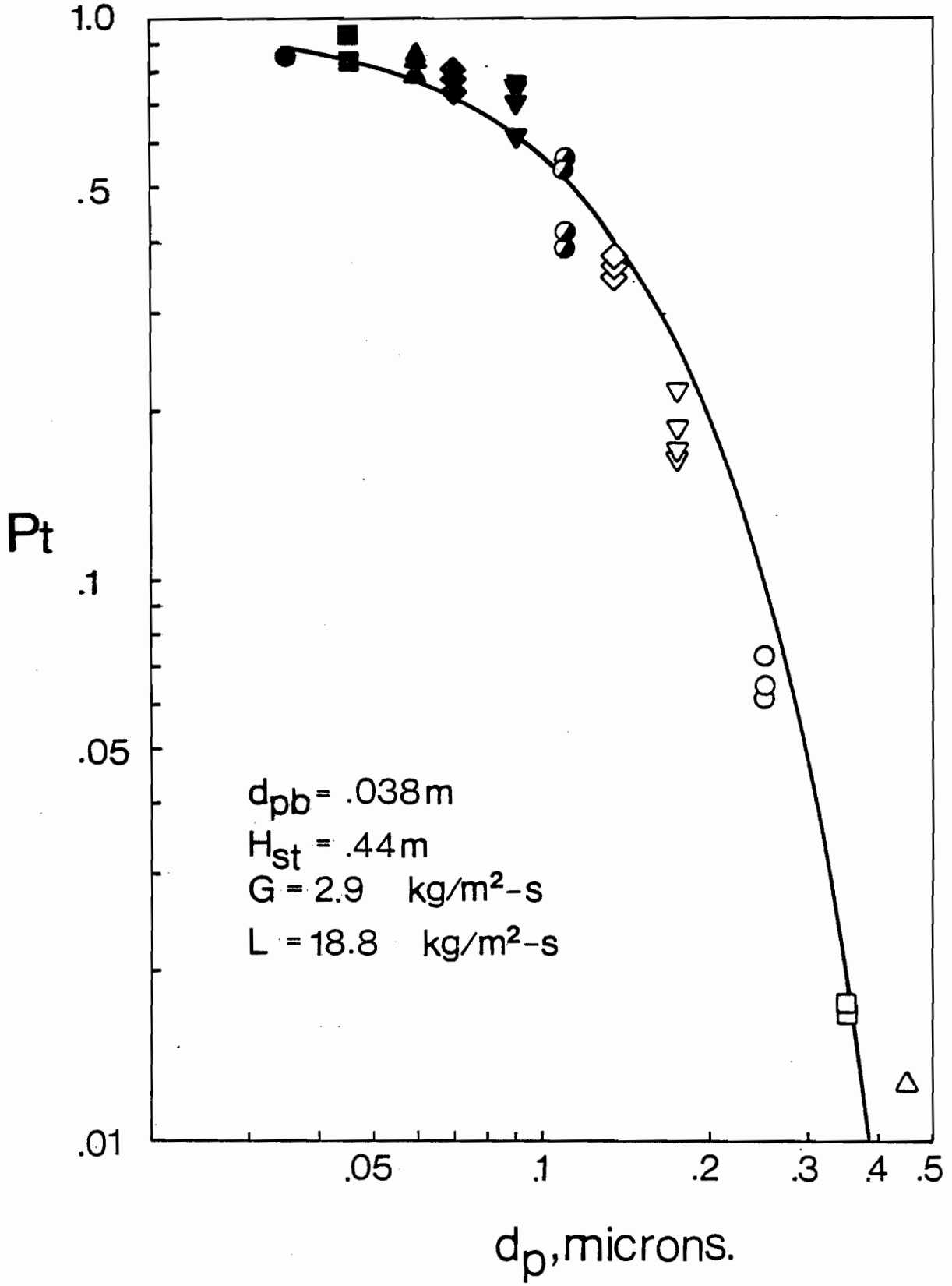

FIGURE 6.52. Effect of size of particle on penetration

that inertial impaction is the dominant mechanism over the 0.35 - 10 μm range of particle size, it is also particularly significant that the correlation fits the experimental data equally well over this entire range. These results, of course, confirm Calvert's et al. (1974) conclusion that the critical size range for particle collection in MBC is between 0.3 and 5 μm. It can be concluded from Figures 6.51 and 6.52 that almost all particles larger than 5 μm are collected in MBC column. For submicron particles, however, efficiency is not very high. This is, of course, to be expected, as inertial impaction is the major mechanism in MBC.

6.2.2. Effect of Hydrophobicity of Particles

The results obtained for effect on collection efficiency of the degree to which particles are hydrophobic or hydrophilic stand in marked contrast to some views in the recent literature. It is, therefore, appropriate to preface the new conclusions which derive from the present study by reference to the current state of development of this aspect of particulate recovery.

As reviewed in section 2.2.1.1 in fact, almost all previous studies of particle collection have assumed, usually implicitly, that all particles which hit a collector are indeed captured. With this simplification, the nature of the surface of the particle is irrelevant. Three studies, those of Goldschmid and Calvert (1963), Montagna (1974) and Allen (1975) are notable exceptions, in that these authors addressed the problem of defining conditions under which particles could come in contact with a liquid collector surface without being captured by the collector. The approach common to these investigations was the attempt

to show the effect of degree of wettability on particle collection by means of changing the contact angle through addition of surfactants. The latter two of the cited authors went further by attempting to incorporate this effect into their models for collection of particles by liquid drops. The common feature of these three studies is the claim that collection efficiency is a function of contact angle over the range from zero to as high as 150^{o}. The author, however, believes that this conclusion should be revised.

The effect on particle collection of degree of hydrophobicity of the particle may be analyzed by considering the change in surface energy which occurs on capture of a particle by liquid. In the process of particle capture, the two reference states are the particle surrounded by gas before coming in contact with the liquid collector, and the particle after penetrating completely into the liquid. The change in total surface energy of the particle during this process is

$$\Delta F = \pi d_p^2 (\gamma_{SL} - \gamma_{SV}) \qquad (6.2.15)$$

Interfacial tension at the solid-liquid interface (γ_{SL}) and surface tension of solid (γ_{SV}) are related to the surface tension of liquid (γ_{LV}) by the well-known Young's relation (Young (1805));

$$\gamma_{SL} = \gamma_{SV} - \gamma_{LV} \cos \theta_c \qquad (6.2.16)$$

where θ_c is the contact angle. From Equations 6.2.15 and 6.2.16,

$$\Delta F = - \pi d_p^2 \gamma_{LV} \cos \theta_c \qquad (6.2.17)$$

If this energy required for the particle to penetrate into the liquid is provided by the kinetic energy of the particle, it follows that

$$\tfrac{1}{2}\, m\, u_p^{\,2} \geq -\, \pi\, d_p^{\,2}\, \gamma_{LV} \cos \theta_c \qquad (6.2.18)$$

or,

$$u_p^{\,2} \geq -\, 12\, \gamma_{LV} \cos \theta_c \,/\, \rho_p\, d_p \qquad (6.2.19)$$

Equation 6.2.19 states the very interesting result that, for particle capture, the square of particle velocity should be greater than or equal to the term on the right hand side of the equation. But, since cosine of all angles between 0 and 90^{o} is positive, it follows that the right hand side of equation 6.2.19 is always negative or zero for contact angles over the range $0 \leq \theta \leq 90^{o}$. From this analysis derives the fundamental conclusion that, for all contact angles up to 90^{o}, the liquid surface does the work on the particle to make it penetrate, even in the limiting case of a particle velocity of zero at impact.

Montagna (1974) and Allen (1975) used a similar approach to the above to find the boundary conditions to be incorporated in their computer program to estimate efficiency of collection by liquid drops (Equations 2.2.8 and 2.2.9). In spite of the fact that hydrophobicity is not involved for $\theta_c \leq 90^{o}$, as shown above, they used these boundary conditions for all cases, i.e. for both the $\theta_c \leq 90^{o}$ and $\theta_c > 90^{o}$ ranges.

In the experimental program to test his theoretical model, Allen (1975) used particles of four materials, namely a paraffin oil, dioctyl phthallate (DOP), talc powder and a paraffin wax, having contact angles with water of 58.2^{o}, 63.49^{o}, 63.4^{o} and 102.17^{o},

respectively. It is significant that the only particulate for which his results were in good agreement with the theoretical predictions was paraffin wax, which is also the only material used with contact angle greater than 90^{o}. For the other three particles, all having $\theta_c < 90^{o}$, experimental collection efficiencies were higher than the values given by his theoretical model. Thus the inconsistency between his experimental results and his theory is explained by the analysis presented in the present study.

Montagna (1975) showed the dependence of collection efficiency on contact angle graphically for 0.84, 1.62 and 5.16 μm sulfur particles, but the scatter of his data for $\theta_c < 90^{o}$ was quite appreciable. The experimental results reported by Goldschmid and Calvert (1963) on the other hand do not show a consistent trend for the effect of contact angle on collection.

Considering the results of these three previous studies of effect of particle wettability, it becomes clear that, although these authors recognized a potentially-important deficiency in the theory of particulate collection, i.e. the assumption of 100% capture of particles on contact with the collector, their treatments contain important shortcomings.

As the analysis of the present study indicates that efficiency of particulate collection should be independent of contact angle for values of $\theta_c < 90^{o}$, this analysis was tested by carrying out collection studies with particulates of three additional materials with $\theta_c < 90^{o}$. The materials chosen for this purpose were silica ($\rho_p = 2200$ kg/m^3), polyvinyl toluene latex ($\rho_p = 1050$ kg/m^3) and DOP particles ($\rho_p = 977$ kg/m^3). Development of the correlation for particle transfer

coefficient (Equation 6.2.14) was carried out using ferrous sulphate particles, which are soluble in water, and naturally have $\theta_c = 0^o$. Silica was chosen because it gives contact angle equal to zero with water, but, in contrast to ferrous sulphate, is totally insoluble. The size of the silica particles used was 2.5 μm. The 2 μm latex particles provided another insoluble particulate, but with a contact angle between 42^o and 52^o. The value of 42^o is the average of ten readings of receding contact angle, while 52^o is the average of ten observations of advancing contact angle. As contact angle advances during the process of particle capture by a water droplet, advancing contact angle is the appropriate measure of wettability for this purpose. Similarly, contact angle for DOP, a liquid aerosol, was determined in the present study to be 63.5^o. Size of DOP particles tested was 2.5 μm.

The experimental results for these particles are given in Table D.2 - D.4 and in Figure 6.53. Although the lines on this figure might appear to be best-fit curves through the experimental data, it is to be emphasized that these curves in fact show particle penetration as predicted by the general correlation 6.2.14. The remarkably close agreement between experimental results for three greatly different types of particles and values predicted from the general correlation for a hydrophilic particle provides convincing experimental confirmation of the analysis given in the present study for effect on collection efficiency of degree of hydrophobicity of particles. Therefore, the correlation developed in this study for particle transfer coefficient (Equation 6.2.14) can be used with confidence not only for all hydrophilic particles, regardless of whether

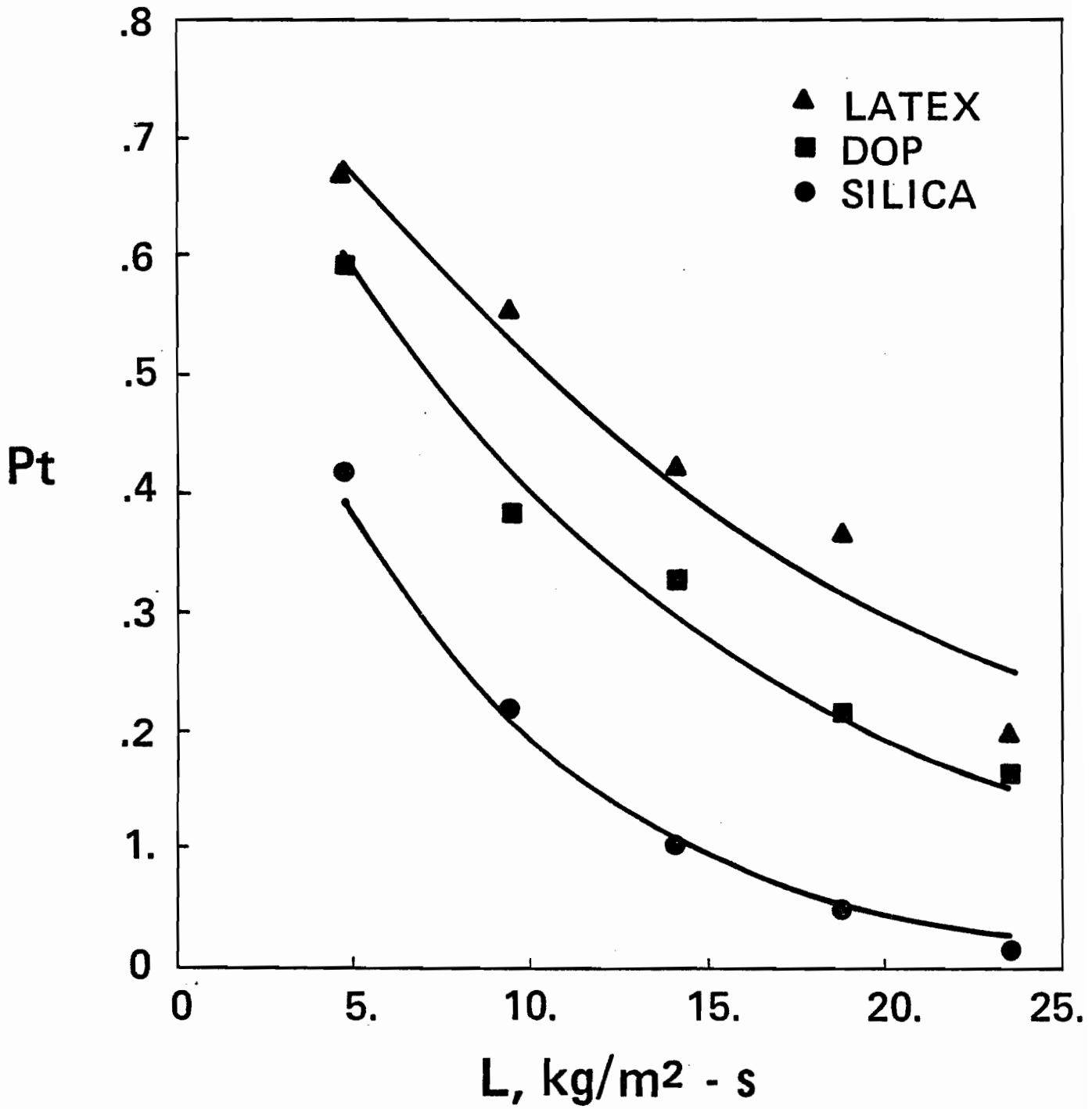

FIGURE 6.53. Penetration of Latex, DOP and Silica particles

these are highly soluble or totally insoluble, but as well for all hydrophobic particles with $\theta_c < 90^o$. Thus the equation developed in the present study in fact covers almost all particles.

In view of the findings of the present study, it is not possible to understand why Mlodzinski and Warych (1975) used two correlations for particle collection in MBC, one for superphosphate particles and one for zinc sulfide particles. Although they specified that zinc sulfide was hydrophobic, no information on contact angle was given. In view of the fact that they chose to give a different correlation for their hydrophobic particle, it is surprising that they made no attempt to introduce Weber number, $We = \rho_p d_p u_G^2/\gamma_{LV}$, into their correlation (Equation 2.3.4), as would be the natural choice. More surprising yet, they introduced the ratio (H_{st}/d_{pb}) into their correlation for zinc sulfide particles, while this term does not appear in their correlation for superphosphate particles (cf Equations 2.3.3. and 2.3.4). Although absolute value of contact angle is very sensitive to contaminants and hence it is customary to report measured θ_c values for specific applications, no such data are provided in the cited study. In any case, the findings of the present study concerning effect of particle wettability lead to the conclusion that the difference in collection efficiencies for the two particles reported by Mlodzinski and Warych is not due to hydrophobicity.

It is relevant to this point to recall that almost all the materials found in nature have contact angles less than 90^o. In fact, this is the reason why flotation processes have been developed for mineral recovery. Even sulfur, known as a highly hydrophobic material,

has a contact angle with water of about 80^{o}. It is therefore apparent that there are very few particulates which are sufficiently hydrophobic to reduce collection efficiency in a wet scrubber. Moreover, it would probably be economic to add a surfactant to reduce the contact angle to less than 90^{o} for an extremely hydrophobic particulate of $\theta_c > 90^{o}$, so as to avoid the reduction in collection efficiency that would otherwise be associated with less than 100% capture of particles of such extremely low wettability. This perspective indicates that, although the general correlation developed in the present study does not give collection efficiency for extremely hydrophobic particles, i.e. those of $\theta_c > 90^{o}$, there would be few if any applications of MBC for particulate recovery for which the efficiency could not be predicted by this equation.

6.2.3. Effect of Diffusiophoresis

An experimental program for study of the effect of positive diffusiophoresis must be guided by the form of the theory of diffusiophoresis, presented in Chapter 4. In this regard, it is particularly significant that Equations 4.4.22, 4.4.24 and 4.4.26 indicate clearly that just one dependable experiment would be sufficient to establish quantitatively the effect of diffusiophoresis. Specifically, as particulate capture by diffusiophoresis is independent of particle size and depends only on the amount of vapor condensed, by performing one experiment with exact knowledge of inlet and outlet gas flow rates, Pt_D may be found from one of the three equations referred to above.

With water as the scrubbing liquid, positive diffusiophoresis implies condensation of water vapor, i.e., inlet air humidity must be appreciably higher than that at the outlet. Thus the inlet air humidity must be significantly above that which corresponds to saturation at the temperature of the inlet water stream. Since MBC is quite efficient for direct contact heat and mass transfer, air leaves the column almost saturated at the exit conditions. Theory and experience establish that the inlet air must be heated and humidified to rather high values to achieve an appreciable contribution to total efficiency by diffusiophoresis. Two practical problems were encountered in this respect during the experiments. First, limitations in the laboratory steam supply used for humidification of air in turn limited the maximum humidities that could be reached in the inlet air. The other problem relates to the control system of the duct heater. The controls provided with this rather large, custom-designed heater were such that, unless the electrical heat input was increased in very small increments, the heater outlet air temperature would fluctuate with a large amplitude. This control deficiency extended the time required to reach steady state in each diffusiophoresis run to several hours. Due to these difficulties, relatively few experiments were made. However, it should be recalled that the theoretical analysis presented earlier indicated that the effect of diffusiophoresis could be determined, in principle, by just a single, accurate experiment.

The dominant variable in determining the amount of particle collection by diffusiophoresis is concentration of the condensing component, as may be seen by reference to Equations 4.4.22, 4.4.24 and 4.4.26. In the present study the maximum inlet humidity that could be attained was about 0.29 kg H_2O/kg dry air for a gas flow rate

2.18 kg/m^2-s. Outlet gas humidity was about 0.005 kg H_2O/kg dry air. Therefore, Equations 4.4.22, 4.4.24 and 4.4.26 imply that particle penetration considering only diffusiophoresis, Pt_D, is about 0.75. The value predicted for Pt_D is in fact obtained more easily if those three basic equations are rewritten in terms of humidity, as follows:

i) For particles moving with the Schmitt-Waldmann velocity:

$$Pt_D = \frac{1 + Y_{out}\sqrt{M_2/M_1}}{1 + Y_{in}\sqrt{M_2/M_1}} \qquad (6.2.20)$$

ii) For particles moving with the gas mean mass velocity:

$$Pt_D = \frac{1 + Y_{out}}{1 + Y_{in}} \qquad (6.2.21)$$

iii) For particles moving with the gas mean molar velocity:

$$Pt_D = \frac{1 + Y_{out}\, M_2/M_1}{1 + Y_{in}\, M_2/M_1} \qquad (6.2.22)$$

For the humidities specified above, the values of Pt_D which derive from the three alternate calculation bases are:

Particle Velocity	Calculation Basis	Pt_D
Schmitt-Waldmann velocity	Equation 6.2.20	0.74
Mean mass velocity	Equation 6.2.21	0.78
Mean molar velocity	Equation 6.2.22	0.69

The difference between these predictions is indeed very small. Moreover, as particle collection due to the aerodynamic mechanisms occurs simultaneously, and as what is measured is total penetration,

$$Pt = Pt_A \; Pt_D \tag{4.4.19}$$

one may expect that it would be difficult to detect experimentally which of the three bases for diffusiophoretic particle velocity is best.

Although theory showed that only a single diffusiophoresis experiment was required, 15 such experiments were actually performed, and the results are given on Figures 6.54 and 6.55. Ferrous sulphate particles of diameter 1.75, 2.5 and 3.5 μm were used. The results for 1.75 μm particles are presented in detail on Figure 6.54 where the uneven broken lines at the top of the figure correspond to the alternate values of Pt_D as predicted by Equations 6.2.20, 6.2.21 and 6.2.22. The even broken line corresponds to penetration due only to inertial collection, as predicted by the correlation (Equation 6.2.14) developed in the present study. The solid lines correspond to the total penetration predicted by Equation 4.4.19 in combination with the three alternate bases for calculating Pt_D. Each of the 5 experimental points represent in turn the average of 15 readings of particle concentration at each condition. As the three solid lines differ so little, and as any one of them would provide a reasonably satisfactory correlation of the experimental data, it is not possible to conclude which of the three expressions for diffusiophoresis particle velocity is best.

The results of the diffusiophoresis experiments for the two larger particle sizes, 2.5 and 3.5 μm, are shown in Figure 6.55, along with the results for the 1.75 m particles. Equation 6.2.21 was used

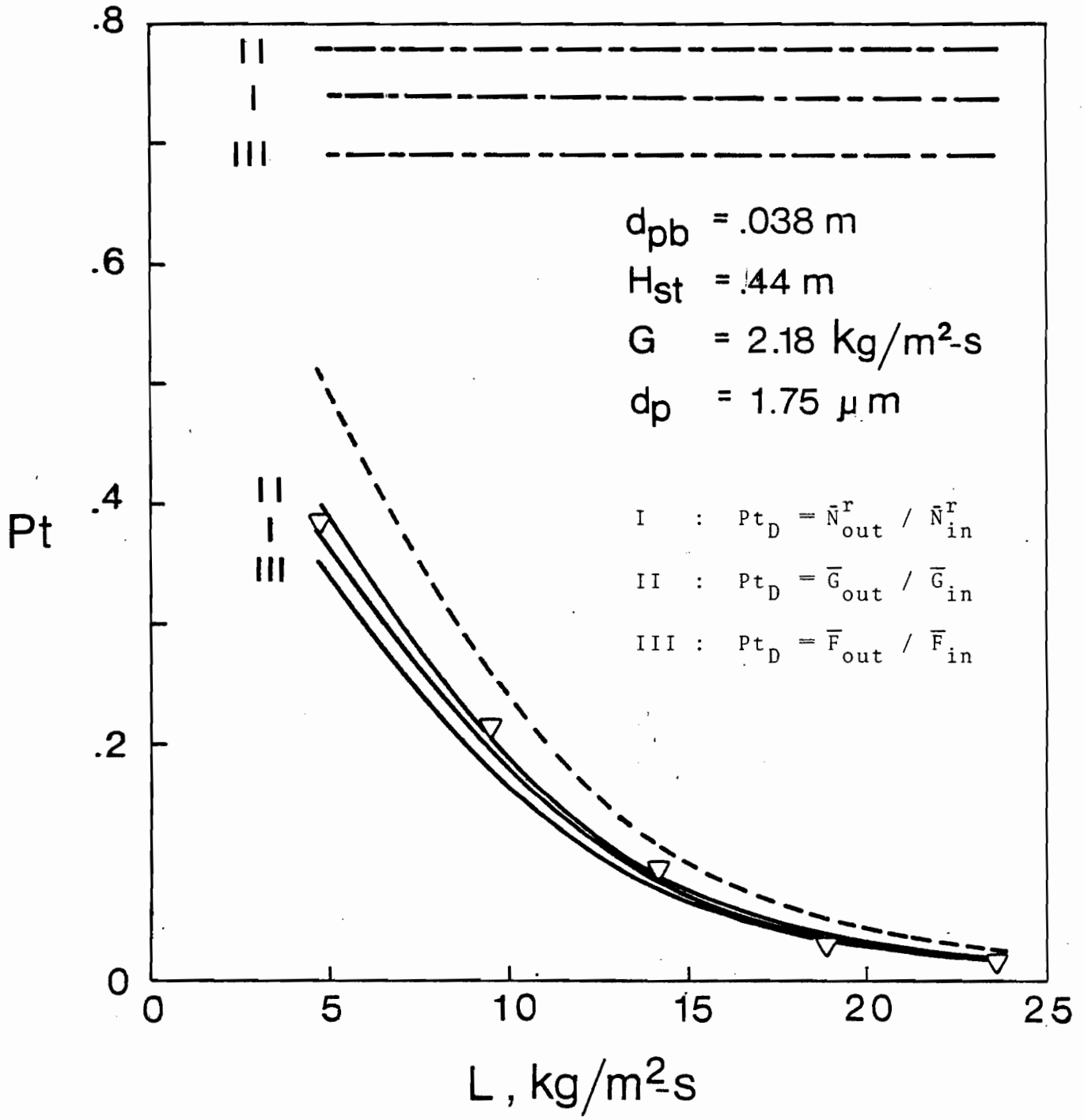

FIGURE 6.54. Comparison of experimental results with three diffusiophoretic velocity expressions

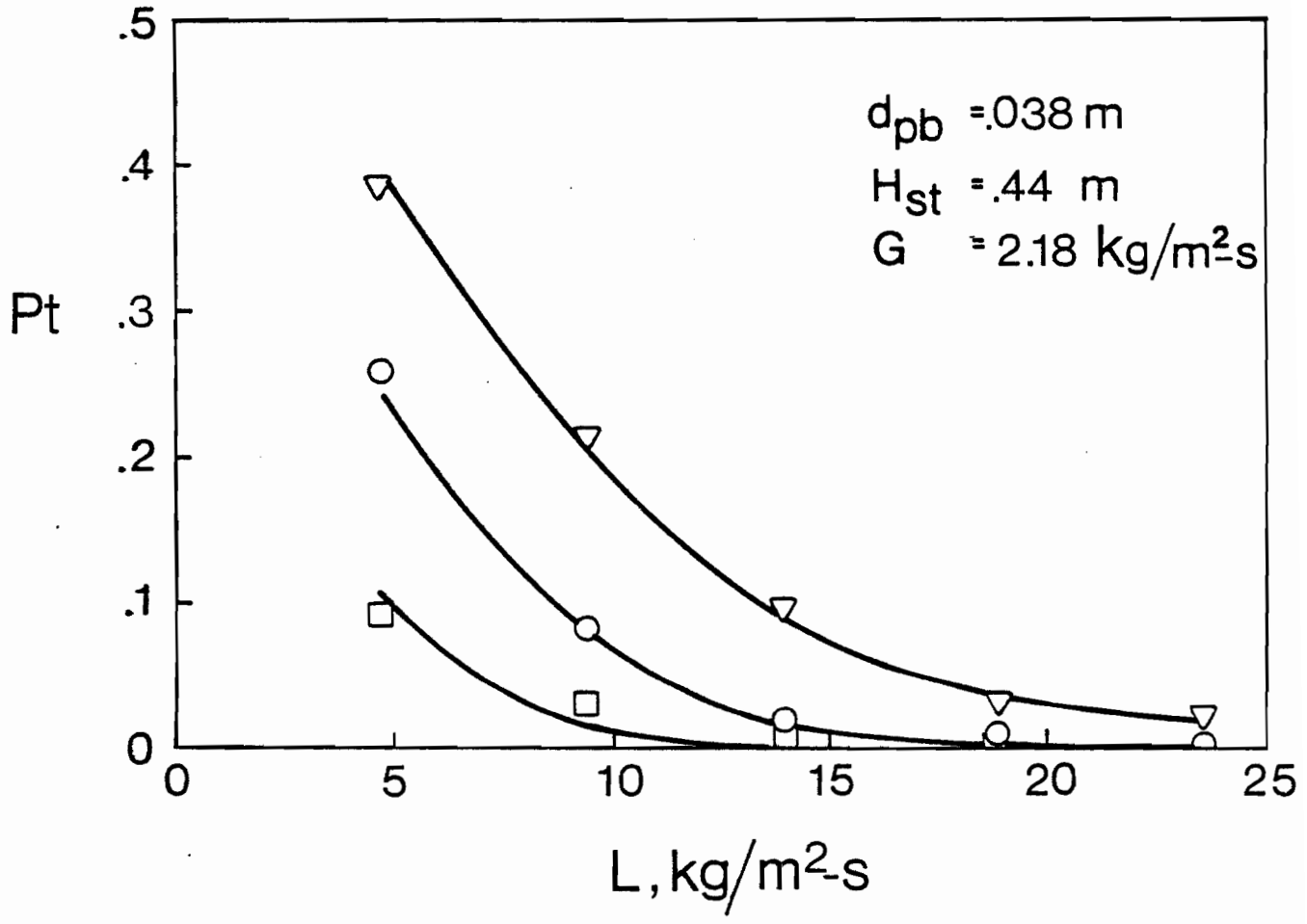

FIGURE 6.55. Penetration in the presence of diffusiophoresis

for all three particle sizes for calculation of overall penetration. The experimental results indicate that the theory presented in Chapter 4 is adequately capable of predicting the overall penetration in MBC in the presence of diffusiophoresis and inertial impaction simultaneously.

As the inlet air was heated to about 90°C in order to reach the high humidities required, one may question whether there could have been an effect of thermophoresis present. As noted in section 2.2.2.2, thermophoretic velocity is normally too small to be significant for normal applications. Although expressions proposed to evaluate thermophoretic velocity are not particularly accurate, they may however be used to make an order of magnitude estimate. Thus at the inlet of the column, where maximum temperature gradient exists between gas and liquid for the present experimental conditions, one may write

$$(\nabla T)_{\infty} \simeq 75/\delta \qquad (6.2.23)$$

where δ = film thickness at the interface.

Since, $k_p = 2.5 \times 10^{-2}$ J/cm-s-°K

$k_{air} = 2.7 \times 10^{-4}$ J/cm-s-°K (Handbook of Chemistry and Physics)

Epstein's expression (Equation 2.2.73) gives

$$u_{pt} \simeq 7 \times 10^{-4}/\delta \qquad (6.2.24)$$

For the same conditions, diffusiophoretic velocity is (from Equation 2.2.68)

$$u_{pd} \simeq 4.3 \times 10^{-2}/\delta \qquad (6.2.25)$$

Assuming film thicknesses for heat and mass transfer to be approximately the same, one may write

$$\frac{u_{pd}}{u_{pt}} \simeq 60 \qquad (6.2.26)$$

Thus, as the particle velocity associated with thermophoresis is in the order of 1/60 of the diffusiophoretic particle velocity, the validity of neglecting thermophoresis is substantiated for the present study.

Over the range of variables studied in the present investigation, the amount of particle collection by diffusiophoresis is less than that by inertial impaction, and the difference between the three alternate bases of calculating diffusiophoretic particle penetration is sufficiently small that the experiments do not discriminate between them. From a practical viewpoint, this lack of ability to discriminate between the three particle velocities is not of great importance since the results differ but little between them. Nevertheless, there are two reasons for which the author would suggest the use of Equation 4.4.24 (or 6.2.21), which assumes particles move with the gas mean mass velocity. The first reason is the fact that Whitmore (1976), based on his study of diffusiophoresis in a small wetted-wall column, concluded that the best expression for diffusiophoretic particle velocity is the one based on the assumption that particles move with the gas mean mass velocity. For an extensive number of runs in this simpler equipment, Whitmore was able to control experimental conditions with the higher accuracy required to discriminate between these three, not greatly different particle velocities. The second reason for recommending the use of gas mean mass velocity is that

in industrial applications this basis would give a more conservative estimate of particle collection, as may be seen from Figure 6.54.

6.2.4. Comparison with Previous Studies of MBC

As reviewed in section 2.3, there are unfortunately very few published studies on particulate recovery in MBC. Moreover, the results of the few available investigations are incomplete and suffer from numerous inconsistencies. There is but one study, Calvert et al. (1974), concerning the effect on penetration of particle size, a critical factor in the evaluation of overall penetration from the relation

$$Pt_{Total} = \Sigma\, Pt(d_p)\, \psi(d_p) \qquad (6.2.27)$$

where $\psi(d_p)$ is the fraction of particles with diameter d_p. The critical size range (0.3 - 5 μm), i.e. the range over which Pt varies from about 5 to 100%, as determined in the present study, agrees with the data reported for the single operating condition by Calvert et al. No other information on the effect on penetration of different variables are available from the publication of Calvert et al. (1974).

In Rowbottom's 1973 study, there is no information concerning the key variable, particle size. Qualitative results reached by Rowbottom on the effect on penetration of variables such as liquid flow rate and gas flow rate, as summarized in section 2.3, do however agree with the present findings.

Mlodzinski and Warych (1975), working with particles of average diameter 6 - 8 μm, naturally obtained high efficiencies. Figure 6.52 and 6.53 show clearly that, for particles of this size, efficiency of MBC is indeed high. Mlodzinski and Warych do include particle size as a variable (Equations 2.3.3 and 2.3.4), but, for reasons discussed in Chapter 2 and in the previous sections of this Chapter, the reliability of their equations is in doubt. Further, their experimental results would be affected significantly by their use of support grids of small open area, as pointed out in section 2.3.

Equations 2.3.1 and 2.3.2 given by Epstein (1971) and Calvert (1972) are not consistent, although the latter is reported to be derived from the former. Equation 2.3.1 incorporates mean diameter of liquid droplets in MBC, whereas there is no published information on size distribution of droplets in MBC. Thus it is not possible to use Epstein's equation. Yet another problem with these interrelated reports is that Calvert's equation, given in the present study as Equation 2.3.2, predicts 100% efficiencies for all particles over the size range 0.01 - 10 μm under moderate flow conditions ($G = 3$ kg/m^2-s and $L = 15$ kg/m^2-s). This result is in considerable variance with the original data of Pollack et al. (1966), on which the correlations of Epstein and Calvert were based.

In summary, although quantitative comparison cannot be made, qualitative conclusions obtained in the present work for the effects of various operating variables such as liquid and gas flow rate agree with the previously reported literature. Beyond such qualitative statements, no meaningful comparisons with previous studies can be made because of the limitations noted for such studies. Thus for the most important findings concerning particulate recovery in MBC, the results of the present study stand alone as new contributions.

6.2.5. Comparison of MBC with Other Scrubbers

Comparison of performance of various scrubbers is a challenging task for design engineers. In order to decide on the best scrubber for a given application and to optimize the design of the type of scrubber selected, a comprehensive understanding of the conditions and requirements of the specific application is necessary, as well as a knowledge of the fundamentals of various scrubbers. It would be incorrect to make a single classification of scrubbers in terms of relative superiority, as a scrubber which is the best choice for one application may be quite inappropriate for another. Also, each scrubber has potential for improvement if its fundamental characteristics are fully appreciated. A good example is a spray column, for which particle collection depends sensitively on the size distribution of liquid droplets. Sparks (1971) established that optimum performance in a spray tower is obtained when the drops are monodisperse. Thus, by improving design of the spray nozzles used, performance of a spray column can be enhanced. Some of the primary data that should be known prior to selection of a scrubber are size distribution, concentration and physical properties of particles, flow rate and temperature of the gas emission, pressure drop or power available for the scrubber, any limitations on scrubbing liquid flow rate, and efficiency of collection required. Both fixed and operating cost of the scrubber facility must also be considered.

Some comparisons may be made of MBC with four alternate scrubbers, i.e. spray columns, sieve plate columns, packed beds and venturi scrubbers. The first three are chosen because MBC operation involves droplets, bubbles and packing. Venturi scrubbers are included because they are known for their characteristically high recovery of very small particles.

Some shortcut methods for comparison of various scrubbers are given in the "Wet Scrubbers System Study Handbook", Calvert (1972), ed., and by Calvert (1977). For example, for quick comparison, penetration is written as

$$Pt = \exp \{- \alpha d_p^{\beta}\} \qquad (6.2.28)$$

Values of the constants α and β are assigned for each type of scrubber. As for any shortcut method, this one involves some drastic assumptions and approximations, and does not include all the relevant information.

On the other hand, it is appropriate to note here that the theory developed in Chapter 4 offers a dependable method of comparison and does not exclude determining factors. Thus particle transfer coefficient, k_p, defined for collection due to aerodynamic mechanisms, is a very useful concept for this purpose. Comparison of k_p values for different scrubbers at corresponding operating conditions would give a clear indication of relative particle removal efficiency.

Unfortunately, such definitive comparisons cannot as yet be made, except for MBC and spray columns, as these are the only scrubbers yet to be analyzed in terms of particle transfer coefficient. Tables D.1 and J.1 include experimental k_p values for MBC and a spray column, respectively. As may be noted, $k_{p,MBC}$ varies between 2.5 and 60, while $k_{p,SC}$ is in the range 0.1 and 12. At comparable flow conditions $k_{p,MBC}$ is about 15 times greater than $k_{p,SC}$. This is the best indication of the extent by which MBC is superior to a spray column.

Comparison of MBC with other scrubbers can also be made by employing the concept of a "cut diameter", which is the diameter of particle for Pt = 0.5 (or E = 0.5). Cut diameter has been considered a convenient parameter in describing the capability of a scrubber. For MBC at liquid and gas flow rates of 18.8 and 2.9 kg/m^2-s, respectively, and H_{st} = 0.44 m, this value can be read from Figure 6.52 as 1.14 μm for ferrous sulphate particles (ρ_p = 1900 kg/m^3). It is generally accepted to lump the effect of particle density and shape into this characteristic value by expressing the cut diameter in terms of aerodynamic diameter, $d_{pa} = d_p \sqrt{c' \rho_p}$, so that, for MBC with L = 18.8 and G = 2.9 kg/m^2-s, d_{pa} = 1.6 μm $(gm/cm^3)^{\frac{1}{2}}$. In order to achieve this separation at these conditions, gas phase pressure drop in MBC is about 9 cm W.C. (water column). For approximately the same pressure drop, Calvert (1977) gives the cut diameter, for sieve plate columns with a foam density* F = 0.4, as about 1.85 μm $(gm/cm^3)^{\frac{1}{2}}$. For packed beds filled with 38 mm stoneware raschig rings, d_{pa} = 1.5 μm $(gm/cm^3)^{\frac{1}{2}}$ for 2 m height and 4.2 μm$(gm/cm^3)^{\frac{1}{2}}$ for 0.25 m height (Calvert et al. (1972)). Even for the lower of these packing heights, pressure drop in the packed column is higher than that of MBC. Thus this simple analysis indicates that MBC is more efficient than any of the three most closely related columns. Furthermore, it is interesting to note that, for the venturi scrubber, a high particle removal, high pressure drop device, in order to obtain the same cut diameter, 1.6 μm $(gm/cm^3)^{\frac{1}{2}}$, about 40 cm W.C. pressure drop is required (Calvert et al. (1972)), as compared to 9 cm for an MBC unit. To achieve this performance, the

---

* Foam density is the ratio of clear liquid height to total foam.

operating conditions for a venturi scrubber should be 85 m/s gas velocity and $Q_L/Q_G = 0.5$ $\ell t/m^3$. Thus the results of the present study show that, in comparison with other wet scrubbing processes, the MBC process is an attractive and competitive scrubber. It may be noted that, if total scrubber power is used instead of gas phase pressure drop, the above analysis yields the same conclusion (Calvert (1977)).

Finally, it may be noted that mobile-bed columns are particularly beneficial for applications which require high mass transfer efficiency as well as particulate recovery.

CHAPTER 7

SUMMARY AND CONTRIBUTIONS TO KNOWLEDGE

Hydrodynamic and particulate recovery characteristics of mobile-bed contacting were studied in a 0.29 m diameter column for mass velocities of gas and liquid over the range $0.5 < G < 5.5$ and $4.7 < L < 33$ kg/m^2-s. Packing of density $157 kg/m^3$, of diameter 38, 25 and 19 mm, was used to obtain static bed heights of 0.29, 0.44 and 0.58 m. Particulates of sizes 0.35 - 5.5 μm, and of four materials, were tested. Diffusiophoresis was studied by addition of steam to a heated inlet air stream. The results obtained can be summarized as follows:

1. Dependence of bed height on gas flow rate is found to be linear over the stable operating region. Beyond this region bed height increases non-linearly as the flooding limit is approached. This transition from linear to non-linear expansion occurs at smaller gas velocities with increasing liquid flow rate and at progressively lower values of G as packing diameter is increased. Over the linear region bed expansion is correlated by:

$$h = 0.147\ G_{mf}\ \Delta/H_{st} \qquad (6.1.8)$$

2. Minimum fluidization velocity, G_{mf}, was determined both visually and from bed expansion data. As results of both methods were in agreement, the combined data were used to obtain the following correlation:

$$G_{mf} = 10.86\ d_{pb}^{0.488}\ 10^{-0.01985\ L} \qquad (6.1.2)$$

It is significant that G_{mf} was found to be independent of H_{st}.

3. Extensive measurements indicated that pressure drop is independent of gas velocity over the stable operating region which corresponds to the linear region of bed expansion. The results for this region are correlated by the following equation:

$$\Delta P_c = 112.17\ L^{0.44}\ d_{pb}^{-0.492}\ H_{st} \qquad (6.1.13)$$

4. The validity of the relation

$$\Delta P_c = (h_L\ \rho_L + h_{pb}\ \rho_{pb})g\ H \qquad (2.1.1)$$

which was first used by Barile et al. (1971) and Tichy and Douglas (1973) was demonstrated by making a macroscopic momentum balance around the MBC column. This equation was used to evaluate liquid holdup for MBC, again for the stable operating region of linear bed expansion. Liquid holdup values thus obtained were correlated by the following equation:

$$h_{L,st} = 1.15 \times 10^{-4} L^{0.826} d_{pb}^{-1.289} \qquad (6.1.14)$$

5. Particle collection mechanisms were classified as aerodynamic and phoretic mechanisms. Characteristic parameters for aerodynamic mechanisms, which are always present in any gas-liquid contactor, were defined for particle collection by drops, by films on spherical packing and from bubbles (Table 2.6 and 2.7). These parameters were applied to make an order-of-magnitude estimate of the relative importance of all aerodynamic mechanisms in MBC. This analysis showed that one mechanism, inertial impaction, is the controlling aerodynamic particle collection mechanism in MBC.

6. A new general theoretical analysis, valid for particle collection in any type of gas-liquid contactor, was developed using the local volume averaged continuity equation (LVACE) of the particles and of the gas phase. A particle transfer coefficient, k_p, analogous to mass transfer coefficient, has been defined for this analysis to account for particle collection by aerodynamic capture mechanisms. Further, it is shown that use of LVACE for the particles facilitates incorporation of any phoretic mechanism into a general theoretical solution for particle capture simultaneously by aerodynamic and phoretic mechanisms. This theoretical treatment was

developed for the two most important industrial cases, i.e. first for particle collection due only to aerodynamic mechanisms, and, second, for particle collection due to the simultaneous occurrence of aerodynamic mechanisms and diffusiophoresis. For the second case, a general solution, as suggested by Whitmore (1976), was presented for three diffusiophoretic velocity expressions.

The new analysis of the present study indicates that particle penetration due to aerodynamic mechanisms is

$$Pt_A = \exp \{- k_p H/u_z\} \tag{4.3.6}$$

while, for simultaneous occurrence of aerodynamic mechanisms and diffusiophoresis, particle penetration is

$$Pt = Pt_A \, Pt_D \tag{4.4.19}$$

where Pt_D is given by one of the expressions in Equations 4.4.22, 4.4.24 and 4.4.26, each corresponding to a different diffusiophoretic particle velocity expression. Whichever expression is chosen, the analysis showed that the effect of diffusiophoresis on overall particle collection efficiency of a scrubber is directly proportional to the amount of the vapor transferred across the gas-liquid interface (Equation 4.4.18). For the most popular case of diffusiophoresis in industry, i.e. condensation of water vapor through air, Pt_D can be expressed in terms of

absolute humidity, as given by Equations 6.2.20, 6.2.21 and 6.2.22.

7. Extensive experiments with ferrous sulphate particles were performed to investigate the effect of liquid and gas flow rate, packing size, static bed height and particle size on particle penetration in MBC. The results gave the following correlation for the particle transfer coefficient of MBC:

$$k_{p,MBC} = 3765\ St^{0.8}\ Re_G^{-2.64}\ Re_L^{2.1}\ (H_{st}/d_{pb})^{1.52} \quad .... (6.2.14)$$

The results show that penetration decreases with increasing liquid flow rate, with decreasing packing size and with increasing static bed height. The effect of gas flow rate on penetration is rather weak. Typically, Pt is either almost independent of or decreases slightly with increasing G. Only for a few cases of high H_{st} does Pt increase somewhat with G. The correlation for particle transfer coefficient was determined using particles over a wide size range, 0.35 - 5.5 μm, and the experimental data fit the correlation equally well over this entire range.

8. A simple theoretical analysis for the effect on particle collection of degree of hydrophobicity indicated that,

for contact angles smaller than, or equal to 90^{o}, hydrophobicity of particles does not affect collection efficiency. This conclusion was checked experimentally using three additional particles: silica (an insoluble solid, $\theta_c = 0^{o}$), latex (an insoluble solid, $\theta_c = 42^{o}$) and DOP (an insoluble liquid, $\theta_c = 63.5^{o}$). The results of all four particulates tested fit well to the general correlation (Equation 6.2.14). This conclusion contrasts to the views of the few previous investigators of effect of degree of hydrophobicity.

9. Effect of diffusiophoresis on particle penetration was investigated by applying the relation $Pt = Pt_A\ Pt_D$, derived from theory, with experimental results obtained by utilizing water vapor condensation from a hot, humid particulate-laden gas stream. The only uncertainty in the theoretical prediction of Pt_D is the choice of diffusiophoretic velocity, i.e. whether particles are assumed to move at the mean molar, mean mass or the Schmitt-Waldmann velocity. However, as predicted Pt_D varied only about ±7% for these three alternate velocities, and as the experimental Pt_D results were equally well represented using any of the three theoretical velocities, the results do not discriminate between them. Due to the small effect of choice of diffusiophoretic velocity, this uncertainty is unimportant practically. Nevertheless,

mean mass velocity would be an appropriate choice for the prediction of Pt_D by Equation 4.4.24 as it gives a slightly more conservative estimate. The corresponding form of this equation for the case of water vapor condensing through air is Equation 6.2.21.

10. Comparison of particulate recovery in MBC with other scrubbers shows that MBC is a competitive scrubber.

11. It is suggested that particle transfer coefficient, introduced in this study, may be a very useful parameter for comparison of different particle collection devices.

SUGGESTIONS FOR FUTURE WORK

In designing the equipment used in this study (Figure 5.1), careful consideration was given to the possibility of extending the research with minor modifications to other aspects of MBC. As there are very few studies of heat and mass transfer at conditions comparable with those preferred by industry, these aspects may be studied extensively. There may be great potential for use of MBC as a cooling tower. Correlations that may be developed for heat and mass transfer coefficients would be very helpful for design of industrial units. For heat transfer studies it would be desirable to improve the temperature control system of the duct heater in order to minimize temperature fluctuations and to reduce experimental time.

A study of gas phase mixing in MBC would definitely help to improve the understanding of this complex phenomenon.

As far as the particulate recovery is concerned, the concentration of particles was limited in the present study to about 10^8 particles/m^3 by the capacity of the spinning disk aerosol generator. By using a different particle injection system, the effect of particle concentration on penetration may be interesting to investigate.

Finally, the test column can be filled with various appropriate packing and be operated as a fixed-bed column. Particulate recovery experiments that may be performed with such a unit can be used to obtain a correlation for particle transfer coefficient of packed beds, similar to Equation 6.2.14 for MBC.

NOMENCLATURE

A	rate of aerodynamic collection, $\#/m^3$-s (4.1.13)
a	interfacial area per unit volume of bed, m^{-1}
a_i	accommodation coefficient, fraction of molecules reflected diffusely from particle's surface (2.2.59)
C	coefficient of discharge (E.1)
c	concentration, $kg.mole/m^3$
c^r	root mass concentration, $kg^{\frac{1}{2}}$-$kg.mole^{\frac{1}{2}}/m^3$, (4.4.7-a)
c'	Cunningham correction factor
D	diffusivity coefficient for gas, m^2/s
D_p	diffusivity coefficient for particle, m^2/s
D_c	column diameter, m
d_b	bubble diameter, m
d_c	collector diameter, m
d_p	particle diameter, m
d_{pb}	packing ball diameter, m
E	efficiency (4.2)
E_D	particle collection efficiency of spherical objects due to diffusion (2.2.39)
E_E	collection efficiency of spherical objects due to electrostatic attraction (2.2.56 and 2.2.57)
E_G	gravitational collection efficiency of spherical objects (2.2.46)
E_I	inertial collection efficiency of spherical objects (2.2.1-a and 2.2.1-b)
E_R	interception efficiency for spherical objects (§2.2.1.2)

$E_{b,D}$	diffusional collection efficiency from bubbles (2.2.43)
$E_{b,G}$	gravitational collection efficiency from bubbles (2.2.49)
$E_{b,I}$	inertial collection efficiency from bubbles (2.2.13)
F	molar flow rate of gas, kg.mole/m^2-s; surface free energy, J
G	mass flow rate of gas, kg/m^2-s
G_{mf}	gas minimum fluidization velocity, kg/m^2-s
g	gravitational acceleration, 9.80665 m/s^2
H	height of mobile-bed, m
H_{st}	static bed height, m
h	dimensionless bed height, $(H-H_{st})H_{st}$
h_G	gas holdup, volume of gas per volume of bed
$h_{G,mf}$	gas holdup at minimum fluidization conditions
h_L	liquid holdup, volume of liquid per volume of bed
$h_{L,st}$	liquid holdup, volume of liquid per static volume of bed
h_{pb}	holdup of packing, volume of packing per volume of bed
$h_{pb,st}$	holdup of packing, volume of packing per static volume of bed
J_p	particle flux with respect to mean mass velocity, #/m^2-s
K	inertial impaction parameter, (2.3.1)
k'_p	area-based particle transfer coefficient, m/s
k_p	volumetric particle transfer coefficient, s^{-1}

L	mass flow rate of liquid, kg/m^2-s
M_i	molecular weight, kg/kg.mole
m_i	molecule mass, kg
m_p	particle's mass, kg
N_i	molar flux of species i with respect to stationary axes, $kg.mole/m^2$-s
N_D	diffusional parameter for spherical collector (2.2.40)
N_E	parameter for electrostatic attraction (2.2.51-2.2.55)
N_G	gravitational parameter for spherical collectors (2.2.45)
N_p	particle flux with respect to stationary axes, $\#/m^2$-s
N_R	interception parameter for spherical collectors (2.2.15)
N^r	root mass flux, $kg^{\frac{1}{2}}$-$kg.mole^{\frac{1}{2}}/m^2$-s, (4.4.7.-b)
$N_{b,D}$	diffusional parameter for bubbles (2.2.44)
$N_{b,G}$	gravitational parameter for bubbles (2.2.50)
$N_{b,I}$	inertial parameter for bubbles (2.2.14)
$\vec{n}$	unit vector
n_p	particle concentration, $\#/m^3$
n_i	mass flux of species i with respect to stationary axes, kg/m^2-s
P	pressure, Pa, (N/m^2)
ΔP_c	pressure drop across the column, Pa
Pt	penetration (4.1)
r	reaction rate, kg/m^3-s
Q	volumetric flow rate, m^3/s

r	radius, m
S_c	column cross sectional area, m^2
S_i	interfacial area, m^2
t	time, s
U	$u/u_{G,\infty}$
u	mean mass velocity, m/s
u_b	bubble velocity, m/s
u_G	superficial gas velocity, m/s
u_{Gi}	interstitial gas velocity, m/s
$u_{G,mf}$	minimum gas fluidization velocity, m/s
$u_{G,\infty}$	undisturbed upstream gas velocity, m/s
u_L	superficial liquid velocity, m/s
u_{Li}	interstitial liquid velocity, m/s
u_p	particle velocity, m/s
u_{pd}	diffusiophoretic velocity of particle, m/s
u_{pe}	electrophoretic velocity of particle, m/s
u_{pm}	magnetophoretic velocity of particle, m/s
u_{pt}	thermophoretic velocity of particle, m/s
$u_{p,ext}$	particle velocity due to an external force, m/s
u_r	relative velocity, m/s
u_T	terminal settling velocity, m/s
u_z	velocity of gas in "z" direction, m/s

u^r	root mass velocity, m/s, (4.4.7-e)
u^*	mean molar velocity, m/s; also $u/u_{G,\infty}$ (2.2.29)
V	volume, m^3
x_i	mole fraction of species i
Y	absolute humidity, kg H_2O/kg dry air
Δ	excess mass velocity, or stirring number, $(G-G_{mf})/G_{mf}$
δ	thickness of the gas film at the interface
θ	dimensionless time, $t\ u_{G,\infty}/d_c$, (2.2.29)
θ_c	contact angle
γ	kinematic viscosity, μ/ρ , m^2/s
γ_{LV}	liquid-vapor surface tension, N/m
γ_{SL}	solid-liquid interfacial tension, N/m
γ_{SV}	solid-vapor surface tension, N/m
ϕ_D	rate of diffusional deposition of particles on spherical objects
$\phi_{b,D}$	rate of diffusional collection by bubbles (2.2.42)
$\phi_{b,G}$	rate of gravitational collection by bubbles (2.2.48)
$\phi_{b,I}$	rate of inertial collection by bubbles (2.2.10)
	mean free path of gas, m
$\sigma_{1,2}$	slip factor (2.2.62 and 2.2.65)
ρ	density, kg/m^3
μ	viscosity, kg/m-s
λ	gas mean free path, m
ψ	fraction of particles (6.2.27)

Overline

-	local volume averaged

Underline

→	vectorial quantity

Superscripts

r	root mass variables (4.4.7)
+	represents general case (4.4.8)

Subscripts

ave	average
b	bubble
c	column, collector
D	diffusion
d	diffusiophoresis
E	electrostatic attraction
e	electrophoresis
ext	external
G	gas, gravitational
I	inertial
i	i^{th} species, interstitial, interface
L	liquid
m	magnetophoresis
mf	minimum fluidization
p	particle
pb	packing ball

R	interception
r	relative
st	based on static volume of bed
T	terminal
t	thermophoresis
1	diffusing component
2	stagnant component

Dimensionless Numbers

$Eu = \Delta P_c / \rho_G \, u_G^2$	Euler number
$Fr = L^2 / d_{pb} \, g \, \rho_L^2$	Froude number
$Kn = \lambda / r_p$	Knudsen number
$Pe = u_G \, d_c / D_p$	Peclet number
$Re = u \, \rho \, d_{pb} / \mu$	Reynolds number
$Sc = \mu_G / \rho_G \, D_p$	Schmidt number
$St = c' \, d_p^2 \, \rho_p \, u_r / 9 \, \mu_G \, d_{pb}$	Stokes number

Mathematical Operations

$\exp x = e^x$

$\ln x$ = the logarithm of x to the base e

∇ = the "del" operator (Vector differential operator)

Σ = addition

REFERENCES

Aitken, J., Trans. Roy. Soc. Edinb., 32, 239 (1883).

Aksel'rud, G., Zh. Fiz. Khim., 27, 1445 (1953).

Aksel'rod, L.S., and M.M. Yakovenko, Teor. Osn. Khim. Tekhnol., 3, No. 1, 148 (1969).

Albrecht, F., Z. Physik, 32, 48 (1931).

Allen, R.W.K., Ph.D. Thesis, McGill University, Montreal, 1975.

Annis, B.K., A.P. Malinauskas and E.A. Mason, J. Aerosol Sci., 3, 55 (1972).

Annis, B.K. and E.A. Mason, J. Aerosol Sci., 6, 105 (1975).

Azarniouch, M.K., Ph.D. Thesis, McGill University, Montreal, 1973.

Bakanov, S.P., and B.V. Derzaguin, Disc. Faraday Soc., 30, 130 (1960).

Balabekov, O.S., P.G. Romankov, E. Ya. Tarat, and M.F. Mikhalev, Zh. Prikl. Khim., 42, No. 7, 1454 (1969).

Barile, R.G., and D.W. Meyer, Chem. Eng. Prog. Symp. Ser., No. 119, 67, 134 (1971).

Beal, S.K., Bettis Atomic Lab. Rep. No. WAPD-TM-765, April 1968.

Beard, K.V., and S.N. Grover, J. Atmos. Sci., 31, 543 (1974).

Bhatia, S.P., T.L.C. Le Souza, M.K. Azarniouch and S. Prahacs, Am. Ind. Hyg. Assoc. Jr., 39, 83 (1978).

Bird, R.B., W.E. Stewart and E.N. Lightfoot, "Transport Phenomena", John Wiley & Sons, Inc., New York (1960).

Blodgett, K.B., Army Air Force Tech. Rept., 5418 (1946).

Blyakher, I.G., L.Ya. Zhivaikin, and N.A. Yurovskaya, Inst. Chem. Eng., 7, 485 (1967).

Brock, J.R., J. Colloid Sci., 17, 768 (1962).

Brock, J.R., J. Colloid Sci., 18, 489 (1963).

Calvert, S., Air Pollution, Stern, A.C., Ed., 3, Academic Press, New York (1968).

Calvert, S., J. Goldschmid, M.D. Leith and D. Mehta, Wet Scrubber System Study Handbook, API Inc., (1972).

Calvert, S., N.C. Jhaveri and S. Yung, EPA-650/2-74-093, October 1974.

Calvert, S., Chem. Eng., 54 (August 29, 1977).

Cawood, W., Trans. Faraday Soc., 32, 1068 (1936).

Chapman, S., and T.G. Cowling, The Mathematical Theory of Non-Uniform Gases", Cambridge Univ. Press, London (1964).

Chen, B.H., Ph.D. Thesis, McGill University, Montreal, 1965.

Chen, B.H., and W.J.M. Douglas, Can. J. Chem. Eng., 46, 245 (1968).

Chen, B.H., and W.J.M. Douglas, Can. J. Chem. Eng., 47, 113 (1969).

Cleaver, J.W., and B. Yates, Proceedings of the 1973 Conference on Particle Technology, IIT, Illinois, Chicago.

Clusius, K., Z. Ver. dt. Ing. Beiheft Verfahrenstechnik, 23 (1941).

Cochet, R., Collogue Internationale, La Physique des Forces Electrostatiques et leurs Applications, p. 331, Centre National de la Recherche Scientifique, Paris (1961).

Das, P.K., Indian J. Meteorol. Jeophys., 1, 137 (1950).

Davies, C.N., Proc. Phys. Soc., 57, 529 (1945).

Davies, C.N., Proc. Roy. Soc. Lond., A289, 235 (1966).

Davies, C.N., Aerosol Science, Academic Press, London (1966).

Derjaguin, B.V., and S.S. Duklin, Dokl. Akad. Nauk., SSSR, (Phys. Chem.), 106, 851 (1956).

Derjaguin, B.V., and S.S. Duklin, Dokl. Akad. Nauk., SSSR, (Phys. Chem.), 111, 613 (1956).

Derjaguin, B.V., and S.S. Duklin, Dokl. Akad. Nauk., SSSR, (Phys. Chem.), 112, 407 (1957).

Derjaguin, B.V., and S.P. Bakanov, Dokl. Akad. Nauk., SSSR, (Phys. Chem.), 2, 41 (1957).

Derjaguin, B.V., and S.P. Bakanov, Kolloid Zh., 21, 377 (1959).

Derjaguin, B.V., and S.P. Bakanov, Dokl. Akad. Nauk., SSSR, (Phys. Chem.), 147, 139 (1962).

Derjaguin, B.V., Y.I. Yalamov, and S. Storozhilova, Coll. Sci., 22, 117 (1966).

Derjaguin, B.V., and S.P. Bakanov, Dokl. Akad. Nauk., SSSR, (Phys. Chem.), 147, 139 (1967).

Derjaguin, B.V., and Ya. I. Yalamov, "Topics in Current Aerosol Research", (Edited by Hidy, G.M. and J.R. Brock), Vol. 3, Pergamon Press, Oxford (1972).

Doganoglu, Y., Ph.D. Thesis, McGill University, Montreal, 1975.

Dorsch, R.G., P.G. Saper and C.F. Kadow, National Adv. Comm. Aeronaut. Tech. Note. 3587 (1955).

Douglas, H.R., I.W.A. Snider, and G.H. Tomlinson, Chem. Eng. Progr., 59 (12), 85 (1963).

Douglas, W.J.M., Chem. Eng. Progr., 60 (7), 66 (1964).

Einstein, A., Z. Phys., 27, 1 (1924).

Environmental Research Corporation (ERC), Operation and Maintenance Manual for the Spinning Disk Aerosol Generator, St. Paul, Minn. (1970).

Epstein, P.S., Z. Physik, 54, 537 (1929).

Epstein, M., C.C. Leivo and C.H. Rowland, Proceedings of 2nd International Lime/Limestone Wet Scrubbing Symposium, V. 1, p. 45, 1971.

Facy, L., Comptes rendus, 246, 102; 246, 3161 (1958).

Flint, L.R., and W.J. Howart, Chem. Eng. Sci., 26, 1155 (1971).

Fond, A., and H. Herne, Nat'l Coal Board (Gt. Brit.), Mining Research Establishment Rept. No. 2068 (1957).

Forney, L.J., and L.A. Spielman, J. Aerosol Sci., 5, (1973).

Freise, V., J. Chem. Physique, 54, 879 (1957).

Friedlander, S.K., A.I.Ch.E.J., 3, 43 (1957).

Friedlander, S.K. and H.F. Johnstone, Ind. Eng. Chem., 49, 1151 (1957).

Fuchs, N.A., The Mechanics of Aerosols, The Macmillan Co., New York (1964).

Garner, F. and R. Keey, Chem. Eng. Sci., 9, 119 (1958).

Garner, F. and R. Suckling, A.I.Ch.E.J., 4, 114 (1958).

Gel'perin, N.I., V.Z. Grishko, V.I. Savchenko and V.M. Shchedro, Khim. Neft. Mashinostroenie, No. 1, 22 (1966).

Gel'perin, N.I., V.I. Savchenko and V.Z. Grishko, Teor. Osn. Khim. Tekhnol., 2, No. 1, 76 (1968).

Glauert, H., Aeronautical Research Committee Rept. 2025, London, (H.M.S.O.) (140).

Goldschmid, Y., and S. Calvert, A.I.Ch.E.J., 9, 352 (1963).

Goldsmith, P., H.J. Delafield, and L.C. Cox, Geo . Pura. Applic., 50, 278 (1963).

Goldsmith, P., H.J. Delafield and L.C. Cox, Q.J. Roy. Met. Soc., 89, 43 (1963).

Goldsmith, P. and F.G. May, Aerosol Science, C.N. Davies, Ed., Academic Press, New York (1966).

Gooding, C.H., T.W. Sigmon and L.K. Monteith, EPA-600/2-77-230 (1977).

Herne, H., Paper presented before the Symposium on Aerodynamic Capture of Particles, Brit. Coal Board, Pergamon Press, London (1960).

Hidy, G.M. and J.R. Brock, The Dynamics of Aerocolloidal Systems, Pergamon Press (1970).

Hirschfelder, J.O., C.F. Curtiss and R.B. Bird, Molecular Theory of Gases and Liquids, John Wiley & Sons Inc., New York (1964).

Hutchinson, P., G.F. Hewitt and A.E. Dukler, Chem. Eng. Sci., 26, 419 (1971).

Jashnani, I.L., Paper presented at the 68th Annual Meeting of the A.P.C.A., #75-30.2, Boston (1975).

Jelinek, Z.K., Particle Size Analysis, John Wiley & Sons Inc., New York (1974).

Johnstone, H.F., and M.H. Roberts, Ind. and Eng. Chem., 41, 2417 (1949).

Khanna, R.T., Ph.D. Thesis, McGill University, Montreal, 1971.

Kielback, A.W., Chem. Eng. Prog., 66, 106 (1959).

Kielback, A.W., Paper presented at A.I.Ch.E. Meeting, Dec. 1960.

Kielback, A.W., Chem. Eng. Prog., Symp. Ser., 57 (35), 51 (1961).

Kito, M., M. Sawada, M. Shimada, M. Takata, T. Sukai and S. Sugiyama, Int. Chem. Eng., 16 (4), 701 (1976).

Kito, M., M. Shimada, R. Iijima, T. Sakai, M. Takata and S. Sugiyama, Int. Chem. Eng., 16 (4), 705 (1976).

Kito, M., Ya. Kayama, T. Sakai, and S. Sugiyama, Int. Chem. Eng., 16 (4), 710 (1976).

Kleinschmidt, R.V., Chem. and Met. Eng., 46, 487 (1939).

Kraemer, H.F. and H.F. Johnstone, Ind. & Eng. Chem., 47, 2426 (1955).

Krainev, N.I., M.I. Niyazov, I.P. Levsh and S.U. Umarav, Zh. Prikl. Khim., 41 (9), 2081 (1968).

Kramers, H.A., and J. Kistemaker, Physica, 10, 699 (1943).

Landahl, H.D. and R.G. Herman, J. Coll. Sci., 4, 103 (1949).

Langmuir, I., U.S. Office of Scientific Research and Development, No. 865, Part 4, Oct. 1942.

Langmuir, I. and K.B. Blodgett, U.S. Army Air Force Tech. Rep. No. 5418, Feb. 19, 1946; U.S. Dept. Commerce Publ. PB 27565, Feb. 1946.

Langmuir, I., J. Met., 5, 175 (1948).

Levich, V., Physico-Chem. Hydrodyn. Acad. Sci. USSR, Moscow (1952).

Levsh, I.P., N.I. Krainev and M.I. Niyazov, Int. Chem. Eng., 8, 311 (1968).

Lewin, L.M., Doklady Akad. Nauk. SSSR, 91 (6), 1329 (1953).

Mason, E.A. and S. Chapman, J. Chem. Phys., 36, 627 (1962).

Mayak, V.I., and V.I. Matrozov, Teor. Osnov. Khim. Tekhnol., 3 (1), 79 (1969).

Merrington, A.C. and E.G. Richardson, The Proceedings of the Physical Society, 59, No. 331, 1 (1947).

Mlodzinski, B. and J. Warych, Chemie-Ing. Techn., 47, Heft 19 (1975).

Montagna, J., Ph.D. Thesis, Wayne State Univ., Detroit, Mich., 1974.

Montgomery, T.L. and M. Corn, J. Aerosol Sci., 1, 185 (1970).

Panthenier, M.M. and M.J. Moreau-Hanot, Phys. Radium, Paris, 3, 590 (1932).

Pollack, W.A., J.P. Tomany and G. Frieling, A.S.M.E. Publication 66-WA/CD-4, 1966.

Ranz, W.E., Univ. I.U., Eng. Expt. Sta. Tech. Rep., No. 3, March 31, 1951.

Ranz, W.E. and J.B. Wong, Ind. and Eng. Chem., 44 (6), 1371 (1952).

Ranz, W.E., Penn. State Univ., State College, Dept. of Eng., Research Rept. No. 66, 1956.

Rohman, H., Z. Phys., 17, 253 (1923).

Rowbottom, R.S., Domtar Lmtd, Research Center, CPAR Project No. 211, December 31, 1973.

Royco Instruments Inc., Operating and Service Manual for Royco Particle Counter Model 202, Menlo Park, Calif., 1963.

Schmitt, K.H., Z. Naturf., 14a, 870 (1959).

Schmitt, K.H. and L. Waldmann, Z. Naturf., 15a, 843 (1960).

Schmitt, K.H., Staub, 21, 173 (1961).

Schmel, G.A., J. Geophys. Res., 75, 1766 (1970); J. Aerosol Sci., 2, 63 (1971).

Sell, W., Forsch. Gebiete Ingenieurw., 2, Suppl. No. 347 (Aug. 1931).

Semrau, K.T., J. Air Poll. Cont. Assoc., 10 (3), 200 (1960).

Shannon, L.J., EPA-650/2-74-027, May 1974.

Slattery, J.C., "Momentum, energy and mass transfer in continua", McGraw-Hill Book Comp., New York (1972).

Sparks, L.E., Ph.D. Thesis, Univ. Washington, 1971.

Stairmand, E.J., Trans. Inst. Chem. Engrs, London, 28, 130 (1950).

Statnick, R.M. and D.C. Drhmel, Jr. of A.P.C.A., 25, 605 (1975).

Stefan, J., Wien Ber., 83, 943 (1881).

Stetter, G., Staub, 20, 244; Ber. Österr. Ahad. Wiss., 169, 91 (1960).

Strauss, W., Industrial Gas Cleaning, Pergamon Press, Oxford, 1966.

Taylor, G.I., Brit. Aeronaut. Research Council, Rep. No. 2024 (1940).

Thring, M.W. and W. Strauss, Jr. of Iron and Steel Inst., 196, 62 (1960).

Tichy, J. and W.J.M. Douglas, Can. J. Chem. Eng., 50, 702 (1972).

Tichy, J., A. Wong and W.J.M. Douglas, Can. J. Chem. Eng., 50, 215 (1972).
Tichy, J. and W.J.M. Douglas, Can. J. Chem. Eng., 51, 618 (1973).
Torobin, L.B. and W.H. Gauvin, Can. J. Chem. Eng., 37, 167 (1949).

Tyndall, J., Proc. R. Inst. Brit., 6, 3 (1870).

Uchida, S., C.S. Chang and C.Y. Wen, Can. J. Chem. Eng., 55, 392 (1977).

UOP (1970)-BECHTEL(1971), in "Wet Scrubber System Study Handbook", A.P.T. Inc., p. 5-156 (1972).

UOP Bulletin No. 608.

Waldmann, L., Z. Natur. Forsch, 14a, 489 (1959).

Waldmann, L., and K.H. Schmitt, in "Aerosol Science", C.N. Davies, Ed., Academic Press, London (1966).

Wang, C.S., M. Beizaie and C. Thien, A.I.Ch.E., 23(6), 879 (1977).

Wet Scrubbers System Study Handbook, Ed. by S. Calvert, J. Goldschmid, D. Leith and D. Mehta, A.P.I. Inc., (1972).

White, H.J., Trans. Am. Inst. Elect. Engrs, 70, 1186 (1951).

Whitmore, P.J., Ph.D. Thesis, Univ. of British Columbia, 1976.

Whitmore, P.J. and A. Meisen, J. Aerosol Sci., 4, 435 (1973).

Whitmore, P.J. and A. Meisen, J. Aerosol Sci., 7, 297 (1976).

Whitmore, P.J. and A. Meisen, Can. J. Chem. Eng., 55, 279 (1977).

Wozniak, M., Int. Chem. Eng.,17(3), 553 (1977).

Young, T., Phil. Trans. Roy. Soc., London, 95, 65 (1805).

APPENDIX A

Experimental results for bed expansion

TABLE A.1. Experimental Results for Bed Expansion

PACKING SIZE = 0.038 M
STATIC BED HEIGHT = 0.29 M

L,KG/M2-S										
4.708	G,KG/M2-S	2.020	2.330	2.690	3.100	3.620	4.100	4.600	5.040	5.470
	HMAX/HST	1.150	1.304	1.626	1.776	2.130	2.506	2.780	2.937	3.290
	HMIN/HST	1.150	1.236	1.274	1.463	1.630	1.734	1.920	2.103	2.250
	HAVG/HST	1.150	1.270	1.450	1.620	1.880	2.120	2.350	2.520	2.770
9.416	G,KG/M2-S	1.870	2.400	2.910	3.420	3.920	4.430	4.920	5.340	
	HMAX/HST	1.210	1.635	1.936	2.230	2.584	2.940	3.190	3.690	
	HMIN/HST	1.210	1.345	1.624	1.730	1.916	2.140	2.250	2.630	
	HAVG/HST	1.210	1.490	1.780	1.980	2.250	2.540	2.720	3.160	
14.124	G,KG/M2-S	1.480	1.850	2.400	2.940	3.430	3.940	4.470	4.930	5.400
	HMAX/HST	1.190	1.363	1.715	2.090	2.290	2.590	2.840	3.240	3.490
	HMIN/HST	1.190	1.277	1.527	1.690	1.830	2.090	2.300	2.640	2.890
	HAVG/HST	1.190	1.320	1.621	1.890	2.060	2.340	2.570	2.940	3.190
18.832	G,KG/M2-S	2.020	2.487	2.710	3.127	3.230	3.700	4.230	4.710	5.110
	HMAX/HST	1.570	1.862	1.920	2.345	2.170	2.380	2.750	3.190	3.700
	HMIN/HST	1.470	1.621	1.640	1.793	1.770	1.980	2.330	2.590	2.900
	HAVG/HST	1.520	1.741	1.780	2.069	1.970	2.180	2.540	2.890	3.300
23.540	G,KG/M2-S	1.070	1.285	1.722	2.243	2.646	2.952	3.190	3.562	3.897
	HMAX/HST	1.138	1.207	1.483	1.724	1.966	2.137	2.345	2.759	3.379
	HMIN/HST	1.138	1.207	1.379	1.552	1.621	1.863	1.897	2.069	2.241
	HAVG/HST	1.138	1.207	1.431	1.638	1.793	2.000	2.121	2.414	2.810

PACKING SIZE = 0.038 M
STATIC BED HEIGHT = 0.44 M

L,KG/M2-S

4.708	G,KG/M2-S	1.760	2.120	2.490	2.980	3.240	3.910	4.390		
	HMAX/HST	1.070	1.200	1.590	2.160	2.470	2.840	3.440		
	HMIN/HST	1.070	1.200	1.350	1.460	1.570	1.800	2.060		
	HAVG/HST	1.070	1.200	1.470	1.810	2.020	2.320	2.750		
9.416	G,KG/M2-S	2.240	2.860	3.420	3.910	4.390				
	HMAX/HST	1.580	2.110	2.480	2.900	3.240				
	HMIN/HST	1.380	1.670	1.780	2.000	2.200				
	HAVG/HST	1.480	1.890	2.130	2.450	2.720				
14.124	G,KG/M2-S	1.083	1.229	1.497	1.720	1.792	2.030	2.378	2.595	3.131
	HMAX/HST	1.000	1.159	1.318	1.377	1.455	1.635	1.955	2.068	2.220
	HMIN/HST	1.000	1.091	1.227	1.263	1.295	1.395	1.500	1.568	1.760
	HAVG/HST	1.000	1.125	1.273	1.320	1.375	1.515	1.727	1.818	1.990
	G,KG/M2-S	3.560	4.030	4.510						
	HMAX/HST	2.710	2.990	3.185						
	HMIN/HST	1.910	2.290	2.545						
	HAVG/HST	2.310	2.640	2.865						
18.832	G,KG/M2-S	1.233	1.442	1.738	1.930	2.166	2.369	2.540	2.642	2.862
	HMAX/HST	1.182	1.318	1.568	1.570	1.841	2.023	1.906	2.250	2.432
	HMIN/HST	1.159	1.273	1.341	1.410	1.477	1.568	1.574	1.682	1.705
	HAVG/HST	1.170	1.295	1.455	1.490	1.659	1.795	1.740	1.966	2.068
	G,KG/M2-S	3.100	3.498	3.950						
	HMAX/HST	2.500	2.841	2.840						
	HMIN/HST	1.818	1.977	2.180						
	HAVG/HST	2.159	2.409	2.510						
23.540	G,KG/M2-S	0.845	1.025	1.147	1.512	2.000	2.576	3.429		
	HMAX/HST	1.000	1.136	1.250	1.409	1.568	2.023	2.818		
	HMIN/HST	1.000	1.091	1.205	1.318	1.432	1.636	2.000		
	HAVG/HST	1.000	1.114	1.227	1.364	1.500	1.830	2.409		

PACKING SIZE = 0.025 M
STATIC BED HEIGHT = 0.29 M

L,KG/M2-S										
4.708	G,KG/M2-S	2.410	2.760	3.160	3.600	4.100	4.520	4.930	5.390	
	HMAX/HST	1.636	1.690	1.940	2.150	2.400	2.774	3.210	3.640	
	HMIN/HST	1.344	1.390	1.540	1.650	1.860	2.190	2.250	2.640	
	HAVG/HST	1.490	1.540	1.740	1.900	2.130	2.482	2.730	3.140	
9.416	G,KG/M2-S	1.790	2.260	2.336	2.820	3.250	3.740	4.210		
	HMAX/HST	1.240	1.635	1.759	1.900	2.122	2.419	2.590		
	HMIN/HST	1.240	1.325	1.345	1.600	1.788	1.981	2.270		
	HAVG/HST	1.240	1.480	1.552	1.750	1.955	2.200	2.430		
14.124	G,KG/M2-S	1.185	1.435	1.879	2.331	2.400	2.692	3.034	3.351	3.570
	HMAX/HST	1.207	1.345	1.690	1.828	1.977	2.000	2.276	2.448	2.621
	HMIN/HST	1.155	1.224	1.310	1.483	1.643	1.586	1.690	1.828	1.966
	HAVG/HST	1.181	1.284	1.500	1.655	1.810	1.793	1.983	2.138	2.293
18.832	G,KG/M2-S	1.023	1.395	1.837	2.297	2.670	3.023	3.325	3.680	
	HMAX/HST	1.224	1.345	1.517	1.690	1.879	2.034	2.241	2.448	
	HMIN/HST	1.172	1.207	1.293	1.448	1.586	1.793	1.828	1.966	
	HAVG/HST	1.198	1.276	1.405	1.569	1.733	1.914	2.034	2.207	
23.540	G,KG/M2-S	1.405	1.740	2.261	2.609	2.942	3.299	3.684		
	HMAX/HST	1.379	1.569	1.759	2.017	2.241	2.328	2.448		
	HMIN/HST	1.259	1.345	1.517	1.655	1.759	1.879	2.069		
	HAVG/HST	1.319	1.457	1.638	1.836	2.000	2.103	2.259		

PACKING SIZE = 0.025 M
STATIC BED HEIGHT = 0.44 M

L,KG/M2-S										
4.708	G,KG/M2-S	2.210	2.580	3.130	3.580	4.120				
	HMAX/HST	1.500	1.715	2.030	2.365	2.880				
	HMIN/HST	1.220	1.385	1.630	1.715	1.920				
	HAVG/HST	1.360	1.550	1.830	2.040	2.400				
9.416	G,KG/M2-S	2.310	2.890	3.370	3.900	4.556	4.800			
	HMAX/HST	1.590	1.940	2.190	2.575	2.893	3.099			
	HMIN/HST	1.390	1.540	1.710	1.945	2.187	2.407			
	HAVG/HST	1.490	1.740	1.950	2.260	2.540	2.753			
14.124	G,KG/M2-S	1.154	1.538	2.063	2.535	2.539	2.915	3.271	3.615	3.650
	HMAX/HST	1.205	1.395	1.818	2.000	2.068	2.295	2.523	2.841	2.751
	HMIN/HST	1.148	1.213	1.364	1.600	1.432	1.568	1.705	1.818	1.989
	HAVG/HST	1.176	1.304	1.591	1.800	1.750	1.932	2.114	2.330	2.370
	G,KG/M2-S	4.140	4.590							
	HMAX/HST	2.920	3.230							
	HMIN/HST	2.200	2.450							
	HAVG/HST	2.560	2.840							
18.832	G,KG/M2-S	1.153	1.557	1.970	2.109	2.570	2.914	3.100	3.258	3.600
	HMAX/HST	1.227	1.455	1.670	1.705	2.030	2.159	2.180	2.295	2.477
	HMIN/HST	1.193	1.295	1.490	1.364	1.630	1.659	1.860	1.727	1.923
	HAVG/HST	1.210	1.375	1.580	1.534	1.830	1.909	2.022	2.011	2.200
23.540	G,KG/M2-S	0.695	0.878	1.417	1.967	2.417	2.847	3.209		
	HMAX/HST	1.000	1.205	1.409	1.682	1.886	2.068	2.295		
	HMIN/HST	1.000	1.114	1.273	1.409	1.500	1.659	1.818		
	HAVG/HST	1.000	1.159	1.341	1.545	1.693	1.864	2.057		

PACKING SIZE = 0.019 M
STATIC BED HEIGHT = 0.29 M

L,KG/M2-S

4.708	G,KG/M2-S	1.124	1.355	1.719	2.160	2.180	3.180	3.700	4.200	4.670
	HMAX/HST	1.000	1.121	1.241	1.475	1.546	1.700	1.873	2.080	2.310
	HMIN/HST	1.000	1.121	1.241	1.225	1.254	1.460	1.631	1.860	2.050
	HAVG/HST	1.000	1.121	1.241	1.350	1.400	1.580	1.752	1.970	2.180
	G,KG/M2-S	5.140								
	HMAX/HST	2.980								
	HMIN/HST	2.300								
	HAVG/HST	2.640								
9.416	G,KG/M2-S	0.950	1.189	1.621	2.300	2.740	3.260	3.770	4.310	4.780
	HMAX/HST	1.000	1.172	1.448	1.667	1.798	1.850	2.050	2.257	2.670
	HMIN/HST	1.000	1.172	1.207	1.333	1.444	1.650	1.730	1.923	2.170
	HAVG/HST	1.000	1.172	1.328	1.500	1.621	1.750	1.890	2.090	2.420
	G,KG/M2-S	5.270								
	HMAX/HST	3.160								
	HMIN/HST	2.600								
	HAVG/HST	2.880								
14.124	G,KG/M2-S	1.190	1.655	1.880	2.204	2.589	2.953	3.293	3.628	3.980
	HMAX/HST	1.224	1.483	1.540	1.655	1.793	1.966	2.138	2.379	2.379
	HMIN/HST	1.224	1.276	1.340	1.379	1.517	1.621	1.862	2.000	2.172
	HAVG/HST	1.224	1.379	1.440	1.517	1.655	1.793	2.000	2.190	2.276
18.832	G,KG/M2-S	0.679	0.849	1.267	1.823	2.180	2.273	2.656	2.840	2.983
	HMAX/HST	1.103	1.207	1.379	1.552	1.680	1.724	1.828	1.880	1.966
	HMIN/HST	1.103	1.207	1.241	1.310	1.500	1.483	1.690	1.740	1.828
	HAVG/HST	1.103	1.207	1.310	1.431	1.590	1.603	1.759	1.810	1.897
	G,KG/M2-S	3.310	3.420	3.648	4.050	4.560				
	HMAX/HST	2.103	2.105	2.276	2.260	2.580				
	HMIN/HST	1.931	1.855	2.103	2.060	2.340				
	HAVG/HST	2.017	1.980	2.190	2.160	2.460				
23.540	G,KG/M2-S	0.906	1.362	1.860	2.330	2.673	3.011	3.371	3.701	4.033
	HMAX/HST	1.345	1.517	1.672	1.966	2.000	2.069	2.276	2.448	2.621
	HMIN/HST	1.276	1.310	1.414	1.690	1.724	1.897	2.000	2.207	2.414
	HAVG/HST	1.310	1.414	1.543	1.828	1.862	1.983	2.138	2.328	2.517

PACKING SIZE = 0.019 M
STATIC BED HEIGHT = 0.44 M

L,KG/M2-S										
4.708	G,KG/M2-S	1.890	1.990	2.540	3.030	3.620	4.230	4.690	5.150	
	HMAX/HST	1.230	1.245	1.650	1.950	2.200	2.525	2.583	2.891	
	HMIN/HST	1.110	1.115	1.210	1.350	1.480	1.515	1.821	2.129	
	HAVG/HST	1.170	1.180	1.430	1.650	1.840	2.020	2.202	2.510	
9.416	G,KG/M2-S	1.840	2.490	3.050	3.570	4.140	4.650			
	HMAX/HST	1.360	1.790	2.113	2.220	2.430	2.690			
	HMIN/HST	1.180	1.290	1.449	1.620	1.890	2.130			
	HAVG/HST	1.270	1.540	1.781	1.920	2.160	2.410			
14.124	G,KG/M2-S	0.796	0.872	0.970	1.334	1.440	1.942	2.040	2.427	2.670
	HMAX/HST	1.057	1.182	1.091	1.386	1.360	1.841	1.850	2.023	2.080
	HMIN/HST	1.057	1.136	1.091	1.227	1.260	1.250	1.370	1.386	1.480
	HAVG/HST	1.057	1.159	1.091	1.307	1.310	1.545	1.610	1.705	1.880
	G,KG/M2-S	2.857	2.954	3.210	3.609	3.700	3.928	4.250	4.700	
	HMAX/HST	2.091	2.409	2.240	2.545	2.477	2.727	2.690	2.990	
	HMIN/HST	1.545	1.659	1.780	1.841	1.923	2.068	2.130	2.370	
	HAVG/HST	1.818	2.034	2.010	2.193	2.200	2.398	2.410	2.680	
18.832	G,KG/M2-S	0.604	0.631	0.760	0.942	1.220	1.566	1.980	2.180	2.636
	HMAX/HST	1.000	1.068	1.100	1.295	1.397	1.477	1.942	1.682	1.864
	HMIN/HST	1.000	1.068	1.100	1.205	1.283	1.250	1.342	1.341	1.500
	HAVG/HST	1.000	1.068	1.100	1.250	1.340	1.364	1.642	1.511	1.682
	G,KG/M2-S	2.660	3.054	3.280	3.441	3.788	3.850	4.320		
	HMAX/HST	2.190	2.182	2.096	2.318	2.636	2.510	2.690		
	HMIN/HST	1.570	1.636	1.722	1.795	2.045	2.110	2.270		
	HAVG/HST	1.880	1.909	1.909	2.057	2.341	2.310	2.480		
23.540	G,KG/M2-S	0.717	1.114	1.795	2.324	2.803	3.154	3.568	3.876	
	HMAX/HST	1.136	1.409	1.750	1.909	2.091	2.318	2.523	2.727	
	HMIN/HST	1.136	1.250	1.318	1.364	1.591	1.750	1.909	2.091	
	HAVG/HST	1.136	1.330	1.534	1.636	1.841	2.034	2.216	2.409	

APPENDIX B

Experimental results for minimum fluidization velocity

TABLE B.1. DATA FOR MINIMUM GAS FLUIDIZATION VELOCITY

determined from bed expansion data

d_{pb} m	H_{st} m	L kg/m^2-s	G_{mf} kg/m^2-s
.038	.29	4.708	1.733
.038	.29	9.4	1.383
.038	.29	14.125	1.057
.038	.29	18.83	.927
.038	.29	23.54	.845
.038	.44	4.708	1.6
.038	.44	9.41	1.287
.038	.44	14.125	1.033
.038	.44	18.83	.893
.038	.44	23.54	.8
.025	.29	4.708	1.667
.025	.29	9.41	1.313
.025	.29	14.125	.9
.025	.29	18.83	.8
.025	.29	23.54	.717
.025	.44	4.708	1.483
.025	.44	9.41	1.366
.025	.44	14.125	.923
.025	.44	18.83	.78
.025	.44	23.54	.695
.019	.29	4.708	1.124
.019	.29	9.41	.95
.019	.29	14.125	.867
.019	.29	18.83	.6
.019	.44	4.708	1.46
.019	.44	9.41	1.157
.019	.44	14.125	.667
.019	.44	18.83	.607
.019	.44	23.54	.483

TABLE B.2. DATA FOR MINIMUM GAS FLUIDIZATION VELOCITY

obtained by visual observation

d_{pb}	H_{st}	L	G_{mf}
m	m	kg/sq.m-s	kg/sq.m-s
0.038	0.29	0	2.555
0.038	0.29	4.708	1.633
0.038	0.29	4.708	1.601
0.038	0.29	4.708	1.571
0.038	0.29	9.400	1.289
0.038	0.29	9.400	1.315
0.038	0.29	14.125	1.087
0.038	0.29	14.125	1.070
0.038	0.29	18.830	1.021
0.038	0.29	18.830	0.949
0.038	0.29	18.830	1.003
0.038	0.29	18.830	0.977
0.038	0.44	0	2.76
0.038	0.44	0	2.72
0.038	0.44	4.708	1.773
0.038	0.44	4.708	1.705
0.038	0.44	9.400	1.459
0.038	0.33	9.400	1.571
0.038	0.44	14.125	1.189
0.038	0.44	14.125	1.178
0.038	0.44	14.125	1.088
0.038	0.44	18.830	0.987
0.038	0.44	18.830	0.931
0.038	0.44	23.540	0.875
0.038	0.44	23.540	0.853
0.025	0.29	0	2.345
0.025	0.29	4.708	1.627
0.025	0.29	9.400	1.358
0.025	0.29	14.125	0.931
0.025	0.29	18.830	0.830
0.025	0.44	0	2.376
0.025	0.44	0	2.397
0.025	0.44	4.708	1.506
0.025	0.44	4.708	1.495
0.025	0.44	9.400	1.119
0.025	0.44	14.125	0.829
0.025	0.44	18.830	0.737
0.019	0.29	0	2.316
0.019	0.29	0	2.296
0.019	0.29	4.708	1.437
0.019	0.29	9.400	1.055
0.019	0.29	14.125	0.761
0.019	0.29	18.830	0.629
0.019	0.44	0	2.197
0.019	0.44	0	2.473

d_{pb}	H_{st}	L	G_{mf}
m	m	kg/sq.m-s	kg/sq.m-s
0.019	0.44	0	2.416
0.019	0.44	4.708	1.341
0.019	0.44	4.708	1.390
0.019	0.44	4.708	1.262
0.019	0.44	4.708	1.303
0.019	0.44	9.400	1.103
0.019	0.44	9.400	1.087
0.019	0.44	9.400	1.070
0.019	0.44	14.125	0.829
0.019	0.44	18.830	0.594
0.019	0.44	18.830	0.567
0.019	0.440	23.540	0.410

APPENDIX C

Experimental results for pressure drop

TABLE C.1. Experimental Results for Pressure Drop

STATIC BED HEIGHT = 0.29 M
PACKING SIZE = 0.038 M

RUN.NU.	LIQUID FLOW RATE,KG/SQ.M-S	GAS FLOW RATE,KG/SQ.M-S	COLUMN PRESSURE DROP,PA
1	0.0	2.52	249.4
2	0.0	2.83	238.3
3	0.0	3.02	247.0
4	0.0	3.05	260.8
5	0.0	3.40	253.3
6	0.0	3.61	253.3
7	0.0	3.95	251.1
8	0.0	4.16	247.1
9	0.0	4.30	238.1
10	0.0	4.74	262.1
11	0.0	4.84	253.4
12	0.0	5.09	273.5
13	0.0	5.22	250.9
14	0.0	5.29	224.9
15	0.0	5.67	241.0

STATIC BED HEIGHT = 0.29 M
PACKING SIZE = 0.038 M

RUN.NU.	LIQUID FLOW RATE,KG/SQ.M-S	GAS FLOW RATE,KG/SQ.M-S	COLUMN PRESSURE DROP,PA
16	4.71	2.39	295.1
17	4.71	2.52	287.3
18	4.71	2.74	283.9
19	4.71	2.69	342.6
20	4.71	2.88	336.7
21	4.71	2.98	291.4
22	4.71	3.33	296.4
23	4.71	3.64	272.6
24	4.71	3.68	331.2
25	4.71	3.90	325.0
26	4.71	3.93	273.8
27	4.71	4.21	295.1
28	4.71	4.14	302.6
29	4.71	4.48	324.3
30	4.71	4.52	297.1
31	4.71	4.74	318.9
32	4.71	4.80	331.7
33	4.71	4.84	308.6
34	4.71	5.06	302.3
35	4.71	5.12	295.2
36	4.71	5.24	303.9
37	4.71	5.32	299.9
38	4.71	5.48	293.8

STATIC BED HEIGHT = 0.29 M
PACKING SIZE = 0.038 M

RUN.NO.	LIQUID FLOW RATE,KG/SQ.M-S	GAS FLOW RATE,KG/SQ.M-S	COLUMN PRESSURE DROP,PA
39	9.41	2.41	390.8
40	9.41	2.96	378.3
41	9.41	3.31	371.8
42	9.41	3.75	395.7
43	9.41	4.03	374.9
44	9.41	4.51	402.1
45	9.41	4.69	377.3

STATIC BED HEIGHT = 0.29 M
PACKING SIZE = 0.038 M

RUN.NO.	LIQUID FLOW RATE,KG/SQ.M-S	GAS FLOW RATE,KG/SQ.M-S	COLUMN PRESSURE DROP,PA
46	14.13	2.30	449.5
47	14.13	2.38	470.6
48	14.13	2.47	497.7
49	14.13	2.69	481.6
50	14.13	2.74	456.4
51	14.13	3.07	486.4
52	14.13	3.16	452.0
53	14.13	3.36	491.4
54	14.13	3.45	440.2
55	14.13	3.67	473.9
56	14.13	3.70	457.5
57	14.13	3.88	454.4
58	14.13	3.97	483.9
59	14.13	4.14	478.1
60	14.13	4.27	444.3
61	14.13	4.28	497.7
62	14.13	4.55	489.5
63	14.13	4.60	496.4
64	14.13	4.85	451.5
65	14.13	5.34	495.4

STATIC BED HEIGHT = 0.29 M
PACKING SIZE = 0.038 M

RUN.NO.	LIQUID FLOW RATE,KG/SQ.M-S	GAS FLOW RATE,KG/SQ.M-S	COLUMN PRESSURE DROP,PA
66	18.83	1.67	559.6
67	18.83	2.14	546.4
68	18.83	2.30	577.8
69	18.83	2.43	525.6
70	18.83	2.64	530.9
71	18.83	2.98	522.4
72	18.83	3.14	501.4
73	18.83	3.21	562.6
74	18.83	3.24	540.2
75	18.83	3.32	503.8
76	18.83	3.37	497.6
77	18.83	3.72	515.1
78	18.83	3.83	518.0
79	18.83	3.84	513.1
80	18.83	4.11	538.2
81	18.83	4.23	521.9
82	18.83	4.23	560.1
83	18.83	4.43	546.3
84	18.83	4.51	549.2
85	18.83	4.58	562.6
86	18.83	4.76	549.2
87	18.83	4.86	565.1
88	18.83	4.99	546.3
89	18.83	5.13	563.9

STATIC BED HEIGHT = 0.29 M
PACKING SIZE = 0.038 M

RUN.NO.	LIQUID FLOW RATE,KG/SQ.M-S	GAS FLOW RATE,KG/SQ.M-S	COLUMN PRESSURE DROP,PA
90	23.54	1.83	699.5
91	23.54	2.51	667.1
92	23.54	3.04	669.0
93	23.54	3.44	666.6
94	23.54	3.97	669.8
95	23.54	4.40	692.5
96	23.54	4.60	701.0
97	23.54	4.91	753.6
98	23.54	5.27	756.3

STATIC BED HEIGHT = 0.29 M
PACKING SIZE = 0.038 M

RUN.NO.	LIQUID FLOW RATE,KG/SQ.M-S	GAS FLOW RATE,KG/SQ.M-S	COLUMN PRESSURE DROP,PA
99	28.25	1.90	815.2
100	28.25	2.24	822.6
101	28.25	3.04	794.2
102	28.25	3.48	773.2
103	28.25	4.00	745.2
104	28.25	4.34	789.0
105	28.25	4.67	784.0
106	28.25	5.08	799.3

STATIC BED HEIGHT = 0.29 M
PACKING SIZE = 0.038 M

RUN.NO.	LIQUID FLOW RATE,KG/SQ.M-S	GAS FLOW RATE,KG/SQ.M-S	COLUMN PRESSURE DROP,PA
107	32.96	1.18	901.1
108	32.96	2.22	876.1
109	32.96	2.28	905.3
110	32.96	2.83	926.5
111	32.96	3.16	939.1
112	32.96	3.43	924.2
113	32.96	3.84	939.4
114	32.96	3.87	971.6
115	32.96	4.23	972.9
116	32.96	4.48	972.9
117	32.96	4.63	982.3
118	32.96	5.05	1004.4
119	32.96	5.08	1000.4

STATIC BED HEIGHT = 0.29 M
PACKING SIZE = 0.038 M

RUN.NO.	LIQUID FLOW RATE,KG/SQ.M-S	GAS FLOW RATE,KG/SQ.M-S	COLUMN PRESSURE DROP,PA
120	37.66	1.37	1046.4
121	37.66	1.92	1098.2
122	37.66	2.04	1058.6
123	37.66	2.51	1112.8
124	37.66	2.66	1144.5
125	37.66	3.23	1192.2
126	37.66	3.38	1183.8
127	37.66	3.60	1167.4
128	37.66	3.97	1192.9
129	37.66	4.06	1171.4
130	37.66	4.52	1181.3
131	37.66	4.60	1173.6
132	37.66	4.90	1139.5

STATIC BED HEIGHT = 0.44 M
PACKING SIZE = 0.038 M

RUN.NO.	LIQUID FLOW RATE,KG/SQ.M-S	GAS FLOW RATE,KG/SQ.M-S	COLUMN PRESSURE DROP,PA
133	0.0	2.31	337.7
134	0.0	2.56	388.7
135	0.0	2.78	394.3
136	0.0	3.02	397.9
137	0.0	3.25	394.6
138	0.0	3.48	387.3
139	0.0	3.76	390.1
140	0.0	3.93	389.5
141	0.0	4.27	392.6

STATIC BED HEIGHT = 0.44 M
PACKING SIZE = 0.038 M

RUN.NO.	LIQUID FLOW RATE,KG/SQ.M-S	GAS FLOW RATE,KG/SQ.M-S	COLUMN PRESSURE DROP,PA
142	4.71	1.78	451.5
143	4.71	1.94	498.3
144	4.71	2.23	491.2
145	4.71	2.24	500.9
146	4.71	2.27	523.9
147	4.71	2.31	510.3
148	4.71	2.64	474.1
149	4.71	2.73	520.6
150	4.71	2.73	518.1
151	4.71	2.74	504.5
152	4.71	2.76	543.9
153	4.71	2.91	525.3
154	4.71	2.94	518.6
155	4.71	2.99	565.2
156	4.71	3.29	517.7
157	4.71	3.32	533.7
158	4.71	3.33	541.3
159	4.71	3.41	533.1
160	4.71	3.41	546.7
161	4.71	3.45	548.1
162	4.71	3.59	572.7
163	4.71	3.69	541.1
164	4.71	3.72	542.7
165	4.71	3.78	533.9
166	4.71	3.79	580.2
167	4.71	3.93	532.0
168	4.71	3.99	530.5
169	4.71	4.03	550.3
170	4.71	4.08	570.2
171	4.71	4.25	541.6
172	4.71	4.27	524.4
173	4.71	4.40	526.3
174	4.71	4.54	518.2
175	4.71	4.62	523.7
176	4.71	4.71	527.5

STATIC BED HEIGHT = 0.44 M
PACKING SIZE = 0.038 M

RUN.NU.	LIQUID FLOW RATE,KG/SQ.M-S	GAS FLOW RATE,KG/SQ.M-S	COLUMN PRESSURE DROP,PA
177	9.41	2.20	645.2
178	9.41	2.47	611.6
179	9.41	2.56	656.5
180	9.41	2.58	623.4
181	9.41	2.72	634.6
182	9.41	2.92	665.2
183	9.41	3.07	607.2
184	9.41	3.24	644.0
185	9.41	3.44	634.1
186	9.41	3.53	681.5
187	9.41	3.70	604.3
188	9.41	3.82	657.7
189	9.41	4.03	609.0
190	9.41	4.18	672.7
191	9.41	4.32	669.0
192	9.41	4.37	607.6
193	9.41	4.43	612.9
194	9.41	4.59	610.9

STATIC BED HEIGHT = 0.44 M
PACKING SIZE = 0.038 M

RUN.NU.	LIQUID FLOW RATE,KG/SQ.M-S	GAS FLOW RATE,KG/SQ.M-S	COLUMN PRESSURE DROP,PA
195	14.13	1.65	697.2
196	14.13	2.10	711.1
197	14.13	2.26	760.3
198	14.13	2.48	720.3
199	14.13	2.61	755.3
200	14.13	2.88	775.3
201	14.13	2.90	699.4
202	14.13	3.21	791.5
203	14.13	3.37	714.2
204	14.13	3.51	762.8
205	14.13	3.66	673.6
206	14.13	3.76	780.3
207	14.13	4.05	712.6
208	14.13	4.10	762.8
209	14.13	4.36	721.7
210	14.13	4.39	774.0
211	14.13	4.66	722.9
212	14.13	4.66	724.1

STATIC BED HEIGHT = 0.44 M
PACKING SIZE = 0.038 M

RUN.NU.	LIQUID FLOW RATE,KG/SQ.M-S	GAS FLOW RATE,KG/SQ.M-S	COLUMN PRESSURE DROP,PA
213	18.83	1.51	943.6
214	18.83	1.77	872.3
215	18.83	2.15	847.8
216	18.83	2.23	878.0
217	18.83	2.47	841.6
218	18.83	2.74	876.9
219	18.83	2.79	847.8
220	18.83	3.11	896.6
221	18.83	3.12	845.3
222	18.83	3.42	857.8
223	18.83	3.44	886.3
224	18.83	3.77	819.0
225	18.83	3.78	918.2
226	18.83	4.02	927.1
227	18.83	4.07	844.1
228	18.83	4.29	961.5
229	18.83	4.37	847.8
230	18.83	4.48	850.3
231	18.83	4.62	911.1
232	18.83	4.72	952.1

STATIC BED HEIGHT = 0.44 M
PACKING SIZE = 0.038 M

RUN.NU.	LIQUID FLOW RATE,KG/SQ.M-S	GAS FLOW RATE,KG/SQ.M-S	COLUMN PRESSURE DROP,PA
233	23.54	1.74	980.4
234	23.54	2.18	995.4
235	23.54	2.55	943.2
236	23.54	2.61	965.3
237	23.54	2.91	925.3
238	23.54	3.23	941.6
239	23.54	3.47	931.9
240	23.54	3.62	870.3
241	23.54	3.78	979.9
242	23.54	3.82	967.9
243	23.54	4.06	976.0
244	23.54	4.14	969.5
245	23.54	4.37	1037.0
246	23.54	4.46	977.9
247	23.54	4.51	1063.0
248	23.54	4.70	979.1
249	23.54	4.71	1034.4

STATIC BED HEIGHT = 0.29 M
PACKING SIZE = 0.025 M

RUN.NO.	LIQUID FLOW RATE,KG/SQ.M-S	GAS FLOW RATE,KG/SQ.M-S	COLUMN PRESSURE DROP,PA
250	4.71	1.58	383.9
251	4.71	1.90	385.1
252	4.71	2.31	386.4
253	4.71	2.76	402.6
254	4.71	3.04	390.1
255	4.71	3.54	362.6
256	4.71	3.90	353.9
257	4.71	4.32	337.6
258	4.71	4.72	355.1
259	4.71	5.08	363.9
260	4.71	5.42	345.1

STATIC BED HEIGHT = 0.29 M
PACKING SIZE = 0.025 M

RUN.NO.	LIQUID FLOW RATE,KG/SC.M-S	GAS FLOW RATE,KG/SQ.M-S	COLUMN PRESSURE DROP,PA
261	9.41	1.83	482.7
262	9.41	2.24	517.7
263	9.41	2.62	515.8
264	9.41	3.11	540.2
265	9.41	3.53	510.2
266	9.41	3.90	522.7
267	9.41	4.31	519.6
268	9.41	4.66	525.2
269	9.41	5.02	542.7
270	9.41	5.30	532.7
271	9.41	5.63	532.7

STATIC BED HEIGHT = 0.29 M
PACKING SIZE = 0.025 M

RUN.NO.	LIQUID FLOW RATE,KG/SQ.M-S	GAS FLOW RATE,KG/SQ.M-S	COLUMN PRESSURE DROP,PA
272	14.12	1.94	604.0
273	14.12	2.34	597.7
274	14.12	2.77	597.7
275	14.12	3.28	577.7
276	14.12	3.74	571.4
277	14.12	4.08	573.9
278	14.12	4.45	592.1
279	14.12	4.84	561.7
280	14.12	5.16	563.9
281	14.12	5.44	612.7

STATIC BED HEIGHT = 0.29 M
PACKING SIZE = 0.025 M

RUN.NO.	LIQUID FLOW RATE,KG/SQ.M-S	GAS FLOW RATE,KG/SQ.M-S	COLUMN PRESSURE DROP,PA
282	18.83	1.51	697.8
283	18.83	1.94	676.5
284	18.83	2.57	637.7
285	18.83	3.05	642.7
286	18.83	3.45	651.5
287	18.83	3.86	640.2
288	18.83	4.26	652.0
289	18.83	4.65	635.2
290	18.83	5.03	626.4

STATIC BED HEIGHT = 0.29 M
PACKING SIZE = 0.025 M

RUN.NO.	LIQUID FLOW RATE,KG/SQ.M-S	GAS FLOW RATE,KG/SQ.M-S	COLUMN PRESSURE DROP,PA
291	23.53	2.02	760.3
292	23.53	2.48	737.8
293	23.53	2.96	709.0
294	23.53	3.35	701.5
295	23.53	3.81	710.2
296	23.53	4.11	700.2
297	23.53	4.53	702.7

STATIC BED HEIGHT = 0.44 M
PACKING SIZE = 0.025 M

RUN.NO.	LIQUID FLOW RATE,KG/SQ.M-S	GAS FLOW RATE,KG/SQ.M-S	COLUMN PRESSURE DROP,PA
298	4.71	1.77	647.4
299	4.71	2.20	656.6
300	4.71	2.67	638.1
301	4.71	2.96	631.1
302	4.71	3.28	639.7
303	4.71	3.59	620.7
304	4.71	3.88	628.2
305	4.71	4.11	616.2
306	4.71	4.42	628.1

STATIC BED HEIGHT = 0.44 M
PACKING SIZE = 0.025 M

RUN.NO.	LIQUID FLOW RATE,KG/SQ.M-S	GAS FLOW RATE,KG/SQ.M-S	COLUMN PRESSURE DROP,PA
307	9.41	1.58	777.4
308	9.41	1.91	822.3
309	9.41	2.31	829.7
310	9.41	2.65	813.1
311	9.41	2.96	810.0
312	9.41	3.28	803.3
313	9.41	3.61	786.9
314	9.41	3.89	797.5
315	9.41	4.20	819.9
316	9.41	4.47	814.4

STATIC BED HEIGHT = 0.44 M
PACKING SIZE = 0.025 M

RUN.NO.	LIQUID FLOW RATE,KG/SQ.M-S	GAS FLOW RATE,KG/SQ.M-S	COLUMN PRESSURE DROP,PA
317	14.12	1.82	918.3
318	14.12	2.05	895.5
319	14.12	2.58	909.5
320	14.12	2.89	883.9
321	14.12	3.27	879.4
322	14.12	3.55	854.8
323	14.12	3.94	910.0
324	14.12	4.22	887.2
325	14.12	4.41	893.3
326	14.12	4.76	884.8

STATIC BED HEIGHT = 0.44 M
PACKING SIZE = 0.025 M

RUN.NO.	LIQUID FLOW RATE,KG/SQ.M-S	GAS FLOW RATE,KG/SQ.M-S	COLUMN PRESSURE DROP,PA
327	18.83	1.42	1007.6
328	18.83	1.96	973.6
329	18.83	2.40	978.5
330	18.83	2.67	959.7
331	18.83	3.05	948.6
332	18.83	3.37	957.0
333	18.83	3.74	941.0
334	18.83	4.03	934.1
335	18.83	4.36	955.3
336	18.83	4.64	969.0

STATIC BED HEIGHT = 0.44 M
PACKING SIZE = 0.025 M

RUN.NO.	LIQUID FLOW RATE,KG/SQ.M-S	GAS FLOW RATE,KG/SQ.M-S	COLUMN PRESSURE DROP,PA
337	23.53	1.03	1100.4
338	23.53	1.42	1114.2
339	23.53	1.87	1077.9
340	23.53	2.36	1094.8
341	23.53	2.73	1057.9
342	23.53	3.07	1063.6
343	23.53	3.38	1072.0
344	23.53	3.74	1078.2
345	23.53	4.02	1026.0
346	23.53	4.31	1037.9

STATIC BED HEIGHT = 0.29 M
PACKING SIZE = 0.019 M

RUN.NO.	LIQUID FLOW RATE,KG/SQ.M-S	GAS FLOW RATE,KG/SQ.M-S	COLUMN PRESSURE DROP,PA
347	4.71	1.82	504.8
348	4.71	2.19	512.7
349	4.71	2.34	537.1
350	4.71	2.55	522.9
351	4.71	2.76	532.9
352	4.71	2.92	561.6
353	4.71	3.02	537.7
354	4.71	3.21	545.2
355	4.71	3.34	516.9
356	4.71	3.53	532.2
357	4.71	3.66	522.8
358	4.71	3.90	528.2
359	4.71	4.25	502.8
360	4.71	4.30	532.9
361	4.71	4.65	510.9
362	4.71	4.97	538.1
363	4.71	5.55	542.7
364	4.71	5.66	525.1

STATIC BED HEIGHT = 0.29 M
PACKING SIZE = 0.019 M

RUN.NU.	LIQUID FLOW RATE,KG/SQ.M-S	GAS FLOW RATE,KG/SQ.M-S	COLUMN PRESSURE DROP,PA
365	9.41	2.02	660.2
366	9.41	2.26	669.6
367	9.41	2.73	661.1
368	9.41	3.08	662.2
369	9.41	3.15	642.7
370	9.41	3.48	663.2
371	9.41	3.50	686.0
372	9.41	3.84	668.0
373	9.41	4.24	675.1
374	9.41	4.63	691.5
375	9.41	4.96	681.5
376	9.41	5.28	663.2
377	9.41	5.58	687.0

STATIC BED HEIGHT = 0.29 M
PACKING SIZE = 0.019 M

RUN.NU.	LIQUID FLOW RATE,KG/SQ.M-S	GAS FLOW RATE,KG/SQ.M-S	COLUMN PRESSURE DROP,PA
378	14.12	1.48	758.8
379	14.12	1.86	745.0
380	14.12	2.18	751.2
381	14.12	2.69	703.5
382	14.12	2.77	760.3
383	14.12	3.18	716.6
384	14.12	3.63	720.6
385	14.12	3.98	702.6
386	14.12	4.31	711.5
387	14.12	4.67	714.9
388	14.12	4.97	726.6
389	14.12	5.35	733.3

STATIC BED HEIGHT = 0.29 M
PACKING SIZE = 0.019 M

RUN.NU.	LIQUID FLOW RATE,KG/SQ.M-S	GAS FLOW RATE,KG/SQ.M-S	COLUMN PRESSURE DROP,PA
390	18.83	1.55	828.6
391	18.83	1.99	825.7
392	18.83	2.47	805.6
393	18.83	2.82	837.8
394	18.83	3.26	789.5
395	18.83	3.65	809.4
396	18.83	4.07	786.5
397	18.83	4.44	805.7
398	18.83	4.77	813.9
399	18.83	5.09	810.3

STATIC BED HEIGHT = 0.29 M
PACKING SIZE = 0.019 M

RUN.NO.	LIQUID FLOW RATE,KG/SQ.M-S	GAS FLOW RATE,KG/SQ.M-S	COLUMN PRESSURE DROP,PA
400	23.53	1.98	962.1
401	23.53	2.50	942.9
402	23.53	2.88	935.3
403	23.53	3.00	945.1
404	23.53	3.25	942.8
405	23.53	3.58	955.5
406	23.53	3.66	931.8
407	23.53	3.69	944.7
408	23.53	4.05	930.3
409	23.53	4.06	924.1
410	23.53	4.37	935.5
411	23.53	4.40	930.3
412	23.53	4.69	938.5
413	23.53	4.72	953.3
414	23.53	5.06	939.1

STATIC BED HEIGHT = 0.44 M
PACKING SIZE = 0.019 M

RUN.NO.	LIQUID FLOW RATE,KG/SQ.M-S	GAS FLOW RATE,KG/SQ.M-S	COLUMN PRESSURE DROP,PA
415	4.71	2.04	800.3
416	4.71	2.11	820.3
417	4.71	2.36	817.5
418	4.71	2.49	885.3
419	4.71	2.75	820.9
420	4.71	2.83	826.5
421	4.71	3.03	831.9
422	4.71	3.21	829.1
423	4.71	3.39	806.8
424	4.71	3.51	826.5
425	4.71	3.67	811.2
426	4.71	3.82	813.4
427	4.71	4.00	800.8
428	4.71	4.16	808.4
429	4.71	4.31	825.9
430	4.71	4.47	812.5
431	4.71	4.61	796.0
432	4.71	4.70	821.5
433	4.71	4.84	808.4

STATIC BED HEIGHT = 0.44 M
PACKING SIZE = 0.019 M

RUN.NO.	LIQUID FLOW RATE,KG/SQ.M-S	GAS FLOW RATE,KG/SQ.M-S	COLUMN PRESSURE DROP,PA
434	9.41	1.75	1068.7
435	9.41	2.23	1048.9
436	9.41	2.25	1038.5
437	9.41	2.63	1075.3
438	9.41	2.64	1016.7
439	9.41	2.91	1017.0
440	9.41	2.93	1076.5
441	9.41	3.24	1035.1
442	9.41	3.28	1071.3
443	9.41	3.58	1006.0
444	9.41	3.58	1053.5
445	9.41	3.85	1047.5
446	9.41	3.95	1021.9
447	9.41	4.18	1022.2
448	9.41	4.22	1050.2
449	9.41	4.46	1030.1
450	9.41	4.58	1006.1
451	9.41	4.74	1048.9
452	9.41	5.03	1029.9
453	9.41	5.27	1031.7

STATIC BED HEIGHT = 0.44 M
PACKING SIZE = 0.019 M

RUN.NO.	LIQUID FLOW RATE,KG/SQ.M-S	GAS FLOW RATE,KG/SQ.M-S	COLUMN PRESSURE DROP,PA
454	14.12	1.61	1152.3
455	14.12	1.83	1122.3
456	14.12	2.15	1136.8
457	14.12	2.31	1158.5
458	14.12	2.52	1116.5
459	14.12	2.75	1149.4
460	14.12	2.90	1137.4
461	14.12	3.10	1088.3
462	14.12	3.15	1114.8
463	14.12	3.38	1145.1
464	14.12	3.50	1108.8
465	14.12	3.77	1091.6
466	14.12	3.80	1115.0
467	14.12	4.13	1119.8
468	14.12	4.36	1139.2
469	14.12	4.64	1128.0
470	14.12	4.92	1104.1
471	14.12	5.18	1106.1

STATIC BED HEIGHT = 0.44 M
PACKING SIZE = 0.019 M

RUN.NO.	LIQUID FLOW RATE,KG/SQ.M-S	GAS FLOW RATE,KG/SQ.M-S	COLUMN PRESSURE DROP,PA
472	18.83	1.91	1236.7
473	18.83	2.08	1221.7
474	18.83	2.30	1227.5
475	18.83	2.52	1212.6
476	18.83	2.69	1230.7
477	18.83	2.96	1203.8
478	18.83	3.28	1216.6
479	18.83	3.62	1248.7
480	18.83	3.91	1224.6
481	18.83	4.20	1203.6
482	18.83	4.47	1199.6
483	18.83	4.71	1215.6
484	18.83	4.96	1191.1
485	18.83	5.23	1228.1

STATIC BED HEIGHT = 0.44 M
PACKING SIZE = 0.019 M

RUN.NO.	LIQUID FLOW RATE,KG/SQ.M-S	GAS FLOW RATE,KG/SQ.M-S	COLUMN PRESSURE DROP,PA
486	23.53	1.55	1349.1
487	23.53	2.30	1363.1
488	23.53	2.52	1403.0
489	23.53	2.73	1366.1
490	23.53	2.78	1364.4
491	23.53	3.07	1371.0
492	23.53	3.09	1328.5
493	23.53	3.38	1306.3
494	23.53	3.43	1373.0
495	23.53	3.75	1357.6
496	23.53	4.03	1342.0
497	23.53	4.32	1337.9
498	23.53	4.58	1333.2
499	23.53	4.92	1308.8
500	23.53	5.20	1343.9

APPENDIX D

Experimental Results for Particulate Recovery in MBC

Listing of Program Used to Calculate Penetration without Diffusiophoresis:

```
C
C       NOMENCLATURE
C
C       CSAUC : CROSS-SECTIONAL AREA OF THE COLUMN , M2.
C       DELTA : STIRRING NUMBER
C       EG    : GAS VOIDAGE, M3/M3.
C       EPBST : VOLUME FRACTION OF PACKING AT STATIC CONDITION , M3/M3.
C       G     : GAS MASS FLUX, KG/M2-S.
C       GMF   : GAS MINIMUM FLUIDIZATION VELOCITY, KG/M2-S.
C       H     : EXPANDED BED HEIGHT, M.
C       HLH   : LIQUID HOLD-UP, M3 WATER/M3 OF EXPANDED BED VOLUME.
C       HLHST : LIQUID HOLD-UP, M3 WATER/M3 OF STATIC BED VOLUME.
C       HST   : STATIC BED HEIGHT, M.
C       HUM   : HUMIDITY, KG WATER VAPOR/KG AIR.
C       KPSC  = PARTICLE TRANSFER COEFF. FOR SPRAY COLUMN, 1/S
C       L     : LIQUID MASS FLUX, KG/M2-S.
C       DP    : PARTICLE DIAMETER, MICRON.
C       DPB   : PACKING BALL DIAMETER, M2.
C       PN    : PARTICLE CONCENTRATION, #/M3
C       PSTAT : STATIC GAS PRESSURE AT INLET
C       PT    : PENETRATION.
C       PTC   : PARTICLE TRANSFER COEFFICIENT, 1/S.
C       QG    : VOLUMETRIC GAS FLOW RATE, FT3/S.
C       QGSI  : VOLUMETRIC GAS FLOW RATE, M3/S
C       REG   : GAS REYNOLDS NUMBER.
C       REL   : LIQUID REYNOLDS NUMBER.
C       ROGIN : GAS DENSITY AT INLET, KG/M3.
C       ROGOUT: GAS DENSITY AT OUTLET, KG/M3.
C       ROL   : WATER DENSITY, KG/M3.
C       ROP   : PARTICLE DENSITY, KG/M3.
C       ST    : STOKE,S NUMBER
C       TDB   : DRY-BULB GAS TEMPERATURE , F.
C       TWB   : WET-BULB GAS TEMPERATURE, F.
C       TL    : LIQUID TEMPERATURE, F.
C       UGO   : SUPERFICIAL GAS VELOCITY , M/S.
C       UGI   : INTERSTITIAL GAS VELOCITY, M/S.
C       ULO   : SUPERFICIAL LIQUID VELOCITY, M/S.
C       ULI   : INTERSTITIAL LIQUID VELOCITY , M/S.
C       UR    : RELATIVE VELOCITY, M/S.
C       VISCG : VISCOSITY OF GAS, KG/M-S, PA-S.
C       VISCL : VISCOSITY OF WATER, KG/M-S, PA-S.
C
0001          DIMENSION X(6),Y(6)
0002          REAL L
0003          READ(5,9) ROP
0004      9   FORMAT(F10.0)
0005          READ(5,10) CSAUC,EPBST,ROL
0006      10  FORMAT(3F10.0)
0007          READ(5,11) (X(I),I=1,6)
0008      11  FORMAT(6F10.0)
0009          READ(5,12) (Y(I),I=1,6)
0010      12  FORMAT(6E10.8)
0011      79  READ(5,17,END=80)DPB,HST
0012      17  FORMAT(2F10.0)
```

```
0013                    WRITE(6,51) DPB,HST
0014            51      FORMAT(1H1,/,5X,'PACKING SIZE =',F6.4,1X,'M',10X,'STATIC BED HEIGH
                       1T =',F5.3,1X,'M',//)
0015                    WRITE(6,52)
0016            52      FORMAT(7X,'G,KG/SQ.M-S',8X,'L,KG/SQ.M-S',6X,'REGAS',10X,'RELIQ',7X
                       1,'DP,MICRON',6X,'PT',8X,'ST',8X,'PTC,1/S',8X,'THEO.PT',///)
0017                    READ(5,15) NRUN
0018            15      FORMAT(I2)
0019                    LINE=0
0020                    DO 70 IN=1,NRUN
0021                    READ(5,18)USGPM
0022            18      FORMAT(F10.0)
0023                    READ(5,19)DPOR,PS1,TDBIN,TWBIN,TDBOUT,TWBOUT,TLIN,TLOUT
0024            19      FORMAT(8F10.0)
                C       CALCULATION OF GAS FLOW RATE
0025                    PSTAT=406.+PS1/2.54
0026                    HUMIN=HUMID(TDBIN,TWBIN)
0027                    HUMOUT=HUMID(TDBOUT,TWBOUT)
0028                    ROG=1.75635*(1.+HUMIN)*PSTAT/((18.+29.*HUMIN)*(460.+TDBIN))
0029                    ROGSI=ROG*16.03
0030                    QG=.9858865*(1.-.32*DPOR/PS1)*(DPOR/ROG)**.5
0031                    GGSI=QG*.3048**3.
0032                    GIN=QG*ROG*.454/CSAOC
0033                    GOUT=GIN*(1.+HUMOUT)/(1.+HUMIN)
0034                    G=(GIN-GOUT)/ALOG(GIN/GOUT)
                C       CALCULATION OF LIQUID FLOW RATE
0035                    L=.9416*USGPM
                C       CALCULATION OF MINIMUM GAS FLUIDIZATION VELOCITY
0036                    GMF=10.86*DPB**.488*10.**(-.01985*L)
                C       CALCULATION OF THE BED HEIGHT
0037                    DELTA=(G-GMF)/GMF
0038                    HCOR=.14681*DELTA*GMF/HST
0039                    H=(1.+HCOR)*HST
                C       CALCULATION OF LIQUID HOLD-UP
0040                    HLHST=1.15E-04*L**.826*DPB**(-1.289)
0041                    HLH=HLHST*HST/H
                C       CALCULATION OF GAS AND LIQUID VELOCITIES
0042                    ROGIN=ROGSI
0043                    DELPC=112.17*L**.44*DPB**(-.492)*HST
0044                    DELPC=DELPC*2.54/248.84
0045                    PSTOUT=PSTAT-DELPC
0046                    ROGOUT=1.75635*(1.+HUMOUT)*PSTOUT/((18.+29.*HUMOUT)*(460.+TDBOUT))
0047                    ROGOUT=ROGOUT*16.03
0048                    ROG=(ROGIN+ROGOUT)/2.
0049                    UGIN=GIN/ROGIN
0050                    UGOUT=GOUT/ROGOUT
0051                    UGJ=(UGIN+UGOUT)/2.
0052                    EPB=CPBST*HST/H
0053                    EG=1.-HLH-EPB
0054                    UGI=UGJ/EG
0055                    ULJ=(L+((GIN-GOUT)/2.))/ROL
0056                    ULI=ULJ/HLH
0057                    UR=UGI+ULI
                C       CALCULATION OF WATER VISCOSITY
```

```
0058                  TL=(TLIN+TLOUT)/2.
0059                  TLC=((TL-32.)/1.8)-8.435
0060                  RECV=2.1482*(TLC+(8078.4+(ABS(TLC))**2.)**.5)-120.
0061                  VISCL=1./(10.*RECV)
                C     CALCULATION OF GAS VISCOSITY
0062                  TG=(TDBIN+TDBOUT)/2.
0063                  VISCG=FLAGR(X,Y,TG,1,6)
                C     CALCULATION OF DIMENSIONLESS NUMBERS
0064                  REG=DPB*UGI*ROG/VISCG
0065                  REL=DPB*ULI*ROL/VISCL
0066                  READ(5,21)KRUN
0067            21    FORMAT(I2)
0068                  DO 70 J=1,KRUN
0069                  READ(5,20)DP,PNIN,PNOUT
0070            20    FORMAT(3F10.0)
0071                  C=1.+(2.E-08*((460.+TG)/1.8)/(DP*1.E-04))*(2.79+.894*EXP(-2.47E+07
                     1*DP*1.E-04/((460.+TG)/1.8)))
0072                  ST=C*((DP*1.E-06)**2.)*ROP*UR/(9.*VISCG*DPB)
                C     CALCULATION OF PARTICLE PENETRATION
0073                  PTTOT=PNOUT/PNIN
0074                  ULNOZ=0.32345*USGPM
0075                  URNOZ=ULNOZ+UGOUT
0076                  D30=3.35*(10*VISCG)**0.2/URNOZ
0077                  RED=D30*URNOZ*ROGOUT/VISCG
0078                  CDRAG=18.5/RED**0.6
0079                  IF(RED.LT.2.) CDRAG=24./RED
0080                  IF(RED.GE.500.) CDRAG=0.44
0081                  UTERMG=(RED/CDRAG*13.076*VISCG*(1000.-ROGOUT)/ROGOUT**2.)**(1./3.)
0082                  STD=C*((DP*1.E-06)**2.)*ROP*UTERMG/(9.*VISCG*D30)
0083                  KPSC=0.0165*L**1.508*G**0.745*STD**(-0.413)
0084                  PTSC=EXP(-1*KPSC*(1.5-H)/UGOUT)
0085                  PT=PTTOT/PTSC
                C     CALCULATION OF PARTICLE TRANSFER COEFFICIENT
0086                  IF(PT.EQ.0.) GO TO 75
0087                  PTLN=ALOG(PT)
0088                  PTC=-(PTLN*UGO/H)
                C     OUTPUT OF THE CALCULATED RESULTS
0089            75    CONTINUE
0090                  PTCTH=3764.762285*ST**.80477*REG**(-2.64264)*REL**2.10754*(HST/DPB
                     1)**1.52217
0091                  PTTHEO=EXP(-PTCTH*H/UGO)
0092                  WRITE(6,53)G,L,REG,REL,DP,PT,ST,PTC,PTTHEO
0093            53    FORMAT(9X,F6.3,12X,F6.3,8X,F8.2,5X,F10.2,8X,F5.2,6X,F6.4,3X,E10.4,
                     43X,F7.3,8X,F6.4,/)
0094                  LINE=LINE+1
0095                  IF(LINE.LT.27) GO TO 70
0096                  WRITE(6,54) DPB,HST
0097            54    FORMAT('1H1,/,5X,'PACKING SIZE =',F6.4,1X,'M',10X,'STATIC BED HEIGH
                     1T =',F5.3,1X,'M',5X,'(CONTINUED)',//)
0098                  WRITE(6,52)
0099                  LINE=0
0100            70    CONTINUE
0101                  GO TO 79
0102            80    STOP
0103                  END
```

```
0001                FUNCTION FLAGR(X,Y,XARG,IDEG,N)
                C   FLAGR USES THE LAGRANGE FORMULA TO EVALUATE THE INTERPOLATING
                C   POLYNOMIAL OF DEGREE IDEG, FOR ARGUMENT XARG, USING THE DATA
                C   VALUES X(1),....,X(N) AND Y(1),....,Y(N). THE DATA X(1),....,X(N)
                C   IS ASSUMED TO BE IN ASCENDING ORDER BUT NOT NECESSARILY EVENLY
                C   SPACED.
0002                DIMENSION X(N),Y(N)
0003                N1=IDEG+1
0004                DO 11 MAX=N1,N
0005                IF(XARG.LT.X(MAX)) GO TO 12
0006             11 CONTINUE
0007                MAX=N
0008             12 MIN=MAX-IDEG
0009                FACTOR=1.
0010                DO 2 I=MIN,MAX
0011                IF(XARG.NE.X(I)) GO TO 2
0012                FLAGR=Y(I)
0013                RETURN
0014              2 FACTOR=FACTOR*(XARG-X(I))
0015                YEST=0.
0016                DO 5 I=MIN,MAX
0017                TERM=Y(I)*FACTOR/(XARG-X(I))
0018                DO 4 J=MIN,MAX
0019              4 IF(I.NE.J) TERM=TERM/(X(I)-X(J))
0020              5 YEST=YEST+TERM
0021                FLAGR=YEST
0022                RETURN
0023                END


0001                FUNCTION HUMID(TDB,TWB)
0002                WBLTHT=1093.4-.55*TWB
0003                PSAT=4.579*EXP(55.932-12253.6/(460.+TWB)-5.0055*ALOG(460.+TWB))
0004                SATHUM=.622*(PSAT/(760.-PSAT))
0005                HUMID=SATHUM-(TDB-TWB)*.227/WBLTHT
0006                RETURN
0007                END
```

TABLE D.1. Experimental Results and Estimated Penetration of Ferrous Sulphate Particles in MBC at Conditions without Diffusiophoresis

PACKING SIZE =0.0380 M STATIC BED HEIGHT =0.290 M

G.KG/SQ.M-S	L.KG/SQ.M-S	REGAS	RELIQ	DP.MICRON	PT	ST	PTC.1/S	THEO.PT
2.309	4.708	10010.83	5085.01	2.50	0.7503	0.8892E-02	2.462	0.7172
2.309	4.708	10010.83	5085.01	3.50	0.5241	0.1713E-01	5.536	0.5694
2.309	4.708	10010.83	5085.01	4.50	0.4428	0.2804E-01	6.980	0.4328
2.309	4.708	10010.83	5085.01	5.50	0.2542	0.4162E-01	11.738	0.3164
2.324	9.416	9165.44	6439.27	2.50	0.5195	0.8176E-02	4.956	0.4817
2.324	9.416	9165.44	6439.27	3.50	0.2518	0.1575E-01	10.437	0.2900
2.324	9.416	9165.44	6439.27	4.50	0.1215	0.2578E-01	15.954	0.1588
2.324	9.416	9165.44	6439.27	5.50	0.0568	0.3827E-01	21.705	0.0797
2.346	14.124	8750.45	7534.77	2.50	0.3018	0.7808E-02	8.281	0.2974
2.346	14.124	8750.45	7534.77	3.50	0.0872	0.1504E-01	16.865	0.1280
2.346	14.124	8750.45	7534.77	4.50	0.0229	0.2462E-01	26.092	0.0471
2.346	14.124	8750.45	7534.77	5.50	0.0100	0.3654E-01	31.831	0.0150
2.364	18.832	8527.16	8432.91	1.75	0.4024	0.3829E-02	5.893	0.3713
2.364	18.832	8527.16	8432.91	2.50	0.1330	0.7617E-02	13.058	0.1785
2.364	18.832	8527.16	8432.91	3.50	0.0314	0.1467E-01	22.411	0.0539
2.364	18.832	8527.16	8432.91	4.50	0.0072	0.2402E-01	31.907	0.0130
2.364	18.832	8527.16	8432.91	5.50	0.0019	0.3565E-01	40.668	0.0026
2.382	23.540	8411.11	9206.02	2.50	0.0997	0.7517E-02	14.204	0.1070
2.382	23.540	8411.11	9206.02	3.50	0.0187	0.1448E-01	24.526	0.0227
2.382	23.540	8411.11	9206.02	4.50	0.0037	0.2370E-01	45.136	0.0036
2.382	23.540	8411.11	9206.02	5.50	0.0002	0.3519E-01	51.626	0.0004
2.742	4.708	10276.45	6026.47	2.50	0.6570	0.9188E-02	3.666	0.6395
2.742	4.708	10276.45	6026.47	3.50	0.4486	0.1773E-01	6.998	0.4688
2.742	4.708	10276.45	6026.47	4.50	0.2701	0.2896E-01	11.424	0.3242
2.742	4.708	10276.45	6026.47	5.50	0.1664	0.4300E-01	15.651	0.2127
2.767	9.416	9771.14	7448.04	2.50	0.4219	0.8750E-02	6.758	0.4251
2.767	9.416	9771.14	7448.04	3.50	0.2429	0.1685E-01	11.082	0.2346

PACKING SIZE =0.0380 M STATIC BED HEIGHT =0.290 M (CONTINUED)

G,KG/SQ.M-S	L,KG/SQ.M-S	REGAS	RELIQ	DP,MICRON	PT	ST	PTC,I/S	THEO.PT
2.767	9.416	9771.14	7448.04	4.50	0.0885	0.2759E-01	18.984	0.1159
2.767	9.416	9771.14	7448.04	5.50	0.0251	0.4095E-01	28.864	0.0517
2.792	14.124	9508.45	8626.95	2.50	0.2890	0.8526E-02	8.992	0.2654
2.792	14.124	9508.45	8626.95	3.50	0.1004	0.1642E-01	16.648	0.1056
2.792	14.124	9508.45	8626.95	4.50	0.0295	0.2688E-01	25.508	0.0353
2.792	14.124	9508.45	8626.95	5.50	0.0066	0.3990E-01	36.312	0.0101
2.822	18.832	9385.46	9600.23	1.75	0.3861	0.4233E-02	6.508	0.3545
2.822	18.832	9385.46	9600.23	2.50	0.1556	0.8421E-02	12.724	0.1647
2.822	18.832	9385.46	9600.23	3.50	0.0416	0.1622E-01	21.750	0.0471
2.822	18.832	9385.46	9600.23	4.50	0.0094	0.2655E-01	31.903	0.0106
2.822	18.832	9385.46	9600.23	5.50	0.0029	0.3941E-01	39.963	0.0019
2.853	23.540	9341.92	10477.06	2.50	0.0873	0.8388E-02	15.988	0.1020
2.853	23.540	9341.92	10477.06	3.50	0.0119	0.1616E-01	29.044	0.0209
2.853	23.540	9341.92	10477.06	4.50	0.0034	0.2644E-01	37.211	0.0032
2.853	23.540	9341.92	10477.06	5.50	0.0011	0.3926E-01	44.675	0.0004
3.105	4.708	10670.25	6948.25	2.50	0.6310	0.9609E-02	4.078	0.5722
3.105	4.708	10670.25	6948.25	3.50	0.4208	0.1850E-01	7.666	0.3883
3.105	4.708	10670.25	6948.25	4.50	0.2261	0.3029E-01	13.169	0.2450
3.105	4.708	10670.25	6948.25	5.50	0.1220	0.4496E-01	18.632	0.1448
3.144	9.416	10341.58	8509.29	2.50	0.4021	0.9326E-02	7.324	0.3680
3.144	9.416	10341.58	8509.29	3.50	0.2172	0.1796E-01	12.277	0.1838
3.144	9.416	10341.58	8509.29	4.50	0.0862	0.2940E-01	19.706	0.0806
3.144	9.416	10341.58	8509.29	5.50	0.0260	0.4364E-01	29.340	0.0314
3.144	9.416	10341.58	8509.29	5.50	0.0268	0.4364E-01	29.101	0.0314
3.163	14.124	10145.04	9680.12	2.50	0.2051	0.9169E-02	11.876	0.2323
3.163	14.124	10145.04	9680.12	3.50	0.0885	0.1766E-01	18.179	0.0843
3.163	14.124	10145.04	9680.12	4.50	0.0261	0.2890E-01	27.335	0.0253

PACKING SIZE =0.0380 M STATIC BED HEIGHT =0.290 M (CONTINUED)

G.KG/SQ.M-S	L.KG/SQ.M-S	REGAS	RELIQ	DP.MICRON	PT	ST	PTC.1/S	THEO.PT
3.163	14.124	10145.04	9680.12	5.50	0.0115	0.4290E-01	33.446	0.0064
3.193	18.832	10064.72	10667.79	1.75	0.3002	0.4582E-02	8.571	0.3323
3.193	18.832	10064.72	10667.79	1.75	0.2815	0.4582E-02	9.028	0.3323
3.193	18.832	10064.72	10667.79	1.75	0.2647	0.4582E-02	9.468	0.3323
3.193	18.832	10064.72	10667.79	2.50	0.0945	0.9113E-02	16.805	0.1472
3.193	18.832	10064.72	10667.79	3.50	0.0340	0.1755E-01	24.075	0.0389
3.193	18.832	10064.72	10667.79	4.50	0.0066	0.2873E-01	35.716	0.0080
3.193	18.832	10064.72	10667.79	4.50	0.0067	0.2873E-01	35.635	0.0080
3.193	18.832	10064.72	10667.79	5.50	0.0045	0.4264E-01	38.539	0.0013
3.268	23.540	10138.53	11660.10	2.50	0.0221	0.9171E-02	26.153	0.0940
3.268	23.540	10138.53	11660.10	3.50	0.0036	0.1766E-01	38.551	0.0182
3.268	23.540	10138.53	11660.10	4.50	0.0002	0.2891E-01	57.602	0.0026
3.268	23.540	10138.53	11660.10	5.50	0.0	0.4291E-01	5.760	0.0003
3.492	4.708	11309.00	7591.52	2.50	0.6397	0.9965E-02	3.897	0.5471
3.492	4.708	11309.00	7591.52	3.50	0.4213	0.1919E-01	7.542	0.3598
3.492	4.708	11309.00	7591.52	4.50	0.2060	0.3141E-01	13.784	0.2188
3.492	4.708	11309.00	7591.52	5.50	0.0989	0.4663E-01	20.188	0.1239
3.492	4.708	11309.00	7591.52	5.50	0.1045	0.4663E-01	19.709	0.1239
3.514	9.416	11030.29	9178.91	2.50	0.4052	0.9781E-02	7.253	0.3574
3.514	9.416	11030.29	9178.91	3.50	0.2008	0.1884E-01	12.889	0.1749
3.514	9.416	11030.29	9178.91	4.50	0.0901	0.3083E-01	19.321	0.0748
3.514	9.416	11030.29	9178.91	5.50	0.0269	0.4577E-01	29.018	0.0284
3.544	14.124	10917.75	10422.41	2.50	0.2479	0.9682E-02	10.492	0.2316
3.544	14.124	10917.75	10422.41	3.50	0.1016	0.1865E-01	17.203	0.0838
3.544	14.124	10917.75	10422.41	4.50	0.0331	0.3052E-01	25.646	0.0251
3.544	14.124	10917.75	10422.41	5.50	0.0114	0.4531E-01	33.633	0.0063
3.584	18.832	10885.45	11480.84	2.50	0.0984	0.9676E-02	16.664	0.1509

PACKING SIZE =0.0380 M STATIC BED HEIGHT =0.290 M (CONTINUED)

G,KG/SQ.M-S	L,KG/SQ.M-S	REGAS	RELIQ	DP,MICRON	PT	ST	PTC,1/S	THEO.PT
3.584	18.832	10885.45	11480.84	3.50	0.0334	0.1864E-01	24.424	0.0405
3.584	18.832	10885.45	11480.84	4.50	0.0089	0.3051E-01	33.960	0.0085
3.584	18.832	10885.45	11480.84	5.50	0.0030	0.4529E-01	41.750	0.0014
3.668	23.540	11001.83	12513.52	2.50	0.0954	0.9768E-02	16.320	0.1004
3.668	23.540	11001.83	12513.52	3.50	0.0032	0.1881E-01	39.787	0.0203
3.668	23.540	11001.83	12513.52	4.50	0.0017	0.3079E-01	44.313	0.0031
3.668	23.540	11001.83	12513.52	5.50	0.0	0.4571E-01	4.431	0.0003
3.864	4.708	11919.91	8392.84	2.50	0.6019	0.1061E-01	4.498	0.5108
3.864	4.708	11919.91	8392.84	3.50	0.4102	0.2044E-01	7.895	0.3203
3.864	4.708	11919.91	8392.84	4.50	0.1867	0.3346E-01	14.871	0.1841
3.864	4.708	11919.91	8392.84	5.50	0.0977	0.4967E-01	20.612	0.0977
3.893	9.416	11744.29	10054.86	2.50	0.3662	0.1048E-01	8.227	0.3345
3.893	9.416	11744.29	10054.86	3.50	0.1809	0.2019E-01	14.006	0.1563
3.893	9.416	11744.29	10054.86	4.50	0.0783	0.3305E-01	20.862	0.0633
3.893	9.416	11744.29	10054.86	5.50	0.0321	0.4907E-01	28.164	0.0226
3.929	14.124	11664.54	11374.41	2.50	0.2128	0.1045E-01	11.984	0.2175
3.929	14.124	11664.54	11374.41	3.50	0.0903	0.2014E-01	18.621	0.0754
3.929	14.124	11664.54	11374.41	4.50	0.0272	0.3296E-01	27.924	0.0214
3.929	14.124	11664.54	11374.41	5.50	0.0106	0.4892E-01	35.228	0.0051
3.974	18.832	11673.58	12495.37	2.50	0.1191	0.1048E-01	15.793	0.1436
3.974	18.832	11673.58	12495.37	3.50	0.0316	0.2019E-01	25.643	0.0373
3.974	18.832	11673.58	12495.37	4.50	0.0079	0.3304E-01	35.905	0.0075
3.974	18.832	11673.58	12495.37	5.50	0.0023	0.4905E-01	45.058	0.0012
4.015	23.540	11711.76	13413.05	2.50	0.0929	0.1053E-01	17.085	0.0987
4.015	23.540	11711.76	13413.05	3.50	0.0372	0.2028E-01	35.445	0.0198
4.015	23.540	11711.76	13413.05	4.50	0.0032	0.3320E-01	41.229	0.0029
4.015	23.540	11711.76	13413.05	5.50	0.0	0.4928E-01	4.123	0.0003

PACKING SIZE =0.0380 M STATIC BED HEIGHT =0.440 M

G.KG/SQ.M-S	L.KG/SQ.M-S	REGAS	RELIQ	DP.MICRON	PT	ST	PTC.1/S	THEO.PT
2.346	4.708	10823.84	4964.23	1.75	0.6545	0.4909E-02	2.634	0.6607
2.346	4.708	10823.84	4964.23	2.50	0.4506	0.9763E-02	4.954	0.4865
2.346	4.708	10823.84	4964.23	3.50	0.2083	0.1880E-01	9.749	0.2949
2.346	4.708	10823.84	4964.23	4.50	0.1354	0.3077E-01	12.426	0.1628
2.313	4.708	10770.88	4983.98	1.35	0.7314	0.3019E-02	1.959	0.7527
2.313	4.708	10770.88	4983.98	1.35	0.7070	0.3019E-02	2.171	0.7527
2.313	4.708	10770.88	4983.98	2.50	0.3765	0.9837E-02	6.118	0.4795
2.313	4.708	10770.88	4983.98	3.50	0.2270	0.1894E-01	9.285	0.2878
2.381	9.416	10188.68	6098.02	1.75	0.4237	0.4621E-02	4.892	0.4587
2.381	9.416	10188.68	6098.02	2.50	0.2272	0.9189E-02	8.443	0.2579
2.381	9.416	10188.68	6098.02	3.50	0.0811	0.1769E-01	14.312	0.1006
2.381	9.416	10188.68	6098.02	4.50	0.0449	0.2896E-01	17.673	0.0329
2.345	9.416	10116.95	6079.25	1.35	0.6227	0.2840E-02	2.721	0.5893
2.345	9.416	10116.95	6079.25	1.75	0.3913	0.4655E-02	5.389	0.4552
2.345	9.416	10116.95	6079.25	2.50	0.1931	0.9256E-02	9.446	0.2545
2.345	9.416	10116.95	6079.25	3.50	0.0791	0.1782E-01	14.569	0.0984
2.390	14.124	9815.95	6869.93	1.75	0.2808	0.4464E-02	6.786	0.3177
2.390	14.124	9815.95	6869.93	2.50	0.1203	0.8877E-02	11.313	0.1362
2.390	14.124	9815.95	6869.93	3.50	0.0364	0.1710E-01	17.706	0.0341
2.390	14.124	9815.95	6869.93	4.50	0.0133	0.2798E-01	23.067	0.0066
2.355	14.124	9733.07	6867.62	1.35	0.4215	0.2739E-02	4.650	0.4561
2.355	14.124	9733.07	6867.62	1.75	0.2495	0.4490E-02	7.473	0.3109
2.355	14.124	9733.07	6867.62	2.50	0.1254	0.8928E-02	11.175	0.1311
2.355	14.124	9733.07	6867.62	3.50	0.0357	0.1719E-01	17.938	0.0320
2.400	18.832	9618.49	7531.60	1.75	0.2011	0.4377E-02	8.157	0.2190
2.400	18.832	9618.49	7531.60	1.75	0.1806	0.4377E-02	8.703	0.2190
2.400	18.832	9618.49	7531.60	2.50	0.0468	0.8705E-02	15.566	0.0713

PACKING SIZE =0.0380 M STATIC BED HEIGHT =0.440 M (CONTINUED)

G.KG/SQ.M-S	L.KG/SQ.M-S	REGAS	RELIQ	DP.MICRON	PT	ST	PTC.1/S	THEO.PT
2.400	18.832	9618.49	7531.60	3.50	0.0258	0.1676E-01	18.596	0.0114
2.400	18.832	9618.49	7531.60	3.50	0.0174	0.1676E-01	20.603	0.0114
2.400	18.832	9618.49	7531.60	4.50	0.0031	0.2744E-01	29.332	0.0013
2.405	23.540	9505.00	8089.44	1.75	0.1543	0.4332E-02	9.154	0.1533
2.405	23.540	9505.00	8089.44	2.50	0.0298	0.8615E-02	17.209	0.0383
2.405	23.540	9505.00	8089.44	3.50	0.0136	0.1659E-01	21.049	0.0040
2.405	23.540	9505.00	8089.44	4.50	0.0030	0.2715E-01	28.479	0.0003
2.858	4.708	11608.32	5386.57	1.75	0.6288	0.5127E-02	2.994	0.6650
2.858	4.708	11608.32	5386.57	2.50	0.4773	0.1020E-01	4.774	0.4919
2.858	4.708	11608.32	5386.57	3.50	0.2871	0.1965E-01	8.054	0.3004
2.858	4.708	11608.32	5386.57	4.50	0.1481	0.3216E-01	12.326	0.1673
2.858	4.708	11608.32	5386.57	4.50	0.1739	0.3216E-01	11.291	0.1673
2.812	9.416	10883.83	6830.03	1.75	0.4362	0.5010E-02	5.106	0.4399
2.812	9.416	10883.83	6830.03	2.50	0.2661	0.9963E-02	8.147	0.2398
2.812	9.416	10883.83	6830.03	3.50	0.0985	0.1918E-01	14.263	0.0890
2.812	9.416	10883.83	6830.03	4.50	0.0100	0.3140E-01	28.342	0.0274
2.869	9.416	11153.99	6539.97	1.75	0.4711	0.4949E-02	4.504	0.4890
2.869	9.416	11153.99	6539.97	2.50	0.2903	0.9846E-02	7.400	0.2881
2.869	9.416	11153.99	6539.97	3.50	0.1162	0.1896E-01	12.881	0.1214
2.869	9.416	11153.99	6539.97	4.50	0.0270	0.3104E-01	21.606	0.0435
2.822	14.124	10625.07	7652.19	1.75	0.2606	0.4907E-02	7.815	0.3141
2.822	14.124	10625.07	7652.19	2.50	0.1146	0.9758E-02	12.588	0.1335
2.822	14.124	10625.07	7652.19	3.50	0.0324	0.1879E-01	19.924	0.0330
2.822	14.124	10625.07	7652.19	4.50	0.0139	0.3075E-01	26.277	0.0063
2.882	14.124	10894.96	7374.13	1.75	0.3346	0.4848E-02	6.188	0.3604
2.882	14.124	10894.96	7374.13	2.50	0.1826	0.9644E-02	9.612	0.1695
2.882	14.124	10894.96	7374.13	3.50	0.0671	0.1858E-01	15.274	0.0494

PACKING SIZE =0.0380 M STATIC BED HEIGHT =0.440 M (CONTINUED)

G,KG/SQ.M-S	L,KG/SQ.M-S	REGAS	RELIQ	DP,MICRON	PT	ST	PTC,1/S	THEO.PT
2.882	14.124	10894.96	7374.13	4.50	0.0079	0.3041E-01	27.338	0.0114
2.823	18.832	10449.65	8267.63	1.75	0.1853	0.4846E-02	9.383	0.2294
2.823	18.832	10449.65	8267.63	2.50	0.0734	0.9636E-02	14.534	0.0773
2.823	18.832	10449.65	8267.63	3.50	0.0172	0.1856E-01	22.601	0.0131
2.823	18.832	10449.65	8267.63	4.50	0.0125	0.3037E-01	24.391	0.0016
2.850	23.540	10421.28	8846.38	1.75	0.1540	0.4829E-02	10.072	0.1715
2.850	23.540	10421.28	8846.38	2.50	0.0348	0.9602E-02	18.082	0.0466
2.850	23.540	10421.28	8846.38	3.50	0.0110	0.1849E-01	24.285	0.0055
2.850	23.540	10421.28	8846.38	4.50	0.0	0.3026E-01	2.429	0.0004
3.177	4.708	11897.07	6342.19	1.75	0.5888	0.5456E-02	3.653	0.5882
3.177	4.708	11897.07	6342.19	2.50	0.3989	0.1085E-01	6.338	0.3975
3.177	4.708	11897.07	6342.19	3.50	0.1910	0.2089E-01	11.418	0.2094
3.177	4.708	11897.07	6342.19	4.50	0.0860	0.3418E-01	16.917	0.0979
3.159	9.416	11503.73	7417.80	1.75	0.4395	0.5335E-02	5.305	0.4287
3.159	9.416	11503.73	7417.80	2.50	0.2457	0.1061E-01	9.059	0.2293
3.159	9.416	11503.73	7417.80	3.50	0.1162	0.2043E-01	13.893	0.0825
3.159	9.416	11503.73	7417.80	4.50	0.0388	0.3343E-01	20.963	0.0245
3.224	14.124	11410.68	8297.62	1.75	0.2972	0.5243E-02	7.377	0.3176
3.224	14.124	11410.68	8297.62	2.50	0.1302	0.1042E-01	12.394	0.1361
3.224	14.124	11410.68	8297.62	3.50	0.0420	0.2007E-01	19.268	0.0341
3.224	14.124	11410.68	8297.62	4.50	0.0193	0.3285E-01	23.995	0.0066
3.251	18.832	11352.32	8968.04	1.75	0.1747	0.5207E-02	10.172	0.2417
3.251	18.832	11352.32	8968.04	2.50	0.0558	0.1035E-01	16.831	0.0846
3.251	18.832	11352.32	8968.04	3.50	0.0195	0.1994E-01	22.970	0.0152
3.251	18.832	11352.32	8968.04	4.50	0.0044	0.3263E-01	31.604	0.0020
3.273	23.540	11331.14	9590.07	1.75	0.1501	0.5203E-02	10.728	0.1840
3.273	23.540	11331.14	9590.07	2.50	0.0317	0.1035E-01	19.519	0.0527

PACKING SIZE =0.0380 M STATIC BED HEIGHT =0.440 M (CONTINUED)

G.KG/SQ.M-S	L.KG/SQ.M-S	REGAS	RELIQ	DP.MICRON	PT	ST	PTC.1/S	THEO.PT
3.273	23.540	11331.14	9590.07	3.50	0.0071	0.1992E-01	28.009	0.0068
3.273	23.540	11331.14	9590.07	4.50	0.0	0.3260E-01	2.801	0.0006
3.426	4.708	12460.42	6371.48	1.75	0.6078	0.5515E-02	3.386	0.6157
3.426	4.708	12460.42	6371.48	2.50	0.3657	0.1097E-01	6.841	0.4302
3.426	4.708	12460.42	6371.48	3.50	0.1717	0.2113E-01	11.984	0.2394
3.426	4.708	12460.42	6371.48	4.50	0.1205	0.3458E-01	14.392	0.1194
3.445	9.416	12171.93	7591.82	1.75	0.4720	0.5407E-02	4.776	0.4559
3.445	9.416	12171.93	7591.82	2.50	0.2816	0.1076E-01	8.062	0.2551
3.445	9.416	12171.93	7591.82	3.50	0.1185	0.2072E-01	13.569	0.0988
3.445	9.416	12171.93	7591.82	4.50	0.0519	0.3391E-01	18.824	0.0320
3.470	14.124	12043.02	8484.62	1.75	0.3637	0.5348E-02	6.108	0.3443
3.470	14.124	12043.02	8484.62	2.50	0.2059	0.1064E-01	9.544	0.1565
3.470	14.124	12043.02	8484.62	3.50	0.0796	0.2049E-01	15.284	0.0432
3.470	14.124	12043.02	8484.62	4.50	0.0167	0.3354E-01	24.705	0.0093
3.499	18.832	11994.98	9199.07	1.75	0.2139	0.5334E-02	8.972	0.2662
3.499	18.832	11994.98	9199.07	2.50	0.0881	0.1061E-01	14.130	0.1000
3.499	18.832	11994.98	9199.07	3.50	0.0236	0.2043E-01	21.794	0.0202
3.499	18.832	11994.98	9199.07	4.50	0.0042	0.3345E-01	31.785	0.0030
3.528	23.540	12001.97	9823.78	1.75	0.1823	0.5340E-02	9.625	0.2095
3.528	23.540	12001.97	9823.78	2.50	0.0291	0.1062E-01	20.007	0.0660
3.528	23.540	12001.97	9823.78	3.50	0.0096	0.2046E-01	26.302	0.0100
3.528	23.540	12001.97	9823.78	4.50	0.0015	0.3349E-01	36.747	0.0011

PACKING SIZE =0.0380 M STATIC BED HEIGHT =0.580 M

G.KG/SQ.M-S	L.KG/SQ.M-S	REGAS	RELIQ	DP.MICRON	PT	ST	PTC.1/S	THEO.PT
2.852	4.708	12293.83	5200.14	1.35	0.6890	0.3377E-02	1.984	0.6511
2.852	4.708	12293.83	5200.14	1.75	0.4761	0.5536E-02	3.954	0.5280
2.852	4.708	12293.83	5200.14	2.50	0.2552	0.1101E-01	7.276	0.3293
2.852	4.708	12293.83	5200.14	3.50	0.1006	0.2121E-01	12.233	0.1522
2.852	4.708	12293.83	5200.14	4.50	0.0329	0.3471E-01	18.195	0.0609
2.852	4.708	12293.83	5200.14	5.50	0.0080	0.5153E-01	25.755	0.0214
2.869	9.416	11925.06	6110.57	1.35	0.5371	0.3288E-02	3.118	0.5071
2.869	9.416	11925.06	6110.57	1.75	0.3130	0.5391E-02	5.828	0.3639
2.869	9.416	11925.06	6110.57	2.50	0.1436	0.1072E-01	9.735	0.1724
2.869	9.416	11925.06	6110.57	3.50	0.0442	0.2065E-01	15.651	0.0508
2.869	9.416	11925.06	6110.57	4.50	0.0156	0.3380E-01	20.877	0.0119
2.869	9.416	11925.06	6110.57	5.50	0.0019	0.5018E-01	31.527	0.0023
2.884	14.124	11721.19	6800.22	1.35	0.4146	0.3237E-02	4.216	0.3980
2.884	14.124	11721.19	6800.22	1.75	0.2185	0.5307E-02	7.284	0.2538
2.884	14.124	11721.19	6800.22	2.50	0.0856	0.1056E-01	11.772	0.0921
2.884	14.124	11721.19	6800.22	3.50	0.0273	0.2033E-01	17.251	0.0176
2.884	14.124	11721.19	6800.22	4.50	0.0062	0.3328E-01	24.336	0.0025
2.884	14.124	11721.19	6800.22	5.50	0.0020	0.4940E-01	29.673	0.0003
2.891	18.832	11605.68	7385.18	1.35	0.2980	0.3211E-02	5.591	0.3138
2.891	18.832	11605.68	7385.18	1.75	0.1242	0.5264E-02	9.633	0.1782
2.891	18.832	11605.68	7385.18	2.50	0.0419	0.1047E-01	14.650	0.0498
2.891	18.832	11605.68	7385.18	3.50	0.0116	0.2016E-01	20.574	0.0062
2.891	18.832	11605.68	7385.18	4.50	0.0019	0.3300E-01	29.060	0.0005
2.891	18.832	11605.68	7385.18	5.50	0.0	0.4899E-01	2.906	0.0000
2.897	23.540	11556.95	7868.59	1.35	0.2436	0.3204E-02	6.349	0.2531
2.897	23.540	11556.95	7868.59	1.75	0.0944	0.5253E-02	10.609	0.1293
2.897	23.540	11556.95	7868.59	2.50	0.0312	0.1045E-01	15.584	0.0285

PACKING SIZE =0.0380 M STATIC BED HEIGHT =0.580 M (CONTINUED)

G,KG/SQ.M-S	L,KG/SQ.M-S	REGAS	RELIQ	DP,MICRON	PT	ST	PTC,1/S	THEO.PT
2.897	23.540	11556.95	7868.59	3.50	0.0071	0.2012E-01	22.218	0.0024
2.897	23.540	11556.95	7868.59	4.50	0.0009	0.3293E-01	31.466	0.0001
2.897	23.540	11556.95	7868.59	5.50	0.0	0.4889E-01	3.147	0.0000

PACKING SIZE =0.0250 M STATIC BED HEIGHT =0.290 M

G,KG/SQ.M-S	L,KG/SQ.M-S	REGAS	RELIQ	DP,MICRON	PT	ST	PTC,1/S	THEO.PT
2.805	4.708	6450.76	2651.50	1.75	0.6971	0.6661E-02	2.830	0.6436
2.805	4.708	6450.76	2651.50	2.50	0.5194	0.1325E-01	5.138	0.4647
2.805	4.708	6450.76	2651.50	3.50	0.2431	0.2551E-01	11.093	0.2728
2.805	4.708	6450.76	2651.50	4.50	0.1399	0.4176E-01	15.426	0.1450
2.805	4.708	6450.76	2651.50	5.50	0.0472	0.6199E-01	23.955	0.0704
2.837	9.416	6388.36	3185.14	1.75	0.5335	0.6593E-02	4.553	0.4895
2.837	9.416	6388.36	3185.14	2.50	0.3389	0.1311E-01	7.840	0.2886
2.837	9.416	6388.36	3185.14	3.50	0.1207	0.2526E-01	15.321	0.1218
2.837	9.416	6388.36	3185.14	4.50	0.0394	0.4134E-01	23.440	0.0437
2.837	9.416	6388.36	3185.14	4.50	0.0386	0.4134E-01	23.584	0.0437
2.837	9.416	6388.36	3185.14	5.50	0.0108	0.6137E-01	32.843	0.0135
2.845	14.124	6356.50	3581.87	1.75	0.4246	0.6560E-02	5.847	0.3752
2.845	14.124	6356.50	3581.87	2.50	0.2085	0.1305E-01	10.702	0.1818
2.845	14.124	6356.50	3581.87	3.50	0.0701	0.2513E-01	18.140	0.0556
2.845	14.124	6356.50	3581.87	4.50	0.0291	0.4114E-01	24.134	0.0136
2.845	14.124	6356.50	3581.87	5.50	0.0052	0.6107E-01	35.864	0.0027
2.854	18.832	6355.89	3900.46	1.75	0.3329	0.6571E-02	7.187	0.2931
2.854	18.832	6355.89	3900.46	2.50	0.1120	0.1307E-01	14.304	0.1183
2.854	18.832	6355.89	3900.46	3.50	0.0317	0.2517E-01	22.548	0.0268
2.854	18.832	6355.89	3900.46	4.50	0.0069	0.4120E-01	32.494	0.0046
2.854	18.832	6355.89	3900.46	5.50	0.0010	0.6117E-01	44.878	0.0006
2.909	23.540	6440.04	4221.49	1.75	0.2328	0.6656E-02	9.243	0.2327
2.909	23.540	6440.04	4221.49	2.50	0.0707	0.1324E-01	16.806	0.0792
2.909	23.540	6440.04	4221.49	3.50	0.0064	0.2550E-01	32.069	0.0136
2.909	23.540	6440.04	4221.49	4.50	0.0022	0.4174E-01	38.793	0.0017
2.909	23.540	6440.04	4221.49	5.50	0.0008	0.6196E-01	44.848	0.0002

PACKING SIZE =0.0250 M STATIC BED HEIGHT =0.440 M

G.KG/SQ.M-S	L.KG/SQ.M-S	REGAS	RELIQ	DP,MICRON	PT	ST	PTC.1/S	THEO.PT
2.393	4.708	6793.79	2030.92	1.75	0.5913	0.6968E-02	2.956	0.5502
2.393	4.708	6793.79	2030.92	1.75	0.6138	0.6968E-02	2.746	0.5502
2.393	4.708	6793.79	2030.92	2.50	0.3505	0.1386E-01	5.898	0.3537
2.393	4.708	6793.79	2030.92	3.50	0.1593	0.2670E-01	10.335	0.1718
2.393	4.708	6793.79	2030.92	3.50	0.1257	0.2670E-01	11.668	0.1718
2.393	4.708	6793.79	2030.92	4.50	0.0590	0.4370E-01	15.925	0.0729
2.393	4.708	6793.79	2030.92	5.50	0.0165	0.6488E-01	23.106	0.0274
2.405	9.416	6717.24	2408.22	1.75	0.4251	0.6901E-02	4.508	0.3931
2.405	9.416	6717.24	2408.22	2.50	0.2070	0.1373E-01	8.301	0.1971
2.405	9.416	6717.24	2408.22	3.50	0.0573	0.2644E-01	15.072	0.0638
2.405	9.416	6717.24	2408.22	4.50	0.0113	0.4328E-01	23.608	0.0167
2.405	9.416	6717.24	2408.22	4.50	0.0110	0.4328E-01	23.756	0.0167
2.405	9.416	6717.24	2408.22	5.50	0.0018	0.6425E-01	33.339	0.0036
2.407	14.124	6680.83	2686.16	1.75	0.3006	0.6889E-02	6.037	0.2866
2.407	14.124	6680.83	2686.16	2.50	0.1316	0.1370E-01	10.185	0.1138
2.407	14.124	6680.83	2686.16	3.50	0.0321	0.2640E-01	17.279	0.0251
2.407	14.124	6680.83	2686.16	4.50	0.0023	0.4321E-01	30.525	0.0042
2.407	14.124	6680.83	2686.16	5.50	0.0	0.6415E-01	3.052	0.0005
2.408	18.832	6698.11	2916.18	1.75	0.2220	0.6911E-02	7.267	0.2146
2.408	18.832	6698.11	2916.18	2.50	0.0587	0.1375E-01	13.687	0.0688
2.408	18.832	6698.11	2916.18	3.50	0.0111	0.2648E-01	21.751	0.0107
2.408	18.832	6698.11	2916.18	4.50	0.0018	0.4334E-01	30.491	0.0012
2.408	18.832	6698.11	2916.18	5.50	0.0	0.6434E-01	3.049	0.0001
2.416	23.540	6757.95	3112.28	1.75	0.0959	0.6982E-02	11.003	0.1672
2.416	23.540	6757.95	3112.28	2.50	0.0205	0.1389E-01	18.237	0.0446
2.416	23.540	6757.95	3112.28	3.50	0.0046	0.2675E-01	25.230	0.0051
2.416	23.540	6757.95	3112.28	4.50	0.0008	0.4379E-01	33.356	0.0004

PACKING SIZE =0.0250 M STATIC BED HEIGHT =0.440 M (CONTINUED)

G,KG/SQ.M-S	L,KG/SQ.M-S	REGAS	RELIQ	DP,MICRON	PT	ST	PTC.1/S	THEO.PT
2.416	23.540	6757.95	3112.28	5.50	0.0	0.6501E-01	3.336	0.0000
2.845	4.708	7268.84	2287.91	1.75	0.5617	0.7551E-02	3.504	0.5301
2.845	4.708	7268.84	2287.91	2.50	0.3509	0.1502E-01	6.362	0.3316
2.845	4.708	7268.84	2287.91	3.50	0.1398	0.2893E-01	11.950	0.1540
2.845	4.708	7268.84	2287.91	4.50	0.0484	0.4735E-01	18.394	0.0620
2.845	4.708	7268.84	2287.91	5.50	0.0151	0.7028E-01	25.479	0.0219
2.862	9.416	7255.95	2692.10	1.75	0.4224	0.7535E-02	4.929	0.3858
2.862	9.416	7255.95	2692.10	2.50	0.2006	0.1499E-01	9.189	0.1908
2.862	9.416	7255.95	2692.10	3.50	0.0733	0.2887E-01	14.944	0.0604
2.862	9.416	7255.95	2692.10	4.50	0.0201	0.4725E-01	22.346	0.0154
2.862	9.416	7255.95	2692.10	4.50	0.0210	0.4725E-01	22.088	0.0154
2.862	9.416	7255.95	2692.10	5.50	0.0054	0.7014E-01	29.914	0.0032
2.869	14.124	7265.21	2986.20	1.75	0.3023	0.7558E-02	6.546	0.2900
2.869	14.124	7265.21	2986.20	1.75	0.3299	0.7558E-02	6.066	0.2900
2.869	14.124	7265.21	2986.20	2.50	0.1274	0.1503E-01	11.272	0.1161
2.869	14.124	7265.21	2986.20	2.50	0.1445	0.1503E-01	10.585	0.1161
2.869	14.124	7265.21	2986.20	3.50	0.0442	0.2895E-01	17.064	0.0260
2.869	14.124	7265.21	2986.20	4.50	0.0105	0.4739E-01	24.940	0.0044
2.869	14.124	7265.21	2986.20	5.50	0.0043	0.7035E-01	29.822	0.0006
2.874	18.832	7307.09	3211.09	1.75	0.2282	0.7609E-02	7.807	0.2278
2.874	18.832	7307.09	3211.09	2.50	0.0801	0.1513E-01	13.337	0.0763
2.874	18.832	7307.09	3211.09	3.50	0.0177	0.2915E-01	21.311	0.0128
2.874	18.832	7307.09	3211.09	4.50	0.0034	0.4771E-01	30.020	0.0015
2.874	18.832	7307.09	3211.09	5.50	0.0	0.7083E-01	3.002	0.0001
2.888	23.540	7391.49	3427.78	1.75	0.1984	0.7697E-02	8.325	0.1815
2.888	23.540	7391.49	3427.78	1.75	0.1542	0.7697E-02	9.621	0.1815
2.888	23.540	7391.49	3427.78	2.50	0.0410	0.1531E-01	16.438	0.0514

PACKING SIZE =0.0250 M STATIC BED HEIGHT =0.440 M (CONTINUED)

G.KG/SQ.M-S	L.KG/SQ.M-S	REGAS	RELIQ	DP.MICRON	PT	ST	PTC.1/S	THEO.PT
2.888	23.540	7391.49	3427.78	3.50	0.0072	0.2949E-01	25.419	0.0065
2.888	23.540	7391.49	3427.78	4.50	0.0014	0.4827E-01	33.969	0.0006
2.888	23.540	7391.49	3427.78	5.50	0.0	0.7165E-01	3.397	0.0000

PACKING SIZE =0.0250 M STATIC BED HEIGHT =0.580 M

G,KG/SQ.M-S	L,KG/SQ.M-S	REGAS	RELIQ	DP,MICRON	PT	ST	PTC,1/S	THEO.PT
2.926	4.708	7925.64	2180.66	1.75	0.3629	0.8123E-02	5.058	0.4077
2.926	4.708	7925.64	2180.66	2.50	0.2119	0.1616E-01	7.743	0.2101
2.926	4.708	7925.64	2180.66	3.50	0.0722	0.3112E-01	13.118	0.0711
2.926	4.708	7925.64	2180.66	3.50	0.0707	0.3112E-01	13.222	0.0711
2.926	4.708	7925.64	2180.66	4.50	0.0255	0.5094E-01	18.307	0.0196
2.926	4.708	7925.64	2180.66	4.50	0.0270	0.5094E-01	18.033	0.0196
2.926	4.708	7925.64	2180.66	5.50	0.0065	0.7561E-01	25.105	0.0045
2.936	9.416	7963.52	2518.98	1.75	0.2784	0.8201E-02	6.105	0.2824
2.936	9.416	7963.52	2518.98	2.50	0.0901	0.1631E-01	11.494	0.1109
2.936	9.416	7963.52	2518.98	3.50	0.0277	0.3142E-01	17.120	0.0241
2.936	9.416	7963.52	2518.98	4.50	0.0070	0.5142E-01	23.672	0.0039
2.936	9.416	7963.52	2518.98	5.50	0.0	0.7633E-01	2.367	0.0005
2.946	14.124	8042.28	2757.03	1.75	0.2104	0.8290E-02	7.179	0.2104
2.946	14.124	8042.28	2757.03	2.50	0.0698	0.1649E-01	12.260	0.0665
2.946	14.124	8042.28	2757.03	3.50	0.0176	0.3176E-01	18.606	0.0101
2.946	14.124	8042.28	2757.03	4.50	0.0041	0.5198E-01	25.318	0.0011
2.946	14.124	8042.28	2757.03	5.50	0.0	0.7716E-01	2.532	0.0001
2.951	18.832	8146.18	2957.22	1.75	0.1239	0.8396E-02	9.336	0.1624
2.951	18.832	8146.18	2957.22	2.50	0.0468	0.1670E-01	13.685	0.0424
2.951	18.832	8146.18	2957.22	3.50	0.0065	0.3216E-01	22.508	0.0047
2.951	18.832	8146.18	2957.22	4.50	0.0020	0.5265E-01	27.677	0.0003
2.951	18.832	8146.18	2957.22	5.50	0.0	0.7815E-01	2.768	0.0000
2.963	23.540	8285.39	3124.57	1.75	0.1122	0.8547E-02	9.577	0.1324
2.963	23.540	8285.39	3124.57	2.50	0.0200	0.1700E-01	17.130	0.0297
2.963	23.540	8285.39	3124.57	2.50	0.0154	0.1700E-01	18.266	0.0297
2.963	23.540	8285.39	3124.57	3.50	0.0029	0.3274E-01	25.609	0.0026
2.963	23.540	8285.39	3124.57	4.50	0.0	0.5359E-01	2.561	0.0001

PACKING SIZE =0.0250 M STATIC BED HEIGHT =0.580 M (CONTINUED)

G.KG/SQ.M-S	L.KG/SQ.M-S	REGAS	RELIQ	DP.MICRON	PT	ST	PTC.1/S	THEO.PT
2.963	23.540	8285.39	3124.57	5.50	0.0	0.7955E-01	0.256	0.0000

PACKING SIZE =0.0190 M STATIC BED HEIGHT =0.290 M

G.KG/SQ.M-S	L.KG/SQ.M-S	REGAS	RELIQ	DP,MICRON	PT	ST	PTC.1/S	THEO.PT
2.377	4.708	4499.55	1291.41	1.75	0.6636	0.8043E-02	2.946	0.6165
2.377	4.708	4499.55	1291.41	2.50	0.4153	0.1630E-01	6.312	0.4312
2.377	4.708	4499.55	1291.41	3.50	0.2305	0.3081E-01	10.543	0.2404
2.377	4.708	4499.55	1291.41	4.50	0.1054	0.5044E-01	16.163	0.1201
2.377	4.708	4499.55	1291.41	5.50	0.0444	0.7487E-01	22.379	0.0543
2.386	9.416	4502.20	1551.79	1.75	0.4546	0.8062E-02	5.260	0.4643
2.386	9.416	4502.20	1551.79	2.50	0.2523	0.1604E-01	9.189	0.2633
2.386	9.416	4502.20	1551.79	3.50	0.0930	0.3089E-01	15.847	0.1042
2.386	9.416	4502.20	1551.79	4.50	0.0174	0.5056E-01	27.051	0.0347
2.386	9.416	4502.20	1551.79	5.50	0.0039	0.7505E-01	37.053	0.0099
2.395	14.124	4533.46	1749.16	1.75	0.3585	0.8116E-02	6.468	0.3564
2.395	14.124	4533.46	1749.16	2.50	0.1606	0.1614E-01	11.529	0.1663
2.395	14.124	4533.46	1749.16	3.50	0.0299	0.3110E-01	22.129	0.0478
2.395	14.124	4533.46	1749.16	4.50	0.0059	0.5090E-01	32.400	0.0109
2.395	14.124	4533.46	1749.16	5.50	0.0018	0.7556E-01	39.796	0.0020
2.410	18.832	4592.41	1904.74	1.75	0.2939	0.8214E-02	7.397	0.2844
2.410	18.832	4592.41	1904.74	2.50	0.1365	0.1634E-01	12.030	0.1122
2.410	18.832	4592.41	1904.74	3.50	0.0079	0.3147E-01	29.204	0.0246
2.410	18.832	4592.41	1904.74	4.50	0.0013	0.5151E-01	40.271	0.0040
2.410	18.832	4592.41	1904.74	5.50	0.0005	0.7647E-01	45.566	0.0005
2.421	23.540	4643.38	2043.29	1.75	0.2106	0.8374E-02	9.179	0.2290
2.421	23.540	4643.38	2043.29	2.50	0.0720	0.1665E-01	15.508	0.0770
2.421	23.540	4643.38	2043.29	3.50	0.0122	0.3208E-01	25.971	0.0130
2.421	23.540	4643.38	2043.29	4.50	0.0002	0.5250E-01	49.356	0.0016
2.421	23.540	4643.38	2043.29	5.50	0.0	0.7793E-01	4.936	0.0001
2.839	4.708	4874.53	1506.18	1.75	0.6775	0.8692E-02	2.898	0.5734
2.839	4.708	4874.53	1506.18	2.50	0.4361	0.1729E-01	6.178	0.3801

PACKING SIZE =0.0190 M STATIC BED HEIGHT =0.290 M (CONTINUED)

G,KG/SQ.M-S	L,KG/SQ.M-S	REGAS	RELIQ	DP,MICRON	PT	ST	PTC,1/S	THEO.PT
2.839	4.708	4874.53	1506.18	3.50	0.2020	0.3330E-01	11.909	0.1941
2.839	4.708	4874.53	1506.18	4.50	0.0648	0.5451E-01	20.376	0.0874
2.839	4.708	4874.53	1506.18	5.50	0.0201	0.8091E-01	29.096	0.0351
2.848	9.416	4902.78	1780.68	1.75	0.4964	0.8799E-02	4.910	0.4335
2.848	9.416	4902.78	1780.68	2.50	0.2710	0.1750E-01	9.153	0.2337
2.848	9.416	4902.78	1780.68	3.50	0.1078	0.3371E-01	15.617	0.0851
2.848	9.416	4902.78	1780.68	4.50	0.0241	0.5517E-01	26.133	0.0257
2.848	9.416	4902.78	1780.68	5.50	0.0054	0.8190E-01	36.548	0.0065
2.864	14.124	4956.86	1974.84	1.75	0.3241	0.8908E-02	7.529	0.3430
2.864	14.124	4956.86	1974.84	2.50	0.1728	0.1772E-01	11.733	0.1555
2.864	14.124	4956.86	1974.84	3.50	0.0446	0.3413E-01	20.782	0.0427
2.864	14.124	4956.86	1974.84	4.50	0.0128	0.5586E-01	29.125	0.0092
2.864	14.124	4956.86	1974.84	5.50	0.0016	0.8292E-01	42.945	0.0016
2.875	18.832	5022.86	2150.78	1.75	0.2393	0.9043E-02	9.219	0.2731
2.875	18.832	5022.86	2150.78	2.50	0.0952	0.1799E-01	15.161	0.1046
2.875	18.832	5022.86	2150.78	3.50	0.0144	0.3464E-01	27.336	0.0218
2.875	18.832	5022.86	2150.78	4.50	0.0019	0.5671E-01	40.258	0.0034
2.875	18.832	5022.86	2150.78	5.50	0.0014	0.8418E-01	42.136	0.0004
2.897	23.540	5112.88	2299.44	1.75	0.2009	0.9211E-02	10.069	0.2261
2.897	23.540	5112.88	2299.44	2.50	0.0137	0.1832E-01	26.932	0.0753
2.897	23.540	5112.88	2299.44	3.50	0.0030	0.3529E-01	36.519	0.0125
2.897	23.540	5112.88	2299.44	4.50	0.0009	0.5776E-01	44.343	0.0015
2.897	23.540	5112.88	2299.44	5.50	0.0	0.8574E-01	4.434	0.0001
3.201	4.708	5166.11	1681.96	1.75	0.5668	0.9351E-02	4.386	0.5406
3.201	4.708	5166.11	1681.96	2.50	0.4114	0.1860E-01	6.864	0.3431
3.201	4.708	5166.11	1681.96	3.50	0.1560	0.3581E-01	14.355	0.1633
3.201	4.708	5166.11	1681.96	4.50	0.0859	0.5862E-01	18.970	0.0676

PACKING SIZE =0.0190 M STATIC BED HEIGHT =0.290 M (CONTINUED)

G.KG/SQ.M-S	L.KG/SQ.M-S	REGAS	RELIQ	DP.MICRON	PT	ST	PTC.1/S	THEO.PT
3.201	4.708	5166.11	1681.96	5.50	0.0190	0.8701E-01	30.604	0.0247
3.226	9.416	5234.22	1975.30	1.75	0.4078	0.9484E-02	6.539	0.4091
3.226	9.416	5234.22	1975.30	2.50	0.2051	0.1886E-01	11.550	0.2113
3.226	9.416	5234.22	1975.30	3.50	0.0862	0.3632E-01	17.867	0.0718
3.226	9.416	5234.22	1975.30	4.50	0.0404	0.5945E-01	23.399	0.0199
3.226	9.416	5234.22	1975.30	5.50	0.0105	0.8825E-01	33.185	0.0046
3.229	14.124	5288.25	2176.30	1.75	0.3067	0.9595E-02	8.238	0.3242
3.229	14.124	5288.25	2176.30	2.50	0.1689	0.1908E-01	12.395	0.1410
3.229	14.124	5288.25	2176.30	3.50	0.0665	0.3675E-01	18.894	0.0362
3.229	14.124	5288.25	2176.30	4.50	0.0205	0.6015E-01	27.101	0.0072
3.229	14.124	5288.25	2176.30	5.50	0.0024	0.8929E-01	41.916	0.0011
3.228	18.832	5347.14	2344.64	1.75	0.2469	0.9762E-02	9.462	0.2626
3.228	18.832	5347.14	2344.64	2.50	0.0760	0.1942E-01	17.436	0.0978
3.228	18.832	5347.14	2344.64	3.50	0.0207	0.3739E-01	26.233	0.0194
3.228	18.832	5347.14	2344.64	4.50	0.0049	0.6120E-01	35.992	0.0029
3.228	18.832	5347.14	2344.64	5.50	0.0016	0.9084E-01	43.466	0.0003
3.256	23.540	5447.47	2493.83	1.75	0.1988	0.9942E-02	10.650	0.2210
3.256	23.540	5447.47	2493.83	2.50	0.0517	0.1977E-01	19.533	0.0724
3.256	23.540	5447.47	2493.83	3.50	0.0034	0.3808E-01	37.525	0.0117
3.256	23.540	5447.47	2493.83	4.50	0.0007	0.6233E-01	48.124	0.0013
3.256	23.540	5447.47	2493.83	5.50	0.0	0.9252E-01	4.812	0.0001
3.542	4.708	5482.23	1831.95	1.75	0.6345	0.9882E-02	3.563	0.5224
3.542	4.708	5482.23	1831.95	2.50	0.3784	0.1965E-01	7.611	0.3233
3.542	4.708	5482.23	1831.95	3.50	0.1693	0.3785E-01	13.910	0.1476
3.542	4.708	5482.23	1831.95	4.50	0.0991	0.6195E-01	18.102	0.0582
3.542	4.708	5482.23	1831.95	5.50	0.0335	0.9195E-01	26.606	0.0201
3.542	9.416	5525.45	2140.17	1.75	0.4530	0.1005E-01	5.913	0.3913

PACKING SIZE =0.0190 M STATIC BED HEIGHT =0.290 M (CONTINUED)

G,KG/SQ.M-S	L,KG/SQ.M-S	REGAS	RELIQ	DP,MICRON	PT	ST	PTC,1/S	THEO.PT
3.542	9.416	5525.45	2140.17	2.50	0.2880	0.1998E-01	9.293	0.1957
3.542	9.416	5525.45	2140.17	3.50	0.0791	0.3848E-01	18.941	0.0630
3.542	9.416	5525.45	2140.17	4.50	0.0210	0.6298E-01	28.838	0.0164
3.542	9.416	5525.45	2140.17	5.50	0.0089	0.9349E-01	35.218	0.0035
3.550	14.124	5588.27	2346.08	1.75	0.3831	0.1019E-01	6.883	0.3125
3.550	14.124	5588.27	2346.08	2.50	0.1523	0.2027E-01	13.502	0.1323
3.550	14.124	5588.27	2346.08	3.50	0.0321	0.3903E-01	24.675	0.0325
3.550	14.124	5588.27	2346.08	4.50	0.0183	0.6388E-01	28.712	0.0061
3.550	14.124	5588.27	2346.08	5.50	0.0048	0.9483E-01	38.238	0.0009
3.569	18.832	5678.88	2527.65	1.75	0.3286	0.1035E-01	7.729	0.2555
3.569	18.832	5678.88	2527.65	2.50	0.1154	0.2059E-01	14.996	0.0932
3.569	18.832	5678.88	2527.65	3.50	0.0255	0.3964E-01	25.470	0.0179
3.569	18.832	5678.88	2527.65	4.50	0.0047	0.6489E-01	37.294	0.0025
3.569	18.832	5678.88	2527.65	5.50	0.0014	0.9631E-01	45.766	0.0003
3.606	23.540	5788.10	2694.86	1.75	0.2066	0.1054E-01	10.695	0.2136
3.606	23.540	5788.10	2694.86	2.50	0.0583	0.2097E-01	19.275	0.0683
3.606	23.540	5788.10	2694.86	3.50	0.0060	0.4038E-01	34.718	0.0106
3.606	23.540	5788.10	2694.86	4.50	0.0006	0.6610E-01	50.352	0.0012
3.606	23.540	5788.10	2694.86	5.50	0.0	0.9812E-01	5.035	0.0001
3.849	4.708	5771.93	1976.13	1.75	0.5177	0.1034E-01	5.190	0.5043
3.849	4.708	5771.93	1976.13	2.50	0.3503	0.2055E-01	8.269	0.3040
3.849	4.708	5771.93	1976.13	3.50	0.1633	0.3958E-01	14.283	0.1330
3.849	4.708	5771.93	1976.13	4.50	0.0626	0.6478E-01	21.838	0.0498
3.849	4.708	5771.93	1976.13	5.50	0.0235	0.9616E-01	29.562	0.0162
3.878	9.416	5857.40	2300.06	1.75	0.3922	0.1054E-01	7.047	0.3810
3.878	9.416	5857.40	2300.06	2.50	0.2281	0.2096E-01	11.127	0.1868
3.878	9.416	5857.40	2300.06	3.50	0.0515	0.4037E-01	22.323	0.0582

PACKING SIZE =0.0190 M STATIC BED HEIGHT =0.290 M (CONTINUED)

G,KG/SQ.M-S	L,KG/SQ.M-S	REGAS	RELIQ	DP,MICRON	PT	ST	PTC,1/S	THEO.PT
3.878	9.416	5857.40	2300.06	4.50	0.0373	0.6608E-01	24.748	0.0146
3.878	9.416	5857.40	2300.06	5.50	0.0077	0.9809E-01	36.592	0.0030
3.889	14.124	5927.72	2517.48	1.75	0.3049	0.1070E-01	8.615	0.3050
3.889	14.124	5927.72	2517.48	2.50	0.1244	0.2127E-01	15.118	0.1268
3.889	14.124	5927.72	2517.48	3.50	0.0480	0.4096E-01	22.025	0.0302
3.889	14.124	5927.72	2517.48	4.50	0.0173	0.6704E-01	29.419	0.0055
3.889	14.124	5927.72	2517.48	5.50	0.0049	0.9952E-01	38.542	0.0008
3.915	18.832	6023.65	2711.83	1.75	0.1990	0.1088E-01	11.379	0.2493
3.915	18.832	6023.65	2711.83	2.50	0.0572	0.2164E-01	20.173	0.0893
3.915	18.832	6023.65	2711.83	3.50	0.0221	0.4167E-01	26.888	0.0167
3.915	18.832	6023.65	2711.83	4.50	0.0	0.6820E-01	2.689	0.0023
3.915	18.832	6023.65	2711.83	5.50	0.0	0.1012E+00	0.269	0.0002

PACKING SIZE =0.0190 M STATIC BED HEIGHT =0.440 M

G,KG/SQ.M-S	L,KG/SQ.M-S	REGAS	RELIQ	DP,MICRON	PT	ST	PTC,1/S	THEO.PT
2.416	4.708	5103.32	1142.84	1.75	0.4636	0.9069E-02	4.157	0.4771
2.416	4.708	5103.32	1142.84	2.50	0.2668	0.1804E-01	7.143	0.2761
2.416	4.708	5103.32	1142.84	3.50	0.1035	0.3475E-01	12.262	0.1129
2.416	4.708	5103.32	1142.84	4.50	0.0124	0.5688E-01	23.719	0.0390
2.416	4.708	5103.32	1142.84	5.50	0.0044	0.8443E-01	29.372	0.0116
2.423	9.416	5193.34	1355.33	1.75	0.3148	0.9277E-02	5.936	0.3379
2.423	9.416	5193.34	1355.33	2.50	0.1188	0.1845E-01	10.940	0.1515
2.423	9.416	5193.34	1355.33	3.50	0.0266	0.3554E-01	18.630	0.0408
2.423	9.416	5193.34	1355.33	4.50	0.0105	0.5818E-01	23.388	0.0086
2.423	9.416	5193.34	1355.33	5.50	0.0	0.8636E-01	2.339	0.0015
2.425	14.124	5298.36	1492.04	1.75	0.2662	0.9479E-02	6.518	0.2625
2.425	14.124	5298.36	1492.04	2.50	0.0958	0.1885E-01	11.549	0.0977
2.425	14.124	5298.36	1492.04	3.50	0.0187	0.3632E-01	19.588	0.0194
2.425	14.124	5298.36	1492.04	4.50	0.0	0.5944E-01	1.959	0.0028
2.425	14.124	5298.36	1492.04	5.50	0.0	0.8824E-01	0.196	0.0003
2.435	18.832	5435.09	1623.26	1.75	0.1379	0.9712E-02	9.436	0.2071
2.435	18.832	5435.09	1623.26	2.50	0.0415	0.1932E-01	15.150	0.0647
2.435	18.832	5435.09	1623.26	3.50	0.0028	0.3721E-01	27.915	0.0096
2.435	18.832	5435.09	1623.26	4.50	0.0008	0.6091E-01	33.723	0.0010
2.435	18.832	5435.09	1623.26	5.50	0.0	0.9042E-01	3.372	0.0001
2.863	4.708	5483.45	1293.41	1.75	0.4088	0.9878E-02	5.240	0.4560
2.863	4.708	5483.45	1293.41	2.50	0.2408	0.1965E-01	8.342	0.2552
2.863	4.708	5483.45	1293.41	2.50	0.2491	0.1965E-01	8.143	0.2552
2.863	4.708	5483.45	1293.41	3.50	0.0508	0.3784E-01	17.465	0.0989
2.863	4.708	5483.45	1293.41	4.50	0.0227	0.6193E-01	22.172	0.0321
2.863	4.708	5483.45	1293.41	5.50	0.0112	0.9193E-01	26.343	0.0088
2.885	9.416	5602.66	1514.09	1.75	0.2923	0.1015E-01	6.899	0.3316

PACKING SIZE =0.0190 M STATIC BED HEIGHT =0.440 M (CONTINUED)

G,KG/SQ.M-S	L,KG/SQ.M-S	REGAS	RELIQ	DP,MICRON	PT	ST	PTC.1/S	THEO.PT
2.885	9.416	5602.66	1514.09	2.50	0.1633	0.2018E-01	10.163	0.1467
2.885	9.416	5602.66	1514.09	3.50	0.0205	0.3887E-01	21.794	0.0387
2.885	9.416	5602.66	1514.09	4.50	0.0135	0.6363E-01	24.152	0.0079
2.885	9.416	5602.66	1514.09	5.50	0.0040	0.9444E-01	30.947	0.0013
2.890	14.124	5724.64	1656.27	1.75	0.1617	0.1039E-01	9.843	0.2637
2.890	14.124	5724.64	1656.27	2.50	0.0436	0.2066E-01	16.927	0.0985
2.890	14.124	5724.64	1656.27	3.50	0.0106	0.3979E-01	24.582	0.0197
2.890	14.124	5724.64	1656.27	4.50	0.0036	0.6512E-01	30.462	0.0029
2.890	14.124	5724.64	1656.27	5.50	0.0	0.9667E-01	3.046	0.0003
2.892	18.832	5853.11	1783.59	1.75	0.1903	0.1066E-01	8.725	0.2141
2.892	18.832	5853.11	1783.59	2.50	0.0236	0.2121E-01	19.711	0.0685
2.892	18.832	5853.11	1783.59	3.50	0.0055	0.4084E-01	27.404	0.0106
2.892	18.832	5853.11	1783.59	4.50	0.0014	0.6685E-01	34.457	0.0012
2.892	18.832	5853.11	1783.59	5.50	0.0	0.9923E-01	3.446	0.0001
2.905	23.540	6012.55	1889.07	1.75	0.1392	0.1095E-01	10.140	0.1839
2.905	23.540	6012.55	1889.07	1.75	0.1431	0.1095E-01	9.995	0.1839
2.905	23.540	6012.55	1889.07	2.50	0.0296	0.2178E-01	18.099	0.0526
2.905	23.540	6012.55	1889.07	3.50	0.0027	0.4194E-01	30.452	0.0068
2.905	23.540	6012.55	1889.07	4.50	0.0	0.6865E-01	3.045	0.0006
2.905	23.540	6012.55	1889.07	5.50	0.0	0.1019E+00	0.305	0.0000

PACKING SIZE =0.0190 M STATIC BED HEIGHT =0.580 M

G.KG/SQ.M-S	L.KG/SQ.M-S	REGAS	RELIQ	DP.MICRON	PT	ST	PTC.1/S	THEO.PT
2.950	4.708	6005.41	1262.38	1.75	0.2834	0.1075E-01	6.169	0.3181
2.950	4.708	6005.41	1262.38	2.50	0.1272	0.2139E-01	10.090	0.1364
2.950	4.708	6005.41	1262.38	3.50	0.0361	0.4118E-01	16.250	0.0342
2.950	4.708	6005.41	1262.38	4.50	0.0051	0.6741E-01	25.848	0.0066
2.950	4.708	6005.41	1262.38	5.50	0.0	0.1001E+00	2.585	0.0010
2.958	9.416	6200.04	1444.96	1.75	0.2447	0.1113E-01	6.627	0.2240
2.958	9.416	6200.04	1444.96	2.50	0.0884	0.2214E-01	11.421	0.0742
2.958	9.416	6200.04	1444.96	2.50	0.0440	0.2214E-01	14.699	0.0742
2.958	9.416	6200.04	1444.96	3.50	0.0238	0.4263E-01	17.597	0.0122
2.958	9.416	6200.04	1444.96	4.50	0.0105	0.6978E-01	21.459	0.0014
2.958	9.416	6200.04	1444.96	5.50	0.0	0.1036E+00	2.146	0.0001
2.962	14.124	6391.96	1516.31	1.75	0.1648	0.1151E-01	8.238	0.1985
2.962	14.124	6391.96	1516.31	2.50	0.0345	0.2289E-01	15.384	0.0601
2.962	14.124	6391.96	1516.31	3.50	0.0077	0.4408E-01	22.238	0.0085
2.962	14.124	6391.96	1516.31	4.50	0.0	0.7214E-01	2.224	0.0008
2.962	14.124	6391.96	1516.31	5.50	0.0	0.1071E+00	0.222	0.0001

PACKING SIZE =0.0380 M STATIC BED HEIGHT =0.440 M

G.KG/SQ.M-S	L.KG/SQ.M-S	REGAS	RELIQ	DP.MICRON	PT	ST	PTC.1/S	THEO.PT
2.858	9.416	11022.79	6558.91	0.35	0.9225	0.2680E-03	0.490	0.9324
2.858	9.416	11022.79	6558.91	0.35	0.9418	0.2680E-03	0.364	0.9324
2.858	9.416	11022.79	6558.91	0.45	0.8957	0.4104E-03	0.669	0.9060
2.858	9.416	11022.79	6558.91	0.55	0.8280	0.5828E-03	1.146	0.8773
2.858	9.416	11022.79	6558.91	0.55	0.8232	0.5828E-03	1.181	0.8773
2.858	9.416	11022.79	6558.91	0.70	0.8480	0.8974E-03	1.001	0.8309
2.858	9.416	11022.79	6558.91	0.70	0.7133	0.8974E-03	2.051	0.8309
2.858	9.416	11022.79	6558.91	0.90	0.8614	0.1421E-02	0.906	0.7648
2.858	9.416	11022.79	6558.91	0.90	0.8447	0.1421E-02	1.024	0.7648
2.858	9.416	11022.79	6558.91	0.90	0.7823	0.1421E-02	1.493	0.7648
2.858	9.416	11022.79	6558.91	0.90	0.8218	0.1421E-02	1.191	0.7648
2.858	9.416	11022.79	6558.91	1.10	0.7438	0.2064E-02	1.797	0.6962
2.858	9.416	11022.79	6558.91	1.10	0.7284	0.2064E-02	1.924	0.6962
2.858	9.416	11022.79	6558.91	1.10	0.7236	0.2064E-02	1.964	0.6962
2.858	9.416	11022.79	6558.91	1.10	0.6960	0.2064E-02	2.200	0.6962
2.858	9.416	11022.79	6558.91	1.10	0.8116	0.2064E-02	1.267	0.6962
2.858	9.416	11022.79	6558.91	1.10	0.6816	0.2064E-02	2.327	0.6962
2.858	9.416	11022.79	6558.91	1.35	0.5833	0.3034E-02	3.272	0.6103
2.858	9.416	11022.79	6558.91	1.35	0.6714	0.3034E-02	2.418	0.6103
2.858	9.416	11022.79	6558.91	1.35	0.6586	0.3034E-02	2.535	0.6103
2.858	9.416	11022.79	6558.91	1.35	0.6102	0.3034E-02	2.998	0.6103
2.858	9.416	11022.79	6558.91	1.35	0.5975	0.3034E-02	3.126	0.6103
2.858	9.416	11022.79	6558.91	1.75	0.4680	0.4974E-02	4.609	0.4795
2.858	9.416	11022.79	6558.91	1.75	0.4634	0.4974E-02	4.669	0.4795
2.858	9.416	11022.79	6558.91	1.75	0.4711	0.4974E-02	4.569	0.4795
2.858	9.416	11022.79	6558.91	1.75	0.4362	0.4974E-02	5.036	0.4795
2.858	9.416	11022.79	6558.91	2.50	0.2560	0.9891E-02	8.271	0.2786

PACKING SIZE =0.0380 M STATIC BED HEIGHT =0.440 M (CONTINUED)

G.KG/SQ.M-S	L.KG/SQ.M-S	REGAS	RELIQ	DP.MICRON	PT	ST	PTC.I/S	THEO.PT
2.858	9.416	11022.79	6558.91	2.50	0.2727	0.9891E-02	7.887	0.2786
2.858	9.416	11022.79	6558.91	2.50	0.2902	0.9891E-02	7.510	0.2786
2.858	9.416	11022.79	6558.91	2.50	0.2661	0.9891E-02	8.036	0.2786
2.858	9.416	11022.79	6558.91	3.50	0.1388	0.1905E-01	11.987	0.1147
2.858	9.416	11022.79	6558.91	3.50	0.1162	0.1905E-01	13.066	0.1147
2.858	9.416	11022.79	6558.91	3.50	0.0985	0.1905E-01	14.069	0.1147
2.858	9.416	11022.79	6558.91	4.50	0.0429	0.3118E-01	19.114	0.0400

PACKING SIZE =0.0380 M STATIC BED HEIGHT =0.440 M

G.KG/SQ.M-S	L.KG/SQ.M-S	REGAS	RELIQ	DP.MICRON	PT	ST	PTC.I/S	THEO.PT
2.891	18.832	10666.57	8060.66	0.35	0.8541	0.2591E-03	0.863	0.8804
2.891	18.832	10666.57	8060.66	0.35	0.8446	0.2591E-03	0.924	0.8804
2.891	18.832	10666.57	8060.66	0.45	0.8397	0.3969E-03	0.956	0.8357
2.891	18.832	10666.57	8060.66	0.45	0.9468	0.3969E-03	0.299	0.8357
2.891	18.832	10666.57	8060.66	0.55	0.8669	0.5636E-03	0.782	0.7882
2.891	18.832	10666.57	8060.66	0.55	0.8428	0.5636E-03	0.936	0.7882
2.891	18.832	10666.57	8060.66	0.55	0.7971	0.5636E-03	1.241	0.7882
2.891	18.832	10666.57	8060.66	0.70	0.7802	0.8680E-03	1.358	0.7139
2.891	18.832	10666.57	8060.66	0.70	0.7405	0.8680E-03	1.644	0.7139
2.891	18.832	10666.57	8060.66	0.70	0.7708	0.8680E-03	1.424	0.7139
2.891	18.832	10666.57	8060.66	0.90	0.7074	0.1375E-02	1.894	0.6140
2.891	18.832	10666.57	8060.66	0.90	0.7570	0.1375E-02	1.523	0.6140
2.891	18.832	10666.57	8060.66	0.90	0.7384	0.1375E-02	1.659	0.6140
2.891	18.832	10666.57	8060.66	0.90	0.6194	0.1375E-02	2.621	0.6140
2.891	18.832	10666.57	8060.66	1.10	0.4172	0.1996E-02	4.784	0.5175
2.891	18.832	10666.57	8060.66	1.10	0.5418	0.1996E-02	3.354	0.5175
2.891	18.832	10666.57	8060.66	1.10	0.5650	0.1996E-02	3.124	0.5175
2.891	18.832	10666.57	8060.66	1.10	0.3902	0.1996E-02	5.150	0.5175
2.891	18.832	10666.57	8060.66	1.35	0.3640	0.2935E-02	5.530	0.4073
2.891	18.832	10666.57	8060.66	1.35	0.3501	0.2935E-02	5.743	0.4073
2.891	18.832	10666.57	8060.66	1.35	0.3758	0.2935E-02	5.355	0.4073
2.891	18.832	10666.57	8060.66	1.75	0.1715	0.4811E-02	9.648	0.2626
2.891	18.832	10666.57	8060.66	1.75	0.1650	0.4811E-02	9.859	0.2626
2.891	18.832	10666.57	8060.66	1.75	0.2193	0.4811E-02	8.303	0.2626
2.891	18.832	10666.57	8060.66	1.75	0.1853	0.4811E-02	9.225	0.2626
2.891	18.832	10666.57	8060.66	2.50	0.0616	0.9569E-02	15.251	0.0978
2.891	18.832	10666.57	8060.66	2.50	0.0614	0.9569E-02	15.269	0.0978

PACKING SIZE =0.0380 M STATIC BED HEIGHT =0.440 M (CONTINUED)

G.KG/SQ.M-S	L.KG/SQ.M-S	REGAS	RELIQ	DP.MICRON	PT	ST	PTC.1/S	THEO.PT
2.891	18.832	10666.57	8060.66	2.50	0.0653	0.9569E-02	14.932	0.0978
2.891	18.832	10666.57	8060.66	2.50	0.0734	0.9569E-02	14.292	0.0978
2.891	18.832	10666.57	8060.66	3.50	0.0169	0.1843E-01	22.328	0.0194
2.891	18.832	10666.57	8060.66	3.50	0.0172	0.1843E-01	22.232	0.0194
2.891	18.832	10666.57	8060.66	4.50	0.0049	0.3016E-01	29.103	0.0029

TABLE D.2. Experimental Results for Silica Particles

PACKING SIZE =0.0380 M STATIC BED HEIGHT =0.440 M

G.KG/SQ.M-S	L.KG/SQ.M-S	REGAS	RELIQ	DP.MICRON	PT	ST	PTC.1/S	THEO.PT
2.860	4.708	11547.67	5750.05	2.50	0.4193	0.1182E-01	5.637	0.3965
2.868	9.416	11089.95	6862.45	2.50	0.2204	0.1142E-01	9.104	0.2088
2.882	14.124	10839.46	7695.62	2.50	0.1056	0.1119E-01	12.778	0.1101
2.886	18.832	10688.04	8390.35	2.50	0.0497	0.1105E-01	16.321	0.0582
2.915	23.540	10664.25	9091.06	2.50	0.0153	0.1101E-01	21.993	0.0305

TABLE D.3. Experimental Results for Latex Particles

PACKING SIZE =0.0380 M STATIC BED HEIGHT =0.440 M

G.KG/SQ.M-S	L.KG/SQ.M-S	REGAS	RELIQ	DP.MICRON	PT	ST	PTC.1/S	THEO.PT
2.806	4.708	11350.49	5813.10	2.00	0.6719	0.3712E-02	2.640	0.6831
2.818	9.416	10886.27	6899.45	2.00	0.5554	0.3576E-02	3.615	0.5273
2.829	14.124	10627.45	7718.79	2.00	0.4220	0.3501E-02	5.007	0.4068
2.834	18.832	10477.06	8376.93	2.00	0.3676	0.3455E-02	5.552	0.3169
2.862	23.540	10456.02	8997.76	2.00	0.1968	0.3444E-02	8.721	0.2503

TABLE D.4. Experimental Results for DOP Particles

PACKING SIZE =0.0380 M STATIC BED HEIGHT =0.440 M

G.KG/SQ.M-S	L.KG/SQ.M-S	REGAS	RELIQ	DP.MICRON	PT	ST	PTC.1/S	THEO.PT
2.856	4.708	11514.99	5858.87	2.50	0.5954	0.5249E-02	3.370	0.6044
2.853	9.416	11017.77	7033.98	2.50	0.3857	0.5085E-02	5.774	0.4193
2.880	14.124	10787.23	7886.35	2.50	0.3280	0.4976E-02	6.375	0.2956
2.871	18.832	10612.73	8554.08	2.50	0.2154	0.4917E-02	8.404	0.2096
2.894	23.540	10563.88	9192.21	2.50	0.1642	0.4908E-02	9.595	0.1505

Listing of Program Used to Calculate Penetration with Diffusiophoresis:

```
C
C       NOMENCLATURE
C
C       CSAOC : CROSS-SECTIONAL AREA OF THE COLUMN , M2.
C       DELTA : STIRRING NUMBER
C       EG    : GAS VOIDAGE, M3/M3.
C       EPBST : VOLUME FRACTION OF PACKING AT STATIC CONDITION , M3/M3.
C       G     : GAS MASS FLUX, KG/M2-S.
C       GMF   : GAS MINIMUM FLUIDIZATION VELOCITY, KG/M2-S.
C       H     : EXPANDED BED HEIGHT, M.
C       HLH   : LIQUID HOLD-UP, M3 WATER/M3 OF EXPANDED BED VOLUME.
C       HLHST : LIQUID HOLD-UP, M3 WATER/M3 OF STATIC BED VOLUME.
C       HST   : STATIC BED HEIGHT, M.
C       HUM   : HUMIDITY, KG WATER VAPOR/KG AIR.
C       KPSC  = PARTICLE TRANSFER COEFF. FOR SPRAY COLUMN, 1/S
C       L     : LIQUID MASS FLUX, KG/M2-S.
C       DP    : PARTICLE DIAMETER, MICRON.
C       DPB   : PACKING BALL DIAMETER, M2.
C       PN    : PARTICLE CONCENTRATION, #/M3
C       PSTAT : STATIC GAS PRESSURE AT INLET
C       PT    : PENETRATION.
C       PTC   : PARTICLE TRANSFER COEFFICIENT, 1/S.
C       QG    : VOLUMETRIC GAS FLOW RATE, FT3/S.
C       QGSI  : VOLUMETRIC GAS FLOW RATE, M3/S
C       REG   : GAS REYNOLDS NUMBER.
C       REL   : LIQUID REYNOLDS NUMBER.
C       ROGIN : GAS DENSITY AT INLET, KG/M3.
C       ROGOUT: GAS DENSITY AT OUTLET, KG/M3.
C       ROL   : WATER DENSITY, KG/M3.
C       ROP   : PARTICLE DENSITY, KG/M3.
C       ST    : STOKE,S NUMBER
C       TDB   : DRY-BULB GAS TEMPERATURE , F.
C       TWB   : WET-BULB GAS TEMPERATURE, F.
C       TL    : LIQUID TEMPERATURE, F.
C       UGO   : SUPERFICIAL GAS VELOCITY , M/S.
C       UGI   : INTERSTITIAL GAS VELOCITY, M/S.
C       ULO   : SUPERFICIAL LIQUID VELOCITY, M/S.
C       ULI   : INTERSTITIAL LIQUID VELOCITY , M/S.
C       UR    : RELATIVE VELOCITY, M/S.
C       VISCG : VISCOSITY OF GAS, KG/M-S, PA-S.
C       VISCL : VISCOSITY OF WATER, KG/M-S, PA-S.
C       PT.EXPT  : EXPERIMENTAL PENETRATION
C       PT.INER  : PENETRATION DUE TO ONLY INERTIAL MECHANISM.
C       PTD.1    : DIFFUSIOPHORETIC PENETRATION EVALUATED BY SCHIMITT- VALDMAN
C                  VELOCITY
C       PT.TOT.1 = PT.INER * PTD1
C       PTD.2    : DIFFUSIOPHORETIC PENETRATION EVALUATED BY MASS VELOCITY
C       PT.TOT.2 = PT.INER * PTD2
C       PTD.3    : DIFFUSIOPHORETIC PENETRATION EVALUATED BY MOLAR VELOCITY
C       PT.TOT.3 = PT.INER * PTD3
C
0001            DIMENSION X(6),Y(6)
0002            REAL L
0003            READ(5,9) ROP
```

```
0004          9     FORMAT(F10.0)
0005                READ(5,10) CSAOC,EPBST,ROL
0006          10    FORMAT(3F10.0)
0007                READ(5,11) (X(I),I=1,6)
0008          11    FORMAT(6F10.0)
0009                READ(5,12) (Y(I),I=1,6)
0010          12    FORMAT(6E10.8)
0011          79    READ(5,17,END=80)DPB,HST
0012          17    FORMAT(2F10.0)
0013                WRITE(6,51) DPB,HST
0014          51    FORMAT(1H1,/,5X,'PACKING SIZE =',F6.4,1X,'M',10X,'STATIC BED HEIGH
                   1T =',F5.3,1X,'M',//)
0015                WRITE(6,55)
0016          55    FORMAT(6X,'G',9X,'L',7X,'HUMIN',5X,'HUMOUT',6X,'DP',6X,'PT.EXPT',3
                   1X,'PT.INER',4X,'PTD.1',3X,'PT.TOT.1',4X,'PTD.2',3X,'PT.TOT.2',4X,'
                   1PTD.3',3X,'PT.TOT.3',//)
0017                READ(5,15) NRUN
0018          15    FORMAT(I2)
0019                LINE=0
0020                DO 70 IN=1,NRUN
0021                READ(5,18)USGPM
0022          18    FORMAT(F10.0)
0023                READ(5,19)DPOR,PS1,TDBIN,TWBIN,TDBOUT,TWBOUT,TLIN,TLOUT
0024          19    FORMAT(8F10.0)
              C     CALCULATION OF GAS FLOW RATE
0025                PSTAT=406.+PS1/2.54
0026                HUMIN=HUMID(TDBIN,TWBIN)
0027                HUMOUT=HUMID(TDBOUT,TWBOUT)
0028                ROG=1.75635*(1.+HUMIN)*PSTAT/((18.+29.*HUMIN)*(460.+TDBIN))
0029                ROGSI=ROG*16.03
0030                QG=.9853865*(1.-.32*DPOR/PS1)*(DPOR/ROG)**.5
0031                QGSI=QG*.3048**3.
0032                GIN=QG*ROG*.454/CSAOC
0033                GOUT=GIN*(1.+HUMOUT)/(1.+HUMIN)
0034                G=(GIN-GOUT)/ALOG(GIN/GOUT)
              C     CALCULATION OF LIQUID FLOW RATE
0035                L=.9416*USGPM
              C     CALCULATION OF MINIMUM GAS FLUIDIZATION VELOCITY
0036                GMF=10.86*DPB**.488*10.**(-.01985*L)
              C     CALCULATION OF THE BED HEIGHT
0037                DELTA=(G-GMF)/GMF
0038                HCOR=.14681*DELTA*GMF/HST
0039                H=(1.+HCOR)*HST
              C     CALCULATION OF LIQUID HOLD-UP
0040                HLHST=1.15E-04*L**.826*DPB**(-1.289)
0041                HLH=HLHST*HST/H
              C     CALCULATION OF GAS AND LIQUID VELOCITIES
0042                ROGIN=ROGSI
0043                DELPC=112.17*L**.44*DPB**(-.492)*HST
0044                DELPC=DELPC*2.54/248.84
0045                PSTOUT=PSTAT-DELPC
0046                ROGOUT=1.75635*(1.+HUMOUT)*PSTOUT/((18.+29.*HUMOUT)*(460.+TDBOUT))
0047                ROGOUT=ROGOUT*16.03
0048                ROG=(ROGIN+ROGOUT)/2.
```

```
0049                UGIN=GIN/ROGIN
0050                UGOUT=GOUT/ROGOUT
0051                UGO=(UGIN+UGOUT)/2.
0052                EPB=EPBST*HST/H
0053                EG=1.-HLH-EPB
0054                UGI=UGO/EG
0055                ULO=(L+((GIN-GOUT)/2.))/ROL
0056                ULI=ULO/HLH
0057                UR=UGI+ULI
                C   CALCULATION OF WATER VISCOSITY
0058                TL=(TLIN+TLOUT)/2.
0059                TLC=((TL-32.)/1.8)-8.435
0060                RECV=2.1482*(TLC+(8078.4+(ABS(TLC))**2.)**.5)-120.
0061                VISCL=1./(10.*RECV)
                C   CALCULATION OF GAS VISCOSITY
0062                TG=(TDBIN+TDBOUT)/2.
0063                VISCG=FLAGR(X,Y,TG,1,6)
                C   CALCULATION OF DIMENSIONLESS NUMBERS
0064                REG=DPB*UGI*ROG/VISCG
0065                REL=DPB*ULI*ROL/VISCL
0066                READ(5,21)KRUN
0067           21   FORMAT(I2)
0068                DO 75 J=1,KRUN
0069                READ(5,20)DP,PNIN,PNOUT
0070           20   FORMAT(3F10.0)
0071                C=1.+(2.E-08*((460.+TG)/1.8)/(DP*1.E-04))*(2.79+.894*EXP(-2.47E+07
                1*DP*1.E-04/((460.+TG)/1.8)))
0072                ST=C*((DP*1.E-06)**2.)*ROP*UR/(9.*VISCG*DPB)
                C   CALCULATION OF PARTICLE PENETRATION
0073                PTTOT=PNOUT/PNIN
0074                PTEXPT=PTTOT*GOUT*ROGIN/(GIN*ROGOUT)
0075                ULNOZ=0.32345*USGPM
0076                URNOZ=ULNOZ+UGOUT
0077                D30=0.65*(10*VISCG)**0.2/URNOZ
0078                RED=D30*URNOZ*ROGOUT/VISCG
0079                CDRAG=18.5/RED**0.6
0080                IF(RED.LT.2.) CDRAG=24./RED
0081                IF(RED.GE.500.) CDRAG=0.44
0082                UTERMG=(RED/CDRAG*13.076*VISCG*(1000.-ROGOUT)/ROGOUT**2.)**(1./3.)
0083                STD=C*((DP*1.E-06)**2.)*ROP*UTERMG/(9.*VISCG*D30)
0084                KPSC=0.0165*L**1.508*G**0.745*STD**(-0.413)
0085                PTSC=EXP(-1*KPSC*(1.5-H)/UGOUT)
0086                PT=PTEXPT/PTSC
                C   OUTPUT OF THE CALCULATED RESULTS
0087           75   CONTINUE
0088                PTCTH=3764.762285*ST**.80477*REG**(-2.64264)*REL**2.10754*(HST/DPB
                1)**1.52217
0089                PTTHEO=EXP(-PTCTH*H/UGO)
0090                RMS=29./18.
0091                SQRMS=RMS**0.5
0092                PTD1=(1.+SQRMS*HUMOUT)/(1.+SQRMS*HUMIN)
0093                PTD2=(1.+HUMOUT)/(1.+HUMIN)
0094                PTD3=(1.+RMS*HUMOUT)/(1.+RMS*HUMIN)
0095                PTOTD1=PTTHEO*PTD1
```

```
                PTOTD2=PTTHEO*PTD2
                PTOTD3=PTTHEO*PTD3
                WRITE(6,53) G,L,HUMIN,HUMOUT,DP,PT,PTTHEO,PTD1,PTOTD1,PTD2,PTOTD2,
               1PTD3,PTOTD3
     53         FORMAT(13F10.4,/)
                LINE=LINE+1
                IF(LINE.LT.27) GO TO 70
                WRITE(6,54) DPB,HST
     54         FORMAT(1H1,/,5X,'PACKING SIZE =',F6.4,1X,'M',10X,'STATIC BED HEIGH
               1T =',F5.3,1X,'M',5X,'(CONTINUED)',//)
                LINE=0
     70         CONTINUE
                GO TO 79
     80         STOP
                END
```

TABLE D.5. Experimental Results and Estimated Penetration of Ferrous Sulphate Particles in MBC at Conditions with Diffusiophoresis

PACKING SIZE =0.0380 M STATIC BED HEIGHT =0.440 M

G	L	HUMIN	HUMOUT	DP	PT.EXPT	PT.INER	PTD.1	PT.TOT.1	PTD.2	PT.TOT.2	PTD.3	PT.TOT.3
2.1319	4.7080	0.2888	0.0061	1.7500	0.3852	0.5084	0.7374	0.3749	0.7806	0.3969	0.6891	0.3504
2.1319	4.7080	0.2888	0.0061	2.5000	0.2599	0.3092	0.7374	0.2280	0.7806	0.2413	0.6891	0.2131
2.1319	4.7080	0.2888	0.0061	3.5000	0.0919	0.1372	0.7374	0.1012	0.7806	0.1071	0.6891	0.0946
2.1713	9.4160	0.2890	0.0056	1.7500	0.2152	0.2593	0.7368	0.1910	0.7801	0.2023	0.6885	0.1785
2.1713	9.4160	0.2890	0.0056	2.5000	0.0814	0.0961	0.7368	0.0708	0.7801	0.0750	0.6885	0.0662
2.1713	9.4160	0.2890	0.0056	3.5000	0.0296	0.0193	0.7368	0.0140	0.7801	0.0148	0.6885	0.0131
2.1918	14.1240	0.2894	0.0056	1.7500	0.0965	0.1112	0.7366	0.0819	0.7799	0.0867	0.6882	0.0765
2.1918	14.1240	0.2894	0.0056	2.5000	0.0187	0.0221	0.7366	0.0163	0.7799	0.0172	0.6882	0.0152
2.1918	14.1240	0.2894	0.0056	3.5000	0.0069	0.0016	0.7366	0.0012	0.7799	0.0012	0.6882	0.0011
2.2041	18.8320	0.2891	0.0049	1.7500	0.0313	0.0364	0.7361	0.0371	0.7795	0.0393	0.6876	0.0347
2.2041	18.8320	0.2891	0.0049	2.5000	0.0102	0.0056	0.7361	0.0041	0.7795	0.0044	0.6876	0.0039
2.2041	18.8320	0.2891	0.0049	3.5000	0.0076	0.0002	0.7361	0.0001	0.7795	0.0001	0.6876	0.0001
2.2167	23.5400	0.2890	0.0046	1.7500	0.0214	0.0268	0.7359	0.0197	0.7794	0.0209	0.6874	0.0184
2.2167	23.5400	0.2890	0.0046	2.5000	0.0034	0.0019	0.7359	0.0014	0.7794	0.0015	0.6874	0.0013
2.2167	23.5400	0.2890	0.0046	3.5000	0.0028	0.0000	0.7359	0.0000	0.7794	0.0000	0.6874	0.0000

APPENDIX E

CALIBRATION OF THE AIR ORIFICE METER

A square-edged stainless steel orifice supplied by Foxboro Corp. was used to measure the air flow rate. It was mounted to the 0.216 m ID (8.5") pipe. The inside diameter of the orifice was 0.1238 m (4.875"). The ratio of the diameters is, therefore,

$$\beta = 0.57353$$

Pressure taps were flange type.

Total volumetric flow rate through the orifice is given by

$$Q_G = \frac{\pi d_o^2}{4} F_a Y \frac{C}{\sqrt{1 - \beta^4}} \sqrt{2 \frac{\Delta P}{\rho}} \qquad (E.1)$$

where F_a is the thermal expansion factor of the orifice metal. For the purpose of the present study it can be taken as one (page 156, ASME (1971)). Y is the expansion factor for gases and can be written as

$$Y = 1 - (0.41 + 0.35\ \beta^4)\ \Delta P/P_1\gamma \qquad (E.2)$$

P is the pressure drop across the orifice and P_1 the static pressure measured at the inlet pressure tap.

Since, for air, the ratio of specific heats of the gas, γ, can be taken as 1.4

$$Q_G = \frac{\pi d_o^2}{4} (1 - 0.32\ \Delta P/P_1) \frac{C}{0.94435} \sqrt{2\ \Delta P/\rho} \qquad (E.3)$$

In order to determine the actual volumetric flow rate, employing the method of "centroid of equal areas" the air velocities at 5 positions corresponding to $r/r_c = 0.3162$, 0.5477, 0.7071, 0.8367 and 0.9487 were measured by a 0.0079375 m (5/16") standard pitot-tube and a micromanometer. Using the average of these velocities, the actual air flow rate is calculated by

$$Q_G = u_{avg}\ \pi d_c^2/4 \qquad (E.4)$$

Using this value, coefficient of discharge for the orifice, C, is evaluated from Equation (E.3) for 12 runs corresponding to different flow rates. The results are given in Table E.1. The average of these values is 0.6259 and this value for G is used in Equation (E.3) to calculate the air flow rate in all the experiments.

TABLE E.1 Experimental Results for the Air Orifice Calibration

Run #	Actual Flow Rate, m^3/s	C
1	.4694	.619374
2	.4611	.616511
3	.4438	.618386
4	.4145	.613558
5	.3878	.62426
6	.3458	.60371
7	.3341	.62963
8	.3064	.627314
9	.2759	.635376
10	.239	.632013
11	.1945	.645902
12	.1537	.645105

APPENDIX F

DESIGN OF THE ENTRAINMENT SEPARATOR

Figure F.1 shows a typical zigzag baffle arrangement. Assuming that particles or droplets are collected at the surface of the baffle due to the centrifugal force created during change of direction of gas flow, Jashnani (1975) offered the following model to predict the collection efficiency of zigzag baffles.

$$E = 1 - \exp(- u_t' n\ w\ \theta / u_G\ b\ \tan\ \theta) \qquad (F.1)$$

where, u_t = drop terminal velocity

n = number of rows (layers) of baffles

w = width of the baffle

θ = angle of the baffle from flow direction, radian

b = distance between the baffles

For calculation of terminal velocity, centrifugal acceleration, a, should be used.

$$a = 2u_G^2/\cos^2\theta\ w\ \cot\ \theta \qquad (F.2)$$

This model implies that the design variables that affect performance of the zigzag baffle are the number of rows, width of the baffle, distance between the baffles and the angle θ. By testing various values for these variables in order to get poor collection for

the maximum particle size used in this study (5.5 μm) and good collection for liquid droplets, in the order of a few hundred microns in size, the following values have been found to be the optimum.

$\theta = 30^{o}$

$n = 4$

$w = .06$ m

$b = .04$ m

Table F.1 gives the predicted efficiencies for various droplet sizes and superficial gas velocities, using the above values and Equation (F.1).

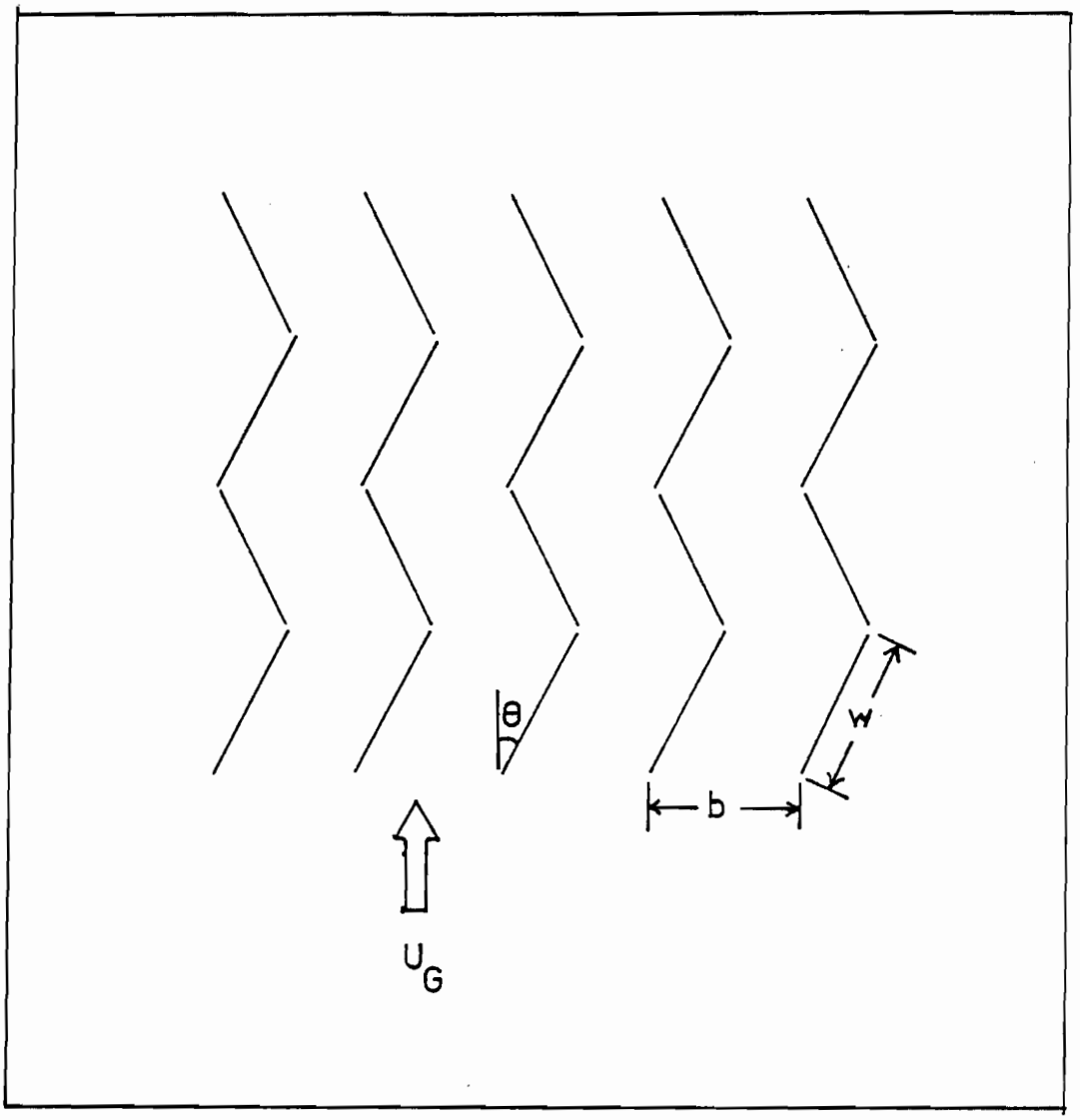

FIGURE F.1. Zigzag baffles

TABLE F.1 Predicted Collection Efficiencies for Zigzag Baffles Used as Entrainment Separator for the Mobile-Bed Contactor

Per cent efficiency as a function of particle diameter and gas velocity.

TETA = 30. BN = 4. W = 6. B = 4.0

Particle diameter in microns, d_p

Gas Velocity, u_G cm per sec	0.3	0.6	1.0	3.0	6.0	10.0	25.0	50.0	100.0	200.0	400.0	800.0
100.	0.01	0.03	0.08	0.68	2.71	7.34	37.88	85.11	99.23	100.00	100.00	100.00
200.	0.01	0.05	0.15	1.36	5.34	14.13	61.42	94.86	99.86	100.00	100.00	100.00
300.	0.02	0.08	0.23	2.04	7.90	20.43	76.03	97.07	99.96	100.00	100.00	100.00
400.	0.03	0.11	0.30	2.71	10.39	26.27	83.62	98.16	99.99	100.00	100.00	100.00
500.	0.03	0.14	0.38	3.37	12.81	31.68	86.34	98.77	99.99	100.00	100.00	100.00
600.	0.04	0.16	0.46	4.03	15.17	36.69	88.38	99.14	100.00	100.00	100.00	100.00
700.	0.05	0.19	0.53	4.69	17.47	41.33	89.97	99.38	100.00	100.00	100.00	100.00

APPENDIX G

CALIBRATION OF THE PRESSURE TRANSDUCER

Calibration of the pressure transducer used for pressure drop measurements across the column was made by a simple U-tube manometer filled with water. It was carried out at static conditions. The results are presented in Table G.1 and in Figure G.1. The straight line in Figure G.1 corresponds to the following equation:

$$\Delta P = 1.27638(mV - 10) \qquad (G.1)$$

where pressure drop is given in units "cm H_2O".

TABLE G.1 Calibration of the Pressure Transducer

ΔP, cm H_2O	mV
.0	10.00
.53	10.46
1.32	11.03
2.51	11.91
3.6	12.78
5.41	14.14
6.68	15.16
8.15	16.32
8.2	16.34
9.68	17.53
11.43	18.89
13.05	20.25
15.16	21.8
17.02	23.21
19.23	24.96
21.26	26.57
23.82	28.43
26.44	30.5
27.79	31.69
29.95	33.45
31.5	34.6
33.15	35.88
34.72	37.22
36.6	38.73
37.82	39.68
39.55	41.07

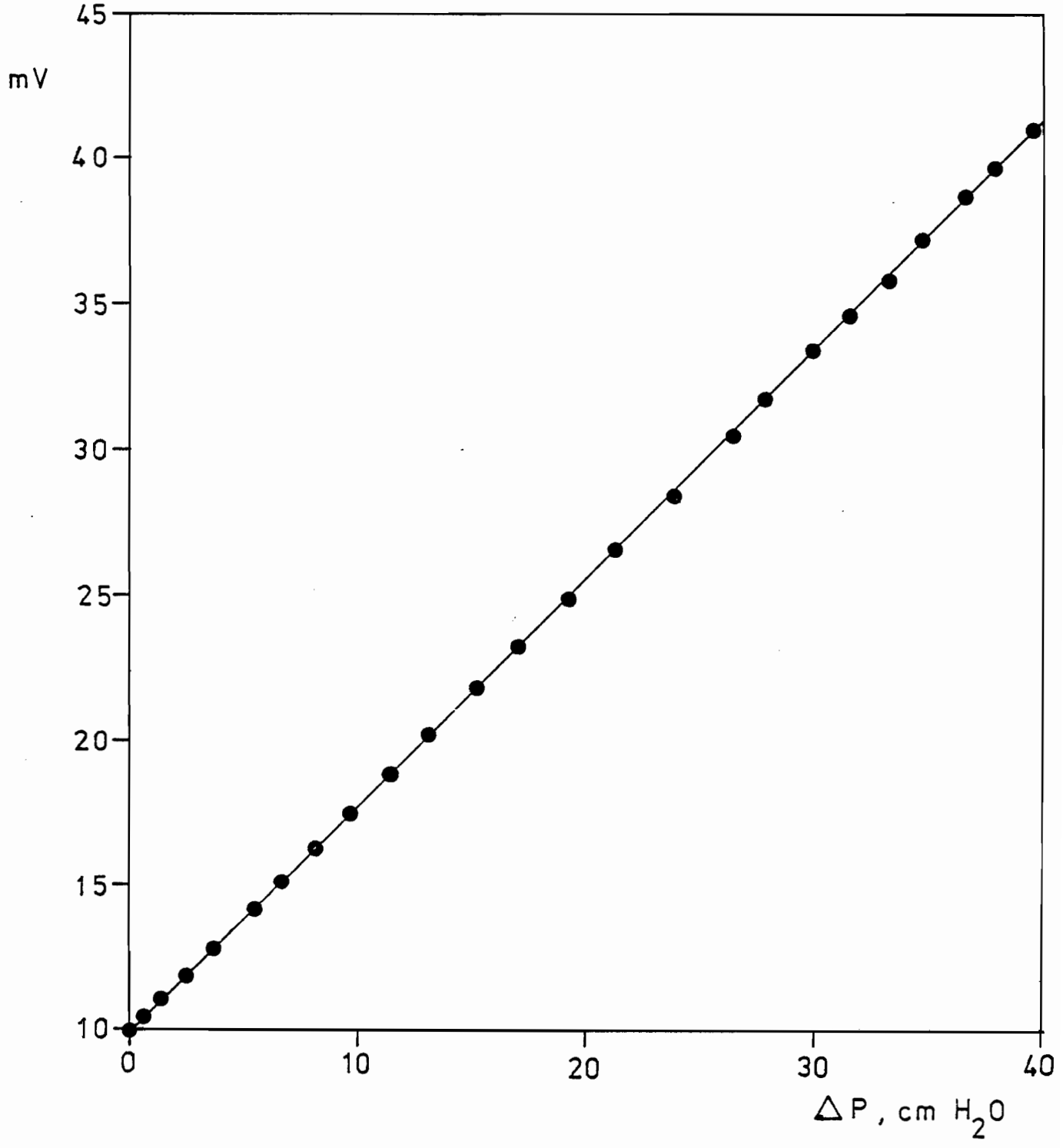

FIGURE G.1. Calibration line of the pressure transducer

APPENDIX H

PRIME CALIBRATION OF THE PARTICLE COUNTER

The Royco Model 202 particle counter must be calibrated periodically. The manufacturers suggest calibration at six month intervals. Due to the high level of use in the present study, this check was made every two weeks. During the whole course of the present work the counter showed a steady and dependable performance.

Prime calibration is carried out by passing particles of known size through the particle counter, comparing the indicated size distribution with a known distribution, and making any necessary calibration adjustments.

Polystyrene latex particles produced by Mr. M. Inoue, Pulp and Paper Research Institute of Canada, were used in this process. These particles were spherical, exceptionally monodispersed and with known physical constants, such as density (1.05 gm/cm^3) and index of refraction (1.595). Three different sizes (0.482, 1.06 and 2.0 μm*) were used. Figure H.1 shows electron micrographs of 0.482 and 1.06 μm particles. The high monodispersity of these latex particles, as shown in this photograph, provides a dependable test for calibrating the particle counter.

These latex particles were dispersed by filtered and compressed dry air stream using a particle generator shown in Figure H.2. The input air causes a partial reduction in pressure over the jet which is half submerged into the aerosol solution so that the aerosol solution

---

* Other 2.0 μm latex particles supplied by Dow Chemical Co. were also used for prime calibration.

is drawn out of the jet and dispersed as a fine mist in which latex particles are carried. By passing the mist through a dryer tube, water evaporates and the end result is a fine dispersion of the latex particles.

From the dryer tube the particles go into the counter. Monitoring the size ranges around the known size of the latex particles, the necessary adjustments to the particle counter can be made so that the size distribution obtained by the counter coincides with the known distribution of the particles. Details of these adjustments are discussed in the manufacturers' service manual.

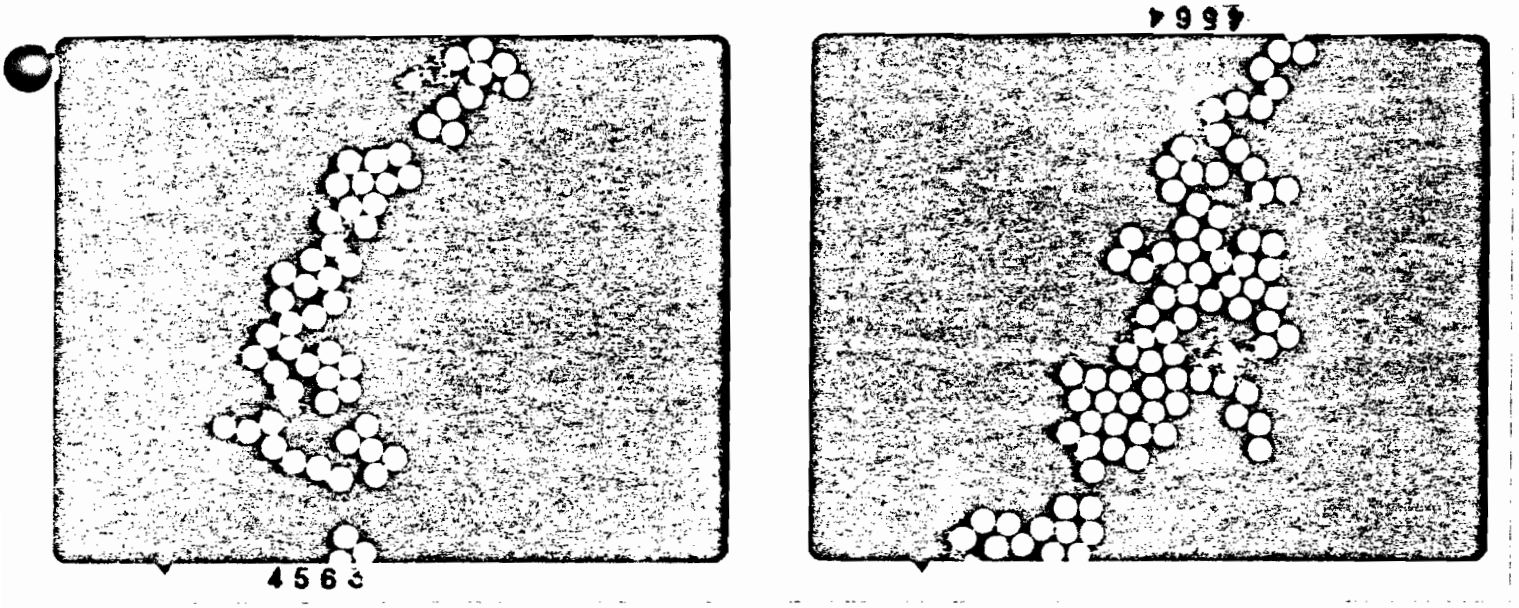

d_p=.482 microns

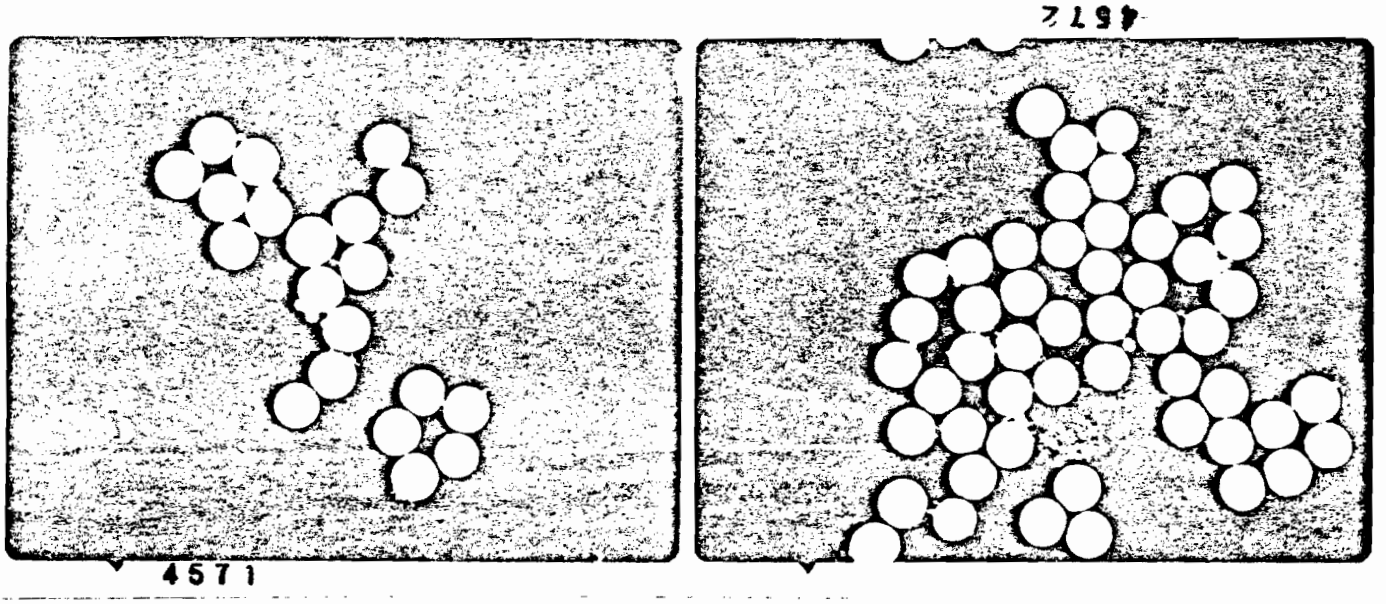

d_p=1.06 microns

FIGURE H.1. Scanning electron microscope photographs of latex particles Magnification 6307 X

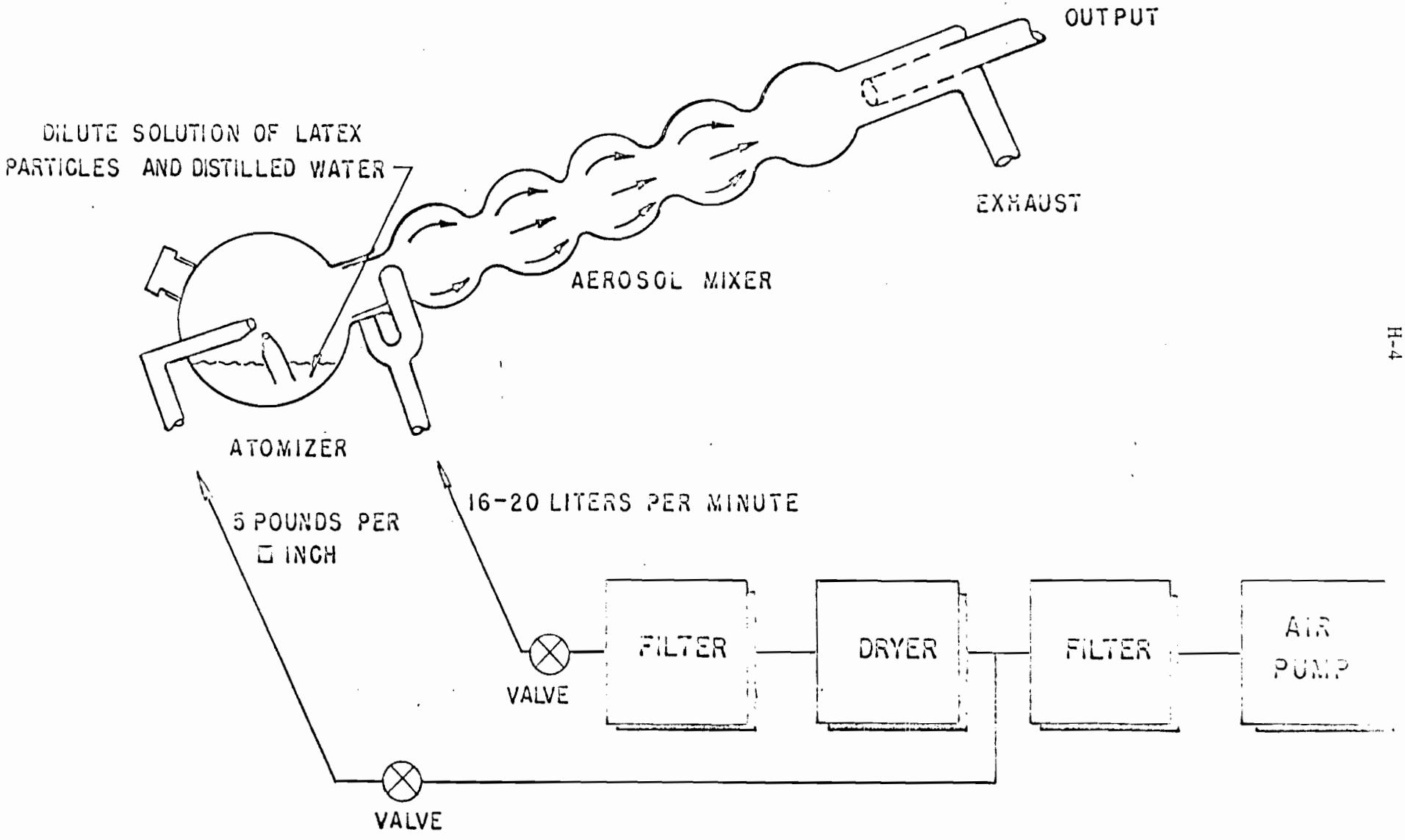

FIGURE H.2. Generator for making an aerosol containing latex particles in air

APPENDIX I

CALIBRATION OF THE SAMPLING SYSTEM

A sampling system was designed to provide isokinetic sampling conditions for particle analysis (Figure 5.11). Decrease of velocity of the aerosol stream while passing through the diverging section of this set-up overcame the difficulty imposed by the constant sampling rate requirement of the Royco particle counter. Since the velocity in the secondary sampling probe, which was connected to the counter, was always constant, 0.4 m/s, by sliding this probe inward or outward the position of its tip was adjusted at the point where the velocity of the main sampled aerosol stream was also 0.4 m/s. In order to speed up this procedure during the experiments a graph was prepared (Figure I.1). After the sampling flow rate was calculated from the velocity measurements at the inlet or outlet of the mobile-bed column, and the rotameter was adjusted accordingly, using this flow rate, the position of the secondary probe was found from Figure I.1 and necessary adjustment was made.

The rotameter used in the sampling system was manufactured by Brooks Inst. Div., Emerson Electric Co., Markham, Ontario, (Tube No. R-6-25-B, steel float). It was calibrated using a dry test-meter. Calibration curve is given in Figure I.2.

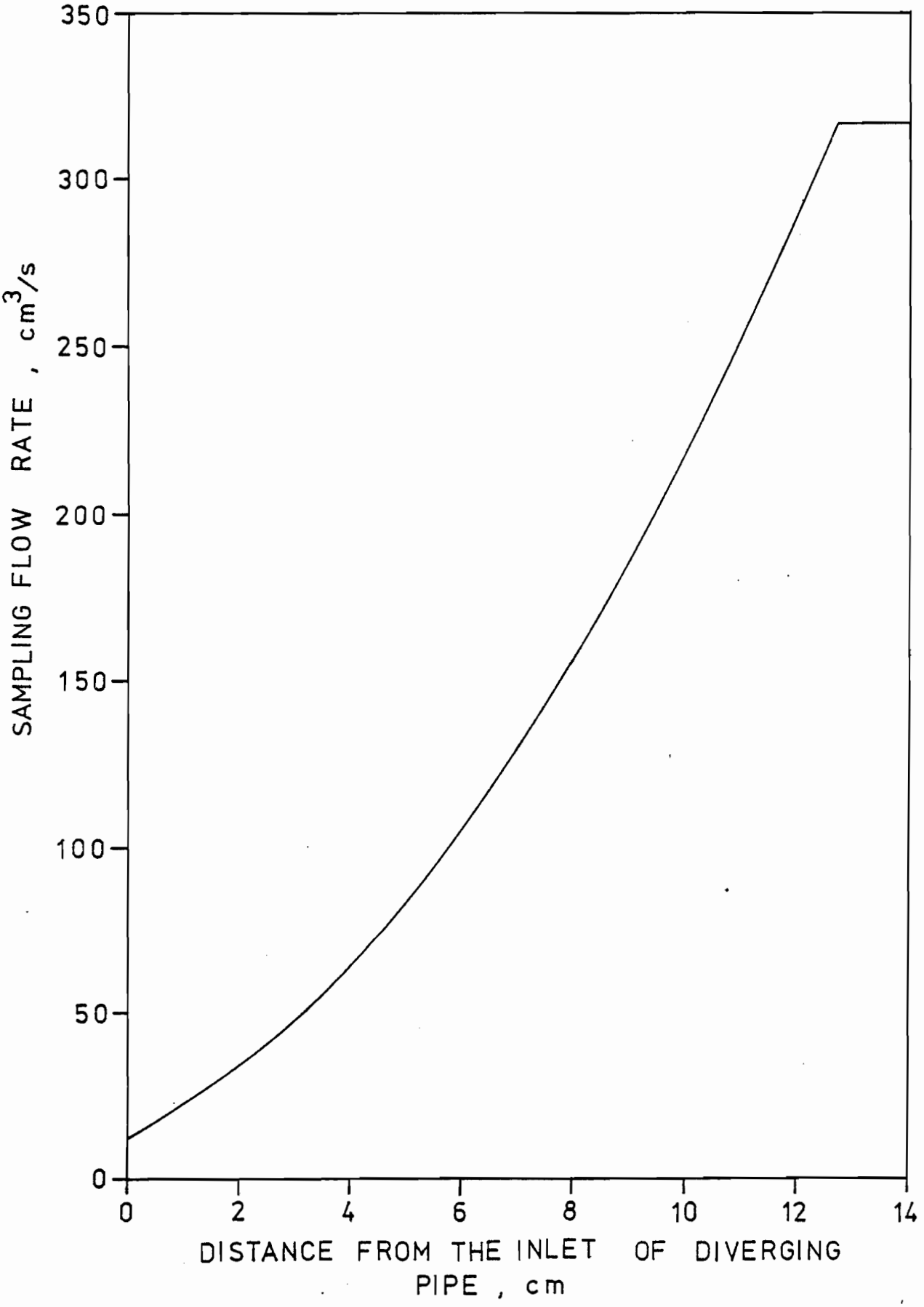

FIGURE I.1. Graph to locate the position of the sliding secondary probe

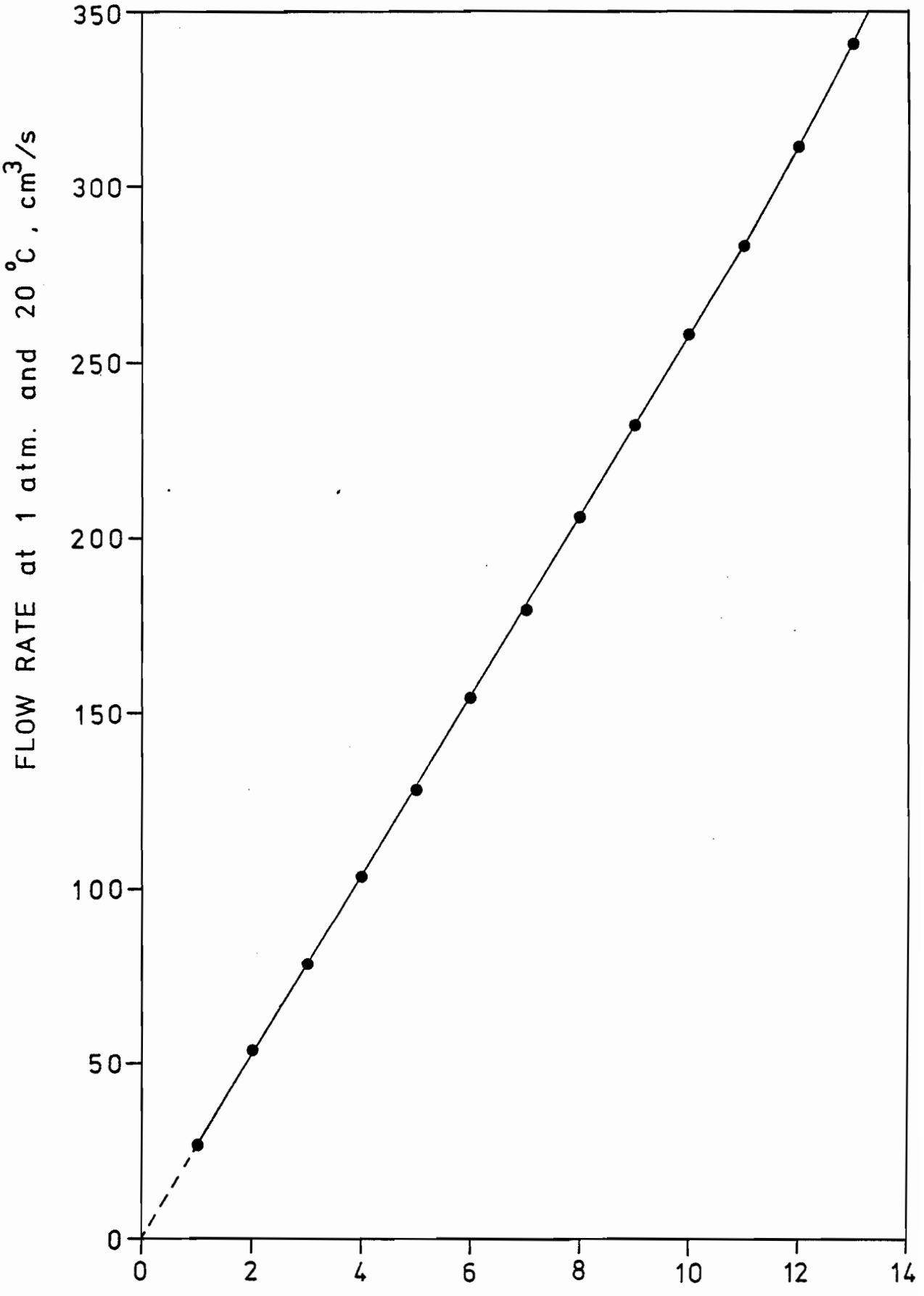

FIGURE I.2. Calibration curve for the air rotameter in the particle sampling system

APPENDIX J

PRESSURE DROP AND PARTICULATE RECOVERY STUDIES IN A SPRAY COLUMN

In order to account for particle collection between the liquid distributor and the top of the mobile-bed, and thus to evaluate particle penetration in active MBC volume from Equation 6.2, the amount of particle collection in the spray column section above the bed must be known. For this reason, the packing was removed so that the entire column of the present study then served as a spray column of height 1.5 m between the liquid inlet distributor and the lower support grid. The results of pressure drop measurements and particle collection experiments are discussed below.

J.1. Pressure Drop

As the assumptions summarized at the beginning of section 6.1.2 are also valid for a spray column, the overall momentum balance yields the following equation:

$$\Delta P = \rho_L \, h_L \, g \, H \qquad (J.1)$$

Liquid holdup in a spray column can be expressed as

$$h_L = L/\rho_L \, u_{Ld} \qquad (J.2)$$

where u_{Ld} is the velocity of liquid droplets with respect to a stationary coordinate system, i.e.

$$u_{Ld} = u_T - u_G \qquad (J.3)$$

Combining Equations J.1, 2 and 3:

$$\Delta P = L\ g\ H/(u_T - u_G) \tag{J.4}$$

In order to estimate the terminal velocity of drops, u_T, required for Equation J.4, the size of the drops should be known. This was evaluated using the equation suggested by Merrington and Richardson (1947),

$$d_{30} = \frac{500}{u_r} \left(\frac{\mu_L}{\rho_L}\right)^{0.2} \tag{J.5}$$

Volume mean diameters thus evaluated were used to find u_T,

$$u_T = (\rho_L - \rho_G) g\ d_{30}^2/18\ \mu_G \tag{J.6}$$

which was then used to calculate pressure drop from Equation J.4.

The agreement between measured pressure drop values and those obtained by Equation J.4 for low and intermediate liquid flow rates ($L = 4.7$, 9.4 and 14.1 kg/m^2-s) is very satisfactory. Figure J.1 shows experimental data for these liquid flow rates and the predictions made by Equation J.4 (solid lines).

At high liquid flow rates (18.8 and 23.5 kg/m^2-s), however, the model described above predicts lower pressure drops than measured experimentally. This is not surprising because liquid holdup at such very high liquid flow rates can no longer be evaluated by Equation J.2, due to the change in break-up length of liquid jets, which changes the overall characteristics of the column. In fact, such high liquid flow rates are not common for a conventional spray column. Nevertheless,

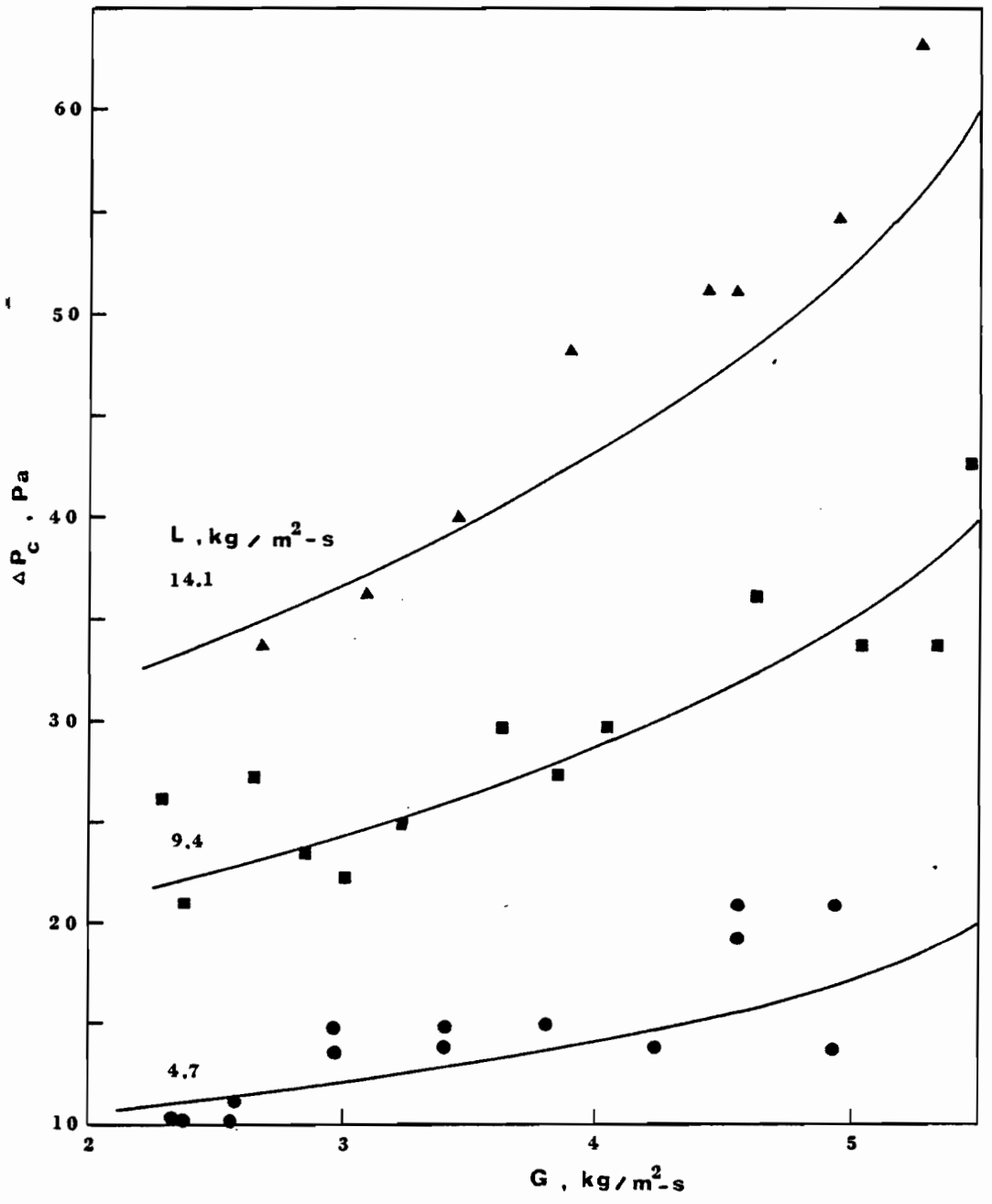

FIGURE J.1. Pressure drop in the spray column

pressure drop data for these high liquid flow rates were correlated by two following equations:

For $L = 18.8$ kg/m^2-s

$$\Delta P = 35.1\ G - 25.9 \qquad (J.7)$$

For $L = 23.5$ kg/m^2-s

$$\Delta P = 30.8\ G + 101.7 \qquad (J.8)$$

J.2. Particulate Recovery

A model for particle collection in a spray tower can be derived by making a material balance over a differential element of volume. This procedure requires the following basic assumptions:

1) Operation is steady state;
2) Water droplets are dispersed uniformly throughout the tower volume;
3) No droplet interactions exist and the overall collection efficiency can be computed by integrating over all of the individual drops;
4) All liquid drops are assumed to be spherical, i.e. no distortions

Using assumption 2, material balance over differential volume element gives:

$$u_G\ S_c\ n_p/z - u_G\ S_c\ n_p/z+\Delta z = C_d\{E_m\ n_p\ u_T\ \frac{\pi\ d_{30}^2}{4}\}S_c\ dz \qquad (J.9)$$

where C_d is the droplet concentration and E_m is the mean droplet efficiency. Integrating Equation J.9

$$Pt = \exp \{-C_d \, E_m \, u_T \, \pi \, d_{30}^2 \, H/4 \, u_G\} \tag{J.10}$$

Due to assumptions 3 and 4, concentration of the droplets in the column is

$$C_d = h_L/(\pi \, d_{30}^3/6) \tag{J.11}$$

or,

$$C_d = 6 \, L/\rho_L \, (u_T - u_G)\pi \, d_{30}^3 \tag{J.12}$$

Substituting Equation J.12 into J.10:

$$Pt = \exp \{- \frac{3}{2} \frac{Q_L}{Q_G} \frac{u_T}{(u_T - u_G)} \frac{E_m \, H}{d_{30}}\} \tag{J.13}$$

Sparks (1971) obtained the same equation by a different approach. By choosing a cylindrical axial volume with diameter equal to volume mean droplet diameter in the column, he arrived at the same expression for particle penetration given as Equation J.13. It may be noted that E_m in this equation can be predicted theoretically, as explained in section 2.2.1.1. Figure J.2 shows the dependence of E_m on Stokes number and is computed theoretically by Allen (1975).

Instead of using this expression directly to evaluate penetration in the spray section, experiments with ferrous sulphate particles were performed to verify the validity of the expression for Pt. It was found that the use of Equation J.13 did not predict the experimental results. The first aspect to be questioned was the validity of Equation J.5 to evaluate volume mean diameter of droplets. However, the

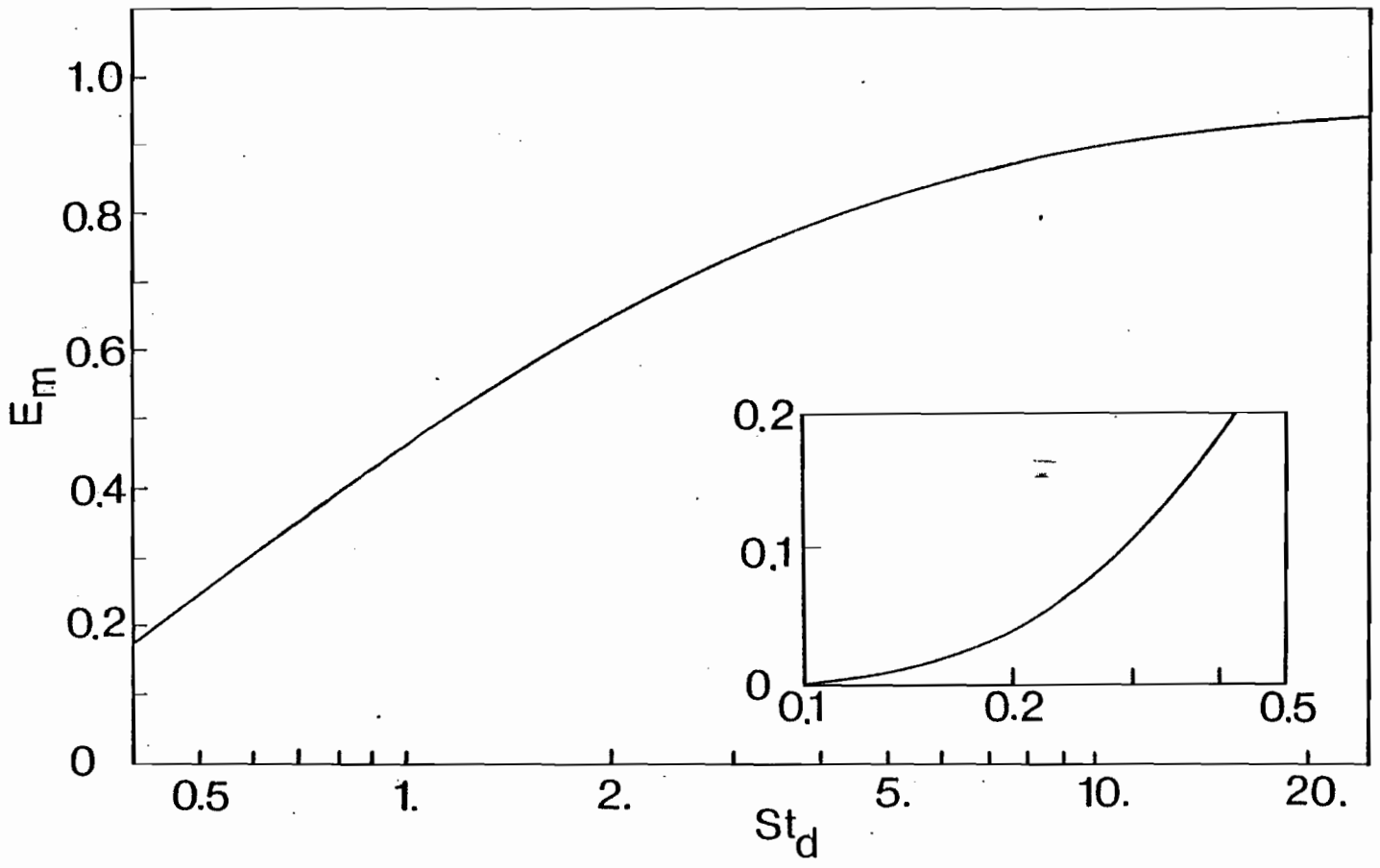

FIGURE J.2. Dependence of theoretical particle collection efficiency of liquid droplets on Stokes number

pressure drop predictions made using this equation agreed with the experimental pressure drop measurements for at least low and intermediate liquid flow rates. This validation with respect to pressure drop indicates that this cannot be the only reason for the failure of Equation J.13. Therefore, these experimental findings show that the problem must be with the validity of assumptions 2, 3 and/or 4 made to derive Equation J.13. Consequently, it is seen that, even for the simplest gas-liquid contactor, a counter-current spray column, a microscopic model may give incorrect results due to some invalid assumptions which it was necessary to introduce because of lack of precise information on gas-liquid contacting phenomena in the column. Furthermore, this shows that use of the theory which involves a particle transfer coefficient, k_p, as developed in Chapter 4, is a more appropriate approach than most of the models currently used for various gas-liquid contactors.

Experimental data obtained from 72 runs for the unit operated as a spray column were, therefore, used to obtain the particle transfer coefficient, $k_{p,SC}$, from Equation 4.3.5. Values of $k_{p,SC}$ thus calculated are correlated by the following equation

$$k_{p,SC} = 0.0165\ L^{1.508}\ G^{0.745}\ St_d^{-0.413} \qquad (J.14)$$

where

$$St_d = c'\ d_p^{\,2}\ \rho_p\ u_r / 9\ \mu_G\ d_{30} \qquad (J.15)$$

Experimental results, calculated values of $k_{p,SC}$ and predicted particle penetration from equations 4.3.6 and J.14 are given in Table J.1. Figure J.3 shows typical experimental results for 3.5 μm particles. Solid lines in this figure are not correlations of each set of runs but, rather, correspond to the predicted penetration using Equation J.14.

It is interesting to note that, over the range of liquid flow rates studied, particle penetration may either increase or decrease with gas flow rate. Two opposing phenomena occur simultaneously as gas velocity increases, i.e. penetration tends to decrease due to increase in inertial collection efficiency of drops, but tends to increase due to shorter residence times of the gas phase as interstitial velocities of both phases increase. Of these opposing effects, the former is predominant for L up to 9.4 kg/m^2-s, the latter for L = 14 kg/m^2-s and higher. Although it is interesting that the data of the present investigation are sufficiently accurate to show the changeover from one effect to the other predominating, Figure J.3 also indicates that, for practical purposes, penetration is effectively independent of gas velocity. This factor suggests design and operation of a spray column used for particulate recovery should be at the highest gas velocity consistent with stable operation and acceptable liquid carry-over.

Figure J.4 shows the agreement between experimental particle penetration data and those evaluated using Equations J.14 and 4.3.6.

TABLE J.1. Experimental Results and Estimated Penetration of Ferrous Sulphate Particles in Spray Column at Conditions without Diffusiophoresis

L kg/m^2-s	G kg/m^2-s	St	Pt_{exp}	$k_{p,SC}$	Pt_{est}
d_p = 2.5 μm					
4.710	2.684	0.106	.8941	0.167	.9094
4.710	3.197	0.119	.9528	0.086	.9059
4.710	3.724	0.130	.9069	0.202	.9035
4.710	4.034	0.139	.8768	0.295	.9003
4.710	4.676	0.152	.8908	0.300	.8975
9.420	2.665	0.150	.8973	0.160	.7163
9.420	3.190	0.163	.7906	0.416	.7143
9.420	3.677	0.174	.8258	0.391	.7129
9.420	4.034	0.183	.6789	0.868	.7095
9.420	4.618	0.195	.8864	0.309	.7068
14.123	2.656	0.194	.4408	1.209	.4790
14.123	3.185	0.207	.5070	1.202	.4823
14.123	3.665	0.218	.5137	1.356	.4852
14.123	4.036	0.227	.4314	1.885	.4844
14.123	4.607	0.239	.4528	2.028	.4846
18.831	2.657	0.238	.1285	3.029	.2671
18.831	3.188	0.251	.1801	3.036	.2749
18.831	3.667	0.261	.2091	3.188	.2813
18.831	4.035	0.271	.1816	3.824	.2823
18.831	4.599	0.283	.2131	3.950	.2856
23.539	2.671	0.282	.0139	6.345	.1234
23.539	3.206	0.295	.0168	7.278	.1314
23.539	3.670	0.305	.0476	6.208	.1371
23.539	4.050	0.314	.0550	6.526	.1399
d_p = 3.5 μm					
4.710	2.684	0.205	.8196	0.297	.8305
4.710	3.197	0.229	.8684	0.251	.8239
4.710	3.724	0.250	.7012	0.734	.8195
4.710	4.034	0.267	.7902	0.528	.8140
4.710	4.676	0.292	.7859	0.626	.8090
9.420	2.665	0.289	.7680	0.391	.5201
9.420	3.190	0.314	.6242	0.835	.5168
9.420	3.677	0.335	.5168	1.348	.5148
9.420	4.034	0.352	.4978	1.563	.5104
9.420	4.618	0.376	.5712	1.437	.5064

L kg/m^2-s	G kg/m^2-s	St	Pt_{exp}	$k_{p,SC}$	Pt_{est}
d_p = 3.5 μm					
14.123	2.656	0.374	.2178	2.249	.2364
14.123	3.185	0.419	.2800	2.252	.2222
14.123	3.665	0.419	.2888	2.529	.2420
14.123	4.036	0.436	.2598	3.022	.2416
14.123	4.607	0.460	.2480	3.569	.2418
18.831	2.657	0.459	.0490	4.452	.07506
18.831	3.188	0.483	.0665	4.801	.07943
18.831	3.667	0.503	.0907	4.890	.08310
18.831	4.035	0.520	.0971	5.228	.08390
18.831	4.599	0.544	.1030	5.808	.08581
23.539	2.671	0.542	.0042	8.121	.01656
23.539	3.206	0.567	.0057	9.203	.01875
23.539	3.670	0.587	.0150	8.563	.0203
23.539	4.050	0.604	.0133	9.720	.0212
d_p = 4.5 μm					
4.710	2.684	0.335	.5697	0.839	.7349
4.710	3.197	0.375	.5748	0.983	.7252
4.710	3.724	0.409	.4843	1.500	.7188
4.710	4.034	0.437	.6023	1.136	.7107
4.710	4.676	0.478	.5756	1.435	.7033
9.420	2.665	0.473	.4600	1.150	.3381
9.420	3.190	0.514	.3438	1.892	.3346
9.420	3.677	0.547	.3596	2.089	.3324
9.420	4.034	0.575	.3652	2.257	.3277
9.420	4.618	0.614	.3740	2.523	.3234
14.123	2.656	0.612	.1010	3.383	.0912
14.123	3.185	0.652	.1416	3.459	.09348
14.123	3.665	0.685	.1687	3.623	.09506
14.123	4.036	0.713	.1070	5.011	.0948
14.123	4.607	0.752	.1492	4.869	.09493
18.831	2.657	0.751	.0146	6.239	.01363
18.831	3.188	0.791	.0292	6.258	.01497
18.831	3.667	0.822	.0323	6.993	.01614
18.831	4.035	0.851	.0438	7.012	.01640
18.831	4.599	0.890	.0394	8.263	.01702
23.539	2.671	0.888	.0029	8.670	.001104
23.539	3.206	0.927	.0026	10.602	.001366
23.539	3.670	0.960	.0090	9.604	.001557
23.539	4.050	0.988	.0039	12.480	.001674

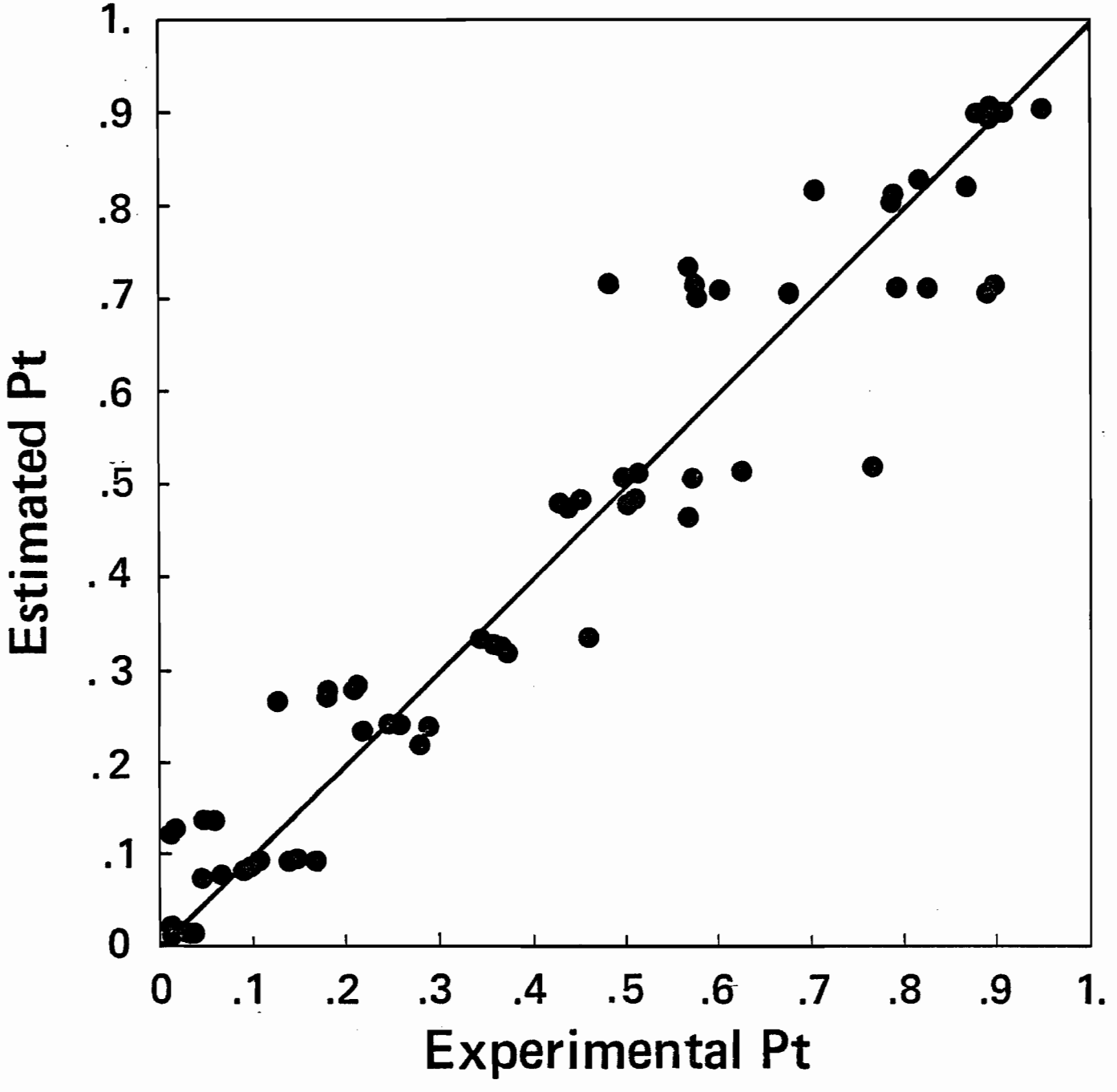

FIGURE J.4. Comparison of experimental and estimated values of penetration in the spray column

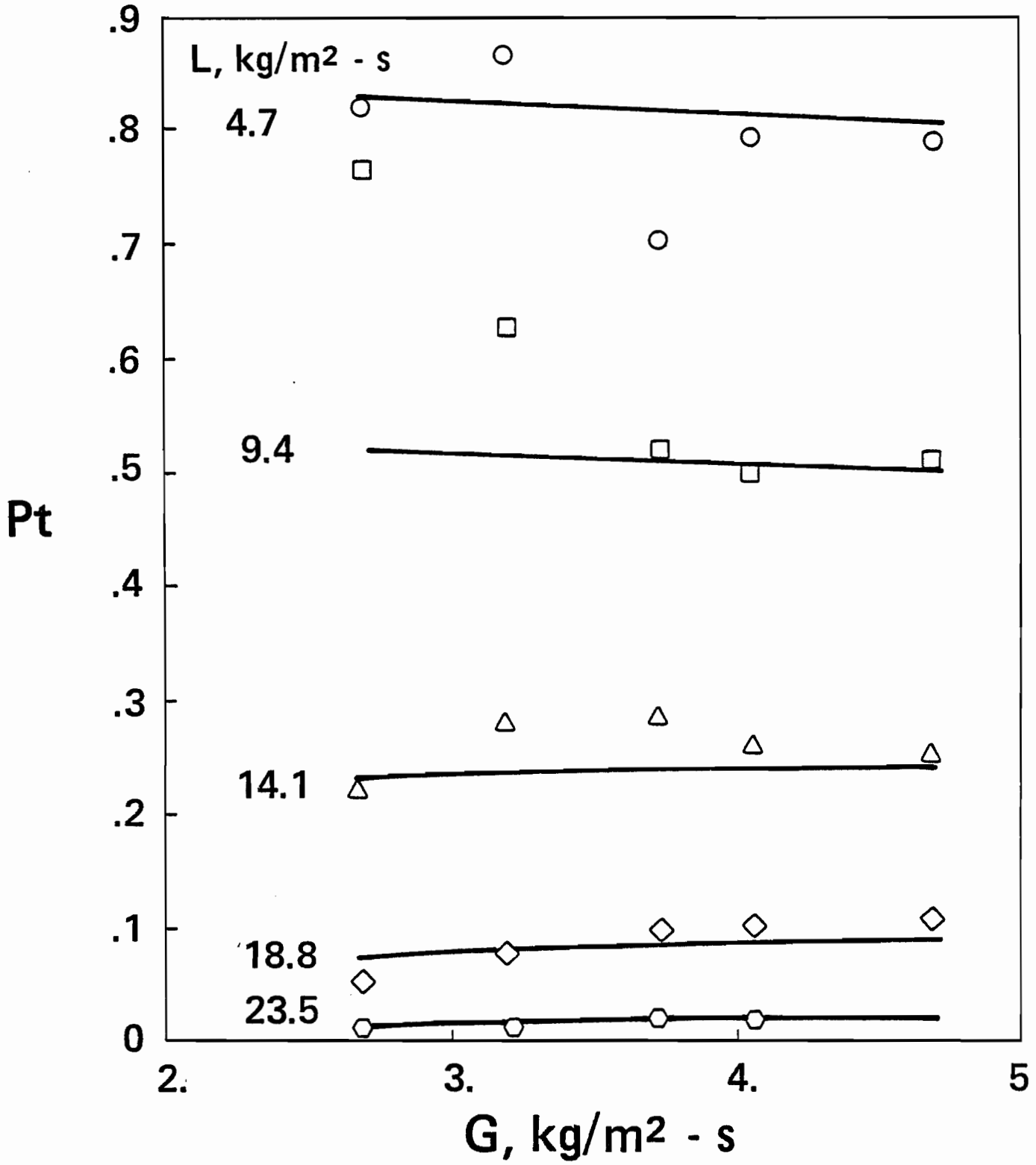

FIGURE J.3. Penetration in the spray column

$d_p = 3.5$ μm